

CHEMICALLY BONDED PHOSPHATE CERAMICS

Twenty-First Century Materials with Diverse Applications

Elsevier Internet Homepage- <http://www.elsevier.com>

Consult the Elsevier homepage for full catalogue information on all books, journals and electronic products and services including further information about the publications listed below.

Elsevier titles of related interest

Books

ELSSNER ET AL.

Ceramics and Ceramic Composites: Materialographic Preparation

ISBN: 0-444-10030-X

OEHLERS and BRADFORD

Composite Steel and Concrete Structural Members

ISBN: 0-08-041919-4

OEHLERS and SERACINO

Design of FRP and Steel Plated RC Structures

ISBN: 0-08-044548-9

OJOVAN and LEE

An Introduction to Nuclear Waste Immobilisation

ISBN: 0-08-044462-8

YEOMANS

Galvanized Steel Reinforcement in Concrete

ISBN: 0-08-044511-X

Elsevier author discount

Elsevier authors (of books and journal papers) are entitled to a **30% discount** off the above books and most others. See ordering instructions below.

Journals

Sample copies of all Elsevier journals can be viewed online for FREE at www.sciencedirect.com, by visiting the journal homepage.

Cement and Concrete Research

Cement and Concrete Composites

Ceramics International

Journal of the European Ceramic Society

To contact the Publisher:

Elsevier welcomes enquiries concerning publishing proposals: books, journal special issues, conference proceedings, etc. All formats and media can be considered. Should you have a publishing proposal you wish to discuss, please contact, without obligation, the publisher responsible for Elsevier's material science programme:

Emma Hurst

Publishing Editor

Elsevier Science Ltd

The Boulevard, Langford Lane

Kidlington, Oxford

OX5 1GB, UK

Phone: +44 1865 843629

Fax: +44 1865 843920

E.mail: e.hurst@elsevier.com

General enquiries, including placing orders, should be directed to Elsevier's Regional Sales Offices – please access the Elsevier homepage for full contact details www.elsevier.com

CHEMICALLY BONDED PHOSPHATE CERAMICS

Twenty-First Century Materials with
Diverse Applications

Arun S. Wagh

*Argonne National Laboratory
9700 S. Cass Avenue
Argonne, IL 60439, USA*



ELSEVIER

2004

Amsterdam – Boston – Heidelberg – London – New York – Oxford
Paris – San Diego – San Francisco – Singapore – Sydney – Tokyo

ELSEVIER B.V.
Radarweg 29
P.O. Box 211, 1000 AE
Amsterdam, The Netherlands

ELSEVIER Inc.
525 B Street, Suite 1900
San Diego, CA 92101-4495
USA

ELSEVIER Ltd
The Boulevard, Langford Lane
Kidlington, Oxford OX5 1GB
UK

ELSEVIER Ltd
84 Theobalds Road
London WC1X 8RR
UK

© 2004 Elsevier Ltd. All rights reserved.

This work is protected under copyright by Elsevier Ltd, and the following terms and conditions apply to its use:

Photocopying

Single photocopies of single chapters may be made for personal use as allowed by national copyright laws. Permission of the Publisher and payment of a fee is required for all other photocopying, including multiple or systematic copying, copying for advertising or promotional purposes, resale, and all forms of document delivery. Special rates are available for educational institutions that wish to make photocopies for non-profit educational classroom use.

Permissions may be sought directly from Elsevier's Rights Department in Oxford, UK: phone (+44) 1865 843830, fax (+44) 1865 853333, e-mail: permissions@elsevier.com. Requests may also be completed on-line via the Elsevier homepage (<http://www.elsevier.com/locate/permissions>).

In the USA, users may clear permissions and make payments through the Copyright Clearance Center, Inc., 222 Rosewood Drive, Danvers, MA 01923, USA; phone: (+1) (978) 7508400, fax: (+1) (978) 7504744, and in the UK through the Copyright Licensing Agency Rapid Clearance Service (CLARCS), 90 Tottenham Court Road, London W1P 0LP, UK; phone: (+44) 20 7631 5555; fax: (+44) 20 7631 5500. Other countries may have a local reprographic rights agency for payments.

Derivative Works

Tables of contents may be reproduced for internal circulation, but permission of the Publisher is required for external resale or distribution of such material. Permission of the Publisher is required for all other derivative works, including compilations and translations.

Electronic Storage or Usage

Permission of the Publisher is required to store or use electronically any material contained in this work, including any chapter or part of a chapter.

Except as outlined above, no part of this work may be reproduced, stored in a retrieval system or transmitted in any form or by any means, electronic, mechanical, photocopying, recording or otherwise, without prior written permission of the Publisher.

Address permissions requests to: Elsevier's Rights Department, at the fax and e-mail addresses noted above.

Notice

No responsibility is assumed by the Publisher for any injury and/or damage to persons or property as a matter of products liability, negligence or otherwise, or from any use or operation of any methods, products, instructions or ideas contained in the material herein. Because of rapid advances in the medical sciences, in particular, independent verification of diagnoses and drug dosages should be made.

First edition 2004

Library of Congress Cataloging in Publication Data

A catalog record is available from the Library of Congress.

British Library Cataloguing in Publication Data

A catalogue record is available from the British Library.

ISBN: 0-08-044505-5

© The paper used in this publication meets the requirements of ANSI/NISO Z39.48-1992 (Permanence of Paper).
Printed in the UK.

Working together to grow
libraries in developing countries

www.elsevier.com | www.bookaid.org | www.sabre.org

ELSEVIER

BOOK AID
International

Sabre Foundation

To my loving family –

Swati, Arati and Raj, Poojan and Jennifer, who kept me on track during the writing of this book by gently but repeatedly asking,

“How is the book coming?”

until it was done.

Arun S. Wagh

This page is intentionally left blank

Foreword I

Dr. Arun Wagh has done the world of materials science a great service by bringing together in a single book an excellent compendium on phosphate ceramics. Moreover, he has stressed the enormous range of low temperature materials—many of them useful in industry and daily life which can accurately be called “chemically bonded ceramics”—a term I coined some twenty years ago to describe materials formed and consolidated by chemical reaction instead of thermal diffusion. While silicates get the enormous majority of attention of the ceramics community, it was Prof. Kingery, my colleague and contemporary from MIT who in the 1950’s first called our attention to phosphate ceramics. Wagh’s book is a much more comprehensive approach to the topic fifty years later. The ceramics community will be indebted to him for another few decades.

In examining Dr. Wagh’s manuscript I was greatly impressed by its diversity of topics and his thoroughness and the detail in each chapter. For students there is just enough on crystal chemistry, on thermodynamics, and on kinetics. It is not too full of equations, just enough. For the researcher this book is an up to date literature review tempered by the good judgment of an expert. For the practicing engineer the book covers a series of applications. I particularly appreciated the chapter on radioactive waste alongside those on dental cements!! It demonstrates the enormous range and versatility of phosphate ceramics. Another valuable strategy for organizing his subject matter on the phosphates, which I found useful, is simply by composition: separate chapters on magnesium, aluminum, zinc, iron, etc. in parallel to the different applications. An “obvious” classification is often the most useful.

In many ways the phosphates provide the richest field for CBC’s (chemically bonded ceramics) because of the P—O bond strengths and the coordination demands of pentavalent phosphorus. Among silicates, room temperature hydration reactions seem to be possible only with Ca-compounds; the magnesium and aluminum anhydrous silicates phases simply do not react. This book documents for the reader the wide application of these separate chemistries as true chemically bonded ceramics.

The organization is logical, the style is very readable with the appropriate amount of thermodynamics and kinetics, not to overwhelm the general reader, but be useful for the professional in the field.

I am sure this book will appear on the shelves of all practicing material scientists interested in cements and related low temperature materials.

Rustum Roy
Founding Director Materials Research Laboratory
Evan Pugh Professor of the Solid State Emeritus
Professor of Science Technology and Society Emeritus
The Pennsylvania State University

Visiting Professor of Medicine
University of Arizona

Distinguished Professor of Materials
Arizona State University

Foreword II

Chemically bonded phosphate ceramics combine the hardness and durability of conventional cements with the easy fabrication of sintered ceramics. For that reason, these room-temperature-setting materials have found applications as structural cements and biomaterials, and in radioactive and hazardous waste treatment. Because of the diverse nature of these applications, the literature on these unique materials is scattered, and no unified treatment could be found in the literature, till now.

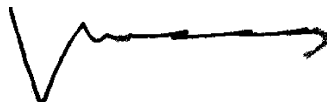
This book by Dr. Arun Wagh is the first comprehensive volume on chemically bonded phosphate ceramics that discusses their chemistry, syntheses, and applications in a single volume.

Dr. Wagh begins by citing examples of chemically bonded ceramics from nature and archeology. Then, he extends the concept to a new class of chemically bonded phosphate ceramics that are man made. He presents the scientific basis for formation of these materials using solution chemistry routes, in general, and Pourbaix diagrams, in particular, and establishes methods for their fabrication. He then goes on to discuss the many actual and possible applications of these materials. Such a comprehensive treatment of this novel subject provides a solid foundation for further research and development by materials researchers. I am confident this book will be a source of baseline information on chemically bonded phosphate ceramics and will inspire further research on these promising engineering materials.

As a radiochemist, I would like to note the great significance of chemically bonded ceramics for high level waste (HLW) treatment. It is well known that for safe storage, transportation, and disposal of radioactive waste streams, it is necessary to convert them to hardened forms. Therefore, the search for and development of a new solid matrix for immobilization of HLW forms are important, indeed.

We, at the Verandsky Institute of Geochemistry and Analytical Chemistry, Russian Academy of Sciences, have recognized this and have already initiated research on these materials for stabilization of some difficult high activity radioactive waste streams. The simple concept of forming these ceramics by acid-base reaction, the resulting room-temperature fabrication processes, and the superior properties of the product ceramics, all presented in this book, are helping us to solve some difficult

problems in the waste treatment area. Scientists and engineers in other fields may also reap the same benefits. This book has laid the foundation for exciting opportunities in materials science.

A handwritten signature in black ink, appearing to read 'Boris Myasoedov'. The signature is stylized, with a large 'V' shape at the beginning and a long, horizontal, slightly wavy line extending to the right.

Boris Myasoedov

Academician Deputy Secretary General for Science,
Russian Academy of Sciences

The Head of the Scientific Counsel on Radiochemistry of the RAS,
Atomic Energy Agency (ROSATOM) RF

Contents

Foreword I	vii
Foreword II	ix
Preface	xv
Abbreviations	xix
1. Introduction to Chemically Bonded Ceramics	1
1.1 Ceramics and Hydraulic Cements	1
1.2 Chemically Bonded Ceramics as Intermediate Products	2
1.3 Acid–Base Cements CBCs	3
1.4 Solidification by Chemical Bonding in Nature	5
1.5 General Definition of Chemically Bonded Ceramics	8
1.6 Nature of the Chemical Bonding in CBCs	9
1.7 Role of Solubility in Chemical Bonding	11
References	12
2. Chemically Bonded Phosphate Ceramics	15
2.1 Review on Phosphate-Bonded Ceramics and Cements	15
2.2 Review on Phosphate-Bonded Dental Cements	16
2.3 Magnesium Phosphate Ceramics	19
2.4 Generalization of Formation of CBPCs	21
2.5 Summary of Literature Survey	22
2.6 Applications of CBPCs	23
References	25
3. Raw Materials	29
3.1 Formation of Phosphoric Acid from Phosphate Rocks	30
3.2 Acid Phosphates	31
3.3 Major Oxides and Oxide Minerals	34
3.4 Aggregates	37
References	41

4. Phosphate Chemistry	43
4.1 Nomenclature	43
4.2 The Effect of pH	44
4.3 Dissolution Characteristics of Phosphoric Acid	45
4.4 Neutralization of the Acid and Formation of Acid Phosphates	46
4.5 Condensed Phosphates	48
4.6 Dissociation (Ionization) Constants of Weak Acids	49
References	50
5. Dissolution Characteristics of Metal Oxides and Kinetics of Ceramic Formation	51
5.1 Dissolution Characteristics as the Basis for Forming CBPCs	51
5.2 Dissolution of Oxides and Formation of Dissolved Cations	52
5.3 Born Equation	55
5.4 Kinetics of Formation of CBPCs	57
5.5 Solubility Product Constant and Its pH Dependence	58
References	62
6. Thermodynamic Basis of CBPC Formation	63
6.1 Review of Basic Thermodynamic Relations	64
6.2 Thermodynamics of Solubility Reactions	66
6.3 Applications of Thermodynamic Parameters to CBPC Formation	67
6.4 Temperature Dependence of Solubility Product Constant	69
6.5 Pressure Dependence of Solubility Product Constants	73
References	73
7. Oxidation and Reduction Mechanisms	75
7.1 Oxidation and Reduction (Redox) Reactions	76
7.2 Redox Potentials	77
7.3 E_H -pH Diagrams	80
7.4 E_H -pH Diagram of Water	81
7.5 Reduction of Iron Oxide and Formation of CBPC	83
References	84
8. Mineralogy of Orthophosphates	85
8.1 Nature of Interatomic Bonds	85
8.2 Rules for Crystal Structure Formation	87
8.3 Major Phosphate Crystal Structures	88
8.4 Relevance to Minerals Constituting CBPC	94
References	95
9. Magnesium Phosphate Ceramics	97
9.1 Solubility Characteristics of MgO and Its Reaction with Acid Phosphates	98

9.2	Controlling Reaction Rates During Formation of Mg-Phosphate Ceramics	98
9.3	Fabrication and Properties of Mg-Based Phosphate Ceramics	103
	References	110
10.	Zinc Phosphate Ceramics	113
10.1	Solubility Characteristics of Zinc Oxide	114
10.2	Formation of Zinc Phosphate Ceramic	115
10.3	Phase Formation in Zinc Phosphate Cements and their Microstructure	117
10.4	Properties of Zinc Phosphate Cements	117
	References	118
11.	Aluminum Phosphate Ceramics	121
11.1	Solubility Enhancement with Temperature, and Formation of Berlinite Phase	123
11.2	Formation of Berlinite Bonded Alumina Ceramic	128
11.3	Consolidation Model of CBPC Formation	131
	References	133
12.	Iron Phosphate Ceramics	135
12.1	Reduction as the Basis for Enhanced Solubility	136
12.2	Ceramic Formation with Iron Oxides	139
12.3	Conclusions	140
	References	141
13.	Calcium Phosphate Cements	143
13.1	Chemistry of Calcium Phosphates	144
13.2	Calcium Phosphate Cements from Calcium Silicates and Aluminates	147
13.3	Adhesion of Portland Cement and CBPCs	151
13.4	Calcium Phosphate Cements with Biomedical Applications	152
13.5	Conclusions	154
	References	154
14.	Chemically Bonded Phosphate Ceramic Matrix Composites	157
14.1	Recycling of Benign Waste Streams in CBPC Value-Added Products	158
14.2	Fiber Reinforcement of CBPC Products	169
14.3	Niche Applications	169
14.4	Energy and Environmental Issues Related to Binder Production . .	174
	References	175

15. Chemically Bonded Phosphate Ceramic Borehole Sealant	177
15.1 Parameters Affecting CBS Slurry Design.	178
15.2 CBS Engineering Properties in Simulated Downhole Environment.	181
15.3 CBS Slurry Designs.	185
15.4 Properties of CBS.	191
15.5 Effect of Individual Components on Slurry Behavior	194
15.6 Conclusions	196
References	196
16. Applications of CBPCs to Hazardous Waste Stabilization.	197
16.1 Test Criterion for Stabilization.	199
16.2 Chemical Kinetics of Stabilization.	200
16.3 General Approach to Phosphate Stabilization.	204
16.4 Conclusions	212
References	212
17. Radioactive Wastes Stabilization.	217
17.1 Nature of the Radioactive Contaminants	219
17.2 Mechanisms of Radioactive Waste Immobilization	221
17.3 Role of Solubility in Immobilization of Radioactive Elements.	221
17.4 Waste Acceptance Criteria	226
17.5 Case Studies in Stabilization of Radioactive Waste Streams.	229
17.6 Macroencapsulation of Large Objects	240
17.7 Other Nuclear Applications	241
17.8 Conclusions	241
References	242
18. Dental Cements and Bioceramics	245
18.1 Bone as a Composite Material.	246
18.2 Chemically Bonded Phosphate-Based Bioceramics	248
18.3 Recent Advances in CBPC-Based Biomaterials.	249
18.4 Calcium-Based CBPC Biomaterials	251
18.5 Conclusions	252
References	253
Appendices	255
A: Thermodynamic Properties of Selected Materials	256
B: Solubility Product Constants	264
C: List of Minerals and Their Formulae	267
Index	269

Preface

Ceramics are associated with terms such as sintering, firing, heat treatment at high temperature, volatilization, melting, thermal shock, and residual stress. Traditional ceramics, such as terra cotta products formed by firing consolidated powders in kilns, have been in use since the beginning of human culture. They provide archeological clues to the life style in ancient times, and are also part of modern day life. Even now, due to their tremendous unexplored potential, ceramics constitute a major field of scientific research and technical innovation and will continue to do so throughout the 21st century.

As first defined by Rustum Roy, chemically bonded ceramics (or simply CBCs) are *inorganic solids consolidated by chemical reactions instead of the conventional high-temperature heat treatment*.

Since the dawn of civilization, human culture has used chemical bonding as an alternative to sintering or other heat treatment to mass produce ceramic products such as building materials. Examples of CBC products include, cements of ancient Egypt and Mesopotamian periods, adobe architecture of native Indians in the American continents, and structures made of lateritic soils in South Asia at places such as Angkor Thom in Cambodia. However, portland cement is the only chemically bonded material that has found wide enough use that it is taken for granted in everyday life. To date, alternative chemical bonding processes have received little attention. This book deals specifically with phosphate-bonded materials, which constitute a class of such alternatives.

In a world of uncertain energy sources, in a market that is ever hungry for novel products, and in a scientific and technologically advanced culture where basic ideas come to fruition within years, depending on sintered ceramics alone or relying on portland type of cements alone seems ill advised, to say the least. This book, building upon a foundation in the history and archeology of CBCs, explores alternative chemically bonded phosphate ceramics (CBPCs), i.e., phosphate-based CBCs that set at room temperature, which have demonstrated potential for wide-ranging novel applications.

At present, there are only a few comprehensive publications on phosphate chemistry, minerals, and materials. Notable ones are *Inorganic Phosphate Materials* by T. Kanazawa [Kodansha, Tokyo, and Elsevier, Amsterdam (1989)], *Phosphate Minerals* by J. Nriagu and P. Moore [Springer-Verlag, Berlin (1984)], and a chapter on CBPCs in *Acid-Base Cements* by A. Wilson and J. Nicholson [Cambridge Univ. Press, Cambridge (1993)]. Much of the background information on phosphate materials is derived from these and other phosphate chemistry books.

The dissolution chemistry and thermodynamic model described in this book is heavily (almost entirely) indebted to Pourbaix's treatment of electrochemical equilibria of inorganic oxides in aqueous solutions. Pourbaix's work is the basis for explaining fundamental processes in the fields of corrosion, water chemistry, geochemistry, and electrochemistry. It is interesting to note that while discussion of corrosion and water chemistry is based on dissociation of metals and oxides, geochemistry and electrochemistry use the same approach in a reverse direction to investigate the syntheses of materials. Pourbaix's diagrams are used in this book in the latter approach, i.e., to find conditions to synthesize CBPCs. Such an approach not only helps in developing new formulations for ceramics such as that of iron phosphates, but also provides a sound scientific basis for the formulations that are reported in the literature, such as zinc and aluminum phosphates.

This book covers the theory behind formation of these ceramics, selection of materials, processing aspects, and their applications. The purpose is to encourage future research into CBCs using the theoretical and experimental methods outlined in this book. It is hoped that future research will establish CBCs as technologically important materials in a class similar to metals, polymers, and sintered ceramics.

The first chapter gives an overview of chemically bonded ceramics. The purpose is to bring CBCs from diverse fields such as materials science, geochemistry, and biomaterials under one umbrella. The second chapter provides a literature survey of the work till 1990. The next six chapters build the theoretical foundation for discussing range of processes and materials that are discussed in next five chapters. The remaining chapters summarize wide-ranging applications of these materials that have been realized since early 1990s.

To be more specific, Chapter 2 provides an overview of *Chemically Bonded Phosphate Ceramics*. It is intended to streamline the earlier literature and present it in a suitable context. Since the many potential applications of CBPCs are likely to affect the raw materials (such as phosphates) market, an overview of the raw materials, their general properties, and their manufacturing processes is given in the third chapter. Chapters 4–7 are devoted to the theoretical basis for formation of phosphate ceramics by chemical reactions, and much of the discussion in these chapters is based on thermodynamics.

Chapter 8 provides a review of the phosphate mineralogy that facilitates discussion on the applications discussed in the latter part of the book. The next five chapters discuss individual phosphate (magnesium, zinc, aluminum, iron, and calcium) ceramics that have potential for use in current and future applications. The approach provided in this book should guide researchers to many more formulations for specific needs in the future.

The last five chapters of the book are devoted to major applications of CBPCs. Chapter 14 covers CBPC matrix composites that are finding commercial applications in the United States. Discussed in Chapter 15 are drilling cements developed mainly by the U.S. Department of Energy laboratories with industrial collaborations. Applications of CBPCs in the stabilization of hazardous and radioactive waste streams are discussed in Chapters 16 and 17. Finally, recent advances in CBPC bioceramics are covered in Chapter 18. Appendixes A, B, and C compile relevant thermodynamic and mineralogy data that were useful in writing the book. They serve as a ready reference to researchers who venture into further development of CBPCs.

The author has received considerable help from the Argonne Libraries in compiling much of the data presented in this book. Assessing the credibility of the data from some of the earlier literature on the thermodynamic potentials of various minerals, cations, and anions is a very difficult task. Obtaining background information from obscure patents and technical reports is also beyond the expertise of the author. Support from the Argonne librarians was indispensable in this respect. Specific mention should be made of Susan Pepalis, Sharon Clark, Swati Wagh, and Karen Schachsnider, who took the burden collectively and provided the responses promptly. Without their help, the author would have been lost in the maize of the knowledge. The author is indebted to Carolyn Primus of Primus Consulting for reviewing Chapters related to biomaterials.

No work is complete till the paper work is done. In this case, that meant arriving at a contract between Argonne National Laboratory as a DOE laboratory, the employer of the author, and Elsevier, Limited, to write and publish the book. The persistence of Emma Hurst, editor of Elsevier, made it possible. The author also thanks Argonne's attorney, Mark Langguth, who was key to finalizing the agreement between Argonne and Elsevier.

Even after writing the draft of the book, preparing a publishable manuscript of that work is an equally daunting task. Accomplishing that task was aided by Joe Harmon as the technical editor, and by Sylvia Hagamann, who put the manuscript in final form. Help from Ramkumar Natarajan in drawing illustrations and inserting the photographs throughout the book is greatly acknowledged. Preparation of the manuscript was partially supported by the Energy Technology Division of Argonne National Laboratory. The author is indebted to Roger Poeppel, Director of the Division, for his help in securing this funding. Preparation of this manuscript was also supported by the U.S. Department of Energy, Office of Technology Development, under Contract No. W-31-109-Eng-38.

June 1, 2004
Argonne, IL
Arun S. Wagh

About the Author

Dr. Arun S. Wagh, is a staff ceramist in the Energy Technology Division at Argonne National Laboratory. His main research project concerns development of chemically bonded phosphate ceramics for stabilization of radioactive waste streams within the U.S. Department of Energy complex. While leading this project, he found a wide range of commercial applications of these materials. He has received several awards for his work, including two R&D 100 awards, which annually recognize one-hundred technologies newly available for commercial use.

Abbreviations

ANL	Argonne National Laboratory
ANS	American Nuclear Society
AASHTO	American Association of State Highway Technology Officials
ASTM	American Society for Testing and Materials
BNL	Brookhaven National Laboratory
BTU	British Thermal Unit
CBC	Chemically Bonded Ceramics
CBPC	Chemically Bonded Phosphate Ceramic
CFR	Code of Federal Register
DCPA	Dicalcium Phosphate Anhydrous
DCPD	Dicalcium Phosphate Dihydrate
DOE	U.S. Department of Energy
DOT	U.S. Department of Transportation
DSC	Differential Scanning Calorimetry
EPA	U.S. Environmental Protection Agency
EDX	Energy Dispersive X-ray Analysis
FAP	Fluoroapatite
FUETAP	Formed Under Elevated Temperature and Pressure
HAP	Hydroxyapatite
IAEA	International Atomic Energy Agency
LI	Leachability Index
MCC	Materials Characterization Center
MCPA	Monocalcium Phosphate Anhydrous
MCPM	Monocalcium Phosphate Monohydrate
MDF	Macro-Defect Free
MHP	Magnesium Hydrogen Phosphate Trihydrate (Newberyite)
MIT	Massachusetts Institute of Technology
MKP	Magnesium Potassium Phosphate Hexahydrate ($\text{MgKPO}_4 \cdot 6\text{H}_2\text{O}$)
MPa	Megapascals
MSW	Municipal Solid Waste
NRC	U.S. Nuclear Regulatory Commission
NSP	Normal Super Phosphate
OCP	Octacalcium Phosphate
PCT	Product Consistency Test
PNNL	Pacific Northwest National Laboratory

psi	Pounds Per Square Inch
PUREX	Plutonium and Uranium Extraction Process
RCRA	Resource Conservation and Recovery Act of the United States
SEM	Scanning Electron Micrograph
TCLP	Toxicity Characteristic Leaching Procedure
TCP	Tricalcium Phosphate
TSP	Triple Super Phosphate
TTCP	Tetracalcium Phosphate
UTS	Universal Treatment Standards
XRD	X-ray Diffraction
XPS	X-ray Photoelectron Spectroscopy
WAC	Waste Acceptance Criteria

Introduction to Chemically Bonded Ceramics

1.1.

CERAMICS AND HYDRAULIC CEMENTS

Ceramics and hydraulic cements are two major classes of inorganic solids that are man made and in common use [1]. Ceramics are formed by compaction of powders and their subsequent fusion at high to very high temperatures, ranging anywhere from ~ 700 to 2000°C . Once fused, the resulting ceramics are hard and dense, and exhibit very good corrosion resistance. These materials have found applications in bricks; pottery; refractory products of alumina, zirconia, magnesia; and high temperature superconductors. There are porous ceramics such as filters and membranes that are also fabricated by the sintering process, but porosity is introduced in them intentionally. Ceramics, in general, are highly crystalline with some glassy phase. If glassy phase dominates, then they are called “glass-ceramics”.

Hydraulic cements are another class of technologically important materials. Examples include Portland cement, calcium aluminate cement, and plaster of Paris. They harden at room temperature when their powder is mixed with water. The pastes formed this way set into a hard mass that has sufficient compression strength and can be used as structural materials. Their structure is generally noncrystalline.

Hydraulic cements are excellent examples of accelerated chemical bonding. Hydrogen bonds are formed in these materials by chemical reaction when water is added to the powders. These bonds are distinct from the bonds in ceramics in which high temperature interparticle diffusion leads to consolidation of powders.

Portland cement is the most common hydraulic cement. It is formed by clinkering a mixture of powders of limestone, sand, iron oxide and other additives at a very high temperature ($\approx 1500^{\circ}\text{C}$). It is mixed with water to form hydrated bonding phases

of dicalcium and tricalcium silicates (Ca_2SiO_4 and Ca_3SiO_5), dicalcium aluminate ($\text{Ca}_2\text{Al}_2\text{O}_6$), and calcium aluminoferrite [$\text{Ca}_4(\text{Fe}_{1-x}\text{Al}_x)\text{O}_5$]. When this cement is mixed with sand and gravel, it bonds them to form cement concrete that is used in construction. Typically, initial bonding occurs in a few hours, but slow curing takes place for weeks to gain full strength.

The preparation of calcium aluminate cements is similar. Here, instead of calcium and silica, calcium and alumina react with water to form hydrated calcium aluminate [2] as the bonding phase. The initial strength gain for this material is faster than that for Portland cement.

Intense research in hydraulic cements has resulted in a wide range of blends that are used in various applications. Accelerated setting formulations have been developed to gain early high strengths. Reducers of water demand have been used to develop macro-defect-free (MDF) cements [3] in which large size pores are eliminated. Pumpable versions of Portland cement for oil drilling applications [4] are common. All the modifications, however, depend on the primary bonds formed by chemical reactions among silica, calcium oxide, alumina and iron oxide.

The main distinction between ceramics and cements is thus how they are produced. Objects that go through intense heat treatment for their consolidation are ceramics, while those formed by chemical reaction at room temperature are cements.

The difference between ceramics and cements, however, goes beyond this definition. From a structural viewpoint, the distinction between ceramics and cements concerns the interparticle bonds that holds them together and provides the necessary strength. Hydraulic cements are bonded by van der Waals forces, while ceramics are formed by either ionic or covalent bonds between their particles. Because covalent and ionic bonds are stronger than van der Waals bonds, ceramics have better strength than cements.

Another major distinction between ceramics and hydraulic cements is the porosity. Ceramics are made dense unless their application requires some degree of porosity. Hydraulic cements, however, are inherently porous. Porosity is <1 vol% for the best ceramics, but typically 15–20 vol% for cements. Ceramics tolerate very high temperatures, and are corrosion resistant in a wide range of pH, while cements are made for use at ambient temperatures and are affected by high temperature as well as acidic environment. Compared to cements, ceramics are more expensive; thus, cement is produced in high volume while ceramics, except few products such as bricks, are specialty products.

1.2.

CHEMICALLY BONDED CERAMICS AS INTERMEDIATE PRODUCTS

The distinctions made between ceramics and hydraulic cements do not cover the many products that have been produced by materials research in the last 50 years. Some of such products are made by partial heat treatment first and then set like cements. There exist products that are made like cements, but exhibit a structure like that of ceramics, because the bonding mechanism in them is covalent and ionic. They have much higher

compressive strength compared to hydraulic cements and they are less corrosion resistant. Some set much more rapidly than hydraulic cements.

Refractory cement is a good example [2]. High-alumina cement paste is mixed with refractory powders such as alumina in the form of corundum (Al_2O_3) that is cast into position, dried and hardened, then fired to make a ceramic. Thus, a chemical route is employed to generate early strength and then ceramic bonds are developed upon firing. Another product that lies between cements and ceramics is the FUETAP cements [5] used for nuclear waste encapsulation. These dense cements are formed by hot pressing. To define such intermediate products, the name chemically bonded ceramics (CBCs) was coined by Roy [6].

Geopolymers are another type of intermediate products that lie between cements and ceramics [7]. A geopolymer is made by pyroprocessing naturally occurring kaolin (alumina-rich clay) into metakaolin. This metakaolin is then reacted with an alkali hydroxide or sodium silicate to yield a rock-like hard mass. Thus, a chemical reaction, which is not fully understood, is employed to produce a hard ceramic-like product. Though this product is produced like cement, its properties are more like a sintered ceramic. It is dense and hard like a rock.

These examples of CBCs are only a few examples of such class of materials. A much wider range of such materials that share attributes of cements and ceramics are formed by acid–base reactions. Such cements are discussed below.

1.3.

ACID–BASE CEMENTS CBCs

Acid–base cements are formed at room temperature but exhibit properties like those of ceramics. They are formed by reaction of an acid with a base. Normally this reaction produces a noncoherent precipitate. If, however, the reaction rate is controlled properly between certain acids and bases, coherent bonds can develop between precipitating particles that will grow into crystalline structures and form a ceramic. The acidic and alkaline components neutralize each other rapidly, and the resulting paste sets rapidly into products with neutral pH.

Much of the initial development in CBCs occurred because of search for suitable dental cements. Wilson and Nicholson [8] have an excellent review of acid–base cements in their book with the same title. They discuss the following three types: polyalkenoate, oxysalt, and phosphate bonded cements.

1.3.1. Polyalkenoate Cements

These are mainly polymeric cements formed by bonding of polyions (or macroions) which are anions with small cations called counterions. Good examples are polycarboxylate cements [9], glass-ionomer cement [10], and polyphosphonic cements [11,12]. Zinc polycarboxylate, glass polyalkenoate, and resin glass polyalkenoate are some examples

of these. They have been developed as dental or bone cements. These materials are dense, quick-setting, and biocompatible. Details may be found in Ref. [8].

1.3.2. Oxysalt Cements

Oxychloride and oxysulfate cements are another class of acid–base cements. These are formed by reaction of a metal oxide such as that of magnesium oxide with a chloride or sulfate of a metal in the presence of water. Magnesium and zinc based oxychloride cements have been developed fully.

Oxychloride cements have several phases, the main one being an oxysalt. Single-phase oxysalts are very insoluble in water and, hence, are suitable for outdoor applications such as structural materials. In practice, however, synthesizing single-phase materials has been difficult. Chlorides and sulfates are also produced as secondary phases, making these cements leachable in water. For this reason, their use has been limited. That does not, however, imply that their potential is limited. If some niche application of these materials is found as in the case of phosphate bonded ceramics, chances are that several other oxysalt cements may be discovered the same way as phosphate bonded ceramics described in this book.

1.3.3. Phosphate Bonded Ceramics

Phosphate bonded ceramics, which is the subject of this book, are formed like cements, but their structure and properties are similar to ceramics. These are also quick-setting and hard materials. They are formed by reaction of metal cations with phosphate anions. The reaction is attained by mixing a cation donor, generally an oxide such as that of magnesium or zinc, with either phosphoric acid or an acid phosphate such as ammonium phosphate solution. Initially, the motivation behind developing these cements was to meet the need of good dental cements, but these products are now finding applications in diverse fields that include structural ceramics, waste management, oil drilling and completions, and bioceramics.

One great advantage with phosphate bonded ceramics in biomaterial or dental applications is the phosphate ions in their structure. Bones contain calcium phosphate, and hence phosphate bonded ceramics are generally biocompatible with bones. While chemically bonded calcium phosphate ceramics have been difficult to produce, magnesium and zinc based phosphate bonded ceramics have been more easily synthesized and used as structural and dental cements.

Phosphate bonded ceramics have several advantages over their cements. Unlike polyalkenoate cements, phosphate based ceramics are entirely inorganic and nontoxic. Unlike Portland cement, which is formed entirely in an alkaline solution, these are acid–base cements, and are neutral. They are stable in a wider range of pH, and since they are made from natural minerals, the raw materials needed for their manufacture are readily available. For the same reason, they are also less expensive compared to other acid–base cements. They are self-bonding, i.e., a second layer will bond intimately to a first set layer. These attributes motivated further research into phosphate bonded materials for

stabilization of radioactive and hazardous wastes at Argonne National Laboratory [13]. These attributes also drew attention of investors for several other applications. This interest spurred the author's group at Argonne to develop an understanding of the formation of these ceramics based on solution chemistry and thermodynamics. The deeper insight gained by this research led to the generalizations about the formation of ceramics using oxides of metals other than magnesium and zinc. This book discusses these generalizations along with development of several novel phosphate bonded cements.

1.4.

SOLIDIFICATION BY CHEMICAL BONDING IN NATURE

Chemical bonding as a means of solidification is very widely observed in nature. Formation of sedimentary rocks, such as carbonate rocks, is an excellent example. Carbonate rocks are formed by the reaction of calcium oxide with the carbon dioxide from the sea water [14]. Sea organisms also use this process and construct seashells. The organisms that flourish in calcium-saturated solutions of sea water change the alkalinity of the solutions slightly and precipitate calcium carbonate, which is used to form protective shelters such as shells and conches.

The lateritic soils that are abundant in tropical region—another good example of strong interparticle bonds that form by chemical reactions in nature. They are red because they are rich in iron oxide (hematite, Fe_2O_3) and also contain alumina (Al_2O_3) and silica. Those soils very rich in alumina are sources of aluminum and are called bauxites. These soils harden when subjected to frequent wetting and drying [15]. Thus, in tropical regions, seasonal rain and then the sun tends to solidify them into hard mass. This property was exploited in constructing the ancient temples in south Asia at places such as Angkor Wat in Cambodia (Fig. 1.1). These monumental structures are made by thatching wet soil into the shape of the temples, which dried and eventually hardened in the rain and sun. One-storey huts of thatched soil are very common in tropical regions like in parts of India, where the soil gains sufficient load-bearing strength to hold lightweight roofs. Similarly, adobe style houses [16] in Central America and the south-west United States built by rammed earth and natural fiber and use the natural property of such soils to bind themselves.

Yet another example of natural chemical bonding is solidification of desert soils to build bird houses in Egypt. Nile silt was mixed with desert grass and river water to make tower shapes on concrete roofs (Fig. 1.2). Holes made in these towers provide shelter to the birds, which eventually are sold for food. The minerals from such rich soils consolidate when they are mixed with water and are dried in the intense sun of the desert.

Solidification of minerals in carbonate rocks or in sea shells, or that of silica and alumina in lateritic or desert soils, is a very slow process. It takes years and centuries and even geological time to consolidate some minerals. Unfortunately, little is known on the exact chemical reactions and the resulting hardening process. As a result, the chemical hardening in nature cannot be translated into technological applications where accelerated hardening and solidification are desired.

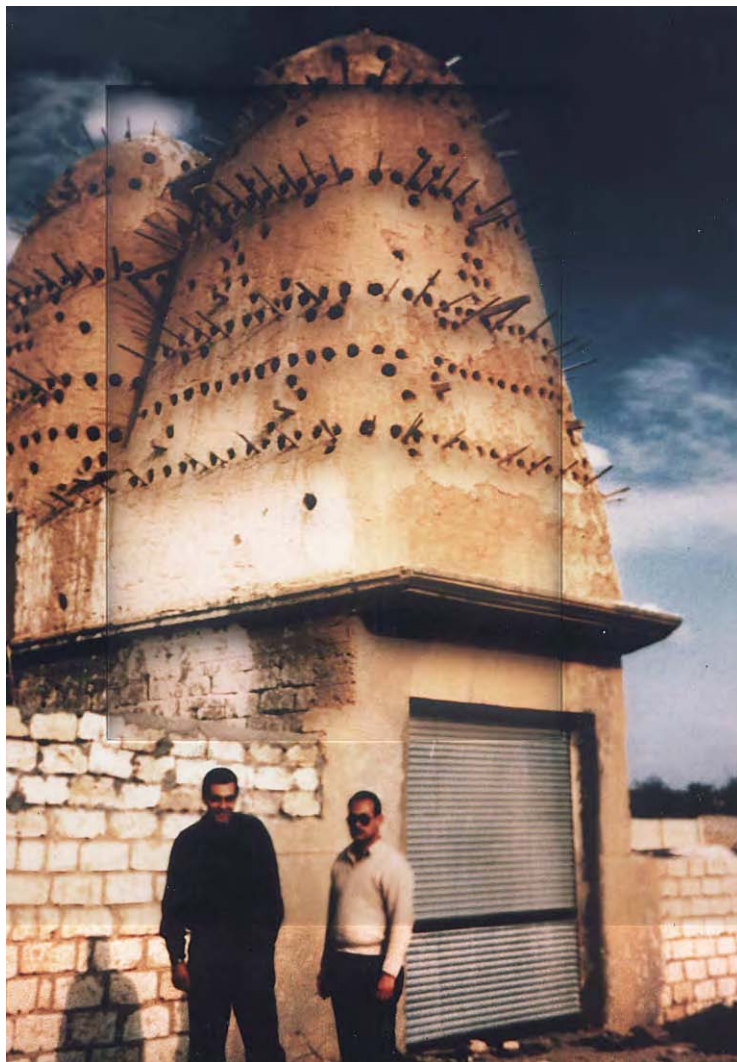
Fig. 1.1.



Temple at Angkor Wat in Cambodia built with thatched lateritic soil. (Photograph: courtesy of Barbara and James Franch.)

The exception is chemical reactions that form mineral rocks. These reactions have been explored by geochemists, and some interesting processes have been proposed to exploit them. A prominent example is the mineral accretion process, developed by W. H. Hilbertz, an architect, to build homes in the ocean [17]. Hilbertz proposes to use this process to

Fig. 1.2.



Bird houses on banks of Nile River made from silt and desert grass.

produce architectural products artificially in oceans. These products could act as barriers for shorelines or construction materials that are produced in the ocean but used on land. The Global Coral Reef Alliance [18] has proposed to grow coral reefs in the ocean and restore marine life by this same process. In this process, a small electric current, generated either by tidal waves or by solar energy enhances the chemical consolidation of carbonates to form solid products (Fig. 1.3). Others have suggested using the process to protect the deteriorating canal structures in Venice [18].

Fig. 1.3.



“Briefcase,” a sculpture made with mineral accretion process (Courtesy: Chris Scala, the artist).

The examples given above indicate the considerable insight to be gained in the chemical bonding of inorganic materials to produce novel ceramics or cements. An improved understanding of the chemistry to form ceramics would accelerate the development of commercial products for modern-day structural materials.

1.5.

GENERAL DEFINITION OF CHEMICALLY BONDED CERAMICS

From a scientific viewpoint, calling all room-temperature-setting materials as cements is a misnomer. Highly crystalline structures, such as phosphate ceramics, are synthesized by chemical reaction at room temperature. They are ceramics because of their crystalline structure, while they are cements because they are formed at room temperature. We would classify such materials as CBCs. If silicates are used to form them, they will be called chemically bonded silicate ceramics. When phosphates are used to form them, they are chemically bonded phosphate ceramics (CBPCs). By using the acronyms CBC and CBPC, we avoid the debate over the words “cements” and “ceramics” as the last letter “C” will stand for either of them.

This definition of CBCs was established by Della Roy and Rustum Roy [6,20,21]. While Della Roy emphasized formation of modified conventional hydraulic cements, Rustum Roy used CBC to mean formation of more general ceramics made at room temperature by techniques such as ultrasonic signals in aqueous phosphate systems. We extend this generalization further to include all inorganic materials that are consolidated into a hard mass by chemical reactions and not by sintering.

Properties of CBCs lie between ceramics and cements. These materials are formed at room temperature like cements, or may be synthesized at slightly elevated temperatures, but their structure is highly crystalline or glass-crystalline composite. The particles in CBCs are bonded by a paste formed by chemical reaction, as in cements, but the particles themselves are mostly crystalline. Their strengths are higher than those of cements but fall short of sintered ceramics. Their corrosion resistance is close to ceramics, but at the same time, they may be vulnerable to erosion like cements. The ease of formation of these ceramics, their rapid setting behavior and low cost make them very attractive for the various applications discussed in this book.

1.6.

NATURE OF THE CHEMICAL BONDING IN CBCs

Whether in minerals or man-made materials, the chemical bonding in CBCs is at room or warm temperatures, and this aspect distinguishes them from conventional sintered ceramics. Most of the CBCs are formed in the presence of water, though Wilson and Nicholson [8] have discussed several nonaqueous cements. In many of the aqueous CBCs, water is bonded chemically within their structure, but in some cases water may be expelled during the reaction. In all cases, their formation is based on dissolution of individual components into an aqueous phase to form cations and appropriate anions. These ions react with each other to form neutral precipitates. If the rate of this reaction is controlled, then the reaction products will form network of connected particles and produce either well-ordered crystals or disordered structures. These CBCs comprise a composite of the crystallized and partly disordered structures.

Consider the case of formation of calcium carbonate in seawater. Seawater is rich in dissolved ions of calcium (Ca^{2+}) and carbonate (CO_3^{2-}) along with other ions that include magnesium (Mg^{2+}) and electrolytes such as sodium (Na^+). Under the right conditions, such as pH and temperature, the calcium and carbonate ions react to form calcium carbonate. Sea organisms provide these right conditions, though the mechanism of changing the pH of the seawater by these organisms is not exactly known. The changed conditions gradually precipitate calcium carbonate, which eventually forms sea shells, conches, and corals as homes of these organisms. In the accretion process, the right conditions are produced in the sea between two electrodes in which a small current deposits calcium on the cathode in the precipitated form of calcium carbonate.

These processes in a marine environment demonstrate that dissolution–precipitation is the basis for forming ceramics of calcium carbonate. This dissolution and recombination process is not limited to seawater. It also occurs in forming carbonate rocks where carbon dioxide (CO_2) dissolves in water to form carbonic acid (H_2CO_3), which reacts with oxides of calcium or magnesium to precipitate calcium or magnesium carbonates. This is nature's way of producing carbonate rocks. These reactions occur so slowly that they are difficult to reproduce in a laboratory environment; however, both calcium and magnesium oxides are slightly soluble in water, and carbonic acid can readily form when atmospheric

carbon dioxide dissolves in water. Thus, dissolution of the constituents plays a major role in these reactions.

Some silicate minerals are also formed in a similar manner. The process is very slow, slower than even carbonate formation, because of the very low solubility of silicate minerals. In clay minerals, or in lateritic soils, silicates dissolve very slowly to form an intermediate product, silicic acid (H_4SiO_4), which subsequently will react with other sparsely soluble compounds and form silicate bonding phases. Thus, a dissolution–precipitation process seems to be crucial to forming some silicate minerals.

Hardening of lateritic soils is a good example. The conditions in which these soils harden indicate that the dissolution–precipitation process may cause hardening. Lateritic soils are rich in alumina (Al_2O_3), silica (SiO_2), and iron oxide in the form of hematite (Fe_2O_3). None of these components dissolve easily in water. However, when they are in the form of very fine particles that are not crystallized, i.e., in amorphous powders, their surface area exposed to water will be large. A minor dissolution that would occur is sufficient for these particles to react with each other in water and precipitate them into products such as aluminosilicates or ferroaluminosilicates. The process is facilitated by the alternate wetting and drying that occurs in the annual tropical rain of the season and sunshine of the summer. Years of wetting–drying cycles will form sufficient crystallized reaction products on the surface of individual particles that will bind two adjacent particles and form a solidified product of laterites.

This process was exploited in binding Jamaican red mud [22]. Red mud is a residue resulting from Bayer process extraction of alumina from its mineral, viz., bauxite. Bauxite is also rich in iron oxide and hence is a typical laterite. Jamaican bauxite is, however, not very rich in silica. Thus, when alumina is extracted by its dissolution in caustic soda (NaOH), the residue left over is very rich in iron oxide. This residue also contains a considerable amount of dissolved caustic soda and dissolved residual alumina which cannot be separated further. Scanning electron micrographs of individual particles show a coating of very fine powdered material on the surface of these particles. This amorphous content is suspected to be alumina or of iron oxide. It is known that after repeated wetting and drying cycles at the banks of ponds, this red mud hardens into chunks. This phenomenon indicates that the amorphous alumina has reacted with whatever silica that exists in the red mud. The process may be accelerated by mixing red mud in a small amount of sodium silicate in a gel form. The high alkalinity of the red mud facilitates reaction between the silica from the sodium silicate solution and the amorphous alumina. This reaction produces aluminosilicates which bind the particles and consolidates the red mud. Upon drying, the red mud forms a solid of sufficient strength that it can be used as a conventional brick.

In hardened lateritic soils, the binding phase is so small that it cannot be isolated and identified. However, needle-shaped crystalline growth was found in silicate-bonded red mud [22]. Such direct evidence is not available for natural soils, but the fact that soils harden when they are rich in alumina after wetting and drying cycles suggests that the dissolution–precipitation phenomenon controls hardening of these lateritic soils.

There is evidence in the literature [14] of clay mineral forming in a laboratory environment. This is another example of CBC formation. Complex clay minerals such as montmorillonite $[(\text{Al},\text{Mg})_8(\text{Si}_4\text{O}_{10})_3(\text{OH})_{10}\cdot 12\text{H}_2\text{O}]$, chlorite $[(\text{Mg},\text{Fe})_3(\text{Si},\text{Al})_4\text{O}_{10}(\text{OH})_2\cdot (\text{Mg},\text{Fe})_3(\text{OH})_6]$, and serpentine $[\text{Mg}_3\text{Si}_2\text{O}_5(\text{OH})_4]$ have been synthesized in

the laboratory at room temperature by employing slow reactions that involve dilute solutions or suspensions of the corresponding oxides or hydroxides. Hardening of these oxides into clay minerals is an excellent example of chemical bonding.

In nature, dissolution caused by carbonic and silicic acids is a slow process. Because formation of carbonate and silicate complexes is very slow and mostly occurs on a geological time scale, it is difficult to reproduce the necessary reactions in the laboratory. On the other hand, acid–base cements may be produced within hours, and controlling the rate of reaction in these materials is easier than accelerating reactions in carbonate and silicate minerals. Acid–base cements have considerable potential for commercial applications by exploiting the solubility of cation donors of oxides in acidic solutions. For this reason, we next explore the dissolution steps involved in formation of these cements in more detail.

1.7.

ROLE OF SOLUBILITY IN CHEMICAL BONDING

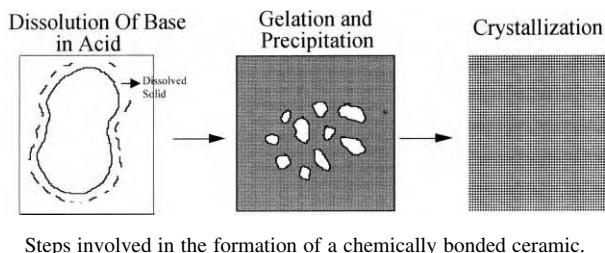
Wilson and Nicholson [8] have summarized the necessary steps that form acid–base cements:

- (a) dissolution of bases in a anion-rich acid solution that forms cations,
- (b) interaction of the cations and anions in the solution to form neutral complexes,
- (c) gelation of these complexes and saturation of the solution with these complexes, and
- (d) precipitation of solids from the saturated gel solution that form a connected network as crystalline, semicrystalline, or disordered solids.

To form a CBC, control over the dissolution of the bases is crucial. The bases that form acid–base cements are sparsely soluble, i.e., they dissolve slowly in a small fraction. On the other hand, acids are inherently soluble species. Typically, a solution of the acid is formed first, in which the bases dissolve slowly. The dissolved species then react to form the gel. When the gel crystallizes, it forms a solid in the form of a ceramic or a cement. Crystallization of these gels is inherently slow. Therefore, bases that dissolve too fast will rapidly saturate the solution with reaction products. Rapid formation of the reaction products will result in precipitates and will not form well ordered or partially ordered coherent structures. If, on the other hand, the bases dissolve too slowly, formation of the reaction products will be too slow and, hence, formation of the gel and its saturation in the solution will take a long time. Such a solution needs to be kept undisturbed for long periods to allow uninterrupted crystal growth. For this reason, the dissolution rate of the base is the controlling factor for formation of a coherent structure and a solid product. Bases should neither be highly soluble nor almost insoluble. Sparsely soluble bases appear to be ideal for forming the acid–base cements.

For acid–base cements, the dissolution of the bases in the acid solution is always partial and never complete. In most cases, saturation of the gel is accomplished even before all the basic material is dissolved. Partial dissolution of individual particles of the base and the subsequent reaction of the dissolved component with the anions saturate the solution with the gel that produces crystals of the reaction products on the surface of the remaining part

Fig. 1.4.



of the base particles and connects them. Subsequently, a ceramic or cement structure is formed. The process is illustrated in Fig. 1.4.

In the case of minerals, the process is slightly different. Particles of minerals that come in contact with water dissolve partially. If these particles are sufficiently close, subsequent recrystallization bridges and binds them. Thus, the binding phase is very small in the entire consolidated product. As a result, identifying this binding phase by means of an analytical technique is difficult. The ability to detect such a binding phase could resolve the controversy over whether ancient Egyptians were or were not the first to conceive the idea of chemically bonding Nile silt to form the rocks on the top of pyramids [23].

If the entire matrix is converted to a binding phase in CBCs, no nuclei for crystallization will remain and the precipitated product will result in a glassy disordered structure that may not have sufficient strength. Thus, the binding phases should be formed only on the surface of the base particles, and chemical conversion of the components should be only partial. The unreacted particles will then form a second phase that will provide rigidity to the matrix. That is the structure an ideal CBC will have.

Overall, this review of minerals and acid–base cements provides insight into formation of CBCs in which control over dissolution of at least one of the participating components is crucial to formation of the ceramic. For this reason, a considerable part of this book is invested in describing the dissolution chemistry of oxides that form CBPCs.

REFERENCES

1. F.P. Glasser, "Cements from micro to macrostructures," *Ceram. Trans. J.*, **89** [6] (1990) 195–202.
2. K. Scrivener and A. Capmas, Calcium Aluminate Cements, in *Lea's Chemistry of Cement and Concrete*, ed. P. Hewlett (John Wiley and Sons, New York, 1998), pp. 709–778.
3. J. Birchall, A. Howard, and K. Kendall, "Flexural strength and porosity of cements," *Nature*, **289** (1981) 388–389.
4. D. Smith, *Cementing*, vol. 4, (Society of Petroleum Engineers, New York, 1990).
5. E.W. McDaniel and D.B. Delzer, "FUETAP concrete," in *Radioactive Waste Forms for the Future*, eds. W. Lutze and R.C. Ewing (Elsevier, New York, 1988), pp. 565–588, Chapter 9.
6. D. Roy, "New strong cement materials: chemically bonded ceramics," *Science*, **235** (1987) 651–658.
7. J. Davidovits, "Recent progress in concretes for nuclear waste and uranium waste containment," *J. Concr. Int.*, **16** [12] (1994) 53–58.
8. A.D. Wilson and J.W. Nicholson, *Acid–Base Cements* (Cambridge University Press, Cambridge, 1993).

9. D.C. Smith, "A new dental cement," *Br. Dent. J.*, **125** (1968) 381–384.
10. A.D. Wilson and B.E. Kent, "The glass-ionomer cement: a new translucent cement for dentistry," *J. Appl. Chem. Biotech.*, **21** (1971) 313.
11. A.D. Wilson and J. Ellis, Poly-vinylphosphonic acid and metal oxide or cermet or glass-ionomer cements, US Patent 5,079,277, (1992).
12. J. Ellis and A.D. Wilson, "Polyphosphonate cements: a new class of dental materials," *J. Mater. Sci. Lett.*, **9** (1990) 1058–1060.
13. A.S. Wagh, D. Singh, and S.Y. Jeong, *Chemically bonded phosphate ceramics for stabilization and solidification of mixed wastes*, Hazardous and Radioactive Waste Treatment Technologies Handbook (CRC Press, Boca Raton, FL, 2001), pp. 6.3.1–6.3.18.
14. K.B. Krauskoff, *Introduction to Geochemistry* (McGraw-Hill Book Co., New York, 1967).
15. M. McNeil, "Lateritic Soils," *Sci. Am.*, **221** [5] (1964) 96–102.
16. E. Toelles, E. Kimbro, F. Webster, and W. Ginell, *Seismic Stabilization of Historic Adobe Structures* (Getty Conservation Institute, Los Angeles, 2000).
17. A. Turnbull, "Ocean-grown homes," in *Popular Mechanics*, September 1997, <http://www.popularmechanics.com/popmech/sci/9709STRSM.html>.
18. W.H. Hilbertz and T. Goreau, Method of enhancing the growth of aquatic organisms, and structures thereby, US Patent 5,543,034, (1996).
19. Key Largo Undersea Park, Key Largo, FL.
20. R. Roy, D.K. Agarwal, and V. Srikanth, "Acoustic wave stimulation of low temperature ceramic reactions: the system $\text{Al}_2\text{O}_3\text{--P}_2\text{O}_5\text{--H}_2\text{O}$," *J. Mater. Res.*, **6** [11] (1991) 2412–2416.
21. T. Simonton, R. Roy, S. Komarneni, and E. Brevel, "Microstructure and mechanical properties of synthetic opal: a chemically bonded ceramic," *J. Mater. Res.*, **1** [5] (1986) 667–674.
22. A.S. Wagh and V. Douse, "Silicate-bonded unsintered ceramics of Bayer process muds," *J. Mater. Res.*, **6** [5] (1991) 1094–1102.
23. J. Davidovits, *The Pyramids—An Enigma Solved* (Hippocrene Books, New York, 1988).

This page is intentionally left blank

Chemically Bonded Phosphate Ceramics

Chemically bonded phosphate ceramics (CBPCs) were discovered and developed as dental cements in the 19th century. This development effort was focused mainly on cements of zinc phosphate. Some silicophosphates were also developed as dental cements. Starting in 1970, magnesium phosphate ceramics have been investigated as structural materials, the main work in this area resulting from fundamental investigations conducted at Brookhaven National Laboratory (BNL) in the United States. Aluminum phosphate was a part of many of these CBPCs, though it did not find niche applications. Some cursory work was also done on iron and copper phosphates, which also did not trickle down to any practical applications. In the 1990s, Argonne National Laboratory developed CBPCs for radioactive and hazardous waste management; the main advance in this area was in the use of magnesium phosphate ceramics. Once formulated for waste management, these ceramics have also found application in structural materials. The birth and growth of CBPCs are reviewed in this chapter.

2.1.

REVIEW ON PHOSPHATE-BONDED CERAMICS AND CEMENTS

A quick review of literature on phosphate cements and ceramics indicates that very little attention has been paid to CBPCs, and a large opportunity exists in developing practical applications of these materials. Westman [1] conducted the first review of work done during 1918–1973 on phosphate ceramic and cement materials. This review appeared in *Ceramic Abstracts* in 1977. He concluded that only 7% of the total number of articles on cements, lime and mortars were on phosphate-bonded materials and also found only one

Table 2.1.

Results of the Literature Search from Ceramic Abstracts.

Years of ceramic abstracts searched	1988–2002
Total number of articles found relevant to phosphate ceramics	2264
Articles in biomaterials and dental cements	68.0%
Structural materials	5.6%
Refractory materials	12.6%
Material structure, properties, etc.	13.9%

reference on phosphate-bonded structural clay products [2]. These references themselves were not all on CBPCs; some were related to the use of phosphates as flocculants and for other purposes. Following the Westman review, Kanazawa [2] conducted a literature survey of the articles that appeared in *Ceramic Abstracts* between the years 1974 and 1987 on phosphate ceramic materials. He concluded that there were only 35 articles on the phosphate-bonded structural products among 874 total articles on phosphates. Not all the articles on structural products dealt with room-temperature-setting phosphates; some were on phosphate ceramics made at elevated temperatures.

Following these two surveys, we conducted a literature review based upon *Ceramic Abstracts* for the years 1988–2002. The results are summarized in Table 2.1. The results presented in Table 2.1 indicate that there has been a significant increase in the literature on CBPCs in recent years. The major thrust of the research has been in biomaterials and dental cements. Though small in number, there have been several articles in structural materials applications, which also include oil well cements. Interest in conventional refractory materials has continued, and as expected, all the applications have been supported by research in materials structure and properties of the CBPCs.

The survey, presented above, however, does not present the full picture of the recent research in the CBPC area. The Abstracts have not covered many modern CBPC applications such as those in radioactive and hazardous waste management. The purpose behind writing this monograph is to cover such areas in which CBPCs have made major inroads. In the process, we have built a discussion on the foundation of basic science and technology behind formation of these materials. We, therefore, hope that this monograph will be a comprehensive source for a wide readership interested in the science of CBPC materials and their applications.

2.2.

REVIEW ON PHOSPHATE-BONDED DENTAL CEMENTS

Wilson and Nicholson [3] give an extensive overview of dental cements in their book. Because such an excellent review already exists, we will only provide milestones in the development of dental phosphate cements and will add other developments that were not covered in the earlier review.

The birth of CBPCs goes back to the discovery of zinc phosphate dental cement in the late 19th century and beginning of the last century [4–11]. Rostaing's patents [4] and Rollins' article [5] are the first documents that provide formulations in which zinc oxide is reacted with phosphoric acid to produce dental cements. Much of the following research are involved in finding ways to retard the fierce reaction between these components so that practical cements could be developed. Calcination of zinc oxide and partial neutralization of phosphoric acid with zinc and/or aluminum hydroxide were recognized as the best methods to retard the chemical reaction. Combination of these two methods gave some good dental cements [12,13] with sufficient time for the dentist to mix and apply them.

The resulting phases in these cements are crystalline. Formation of major phases depends on time of curing and presence of water during curing and is also influenced by other components, such as aluminum oxide, in the mixture. However, in simple systems of zinc oxide and phosphoric acid solutions, investigations revealed formation of partially soluble zinc hydrophosphates [$\text{Zn}(\text{H}_2\text{PO}_4)_2 \cdot 2\text{H}_2\text{O}$, and $\text{ZnHPO}_4 \cdot 3\text{H}_2\text{O}$] that gradually converted to hopeite [$\text{Zn}_3(\text{PO}_4)_2 \cdot 4\text{H}_2\text{O}$] [14–20].

The aluminum in the zinc phosphate cements was considered very important. van Dalen [21] recognized its importance first. The reaction of zinc oxide and phosphoric acid was greatly moderated by aluminum. This effect was attributed to formation of an aluminum phosphate gelatinous coating on zinc oxide particles. In fact, Wilson and Nicholson believe that the gelatinous substance may even be zinc aluminophosphate phase [3], which subsequently crystallizes into hopeite and aluminophosphate amorphous gel ($\text{AlPO}_4 \cdot n\text{H}_2\text{O}$).

The resulting zinc phosphate cement in such formulations is an opaque solid that consists of excess zinc oxide coated and bonded by, possibly, aluminum phosphate and zinc phosphate gels. The cement is porous and permeable to dyes [22]. The resulting cement, in spite of this porosity, has high compressive and tensile strengths, 70–131 (10,000–18,600 psi) and 4.3–8.3 MPa (600–1186 psi), respectively. These values are several times higher than the corresponding strengths of conventional cements; for example, Portland cement has compressive and tensile strengths of only ≈ 30 and 1 MPa, respectively.

In parallel to the work on zinc phosphate cements, "porcelain" dental cements also were developed. Steenbock [23] was the first to produce silicophosphate dental cement using 50 wt% concentrated phosphoric acid solution and an aluminosilicate glass. Schoenbeck [24] introduced fluoride fluxes in these glasses and vastly improved the dental cements. Fluorides lower the temperature of fusion of the glasses used in forming these cements. The same fluorides impart better translucency to the cement, and have some therapeutic effects. As a result, fluorides have become a part of modern dental cements.

Wilson *et al.* [25] analyzed various brands of commercial cements and specified their possible composition, properties, and microstructure. Wilson *et al.* report the most representative and comprehensive data on commercial porcelain dental cements. These cements consist of powdered alumina–lime–silica glass mixed with phosphoric acid that formed a hard and translucent product. The starter glass powder consists of 31.5–41.6 wt% silica, 27.2–29.1 wt% alumina, 7.7–9.0 wt% calcium oxide, 7.7–11.2 wt% sodium oxide, 13.3–22 wt% fluorine and small amounts of phosphorous and zinc oxides. Often very small amounts of magnesium and strontium oxides are also present.

The phosphoric acid is partially neutralized by aluminum and zinc oxides. Wilson's detailed analysis led to the following general conclusions on these cements:

1. They consist of original glass particles bonded by reaction products. Unlike zinc phosphate cements, they show no evidence of a crystalline structure and contain mainly glassy phases. As in the case of zinc phosphate cement, however, only a small amount of original glass reacts to form the bonding phases, and much of the glass remains unreacted and becomes part of the product.
2. The setting time depends on the extent of dilution of the phosphoric acid. Up to ≈ 70 wt% concentrated acid gives a faster setting time of < 5 min, while lower concentrations exponentially increases the setting time. A certain amount of water, however, is necessary for good reaction and gain-in-strength. Best strength (compressive) is obtained when the phosphoric acid is diluted to 50 wt%. This strength ranges from 220 to 325 MPa, and the setting time is as less as 3 min to a maximum of 24 min.
3. Stronger cements seem to contain more crystallites in the bonding phases than weaker cements, indicating that crystallization is the key for the formation of better cements.

These cements are formed by a similar process to the silicate minerals described in Chapter 1, the difference being the rate. Silicate minerals are formed at a rate lower by orders of magnitude compared with dental cements. In the case of dental cements, the phosphoric acid releases protons in the solution and lowers its pH. This decomposes the glass and releases silicon in the solution, and silicic acid forms as an intermediate product [26,27]. Simultaneously, cations such as Al^{3+} , Ca^{2+} , and Na^+ and the anion F^- are also released [28]. The cations and anions are attracted to each other, and neutral bonding phases form. Such a bonding network, especially that of aluminum, results in gelation and subsequent polymerization of a hard product.

Wilson and Kent [28] followed the precipitation of individual ions in the solution and showed that aluminum and calcium precipitate within the setting time of 5 min after the slurry is mixed. Zinc precipitation takes longer, about 30 min, while sodium and fluorine do not precipitate completely. These observations imply that aluminum and calcium are responsible for the early strength of the cement, while zinc provides gradual increase in strength. As the setting could take place even over a year [28,29], one could assume that the strengthening is a continuing process in such cements.

These cements attain an ultimate compressive strength of 255 MPa (36,500 psi), which is probably the highest strength achieved by any purely inorganic cement. Wilson and Nicholson [3] also reviewed other properties of these cements. Overall, these cements have a flexural strength of 24.5 MPa (3500 psi), a tensile strength of 13.6 MPa (2000 psi), a fracture toughness of $0.12\text{--}0.3 \text{ MPa}\cdot\text{m}^{1/2}$, and a disintegration of 0.34–3.8%. The weakest property is the fracture toughness, which indicates that this cement is very brittle. Also the disintegration, especially in an acid medium at a pH of 4, is high. The advantage of these cements, however, is that their translucency and color can be matched with tooth enamel. Because of these two properties, these cements have been mostly used for restoring front teeth.

Another dental cement is zinc silicophosphate, a mixture of zinc phosphate and silicophosphate described above [30]. Cation-releasing powder is formed by mixing

aluminosilicate glass and zinc oxide. Its properties lie between those of zinc phosphate and silicate cements. For example, the compressive strength is 101–171 MPa (14.3–24.4 psi) [31], less than that of silicate cement, but higher than that of zinc phosphate cement. Its main advantage, however, is sustained release of fluorine, which is invaluable in dentistry [32]. This fluorine is absorbed by the tooth enamel and, hence, is protected from caries-producing debris and plaque.

Other silicophosphate cements that use cation-releasing silicates are based on wollastonite [33], and serpentinite [34,35]. Naturally occurring phosphate cements have also been known [36]. In these cements, silicates are sparsely soluble and release cations (Ca^{2+} , and Mg^{2+}), which react with the phosphate anions to form hydrophosphates and eventually convert to phosphates. This process is similar to that involving zinc phosphate cements, in which hydrophosphates form first, then convert to phosphates during aging.

2.3.

MAGNESIUM PHOSPHATE CERAMICS

Unlike silicophosphate cements, magnesium phosphates are highly crystalline, and hence they may be appropriately called room-temperature-setting ceramics rather than cements. Various magnesium-phosphate-based ceramics were developed for use in structural materials during the second half of the last century. These include magnesium ammonium phosphate ceramic grout for rapid repair of roads in cold regions, and for repair of industrial floors and airport runways [37], and magnesium potassium phosphate ceramics for stabilization and solidification of low-level radioactive and hazardous wastes [38]. A few commercial products have also appeared on the American and European markets.

Magnesium-phosphate-based ceramics were discovered first during 1939–1940 by Prosen [39,40] and Earnshaw [41,42] as investment materials for casting alloys. Several patents have been also issued in Europe and the U.S. on similar materials [43–46], in which magnesium oxide is reacted with phosphoric acid or with a source of phosphorous pentoxide (P_2O_5). However, the resulting products set very rapidly and thus allow very little working time. In addition, they are water soluble and hence not practical for structural material applications [47]. They form water-soluble magnesium dihydrogen phosphate $[\text{Mg}(\text{H}_2\text{PO}_4)_2 \cdot n \text{H}_2\text{O}]$ as a reaction product. Practical ceramics with very low solubility can be formed by an additional cation provided as a soluble phosphate. This cation replaces the hydrogen in the $\text{Mg}(\text{H}_2\text{PO}_4)_2$ part of the compound. Salts such as ammonium mono- or di-hydrogen phosphate [48,49], ammonium polyphosphate [50], aluminum hydrophosphate [47–51], sodium polyphosphate [52], or potassium dihydrogen phosphate [38] provide the necessary additional cation.

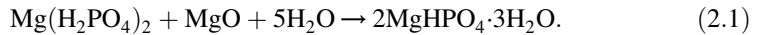
As discussed earlier, ceramic is formed by the reaction of calcined magnesium oxide (MgO) with a solution of phosphoric acid or an acid phosphate in these products. The quick-setting reaction results in products similar to those found in zinc phosphate ceramics. The major products can be represented by the formula, $\text{Mg}(\text{X}_2\text{PO}_4)_2 \cdot n \text{H}_2\text{O}$ or $\text{MgXPO}_4 \cdot n \text{H}_2\text{O}$, where X is hydrogen (H), ammonium (NH_4), sodium (Na), or potassium (K). The reaction products are listed in Table 2.2.

Table 2.2.

Phases found in magnesium phosphate ceramics

Formula	Name	Reference
$\text{Mg}(\text{H}_2\text{PO}_4)_2 \cdot 2\text{H}_2\text{O}$	Magnesium dihydrogen phosphate	[52]
$\text{Mg}(\text{H}_2\text{PO}_4)_2 \cdot 4\text{H}_2\text{O}$	Magnesium dihydrogen phosphate	[52]
$\text{MgHPO}_4 \cdot 3\text{H}_2\text{O}$	Newberyite	[53]
$\text{MgHPO}_4 \cdot \text{H}_2\text{O}$, $\text{MgHPO}_4 \cdot 2\text{H}_2\text{O}$	Haysite	[54]
$\text{Mg}(\text{NH}_4\text{HPO}_4)_2 \cdot 4\text{H}_2\text{O}$	Schertelite	[55–58]
$\text{MgNH}_4\text{PO}_4 \cdot 4\text{H}_2\text{O}$	Struvite	[55–58]
$\text{MgNH}_4\text{PO}_4 \cdot \text{H}_2\text{O}$	Dittmarite	[55–58]
$\text{MgK}(\text{PO}_4)_2 \cdot 6\text{H}_2\text{O}$	Magnesium potassium phosphate	[37]
$\text{Mg}_3(\text{PO}_4)_2 \cdot 4\text{H}_2\text{O}$	Magnesium phosphate	[48]

Among the phases listed in Table 2.2, newberyite, struvite, magnesium potassium phosphate, and magnesium phosphate are the most stable. The first two phases in Table 2.2 are water soluble [47]. They are formed when magnesium oxide is reacted directly with phosphoric acid. If, however, this reaction is retarded by using a small amount of boric acid (< 1 wt% of MgO), these phases convert to more insoluble newberyite during curing of the ceramics. The conversion may be represented by the reaction:



Such curing reactions are very common in these ceramics. For example, Abdelrazig and coworkers [54–56] showed that struvite formation in magnesium ammonium phosphate ceramics occurs in a stepwise fashion. Initially, schertelite is formed, but as the curing continues, reaction of schertelite with excess MgO results in struvite and dittmarite formation. If sufficient water is available, then the reaction continues to form hexahydrate struvite. These reactions indicate that curing produces phases that are most stable in a given composition, and availability of excess MgO and water governs the composition of the final product. Sarkar [59,60] also arrived at similar conclusions.

Newberyite has been found to be the most stable phase in ceramics formed by the reaction of MgO and $\text{Al}(\text{H}_2\text{PO}_4)_3$. Detailed study by Finch and Sharp [47] showed that the newberyite content is a maximum, when the ratio of $\text{MgO} : \text{Al}(\text{H}_2\text{PO}_4)_3$ is 4 : 1. Interestingly, these investigators did not detect any phases containing both Mg and Al, such as $\text{Al}(\text{MgPO}_4)_3$, but Al always formed $\text{AlPO}_4 \cdot n\text{H}_2\text{O}$. Because AlPO_4 is one of the most thermodynamically stable phases, its formation is preferred over other phosphates of Al.

In the case of reaction of MgO with KH_2PO_4 , the product is invariably $\text{MgKPO}_4 \cdot 6\text{H}_2\text{O}$. No evidence of newberyite has been found. If, however, H_3PO_4 is neutralized partially with K_2CO_3 , and then reacted with MgO, one finds the coexistence of newberyite and $\text{MgKPO}_4 \cdot 6\text{H}_2\text{O}$ [61]. In the first case, a stoichiometric amount of MgO and KH_2PO_4 is used and forms the most stable phase of $\text{MgKPO}_4 \cdot 6\text{H}_2\text{O}$. In the second case, available K is consumed in forming $\text{MgKPO}_4 \cdot 6\text{H}_2\text{O}$, and additional MgO reacts with available H_3PO_4 to form newberyite.

These observations with a range of magnesium phosphate ceramics suggest the following guiding principle for forming most stable ceramics:

Among all possible reaction products, a given composition will form the most stable phases during curing through intermediate steps of less stable phases.

We will explore this principle in more detail in Chapters 4–6 on the basis of the dissolution characteristics of the reaction products and their thermodynamic stability.

As was discussed in Chapter 1, the common feature of these ceramics is that a portion of the MgO always remains unreacted. When MgO dissolves and reacts with the acidic solution, the dissolution and subsequent reaction occur on the particle surface of MgO. The reaction produces a protective coating of less soluble products on the particle surface that inhibits the reaction of the acid solution from the core of individual MgO particles. Prevalence of unreacted MgO, in fact, is good for the overall strength and integrity of the ceramic because unreacted MgO can act as a second phase that will resist crack propagation within the ceramic and improve its fracture toughness.

2.4.

GENERALIZATION OF FORMATION OF CBPCs

As early as 1950, Kingery [62] explored formation of generalized CBPCs by reacting phosphoric acid solution with different cation donor oxides. He performed this study in order to identify reactions that may lead to CBPCs as precursors to refractories. He determined, in each case, whether the reaction sets into a ceramic, and if it does, what is the setting time and maximum temperature on a 0.5 cm^3 sample. Using the X-ray diffraction technique, he also tried to identify the phases in the set ceramic.

Kingery's work demonstrated that the formation of CBPCs is not limited to the reaction between phosphoric acid and MgO or ZnO, but may include most other metal oxides. In all the cases that formed a ceramic, the reaction products were either mono- or dihydrogen phosphates of the respective oxides. With certain metal oxides, the products were anhydrous, and the reaction products did not set into a ceramic. For example, mercury (Hg) and lead (Pb) formed $\text{Hg}_3(\text{PO}_4)_2$ and $\text{Pb}_3(\text{PO}_4)_2$, respectively, as precipitates and did not consolidate into a solid. Furthermore, formation of a ceramic depended on the valence of the oxide used. In the case of Pb, instead of PbO or PbO_2 , Kingery used Pb_3O_4 , and formed $\text{Pb}(\text{H}_2\text{PO}_4)_4$ that set into a solid form.

Other investigators besides Kingery also attempted to form ceramics of oxides other than those of Mg and Zn. For example, Fedorov *et al.* [63] used a mixture of copper oxide (CuO) and metallic copper and developed a bonding agent for metals. They also cite formation of phosphate glues with ZrO_2 and CaZrO_3 in combination with Ni, Cr, and Ti. These studies differ from Kingery's or any other work discussed earlier because a metal component always participates in the reaction. The effect of the metals on the reaction kinetics will be discussed in Chapter 7.

We have already discussed use of silicates as cation donors in forming CBPCs. In a manner similar to use of silicates, Sychev *et al.* [64], and Sudakas *et al.* [65] showed that

slightly soluble magnesium titanates (Mg_2TiO_4 , MgTiO_3 , and $\text{Mg}_2\text{Ti}_2\text{O}_5$) also form CBPCs. In these cases, the bonding phase is again newberyite. These studies imply that compounds that are slightly soluble and provide cations in solution to form these ceramics.

Much of the work reported in the literature concerns formation of ceramics with divalent metal oxides or their compounds. Except for Kingery [62], few have attempted to synthesize room-temperature-setting ceramics using trivalent and quadrivalent oxides. Kingery claims formation of ceramics using $\text{Al}_2\text{O}_3 \cdot x\text{H}_2\text{O}$, Pb_3O_4 , $\text{Cr}_2\text{O}_3 \cdot x\text{H}_2\text{O}$, Fe_2O_3 , Fe_3O_4 , La_2O_3 , Y_2O_3 , $\text{Ti}(\text{OH})_4$, ThO_2 , and V_2O_5 . Some work by Russians [66,67] and by Wagh *et al.* [68,69] also demonstrated that ceramics may be formed by reacting Fe_3O_4 with phosphoric acid. The resulting products in each case are hydrophosphates. Some of those reaction products found by Kingery, such as $\text{Al}(\text{H}_2\text{PO}_4)_3$, are water soluble. In addition, some may contain amorphous products that are water soluble and may not be detectable by techniques such as X-ray diffraction. Thus, Kingery's limited study, though very useful, does not ensure formation of practical insoluble ceramics. It, however, demonstrates that a generalized approach to formation of ceramics is possible, a wider range of ceramics may be formed provided their kinetics of formation is better understood.

2.5.

SUMMARY OF LITERATURE SURVEY

The literature reviewed in this chapter reveals several common guiding features for further study of CBPCs. These are listed below:

1. Concentrated phosphoric acid and a metal oxide do not seem to form a ceramic. The reaction product is crystalline, but a precipitate.
2. When a partially neutralized phosphoric acid solution is reacted with a metal oxide, a ceramic formed with a reaction product $\text{M}_x\text{B}_y(\text{PO}_4)_{(x+y)/3}$, where M stands for a metal, and B can be hydrogen (H) or another metal such as aluminum (Al). The phosphoric acid in these reactions is partially neutralized by dilution or by reaction of an oxide of B.
3. If B is hydrogen, and $y > 1$, generally the product is soluble in water, and hence the product by itself can be reacted with an oxide of M, and a less soluble ceramic can be formed.
4. In most CBPC products, M is a divalent metal, though limited studies have been reported with tri- and four-valent metal oxides. Ceramics of Mg and Zn have been extensively developed. If M is a monovalent metal, it leads to soluble reaction products and cannot be used to form a ceramic. However, B can be a monovalent metal, when M is either divalent or has valency > 2 .
5. Silicates and other minerals such as titanates containing divalent metals have been used in place of oxides. Silicates provide a translucent structure to the product. Aluminum also gives a denser and stronger structure.

These observations imply that, forming a phosphate ceramic requires either diluted phosphoric acid or a partially neutralized phosphate solution as a source of anions, and a sparsely soluble (slightly soluble) oxide or a mineral to provide cations. All ceramics are formed in an aqueous solution. In general, the following scheme seems to work best.

Phosphoric acid may be diluted with water. This step provides the water fraction needed to form the ceramic. Monovalent alkali metal oxides, with their high aqueous solubility, may be used for partial neutralization of the acid, while sparsely soluble divalent oxides are good candidates for providing the cations. In particular, oxides of Mg, Ca, and Zn are preferred because they are inexpensive compared to similar oxides, and unlike oxides of Pb, Cr, Cd, Hg, and Ni, they are not environmentally hazardous (see Chapter 16).

Aluminum oxide is the only trivalent oxide that has been used to form a ceramic; some heat treatment is needed. Kingery claims to have observed a setting reaction between trivalent iron oxide and phosphoric acid, but this reaction may have been caused by traces of magnetite in the trivalent oxide. Pure trivalent iron oxide such as hematite (Fe_2O_3) does not react with phosphoric acid. Overall, trivalent metal oxides have a solubility that is only marginal and falls below that of even sparsely soluble divalent oxides, while the solubility of oxides of most quadrivalent metals (zirconium is an exception) is too low to form a ceramic.

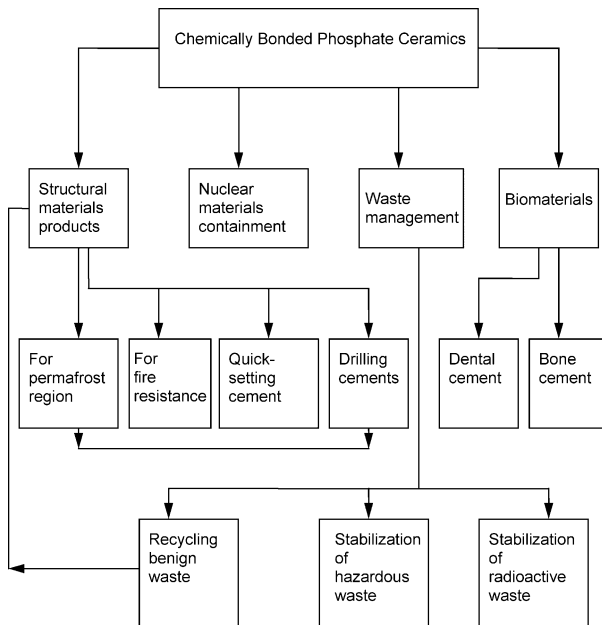
Overall the cation donors remain the key parameter in determining formation of the ceramics in a diluted or partially neutralized phosphate solution. For this reason, Chapters 4–6 are devoted to a dissolution model for the formation of these ceramics. In Chapters 9–13, this model will then be used to discuss formation of ceramics from common oxides.

2.6.

APPLICATIONS OF CBPCs

Though much of the earlier work on CBPCs is focused on Zn and Mg ceramics for use as dental cements or as rapid-setting cements, a very wide range of applications of CBPCs has been realized in recent years. Figure 2.1 gives an overview of these applications. These include use of these ceramics for: (1) waste management applications [37], such as stabilization and solidification of radioactive and hazardous wastes, (2) recycling of benign wastes such as coal ashes [69] and mineral wastes in producing construction products, (3) oil field cements, and (4) dental materials. The CBPCs are most suitable for applications in the waste management area. The phosphate reactions convert most of the hazardous contaminants and fission products into nonleachable phosphate reaction products, and the phosphate ceramic itself encapsulates these insoluble reaction products, as well as the most insoluble oxides of transuranic elements into a dense and durable matrix. Chapters 16 and 17 include extensive discussion on these topics. CBPCs exhibit properties between conventional cements and sintered ceramics. Their strengths are generally higher and their stability in acidic aqueous environment is much better than those of conventional cements. In addition, CBPCs

Fig. 2.1.



Potential applications of CBPCs.

have the ability to incorporate a very large amount of benign waste, such as fly ash and mineral wastes in forming these products. Using them as nonflammable adhesives to replace flammable polymers such as urea formaldehyde, one can develop nonflammable and less expensive particle boards that can be formed without worry about release of volatile organic compounds into the atmosphere. For this reason, they are being considered for a wide range of applications in construction industry (see Chapter 14). Because of their superior mechanical properties and their ability to bind rocks and other earth materials, and unlike conventional cements, they set even in the presence of hydrocarbons; they are thus being considered as drilling cements in oil fields. Chapter 15 covers these applications. Since these materials are phosphates and compatible with bones, they have applications as dental cements and biomaterials, as discussed in Chapter 18.

Development of superior CBPC products for the wide-ranging applications shown in Fig. 2.1 requires a fundamental understanding of their kinetics of formation and their properties. This topic is extensively addressed in Chapters 4–6. The dissolution model described in these chapters also helps in understanding the role of individual components in formation of ceramics and the end performance of the ceramics. In addition, the dissolution model explains how hazardous and radioactive components are stabilized in a phosphate matrix. The stabilization mechanisms are discussed in Chapters 16 and 17.

REFERENCES

1. A.E.R. Westman, *Phosphate ceramics*, Topics in Phosphorus Chemistry, vol. **9**. (Wiley, New York, 1977), pp. 231–381.
2. *Inorganic Phosphate Materials*, ed. T. Kanazawa (Elsevier, New York, 1989), pp. 1–8.
3. A.D. Wilson and J.W. Nicholson, *Acid–Base Cements* (Cambridge Univ. Press, Cambridge, 1993).
4. C.S. Roastaing di Rostagni, Verfahren zur darstellung von kitten für zahnärztliche und ähnliche zwecke, bestehend von gemischen von pyrophosphaten des calciums oder bariums mit den pyrophospheten des zinks oder magneiums. German Patent 6015 (Berlin) (1878). Also in *Correspondenz-Blatt für Zahnärzte* 10 (1881) 67–69.
5. W.H. Rollins, “A contribution to the knowledge of cements,” *Dent. Cosmos*, **21** (1979) 574–576.
6. E.S. Gaylord, “Oxyphosphates of zinc,” *Arch. Dent.*, **33** (1989) 364–380.
7. W.B. Ames, “Oxyphosphates,” *Dent. Cosmos*, **35** (1893) 869–875.
8. H. Fleck, “Chemistry of oxyphosphates,” *Dent. Items Interest*, **24** (1902) 906.
9. W. Souder and G.C. Paffenbarger, *Physical Properties of Dental Materials* (Natl Bur. Standards (U.S.), Gaithersburg, MD, 1942), Circ. No. C433.
10. W.S. Crowell, “Physical chemistry of dental cements,” *J. Am. Dent. Assoc.*, **14** (1927) 1030–1048.
11. E.W. Skinner, *Science of Dental Materials*, 3rd ed. (W.B. Saunders Co., Philadelphia, 1947).
12. N.E. Eberly, C.V. Gross, and W.S. Crowell, “System zinc oxide, phosphorous pentoxide, and water at 25° and 37°,” *J. Am. Chem. Soc.*, **42** (1920) 1433.
13. G.C. Paffenbarger, S.J. Sweeney, and A. Isaacs, “A preliminary report on zinc phosphate cements,” *J. Am. Dent. Assoc.*, **20** (1933) 1960–1982.
14. A.B. Wilson, G. Abel, and B.G. Lewis, “The solubility and disintegration test for zinc phosphate dental cements,” *Br. Dent. J.*, **137** (1974) 313–317.
15. W.S. Crowell, “Physical chemistry of dental cements,” *J. Am. Dent. Assoc.*, **14** (1929) 1030–1048.
16. B.W. Darwell, “Aspects of chemistry of zinc phosphate cements,” *Aust. Dent. J.*, **29** (1984) 242–244.
17. F. Halla and A. Kutzeilnigg, “Zur kennetnis des zinkphosphatzements,” *Z. Für Stomatol.*, **31** (1933) 177–181.
18. D.F. Vieira and P.A. De Arujo, “Estudo a cristizacao de cemento de fostato de zinco,” *Rev. Faculdade Odontol. Univ. São Paolo*, **1** (1963) 127–131.
19. J. Komarska and V. Satava, “Die chemischen prozasse bei der abbinding von zinkphosphatzementen,” *Deutsche Zahnärztliche Z.*, **25** (1970) 914–921.
20. A.D. Wilson, ed. J.A. von Fraunhofer, *Zinc Oxide Dental Cements*, vol. **5**. (Butterworths, Boston, 1975), Chapter 5.
21. E. van Dalen, Oriënteerende onderzoekingen over tandcementen, Thesis, Delft Univ., Netherlands (1933).
22. P.J. Wisth, “The ability of zinc phosphate and hydrophosphate cements to seal space bands,” *Angle Orthod.*, **42** (1972) 395–398.
23. P. Steenbock, Improvements in and relating to the manufacture of a material designed to the production of cement, British Patent 15,181, 1904.
24. F. Schoenbeck, Process for the production of tooth cement, US Patent 897,160, 1908.
25. A.D. Wilson, B.E. Kent, D. Clinton, and R.P. Miller, “The formation and microstructure of the dental silicate cement,” *J. Mater. Sci.*, **7** (1972) 220–228.
26. A.D. Wilson and R.F. Bachelor, “Dental silicate cements. I. The chemistry of erosion,” *J. Dent. Res.*, **46** (1967) 1075–1085.
27. A.D. Wilson and R.F. Mesley, “Dental silicate cements. VI. Infrared studies,” *J. Dent. Res.*, **47** (1968) 644–652.
28. A.D. Wilson and B.E. Kent, “Dental silicate cements. IX. Decomposition of the powder,” *J. Dent. Res.*, **49** (1970) 21–26.
29. A.D. Wilson and B.E. Kent, “Dental silicate cements. V. Electrical conductivity,” *J. Dent. Res.*, **44** (1968) 463–470.
30. G.C. Paffenbarger, I.C. Schoonover, and W. Souder, “Dental silicate cements: physical and chemical properties and a specification,” *J. Am. Dent. Assoc.*, **25** (1938) 32–87.

31. A.D. Wilson, S. Crisp, and B.G. Lewis, "The aqueous erosion of silicophosphate cements," *J. Dent.*, **10** (1982) 187–197.
32. K.R. Anderson and G.C. Paffenbarger, "Properties of silicophosphate cements," *Dent. Prog.*, **2** (1962) 72–75.
33. C.E. Semler, "A quick-setting wollastonite phosphate cement," *Am. Ceram. Soc. Bull.*, **55** (1976) 983–988.
34. M.S. Ter-Grigorian, V.V. Beriya, E.N. Zedginidze, and M.M. Sychev, "Problem of the setting of serpentinite–phosphate cement," *Chem. Abstr.*, **101** (1984), No. 156469.
35. M.S. Ter-Grigorian, E.N. Zedginidze, M.M. Sychev, S.M. Papuashvili, L.K. Teideishvili, and R.I. Dateshitze, "Study of serpentinite–phosphate cement during heat treatment at 110–1200 degrees C," *Chem. Abstr.*, **96** (1982), No. 23920.
36. K.P. Krajewski, "Early diagenetic phosphate cements in the Albeian condensed glauconitic limestone of the Tatra Mountains, Western Carpathians," *Chem. Abstr.*, **10** (1984), No. 114382.
37. B. El-Jazairi, "Rapid repair of concrete pavings," *Concrete*, (London), **16** [9] (1982) 12–15.
38. A.S. Wagh, D. Singh, and S.Y. Jeong, "Chemically bonded phosphate ceramics," in *Handbook of Mixed Waste Management Technology*, ed. C. Oh (CRC Press, Boca Raton, 2001), pp. 6.3.1–6.3.18.
39. E.M. Prosen, Refractory materials for use in making dental casting, US Patent 2,152,152, 1939.
40. E.M. Prosen, Refractory material suitable for use in casting dental investments, US Patent 2,209,404, 1941.
41. R. Earnshaw, "Investments for casting cobalt–chromium alloys, part I," *Br. Dent. J.*, **108** (1960) 389–396.
42. R. Earnshaw, "Investments for casting cobalt–chromium alloys, part II," *Br. Dent. J.*, **108** (1960) 429–440.
43. F.G. Sherif and Edwin S. Michaels, Fast-setting cements from liquid waste phosphorous pentoxide containing materials, US Patent 4,487,632, 1984.
44. F.G. Sherif and E.S. Michaels, Fast-setting cements from solid phosphorous pentoxide containing materials, US Patent 4,505,752, 1985.
45. F.G. Sherif and A.G. Ciamei, Fast-setting cements from superphosphoric acid, US Patent 4,734,133, 1988.
46. F.G. Sherif and F.A. Via, Production of solid phosphorous pentoxide containing materials for fast-setting cements, US Patent 4,755,227, 1988.
47. T. Finch and J.H. Sharp, "Chemical reactions between magnesia and aluminium orthophosphate to form magnesia-phosphate cements," *J. Mater. Sci.*, **24** (1989) 4379–4386.
48. T. Sugama and L.E. Kukacka, "Magnesium monophosphate cements derived from diammonium phosphate solutions," *Cem. Concr. Res.*, **13** (1983) 407–416.
49. F.G. Sherif, F.A. Via, L.B. Post, and A.D.F. Toy, Improved fast-setting cements from ammonium phosphate fertilizer solution, European Patent No. EP0203485, 1986.
50. T. Sugama and L.E. Kukacka, "Characteristics of magnesium polyphosphate cements derived from ammonium polyphosphate solutions," *Cem. Concr. Res.*, **13** (1983) 499–506.
51. J. Ando, T. Shinada, and G. Hiraoka, "Reactions of monoaluminum phosphate with alumina and magnesia," *Yogyo-Kyokai-Shi*, **82** (1974) 644–649.
52. E.D. Demotakis, W.G. Klemperer, and J.F. Young, "Polyphosphate chain stability in magnesia-polyphosphate cements," *Mater. Res. Symp. Proc.*, **45** (1992) 205–210.
53. A.P. Belopolsky, S.Ya. Shpunt, and M.N. Shulgina, "Physicochemical researches in the field of magnesium phosphates (the system $\text{MgO}-\text{P}_2\text{O}_5-\text{H}_2\text{O}$ at 80°C)," *J. Appl. Sci. (USSR)*, **23** (1950) 873–884.
54. B.E.I. Abdelrazig and J.H. Sharp, "Phase changes on heating ammonium magnesium phosphate hydrates," *Thermochim. Acta*, **129** (1988) 197–215.
55. B.E.I. Abdelrazig, J.H. Sharp, and B. El-Jazairi, "Microstructure and mechanical properties of mortars made from magnesia-phosphate cement," *Cem. Concr. Res.*, **19** (1989) 228–247.
56. B.E.I. Abdelrazig, J.H. Sharp, and B. El-Jazairi, "The chemical composition of mortars made from magnesia-phosphate cement," *Cem. Concr. Res.*, **18** (1988) 415–425.
57. B.E.I. Abdelrazig, J.H. Sharp, P.A. Siddy, and B. El-Jazairi, "Chemical reactions in magnesia-phosphate cements," *Proc. Br. Ceram. Soc.*, **35** (1984) 141–154.
58. S. Popovics, N. Rajendran, and M. Penko, "Rapid hardening cements for repair of concrete," *ACI Mater. J.*, **84** (1987) 64–73.
59. A.K. Sarkar, "Phosphate cement-based fast-setting binders," *Ceram. Bull.*, **69** [2] (1990) 234–238.
60. A.K. Sarkar, "Hydration/dehydration characteristics of struvite and dittmarite pertaining to magnesium ammonium phosphate cement system," *J. Mater. Sci.*, **26** (1991) 2514–2518.

61. A. Wagh, D. Singh, and S. Jeong, Method of waste stabilization via chemically bonded phosphate ceramics, US Patent No. 5,830,815, 1998.
62. W.D. Kingery, "Fundamental study of phosphate bonding in refractories: II, cold-setting properties," *J. Am. Ceram. Soc.*, **33** [5] (1950) 242–250.
63. N.F. Fedorov, L.V. Kozhevnikova, and N.M. Lunina, Current-conducting phosphate cements, UDC 666.767.
64. M.M. Sychev, I.N. Medvedeva, V.A. Biokov, and O.S. Krylov, Effect of reaction kinetics and morphology of neoformation on the properties of phosphate cements based on magnesium titanates, *Chem. Abstr.*, **96** No. 222252e.
65. G.L. Sudakas, L.I. Turkina, and A.A. Chernikova, Properties of phosphate binders, *Chem. Abstr.*, **96**, No. 202,472.
66. S.L. Golynko-Wolfson, M.M. Sychev, L.G. Sudakas, and L.I. Skoblo, Chemical basis of fabrications and applications of phosphate binders and coatings, Leningrad, Khimiya (1968).
67. L.I. Turkina, L.G. Sudakas, V.A. Paramonova, A.A. Chernikova, *Inorganic Materials* (Plenum Publishers, New York, 1990), Translated from Russian Original **26**[7], pp. 1680–1685.
68. A.S. Wagh, S.Y. Jeong, D. Singh, A.S. Aloy, T.I. Kolytcheva, E.N. Kovarskaya, and Y.J. Macharet, "Iron-phosphate-based chemically bonded phosphate ceramics for mixed waste stabilization," *Proceedings on Waste Management '97, March 2–6 1997*, (1997).
69. A.S. Wagh, S. Jeong, and D. Singh, "High strength phosphate cement using industrial byproduct ashes," in *Proceedings of First International Conference on High Strength Concrete*, eds. H.I. Kona, A. Azizinamini, D. Darwin, and C. French (Amer. Soc. Civil Eng., Reston, VA, 1997), pp. 542–553.

This page is intentionally left blank

Raw Materials

The various CBPC products discussed in the last chapter reveal that CBPC powder consists of one or more sparsely soluble oxides and an acid phosphate. When this mixture is stirred in water, the acid phosphate dissolves first and makes the solution acidic, in which the sparsely soluble alkaline oxides dissolve and an acid–base reaction is initiated. This reaction produces slurry that subsequently hardens and a ceramic hard product is formed. If the acid phosphate is phosphoric acid solution, the setting reaction is too rapid. Such a process becomes impractical for production of large ceramic objects because the rapid acid–base reaction is exothermic and that boils the reaction slurry. Therefore, less acidic acid phosphates (such as dihydrogen phosphates) are preferred for fabrication of practical ceramics.

In most applications, a small amount of binder powders is mixed with a large volume of inexpensive fillers and then the entire mixture is stirred in water to form the reaction slurry. For example, if the phosphate binders are used for manufacturing construction products, invariably the fillers are sand, gravel, ash, soil, or some mineral waste. The phosphate binders provide adhesion between the particles of these fillers and bind them into a solid object. Thus, these mixtures mimic conventional concrete mixtures in which Portland cement binder is mixed with large volume of sand and gravel to produce cement concrete. When phosphate binders are used, the products may be termed as “phosphate concrete”. In waste stabilization, the waste itself becomes the filler and the final product is termed as a “waste form”.

Generally, a small amount of the binder is used in cement or phosphate concrete; the major volume of the concrete is aggregates. The small amount of binder keeps the overall cost of the product low. The components of the aggregates, however, do not participate in the setting reaction. On the other hand, in the case of a CBPC the reaction of the aggregate will entirely depend on its solubility in the acidic phosphate solution. Since silica (SiO_2) is insoluble in an acid solution, it is safe to assume that it will not participate in any setting

reaction, but will remain as inactive filler in the final product. Few silicates such as wollastonite (CaSiO_3) are sparsely soluble. They react and participate in forming a binding phase. Even fly ash is found to contain such silicate components and therefore it participates in the chemical reaction that forms the final CBPC product [1]. When CBPCs are used for waste stabilization, the reaction between the hazardous or radioactive contaminants and phosphates is important, because these reactions ultimately convert these contaminants into insoluble phosphate products that are chemically immobilized and do not leach into groundwater. Thus, while developing a CBPC product of desired properties, it is essential that one not only studies the dissolution characteristics of the binder components, but also has a good knowledge of the solubility of the additives and fillers.

Solubility of fillers is also important in dental cements and biomaterials. Unlike in construction cements, the cost of the end product is not a major issue in dental cements, but purity, biocompatibility, and performance of the final product is very important. Each filler component has its own role in modifying the behavior of the final product. As we shall see later in Chapter 18, wollastonite improves the flexural strength and toughness of the dental cements because the grains of wollastonite have elongated needle shape (acicular). Hydroxyapatite is added to provide biocompatibility to the product. Attributes of these fillers govern the final properties of the products and hence it is necessary that, not only one understands detailed properties of the binder components, but also that of the additives and filler components. For this reason, this chapter is devoted to describe the genesis and properties of the binder and important filler components.

3.1.

FORMATION OF PHOSPHORIC ACID FROM PHOSPHATE ROCKS

The major deposits of phosphate ores are in Florida in the United States, Kola in Russia, and Morocco [2,3]. They consist of minerals of calcium and aluminum phosphates [2]. These ores are processed to extract these minerals; the most important among these minerals is calcium fluorophosphate ($\text{Ca}_{10}\text{F}_2(\text{PO}_4)_6$). Richness of phosphate in these rocks and the extracted products is measured in terms of P_2O_5 content in them.

Phosphate chemicals are used in large scale in manufacture of phosphate fertilizers. Figure 3.1 shows the flow chart of production of acid-phosphates used as fertilizer chemicals. These acid-phosphates are also potential ingredients in manufacture of CBPC products.

Ortho phosphoric acid (H_3PO_4), which is referred to as phosphoric acid here after, is the first and the most important product extracted from the phosphate ore. When the ore is reacted with sulfuric acid (H_2SO_4), phosphoric acid is formed by the following reaction

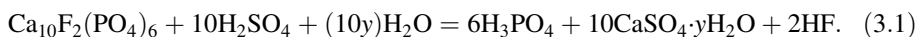
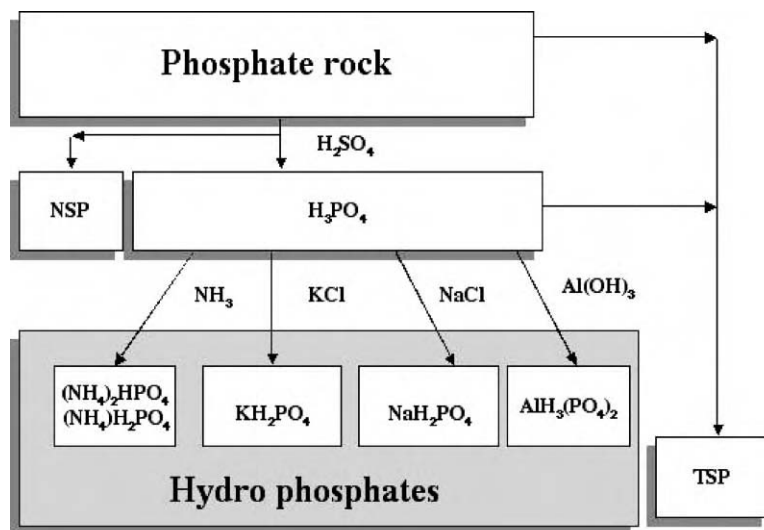


Fig. 3.1.



Flow chart of acid-phosphate production from phosphate ores.

Here, $y = 0, 0.5\text{--}0.7$, or 2 . The second term on the right-hand side represents gypsum in various forms. It is separated and discarded, while the third term, which is hydrofluoric acid, is removed and either used or disposed off safely.

Depending on the purity and concentration, phosphoric acid is sold in different grades. Generally, commercial grade phosphoric acid is 70 and 85 wt% concentrated. The pH of this acid is zero and hence it is a strong acid. For all practical applications in forming CBPC products however, either this acid is diluted, or reacted with alkali metals to form acid-phosphates with a $\text{pH} > 1$. Figure 3.1 illustrates formation of these acid-phosphates.

Even diluted phosphoric acid is too acidic in forming CBPC. Furthermore, transportation and storage of liquid acid has risks of spillage and accidents. Partially neutralized acid-phosphates, on the other hand, are powders and are less acidic and hence are more suitable for transportation, handling, and storage. Therefore, such acid phosphates are preferred in manufacture of CBPC products.

3.2.

ACID PHOSPHATES

Typical acid-phosphates used in forming CBPCs are hydrophosphates of ammonia, calcium, sodium, potassium, and aluminum. Reacting their chlorides, nitrates, oxides (or hydroxides) or carbonates with phosphoric acid, hydrophosphates are formed.

As mentioned before, these hydrophosphates are used in commercial fertilizers. Hydrophosphates of calcium $[\text{Ca}(\text{H}_2\text{PO}_4)_2 \cdot \text{H}_2\text{O}]$ and ammonium $[(\text{NH}_4)_2\text{HPO}_4$ and $(\text{NH}_4)\text{H}_2\text{PO}_4]$ are the most commonly used fertilizers, while potassium hydrophosphate (KH_2PO_4) is also used where the soil needs potash.

It is economical to use only a small amount of binder with maximum available P_2O_5 value and large amount of locally available fillers in forming CBPC products. This way, only a small amount of the P_2O_5 -rich binder is transported to the site of use and high transportation costs of the bulk fillers are avoided. Therefore, purity of hydrophosphates with maximum P_2O_5 is a major factor in the cost of CBPC production.

P_2O_5 content of candidate acid-phosphates is given in Table 3.1. For comparison, we have also included commercially available phosphoric acid (85% concentrated) and a calcium hydrophosphate fertilizer called triple super phosphate (TSP) in this table.

One immediate conclusion that may be drawn from Table 3.1 is that all pure acid-phosphates and the phosphoric acid contain P_2O_5 in a narrow range of 50–60 wt%; phosphoric acid has the highest amount while KH_2PO_4 has the least. TSP is an impure $\text{Ca}(\text{H}_2\text{PO}_4)_2 \cdot \text{H}_2\text{O}$, and hence its yield of P_2O_5 is low. Thus, one may conclude that phosphoric acid should be the most economical for use in CBPC products. However, because it is a liquid, one prefers use of acid phosphates rather than the acid itself for CBPC production.

Among the acid-phosphates, hydrophosphates of ammonium, aluminum $[\text{AlH}_3(\text{PO}_4)_2 \cdot \text{H}_2\text{O}]$, and sodium $(\text{NaH}_2\text{PO}_4)$ also have higher concentration of P_2O_5 and hence are potential raw materials in forming CBPCs. Ammonium hydrophosphate and its CBPC products, however, release ammonia during formation of CBPCs and even after, particularly when large size samples are made. NaH_2PO_4 ceramics contain Na-glassy phase in it, and the end product is not very tough. Such ceramics tend to develop microcracks over time. Because Na is a light atom, its aqueous leachability is also comparatively high. $\text{AlH}_3(\text{PO}_4)_2 \cdot \text{H}_2\text{O}$ is too acidic, reacts too rapidly, and hence large size objects are difficult to make with this raw material. Similar is the problem with calcium hydrophosphate. Thus, ironically, KH_2PO_4 , though has comparatively lower content of P_2O_5 , is the most useful acid phosphate. It is not too acidic, it is a powder, and it produces excellent ceramics. Therefore, KH_2PO_4 has been the most useful raw material in production of objects of large size or in a continuous production process. In batch processes or when smaller objects are produced, or often in combination with KH_2PO_4 , other phosphates are very useful. For this reason, individual acid-phosphates that are used in forming ceramics are discussed below in detail.

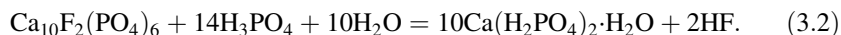
Table 3.1.

P_2O_5 Content of Candidate Acid Phosphates.

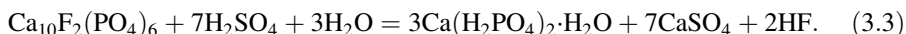
Phosphate P_2O_5 (wt%)	85% H_3PO_4 61.6	NaH_2PO_4 59.2	KH_2PO_4 52.2	$(\text{NH}_4)\text{H}_2\text{PO}_4$ 61.7	$(\text{NH}_4)_2\text{HPO}_4$ 53.8
Phosphate P_2O_5 (wt%)	$\text{Ca}(\text{H}_2\text{PO}_4)_2 \cdot \text{H}_2\text{O}$ 56.4	$\text{Mg}(\text{H}_2\text{PO}_4)_2 \cdot \text{H}_2\text{O}$ 60	$\text{AlH}_3(\text{PO}_4)_2 \cdot \text{H}_2\text{O}$ 59.7	TSP (70 wt% pure) 39.5	

3.2.1. Calcium Hydrophosphate Fertilizers

Because calcium is one of the major components of phosphate ore, it is possible to produce calcium hydrophosphate by reaction of the ore with phosphoric acid. The reaction is given by [3]



The first term on the right-hand side, i.e., calcium hydrophosphate is not in pure form in actual process. It contains impurities from the ore and is sold commercially as TSP fertilizer. It is also possible to produce a similar phosphate product by reacting phosphate ore with sulfuric acid. The reaction proceeds according to reaction 3.3 [3]



Once the hydrofluoric acid (HF) is removed, the end product is a solid mass of calcium hydrophosphate and gypsum. This solid is termed as normal super phosphate (NSP). Though this fertilizer is an inexpensive product, because available P_2O_5 in NSP is very small (5–8%), it is not a good raw material for economic production of CBPCs. However, TSP can be used in some applications. Details of TSP use in ceramic formation are discussed in Chapter 13.

3.2.2. Monopotassium Phosphate

Commercially available pure KH_2PO_4 , when reacted with MgO , produces high quality ceramics [4]. This raw material is comparatively more expensive than other hydrophosphates, but a very large proportion of fillers can be incorporated in the ceramic formation and hence the net cost of the binder components in making products is less. The binder formed by reaction of KH_2PO_4 and MgO has been studied extensively at Argonne National Laboratory and is named as “Ceramicrete”. Details of Ceramicrete are discussed in Chapter 9 and its subsequent applications from Chapter 14 onwards.

Monopotassium phosphate (MKP) is formed by reaction of chloride or carbonate of potassium with phosphoric acid and the phosphate is derived as a crystalline material in a pure form. Its main commercial applications are, food ingredient in cold drinks and in detergents, and now CBPCs have provided a new avenue for its commercial use.

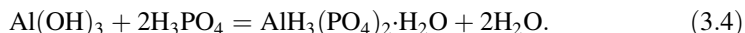
3.2.3. Magnesium Dihydrogen Phosphate

Similar to calcium dihydrogen phosphate, one may use magnesium dihydrogen phosphate ($\text{Mg}(\text{H}_2\text{PO}_4)_2 \cdot \text{H}_2\text{O}$) as an acid phosphate [5]. Not many commercial applications of this product have been identified and hence its commercial availability has been limited. As a result, though this product can produce excellent ceramics, it can only be used in specialty products such as dental cements. Formation of magnesium phosphate ceramics with this acid phosphate is discussed in Chapter 9 and its use in dental cement in Chapter 18.

3.2.4. Aluminum Hydrophosphate

As discussed in Chapter 2, use of $\text{AlH}_3(\text{PO}_4)_2 \cdot \text{H}_2\text{O}$ was recognized during development of early dental cements. Finch and Sharp [6] studied the detailed chemistry of reaction of magnesium oxide and this acid phosphate that forms excellent ceramics.

This acid-phosphate is formed when a mixture of aluminum hydroxide and phosphoric acid solution is heated between 100 and 120°C. The reaction is represented as



Details of such reaction and formation of aluminum phosphate ceramics are discussed in Chapter 11. Unfortunately, this acid phosphate also has limited use in other applications, and hence its commercial availability is limited.

3.2.5. Ammonium Acid Phosphates

Among all ammonia based phosphate fertilizer chemicals, monoammonium phosphate (MAP), $(\text{NH}_4)\text{H}_2\text{PO}_4$, and diammonium phosphate (DAP), $(\text{NH}_4)_2\text{HPO}_4$ have played a major role in forming CBPCs. As discussed in Chapter 2, Sugama and his group [7,8] developed ceramics using these two acid phosphates and subsequently Abelrazig and his group [9–11] and Popovic *et al.* [12] developed structural materials using these ceramics (see Chapter 9).

These ammonium phosphates are made by reacting ammonium nitrate with phosphoric acid. The resulting compounds are very soluble in water. During formation of ceramics, ammonia is released and phosphate reacts with metal cations such as magnesium and forms the CBPC. Because of the evolution of ammonia, it is used for outdoor applications such as road repair material and hardly any indoor applications have been found for these products.

3.3.

MAJOR OXIDES AND OXIDE MINERALS

The literature review in Chapter 2 reveals that divalent metal oxides such as oxides of calcium, magnesium, and zinc (CaO , MgO , and ZnO) are the major candidates for forming phosphate ceramics. These oxides are sparsely soluble in acidic solution, and as we shall see in Chapter 4, they are the most suitable ones to form ceramics. In addition, following the methods discussed in subsequent chapters in this book, aluminum oxide (alumina, Al_2O_3) and iron oxide (Fe_2O_3), which are abundant in earth's crust have excellent potential to form low cost CBPCs. For this reason, we have provided relevant information on these oxides. Table 3.2 gives some details.

Table 3.2.

Candidate Metal Oxides, Abundance of their Metals in Earth's Crust, their Solubility, and CBPC Forming Temperature.

Metal Oxide	Metal Abundance (wt%) [13]	Aqueous Solubility	Potential to Form CBPC	CBPC Forming Temperature (°C)
MgO	2.09	Sparingly soluble. Higher in acidic solutions and decreases with pH	High volume structural products, and in waste management	Ambient and cold
CaO	3.63	Sparingly soluble. Higher in acidic solutions and decreases with pH	Low volume in dental cements and biomaterials	Ambient
Al ₂ O ₃	8.13	Very low solubility, but increases in acidic and alkaline solutions (amphoteric)	Good at warm temperature	Warm, ≈ 150°C
ZnO	0.007	Sparingly soluble. Higher in acidic solutions and decreases with pH	In small volume in dental cements	Ambient
Fe ₂ O ₃	5.00	Insoluble	Good at ambient temperature by reduction	Ambient

3.3.1. Calcium Oxide

Calcium occurs mainly as calcium carbonate and calcium silicate on earth's crust; both are found in limestone. By heating the limestone, carbon dioxide is driven away to obtain calcium oxide. Because of its abundance in nature, it is an inexpensive raw material and is used in various industries including in cement manufacture to tooth pastes. It is available in different grades based on the particle size, purity, and reactivity.

Because calcium oxide is a fairly reactive powder, it forms calcium hydroxide when in contact with water. This reaction is exothermic and hence heats water during formation of the hydroxide. Because of this excess heat, it cannot directly be used to form phosphate ceramics by reacting it with an acid phosphate solution and must be used in a less soluble form as sparsely soluble silicate or hydrophosphate. In spite of this difficulty, because human bones contain calcium phosphate, there have been sufficient efforts in developing methods of forming biocompatible CBPCs of calcium phosphate by using partially soluble phosphates of calcium rather than using oxide itself. A similar approach may also be taken if one uses partially soluble silicate or aluminate of calcium. These routes are discussed in Chapter 13.

3.3.2. Magnesium Oxide

Like calcium, magnesium oxide occurs in minerals such as magnesite (magnesium carbonate), and dolomite (a mixture of calcium and magnesium carbonates). It is the

eighth most abundant element in earth's crust. It is extracted either from these rocks or from magnesium chloride derived from seawater by electrolysis. It is the most common raw material used in forming CBPCs. This is because its solubility is not as high as that of calcium oxide, nor as low as other commonly available oxides such as silica and iron oxide. Upon dissolving in water, it does not release excessive heat either. Therefore, number of magnesium based CBPCs have been developed as structural materials and for waste management applications. Development of magnesium based CBPCs will be discussed in Chapter 9 and their applications from Chapter 14 onwards. It is available in various reactivity grades based on the temperature and duration at which it is heat treated. Hard burnt and dead burnt grades are most useful for CBPC formation. Its reactivity and heat treatment are discussed in Chapter 8.

3.3.3. Aluminum Oxide

Aluminum is the second most abundant metal on earth's crust. It is a common metal in tropical soils called laterites (red soils). It is extracted from bauxite that is a rich laterite by Bayer process that involves dissolution and separation of the oxide in caustic soda solution between 150 and 250°C and 20 atm of pressure. Though abundant and inexpensive, alumina based CBPCs are difficult to form because even in an acid solution the solubility of alumina is very low. This solubility, however, can be enhanced by a mild thermal treatment and suitable CBPCs can be formed. Alumina is available commercially as calcined alumina called corundum, or as its hydrated forms such as aluminum hydroxide ($\text{Al}(\text{OH})_3$), as bohmite, ($\text{Al}_2\text{O}_3 \cdot 3\text{H}_2\text{O}$), gibbsite ($\text{Al}_2\text{O}_3 \cdot \text{H}_2\text{O}$) or in impure forms as in kaolin clay. These mineral forms and their use in ceramic formation are discussed in Chapter 11.

3.3.4. Iron Oxide

Iron is the third most abundant metal on earth's crust. Its oxide minerals are wüstite (FeO), hematite (Fe_2O_3), and magnetite (Fe_3O_4); the last one may be considered as a mixture of the first two [14]. FeO and Fe_3O_4 readily form CBPCs because their solubility is sufficiently high, but Fe_2O_3 is one of the most stable oxides and hence cannot be reacted easily with an acid phosphate to form a CBPC product. It can, however, be partially reduced to form CBPCs, and because of the abundance of this oxide in the nature and low cost, its CBPCs are practical ceramics that may find high volume usage. Formation of the CBPCs of this oxide is discussed in Chapter 12.

3.3.5. Zinc Oxide

Zinc is not a very common metal and as we notice from Table 3.1, its availability on earth's crust is low. It is found mainly as zinc sulfide in ores such as sphalerite and zinc blende, and as carbonates in smithsonite and silicate in calamine. The oxide is extracted by roasting these ores. The first discovery of zinc based CBPC as a dental material occurred

during 1879–1881 [15,16]. Improvements in zinc based dental cements continued for next several decades (see Chapter 2) and zinc phosphate became one of the most important early CBPCs. Unfortunately, it could be produced in a small scale as dental cement that is formed within minutes. Producing this material in a large scale requires slowing down its reaction with phosphoric acid solution. This has not been pursued and hence this material did not find its use in other applications. The cost of zinc oxide may also be a contributing factor that discouraged its use. Detailed formation of zinc phosphate cements is discussed in Chapter 10.

3.4.

AGGREGATES

Aggregates are typically high volume, low cost materials available at every site where concrete is used. They form the bulk part of CBPCs in most applications. Being inexpensive, they reduce the overall cost of the product and hence are key to production of viable CBPC products.

3.4.1. Sand

Sand is the most abundant material and is available almost everywhere. It is also the most common aggregate used in the conventional concrete industry, and in few construction industry applications that CBPCs have found, sand is the major ingredient.

Sand consists of mainly crystalline silica (quartz) and its aqueous solubility is negligible. As a result, it does not participate in the reaction that forms CBPCs. However, because sand is made of hard particles, it improves mechanical properties of CBPC products, especially the toughness. Being low cost filler, it can also be used in a large percentage of CBPC products.

3.4.2. Fly Ash

In addition to sand, the most important bulk additive in CBPC is fly ash. As we shall see in Chapter 14, fly ash is not just a filler; it seems to participate in the chemical reaction that forms CBPCs. As a result, the CBPC products containing fly ash have considerably better mechanical properties and provide a dense structure to the body of the ceramic. Therefore, fly ash has been a major ingredient in products in CBPC construction materials and oil well cements.

Fly ash is produced at utility plants that burn coal or oil to produce electricity. Therefore, it is an industrial high volume by-product. It consists of very fine powder, typically of fine particle size ($< 10 \mu\text{m}$). It is available in two grades called Class C and Class F ash. This classification is based on the composition of the ashes. Table 3.3 provides typical range of different oxide components found in the two ashes.

Table 3.3.

Composition of Typical Class C and F Coal Ashes.

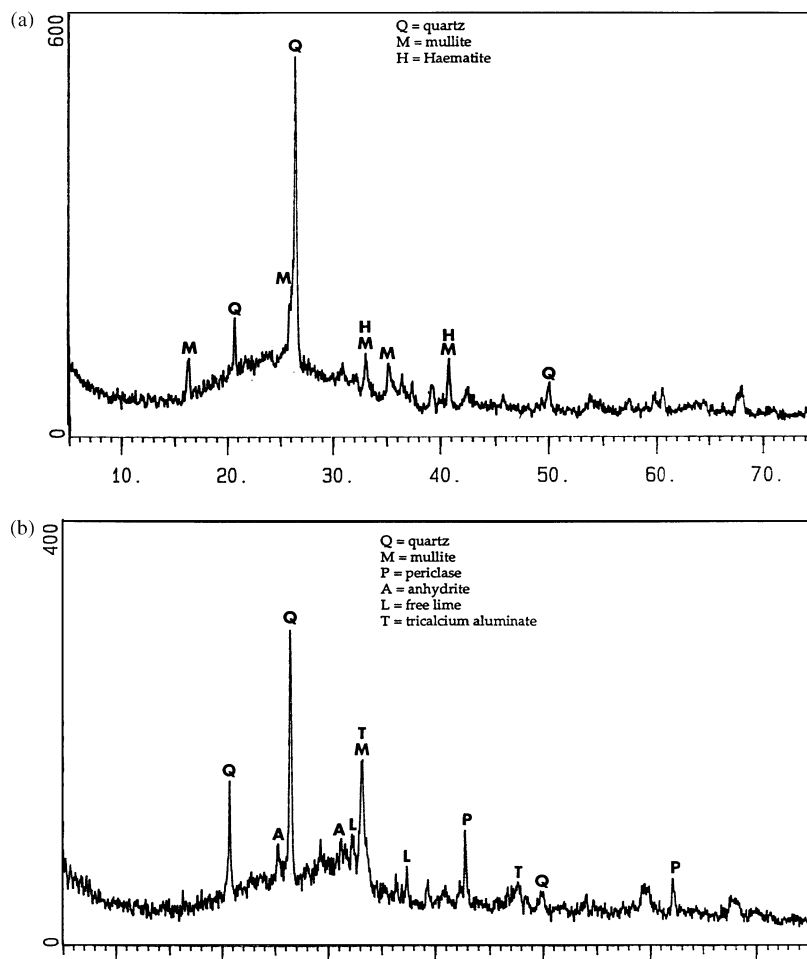
Element	Class F	Class C
Al	11.5	9.74
Ca	1.54	16.8
Fe	4.16	3.44
K	2.31	—
Si	21.8	16.5
C	8.78	0.08

As Table 3.3 indicates, the content of calcium in Class C ash is higher and carbon content is lower when compared with Class F ash. The high content of calcium is a result of its high content in the coal that is used when this ash is produced. Also this ash is produced when the coal is fully burned and hence there is hardly any residual carbon left in the ash. Comparatively content in Class F ash is high. As a result, Class F ash is grayish black in color while Class C ash is usually beige. Figure 3.2 shows a typical X-ray diffraction output of Class F and C ash. The peak found at $\approx 27^\circ$ is that of crystalline silica. As one may notice from the scanning electron micrograph in Fig. 3.3, this silica is found mainly in the form of silica spheres. These are hollow spheres called cenospheres or extensospheres that can be separated from the ash and used as additives in light weight cements and other similar products. One may notice in Fig. 3.2, that at the base of the silica peak, there is also a broad hump that represents the silica that is amorphous or microcrystalline. With its large surface area available for reaction, this amorphous silica plays a major role in forming superior CBPC products. As a result, fly ash is a good additive in CBPC structural material products. Use of fly ash in CBPC products will be discussed in Chapter 14.

In addition to the utility plant fly ash, one may also use volcanic fly ash, ash produced from burning municipal solid waste or any other combustion product that contains ash. The role of ash is also important in management of hazardous and radioactive waste because often such waste, if combustible, is incinerated to reduce its volume. The incinerated ash now is richer in inorganic hazardous components and needs to be stabilized. CBPC processes are ideal for stabilizing such ash because, phosphates are ideal materials to stabilize hazardous and radioactive contaminants, but as mentioned before, ash improves the physical and mechanical properties of the end products. Stabilization of such ashes is discussed in Chapters 16 and 17.

As we shall see later, CBPC processes also accommodate range of other high volume and low cost fillers such as mineral and industrial waste streams and soil. This is an attractive feature of the CBPC because using these locally available fillers, major material cost of the CBPC products can be reduced. For the same reason, CBPC processes are also most useful in stabilizing different waste streams. Thus, one may conclude that a wide range of aggregates can be used in a CBPC and their use is not limited significantly by the composition of the aggregates.

Fig. 3.2.

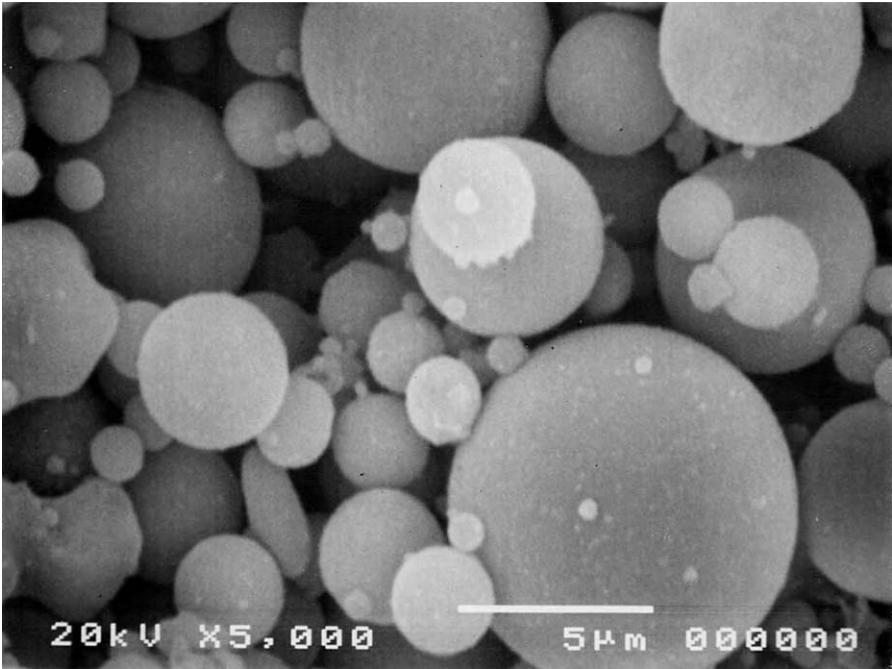


X-ray diffraction output of Class F and C fly ash.

3.4.3. Calcium Silicate (Wollastonite, CaSiO_3)

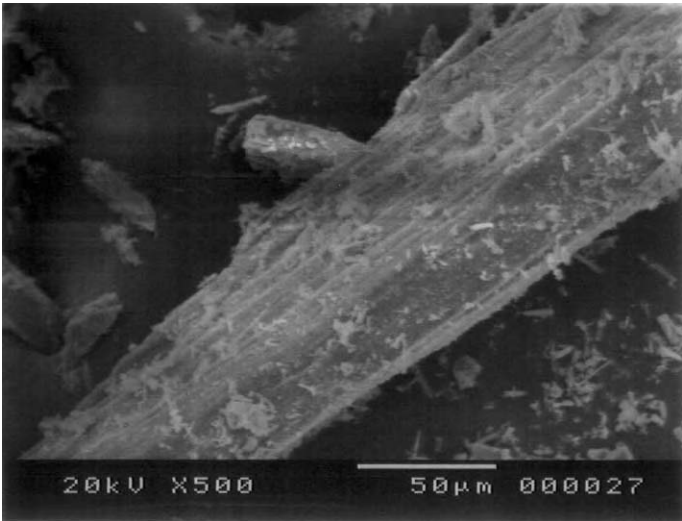
A wide range of silicates is available in nature in varying degrees of solubility. These minerals can be used in CBPCs as a source of soluble silica and enhance mechanical properties of the products such as compressive strength. Among them, calcium meta-silicate or wollastonite is the most important one. This is because, this mineral is abundant in nature and hence is available at a low cost, it is sparsely soluble and hence participates in the setting reaction during formation of CBPC products, and its crystal structure is acicular that provides better toughness, and flexural properties to the end product.

Fig. 3.3. _____



Scanning electron micrograph of cenospheres in Class C fly ash.

Fig. 3.4. _____



Scanning electron micrograph of wollastonite.

Wollastonite is found in crystalline limestones and is mined where it is sufficiently high in concentration and forms major part of the rock mass. Such places are states of New York and California in the United States, Brittany, Germany, Rumania, and Mexico [13].

Commercially, wollastonite is available in pure form and with different aspect ratio (length-to-diameter ratio of grains). Figure 3.4 shows the microstructure of a typical commercially available wollastonite mineral. The structure of individual grains is acicular and hence the mineral is identified by the aspect ratio (length-to-diameter ratio) of the grains. As we shall see in Chapter 14, this fibrous nature of this mineral provides sites for crack deflection in the CBPC composite formed by this mineral, increases the tortuosity of the crack propagation which leads to a tougher material. Thus, in addition to providing a source of soluble silica, its morphological structure also helps in forming a product with enhanced mechanical properties. For this reason, wollastonite is a preferred mineral in CBPC products [17].

REFERENCES

1. A.S. Wagh, S. Jeong, and D. Singh, "High strength phosphate cement using industrial byproduct ashes," in *Proceedings of the First International Conference on High Strength Concrete, Kona, HI*, eds. A. Azizinamini, D. Darwin, and C. French (Amer. Soc. Civil Eng., Reston, VA, 1997), pp. 542–553.
2. *Inorganic Phosphate Materials*, ed. T. Kanazawa (Kodansha/Elsevier, Tokyo/Oxford, 1989), pp. 1–13.
3. Kirk-Othmer, *Encyclopedia of Chemical Technology*, 3rd ed., vol. 10. (Wiley Interscience, New York, 1982), p. 62.
4. A.S. Wagh, D. Singh, and S.-Y. Jeong, Method of waste stabilization via chemically bonded phosphate ceramics, US Patent No. 5,830,815, 1998.
5. S.-Y. Jeong and A.S. Wagh, Formation of chemically bonded ceramics with magnesium dihydrogen phosphate binder, Invention Report ANL-IN-99-037, 1999. Filed for patent.
6. T. Finch and J.H. Sharp, "Chemical reactions between magnesia and aluminium orthophosphate to form magnesia-phosphate cements," *J. Mater. Sci.*, **24** (1989) 4379–4386.
7. T. Sugama and L.E. Kukacka, "Magnesium monophosphate cements derived from diammonium phosphate solutions," *Cem. Concr. Res.*, **13** (1983) 407–416.
8. T. Sugama and L.E. Kukacka, *Cem. Concr. Res.*, **13** (1983) 499–506.
9. B.E.I. Abdelrazig, J.H. Sharp, and B. El-Jazairi, "Microstructure and mechanical properties of mortars made from magnesia-phosphate cement," *Cem. Concr. Res.*, **19** (1989) 228–247.
10. B.E.I. Abdelrazig, J.H. Sharp, and B. El-Jazairi, "The chemical composition of mortars made from magnesia-phosphate cement," *Cem. Concr. Res.*, **18** (1988) 415–425.
11. B.E.I. Abdelrazig, J.H. Sharp, P.A. Siddy, and B. El-Jazairi, "Chemical reactions in magnesia-phosphate cements," *Proc. Br. Ceram. Soc.*, **35** (1984) 141–154.
12. S. Popovics, N. Rajendran, and M. Penko, "Rapid hardening cements for repair of concrete," *ACI Mater. J.*, **84** (1987) 64–73.
13. C. Klein and C. Hurlbut, Jr., *Manual of Mineralogy* (Wiley, New York, 1977), p. 153.
14. *ibid*, pp. 406–408.
15. C.S. Roastaing di Rostagni, Verfahrnung zur Darstellung von Kitten für zahnärztliche und ähnliche Zwecke, bestehend von Gemischen von Pyrophosphaten des Calciums oder Bariums mit den Pyrophospheten des Zinks oder magneiums. German Patent 6015, Berlin, 1878. Also in *Correspondenz-Blatt für Zahnärzte*, **10** (1881) 67–69.
16. W.H. Rollins, "A contribution to the knowledge of cements," *Dent. Cosmos.*, **21** (1979) 574–576.
17. A. Wagh, S. Jeong, D. Lohan, and A. Elizabeth, Chemically bonded phosphosilicate ceramic, US Patent No. 6,518,212 B1, 2003.

This page is intentionally left blank

Phosphate Chemistry

4.1.

NOMENCLATURE

Phosphorous is a five-valent element, and its natural oxide is P_2O_5 , phosphorous pentoxide. It is a highly hygroscopic powder and readily reacts with water to form phosphoric acid (H_3PO_4). This acid when reacted with various alkaline compounds forms phosphates. These and other modified compounds are linear or chain, cyclic or ring, and branch chain polymers. Because these compounds are polymeric, phosphates can provide a continuous structure and, hence, form good ceramics. The reader is referred to *Topics in Phosphorus Chemistry* by Westman [1] for details. Because of the variety of polymeric compounds formed by phosphorous, a systematic nomenclature is used in phosphate chemistry.

Linear or chain polymers are represented by the formula

$$M_{(n+2)}(P_nO_{(3n+1)})_x, \quad (4.1)$$

where M is an x -valent cation and n is an integer. nx represents the number of phosphorous atoms in the molecule or the “chain length”. For $n = 1$, one uses the prefix “ortho” and for $n = 2$, the prefix “pyro”. Thus, if M is hydrogen ($x = 1$), and $n = 1$, formula 4.1 yields H_3PO_4 , which is orthophosphoric acid that is simply called as phosphoric acid. For $n = 2$, the formula yields $H_4P_2O_7$, pyrophosphoric acid. If M is a monovalent metal, such as sodium, the formula yields Na_3PO_4 (sodium orthophosphate) for $n = 1$, and $Na_3P_2O_7$ (sodium pyrophosphate) for $n = 2$, respectively. If M is a divalent metal such as calcium ($x = 2$), the formula yields $Ca_3(PO_4)_2$ (calcium orthophosphate) for $n = 1$ and $Ca_4(P_2O_7)_2$ which is the same as $Ca_2P_2O_7$ (calcium pyrophosphate) for $n = 2$. As in the case of phosphoric acid, since most compounds referred to in this book are orthophosphates,

we will drop the prefix “ortho” and simply call orthophosphates as phosphates. Thus, sodium orthophosphate will be sodium phosphate and calcium orthophosphate, calcium phosphate. For $n = 3, 4$, etc., one uses the words tripolyphosphate, tetrapolyphosphate, etc., and the corresponding acids are tripolyphosphoric and tetrapolyphosphoric acids.

Phosphates with ring or cyclic structures are represented by the general formula

$$[M(PO_3)_x]_n, \quad (4.2)$$

where $n > 2$. For these, the prefix “meta” is used. Thus, H_3PO_3 , Na_3PO_3 , and $Ca_3(PO_3)_2$ are metaphosphoric acid, sodium metaphosphate, and calcium metaphosphate, respectively.

Formula 4.1 is written for a single cation in the molecule. It is possible to have more than one cation in the chain. In the case of orthophosphates, examples include various hydrophosphates, or products such as magnesium potassium phosphate or zinc alumino phosphates that were discussed in Chapter 2. A generalization of formula 4.1 for orthophosphates may be made by replacing M by AB , where the total valency of A and B is equal to x , and $n = 1$. Thus, the general formula becomes

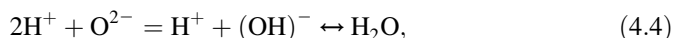
$$A_mB_n(PO_4)_{(mx+ny)/3}. \quad (4.3)$$

When $A = B = M$, and hence $x = y$, we obtain the formula 4.1 with $m + n = 3$. Writing $A = Mg$, $B = K$, $m = 1$, and $n = 1$ in formula 4.3, we obtain $MgKPO_4$, since in this case $x = 2$ and $y = 1$, which is a neutral and insoluble compound. As discussed in Chapter 2, such molecules with more than one cation form CBPCs. If either A or B is H , then these compounds are acid phosphates and often are used as components to produce the ceramics. Examples are the soluble compounds of metals, such as KH_2PO_4 , $(NH_4)_2HPO_4$, or $Al(H_2PO_4)_3$. Thus, compounds with more than one type of cations can be binder components or the final ceramic products, depending on whether they are soluble and acidic or insoluble and neutral.

4.2.

THE EFFECT OF pH

The acid–base reactions that form CBPCs are all carried out in an aqueous solution. In these reactions, either synthesis or dissociation of water may occur, involving ionized species of protons and hydroxyl ions. These reactions are given by



where the forward reaction is the synthesis of water, and the reverse is dissociation of water. The extent to which H^+ and $(OH)^-$ will react when they are released in water by the dissolution of the oxides and the acid phosphates will greatly influence the rate of the reaction represented by Eq. 4.4. Therefore, the reaction between H^+ and $(OH)^-$ is of fundamental interest. Experimentally, when these ions are released in water, all of them do not fully react. The reaction proceeds till H^+ and $(OH)^-$ have equal concentrations of

10^{-7} mol. Such a solution is called “neutral”. Thus, the ionization constant of water is defined by

$$\langle \text{H}^+ \rangle \langle (\text{OH})^- \rangle / \langle \text{H}_2\text{O} \rangle = 10^{-14} \text{ at } 25^\circ\text{C}. \quad (4.5)$$

The angle brackets in Eq. 4.15 represent molar concentrations of the particular species. In practice, one may select 1 mol of water for study, which means $\langle \text{H}_2\text{O} \rangle = 1$ in Eq. 4.5. Furthermore, it is customary to represent the negative logarithm to base 10 of the molar concentrations in Eq. 4.5:

$$-\log \langle \text{H}^+ \rangle \langle (\text{OH})^- \rangle = 14. \quad (4.6)$$

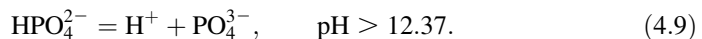
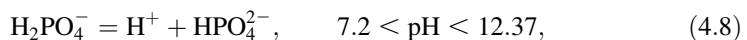
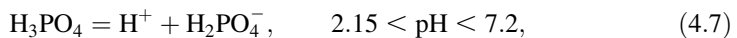
When $\langle \text{H}^+ \rangle = \langle (\text{OH})^- \rangle$, the solution is neutral water, and $-\log \langle \text{H}^+ \rangle = -\log \langle (\text{OH})^- \rangle = 7$. If more H^+ remains in the water, then it is acidic ($\text{pH} < 7$), while more hydroxyl ions remain, then the solution pH will be higher than 7.

Similar to dissociation of water, all soluble acid phosphates, and soluble oxides dissociate or dissolve in water. When acid phosphates dissociate in water, they lower the pH of the solution by releasing protons (H^+), while most of the oxides or hydroxides when mixed with water release hydroxyl ions (OH^-) by removing protons from the solution. As a result, initially neutral water becomes richer in protons when acid phosphates are dissolved in it and the pH becomes < 7 . On the other hand, for certain oxides such as those of alkaline elements (e.g., Na, K, Mg, and Ca), the pH is increased because the solution becomes deficient in protons. Thus, the pH scale is a good indicator of the extent of release of protons and hydroxyl ions and will be used throughout this book to represent the extent of acid–base reactions.

4.3.

DISSOLUTION CHARACTERISTICS OF PHOSPHORIC ACID

For example, consider phosphoric acid, which when mixed in water, loses hydrogen and forms protons (H^+) and anions (H_2PO_4^- , HPO_4^{2-} , and PO_4^{3-}) of phosphates. The number of protons lost during the dissolution depends on the pH in which this dissociation takes place. These dissociation reactions are represented by the following equations:



The dissociated species are the dominant species in the pH ranges given in Eqs. 4.7–4.9. At $\text{pH} < 2.15$, nonionic H_3PO_4 is dominant and therefore, this region is not useful in forming ceramics, because it will not contribute to the aqueous acid–base reaction.

In the pH range of 2.15–7.2, the dominant species is H_2PO_4^- , and one finds only minor amount of H_3PO_4 and HPO_4^{2-} . At $\text{pH} > 7.2$, the dominant species is HPO_4^{2-} , while minor species will be H_2PO_4^- and PO_4^{3-} and so on.

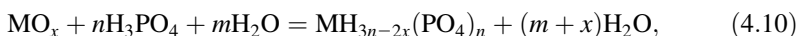
In agreement with the literature survey given in Chapter 2, a pH of 0–2.15 is not a suitable range to form CBPCs, because the acid–base reactions are very violent and do not form a homogeneous consolidated solid. The pH 2.15–7.2 range seems to be ideal, because in this range an alkaline oxide can be mixed with the acid solution, and a controllable reaction can occur. Thus, the reaction given by Eq. 4.8 is the most applicable for forming CBPCs.

4.4.

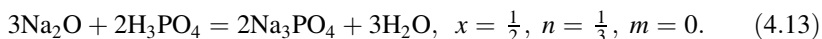
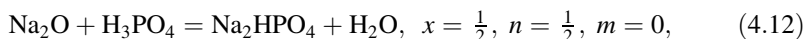
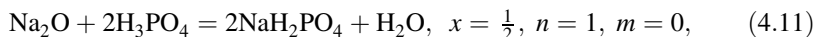
NEUTRALIZATION OF THE ACID AND FORMATION OF ACID PHOSPHATES

Metal oxides, such as that of Mg or Al, will dissolve in a phosphate solution to the extent their solubility allows. The dissolved part of these oxides reacts with the phosphate anions and forms the corresponding hydrophosphates or phosphates. For example, at pH < 2.15, the spontaneous reaction between MgO with nonionic H_3PO_4 will occur. Also a minor phase of $\text{Mg}(\text{H}_2\text{PO}_4)_2$ will form by the reaction of the dissolved part of MgO and H_2PO_4^- . In the pH range of 2.15–7.2, the dominant reaction product is $\text{Mg}(\text{H}_2\text{PO}_4)_2$, but minor phases such as MgHPO_4 are also formed. In the range 7.2–12.37, the major phase is MgHPO_4 and other minor phases are also formed. Thus, it is possible to produce a desired metal hydrophosphate by introducing the metal oxide in these specific pH ranges. If the rate of reaction is controlled, these hydrophosphates consolidate and form CBPCs. Thus, the aqueous acid–base reactions are the basis for forming CBPCs. Because the acid solutions always contain more than one phase, and also because all metal oxide added to the solution does not dissolve, the resulting ceramic has more than one phosphate phases and contains always some unreacted metal oxide.

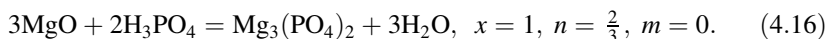
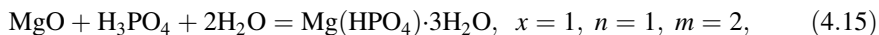
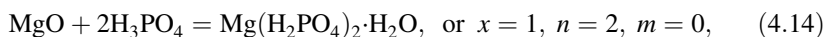
A typical acid–base reaction between a metal oxide and phosphoric acid may be written as



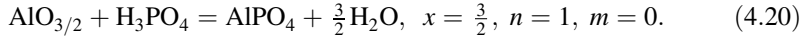
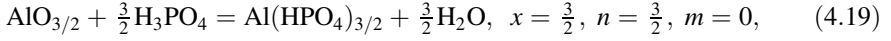
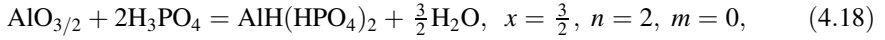
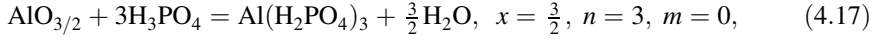
where x denotes half of the valency of M, $n \geq (2/3)x$, and m is an arbitrary integer that decides the amount of water to be added in the reaction. This water and any other formed during the reaction may remain within the system as water of crystallization or may be released as free water. The different products for the reaction of sodium oxide (Na_2O) are as follows:



The products from magnesium oxide (MgO) are the following:



Similarly, reactions for aluminum oxide (Al_2O_3) yield the following products:



Other choices of n will give linear combinations of these primary reactions, or these reactions and additional H_3PO_4 . For example, if we select $x = 1$ and $n = 3$ for Mg, we obtain $\text{Mg}_4\text{H}(\text{PO}_4)_3$, which is the same as $\text{MgHPO}_4 + \text{Mg}_3(\text{PO}_4)_2$. Similarly, by selecting $x = 3/2$ and $n = 4$ for Al, we obtain $\text{AlH}_9(\text{PO}_4)_4$, which is the same as $\text{Al}(\text{H}_2\text{PO}_4)_3 + \text{H}_3\text{PO}_4$.

According to Eq. 4.10, each of these reactions will be dominant at different pH that is determined by Eq. 4.4, and hence, is dependent on the speciation of H_3PO_4 in the aqueous solution. For example, for $7 \geq \text{pH} \geq 2$, H_3PO_4 will produce H_2PO_4^- . In acidic solution, i.e., in the presence of H^+ , MgO will also partially dissolve to form cations of Mg by the dissolution reaction



The notation (aq) attached to the Mg ion denotes that it is an aqueous species. Formation of this aqueous species will be discussed later. It suffices to state that it is an intermediate product formed by dissolution of MgO. This $\text{Mg}^{2+}(\text{aq})$ combines with the H_2PO_4^- produced by the dissolution reaction given in Eq. 4.14 to produce $\text{Mg}(\text{H}_2\text{PO}_4)_2$ by the reaction



As an alkaline oxide dissolves in an acid solution and reacts with the acidic ions, partial neutralization of the solution will occur. This will correspondingly change the speciation of the acidic ions. Because the solubility of highly acidic intermediate species is higher than less acidic ones, they are more reactive. Therefore, they react with more oxides and produce even more neutral products. For example, $\text{Mg}(\text{H}_2\text{PO}_4)_2$ will form less acidic MgHPO_4 by the following reaction:



Similarly, $\text{Al}(\text{H}_2\text{PO}_4)_3$ neutralizes $\text{AlO}_{3/2}$ by the reaction,



Reactions 4.23 and 4.24 imply that partially acidic phosphate salts are only intermediate phases. Consequently, it is possible to select these intermediate components as the starter powders to react them with oxides and form more neutral salts to form ceramics. As we shall see later, selection of the intermediate products as the acid components helps in slowing down the acid–base reaction and creating conditions in which homogeneous ceramics are formed.

Table 4.1.Solubilities (mol/100 g H₂O) of Various Acid Phosphates [3].

Solubility (mol/100 g H ₂ O)	NaH ₂ PO ₄	KH ₂ PO ₄	(NH ₄)H ₂ PO ₄	Ca(H ₂ PO ₄) ₂
Grams	48.5	20	28.57	30.01 ^a
Moles	0.4042	0.147	0.2484	0.128

^aFrom Ref. [4].

The above discussion indicates that acidic phosphate salts may play an important role in forming CBPCs. To use acid phosphates as the acidic components in acid–base reactions, primary requirement is solubility in water. Table 4.1 lists solubilities of some of the common hydrogen phosphates that are available in the literature and are useful intermediate phases during formation of CBCs.

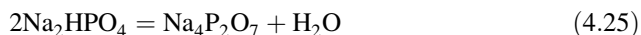
When these acid phosphates are used as anion donors in the formation of CBPC, phosphates with lower solubility are formed. For example, H₃PO₄ readily dissolves in water, and the acid–base reaction in the CBPC process is too rapid. The resultant products are precipitates of acid phosphates that are soluble in water. On the other hand, for the acid phosphates formed by partial neutralization of H₃PO₄ that are listed in Table 4.1, the process is slightly slower, and hence one has better control over formation of a coordinated network of phosphate reaction products that are less soluble. For this reason, neutralization of phosphoric acid and formation of the acid phosphate was the common route followed by earlier workers as discussed in Chapter 2.

Even among the acid phosphates, those with lower solubility are preferred. Acid phosphates such as KH₂PO₄ allow longer working time while synthesizing a ceramic compared to those of higher solubility, such as NaH₂PO₄ or MgH₂PO₄ or even (NH₄)H₂PO₄. For this reason, CBPCs produced with KH₂PO₄ can be used in large-scale applications while other formulations cannot.

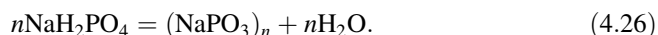
4.5.

CONDENSED PHOSPHATES

Orthophosphates are monomers. Their condensation polymerization leads to compounds such as pyrophosphates or metaphosphates, which have structures of long chain or ring polymers. These phosphates are formed by linkages of PO₄ tetrahedra with shared oxygen atoms, such that the skeletons with alternating P and O atoms, either in chains or rings, are formed by heat treatment of orthophosphates, as in the following example:



and



The latter reaction can form long chain phosphates, where n is theoretically infinite. Being formed by heat treatments, these phosphates are excellent candidates for high-temperature ceramics and glasses. Because the subject of this volume is low-temperature ceramics, we will not discuss the condensed phosphates in detail, except in one case in Chapter 15, where cements for geothermal wells are discussed with sodium metaphosphate. However, bear in mind that CBPCs can be precursors to high temperature phosphates and glasses. For this reason, as we have seen in the literature survey presented in Chapter 3, early interest in CBPCs was the formation of refractory shapes at room temperature, which were then fired to produce the final refractory components.

4.6.

DISSOCIATION (IONIZATION) CONSTANTS OF WEAK ACIDS

Strong acids and bases react violently and produce heat and, hence, are not very useful in forming CBCs. Therefore, in the entire study of CBPCs, we will be dealing with phosphoric acid, which is a weak acid in that it dissolves in water slowly compared with strong acids such as hydrochloric acid. Acid phosphates such as KH_2PO_4 and $\text{Al}(\text{H}_2\text{PO}_4)_3$ and weak bases such as oxides of Mg and Al dissolve slowly in water. To represent how slowly the weak acids or bases dissolve in water and to what extent, the term “dissociation (ionization) constant” is used.

Dissociation constants, which are chemical equilibrium constants for dissolution of acids, are defined in a manner similar to the definition of pH in the case of water. As discussed before, a weak acid such as H_3PO_4 goes through step-by-step ionization in water given by Eqs. 4.7–4.9. In each step, the dissociation constant is experimentally found to be

$$-\log\langle\text{H}^+\rangle\langle\text{H}_2\text{PO}_4^-\rangle = 2.15, \quad (4.27)$$

$$-\log\langle\text{H}^+\rangle\langle\text{HPO}_4^{2-}\rangle = 7.2, \quad (4.28)$$

$$-\log\langle\text{H}^+\rangle\langle\text{PO}_4^{3-}\rangle = 12.37. \quad (4.29)$$

Note that, as customary, we have assumed that 1 mol of the acid is selected for the dissolution in each case.

Similar analyses can be carried out for acidic or alkaline salts that are weakly soluble. One may define a dissociation constant, pK_{so} , for a dissociation reaction of a dihydrogen phosphate of a n -valent metal, given by

$$\text{M}(\text{H}_2\text{PO}_4)_n = \text{M}^{n+} + n(\text{H}_2\text{PO}_4)^{n-}. \quad (4.30)$$

In this case

$$pK_{\text{so}} = -\log[\langle\text{M}^{n+}\rangle\langle\text{H}_2\text{PO}_4^{n-}\rangle]. \quad (4.31)$$

Similar to Eqs. 4.27–4.29, Eq. 4.31 is written for 1 mol of $\text{M}(\text{H}_2\text{PO}_4)_n$. Table 4.2 provides the dissociation constants for some of the most important acid phosphate salts used as reactants to produce CBPCs or their reaction products.

Table 4.2.

Dissociation Reactions and the Respective Constants of Weak Acid Phosphates [2–4].

Phosphate	Dissociation Reaction	pK_{so}
KH_2PO_4	$KH_2PO_4 = K^+ + H_2PO_4^-$	0.15
$(NH_4)H_2PO_4$	$(NH_4)H_2PO_4 = NH_4^+ + H_2PO_4^-$	−0.69
$Mg(H_2PO_4)_2 \cdot 2H_2O$	$Mg(H_2PO_4)_2 \cdot 2H_2O = Mg^{2+} + 2H_2PO_4^- + 2H_2O$	2.97
$Ca(H_2PO_4)_2 \cdot H_2O$	$Ca(H_2PO_4)_2 \cdot H_2O = Ca^{2+} + 2H_2PO_4^- + H_2O$	1.146

As shown in Table 4.2, the dissociation constants of the acid phosphates vary widely. $(NH_4)H_2PO_4$ and KH_2PO_4 have low pK_{so} as well as low molar solubilities (see Table 4.1) and hence are suitable to form a ceramic. Salts with higher pK_{so} can form ceramics in small volumes but cannot be used for practical ceramics, because their solubility is high and the acid–base reactions are too rapid and also exothermic.

Similarly, the dissociation constants of phosphoric acid or its subsequent ions, given in Eqs. 4.28 and 4.29, are comparable to the highest value of pK_{so} given in Table 4.2 or even higher. Thus, use of phosphoric acid that furnishes phosphate ions is not useful in forming practical ceramics. For this reason, as noted in Chapter 2, researchers have resorted to some neutralization of the acid by dissolving oxides of Al or Zn to produce dental cements.

In addition to these acid phosphates, Sugama and Kukacka [5] also used $(NH_4)_2HPO_4$ which is an alkaline phosphate to react with MgO and produce ceramics. Such monohydrogen phosphate salts may often be used because their solubility is lower than the dihydrogen phosphates, but generally, the solubility of such salts, except for that of ammonium, is too low. Furthermore, these are not acid salts and hence the reaction with an oxide is not an acid–base reaction. For these reasons, detailed discussion of these salts is not included here.

REFERENCES

1. A.E.R. Westman, *Topics in Phosphorous Chemistry*, vol. **9**. (Wiley, New York, 1977), pp. 239–253.
2. V. Snoeyink and D. Jenkins, *Water Chemistry* (Wiley, New York, 1980), pp. 243–315.
3. F.L. William, *Solubilities of Inorganic and Metal Organic Compounds*, 4th ed., vol. **II**. (American Chemical Society, Washington, DC, 1965).
4. W.F. Linke, *Solubilities*, vol. **II**. (American Chemical Society, Washington, DC, 1965), p. 618.
5. T. Sugama and L.E. Kukacka, “Magnesium monophosphate cements derived from diammonium phosphate solutions,” *Cem. Concr. Res.*, **13** (1983) 407–416.

Dissolution Characteristics of Metal Oxides and Kinetics of Ceramic Formation

5.1.

DISSOLUTION CHARACTERISTICS AS THE BASIS FOR FORMING CBPCs

When powders of metal oxides are stirred in solvent such as an acid-phosphate solution, they dissolve slowly in the solvent and release cations in the solution. These cations react with the phosphate anions within the solvent and form a precipitate of salt molecules. Under the right conditions, these molecules form an ordered structure and grow into crystals. This ordered crystalline solid of the reaction products is the CBPC. Thus, CBPC formation is a result of the following three steps:

1. The acid phosphates dissolve in water, release phosphate anions, and form an acid-phosphate solution of low pH.
2. The oxides dissolve gradually in the low pH solution and release cations.
3. The phosphate anions react with the newly released cations and form a coordinated network and consolidate into a CBPC.

The right conditions to form a CBPC are governed by the rate of reactions that control each of these three steps. Since acid phosphates selected for use in the CBPC process are soluble, their dissolution rate is comparatively high and, hence, uncontrollable. The phosphate reaction between dissolved cations and anions described in step 3 is also inherently fast and, again, cannot be controlled. Thus, the only reaction that can be controlled is the dissolution of oxides given in step 2. By selecting suitable oxides with appropriate reaction rates for forming CBPCs, one may allow sufficient time to mix the components in water and pour the slurry in molds, or spray the slurry, or apply it in any other suitable manner to form a ceramic. On the other hand, an oxide that dissolves fast

will also react too fast and produce only a precipitate but not a well-coordinated network of phosphate ceramics. If the dissolution rate is too low, the oxide powder will remain mostly unreacted in the solution as powder. In such cases, the product resulting from the slow reaction forms a thin coating on the surface of individual particles of the oxides. This coating acts like a shield and inhibits further dissolution of the powder. This hinders formation of a ceramic. For this reason, it is crucial that appropriate oxides, based on their moderate solubility, are selected to synthesize CBPCs. The dissolution rate of such oxides is key to formation of CBPCs and is the subject of this chapter.

The dissolution of acid phosphates, or that of oxides, is an endothermic or heat absorbing reaction. As a result, there is some cooling effect on the slurry due to the first two steps given above. However, the acid–base reaction described in step 3 is inherently exothermic, i.e., it generates heat during the reaction. The amount of net heat generated and the rate at which it is produced are also important factors in forming the CBPCs. The heating due to the acid–base reaction more than compensates for the initial cooling resulting from the dissolution steps, and the net effect of all three steps is to heat the slurry. The net rate of heating of the slurry will depend on the amount of heat dissipated during the ceramic formation. This rate will also depend on the amount of the slurry mixed, ambient conditions in which it is mixed, and the speed with which it is mixed. When CBPCs are formed in a large scale, say in a 55 gal drum [1], it is quite common for condensation to occur on the container drum initially due to the dissolution of the first two steps and for heating to occur due to the acid–base reaction of the third step. The same dramatic effect of cooling and heating may not be found when mixing is done in a small beaker. For these reasons, processing conditions are an important factor in forming ceramics.

In addition to the processing conditions, as stated before, solubility is key to forming these ceramics. Both the solubility and the amount of heat generated or absorbed during the three steps of formation depend on the intrinsic thermodynamic properties of the oxides and acid phosphates. Thus, selection of particular oxides and the acid phosphates should be based upon their thermodynamic properties.

This chapter is devoted to the behavior of the powders of the candidate acid phosphates and oxides in solution. Taking into account the intermediate products formed by the dissolution of individual components, a model for kinetics of ceramic formulation is presented. Once the solubility characteristics of the binder components is established, the solubility will be related to the thermodynamic properties of these components and the amount of heating and cooling will be estimated from the thermodynamic properties. That will be done in Chapter 6.

5.2.

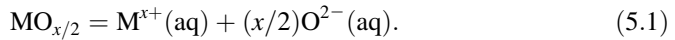
DISSOLUTION OF OXIDES AND FORMATION OF DISSOLVED CATIONS

As discussed before, when an oxide is stirred in any acidic phosphate solution, the solubility of the oxide controls the reaction. Except for oxides of alkaline metals (Group I

in the Periodic Table), all other metal oxides (or their hydroxides) exhibit low to very low aqueous solubility. Oxides of low solubility are the best candidates to form CBPC. They dissolve sufficiently slowly in acidic phosphate solution and allow slow mixing of the slurry without spontaneous reaction. Slow mixing forms good slurry that can be poured in suitable molds even in large forms. Oxides of low solubility are categorized as “sparsely soluble solids”, and they are the best candidates to form CBPCs.

The solubility of such solids is only a fraction of that of the acid phosphates that we discussed in the last chapter. A sparsely soluble oxide (or its hydroxide) dissolves in acidic solution in two steps. The first step is ionization or dissociation. When stirred in water, the oxide decomposes into its cations and anions. This decomposition occurs because of collisions between the oxide molecules and the polar molecules of water. Second is a screening step in which the two charged ions resulting from this dissociation are kept separate by the water molecules. These steps are described in detail below.

Consider, for example, an x -valent metal oxide represented by the notation $\text{MO}_{x/2}$. Dissociation of such an oxide is expressed by

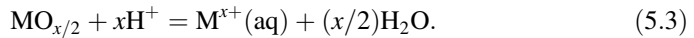


The notation “aq” stands for dissolved species. Throughout the text in this book, we have used this notation for cations to distinguish them from the solids. Anions are also aqueous, but as is customary in most text books, we have avoided using this explicit notation for anions for the sake of simplicity. During dissolution, the charges of these ions are screened by the rearrangement of polar water molecules, which keeps the ions apart from each other and prevents them from recombining. These screened and stable ions are called “aquosols” in the conventional sol–gel process of forming ceramics [2]. This screening procedure will be discussed in more detail in Section 5.3.

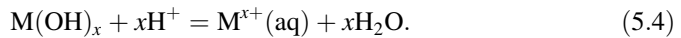
In the second step, the oxygen ion produced by reaction 5.1 combines with protons released by the acid component in the solution, and water is produced



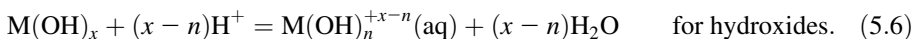
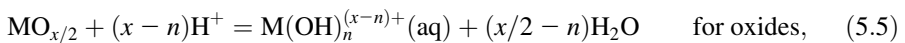
Reactions 5.1 and 5.2 combine to give



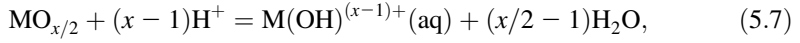
A similar reaction for the metal hydroxide may be written as



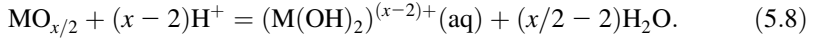
Reactions 5.3 and 5.4 represent complete dissolution of the metal oxide and its hydroxide, respectively. These reactions occur in a highly acidic medium where sufficient protons are available. In practice, however, partial neutralization of the acid solution due to reaction Eq. 5.2 also raises the pH. Thus, as the solution pH is raised, only partial ionization of the oxides occurs. This results in the following reactions:



Reactions 5.5 and 5.6 represent the basic dissolution of the oxide or the hydroxide of a metal of valency x , and they form the basis for discussion of the CBPC processes. When $n = 0$ in reactions 5.5 and 5.6, we regain reaction 5.3 and 5.4, respectively; these occur in highly acidic conditions. As the pH of the medium increases, reactions with increasing n occur. For example, for slightly higher pH, we put $n = 1$ and have

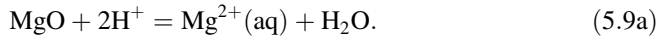


while for $n = 2$, we obtain for corresponding higher pH ranges,

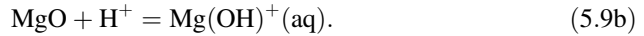


For $x > n$, the dissolution reaction occurs in acidic medium. If $x = n$, the reaction is in a neutral solution, while for $x < n$, the reaction is in an alkaline solution. Depending on the type of reaction needed and the solution pH, one can select the desired reaction for practical development of CBPCs. This is best illustrated by the two most useful oxides: one a divalent oxide, MgO, and the other a trivalent oxide, Al_2O_3 .

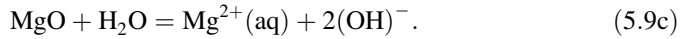
For Mg, $x = 2$, and $n = 0$, reaction 5.8 is



For $x = 2$, and $n = 1$, reaction 5.8 is

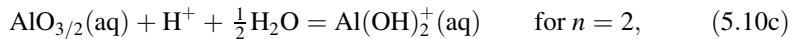
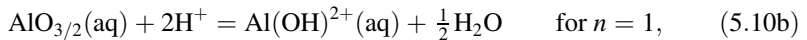
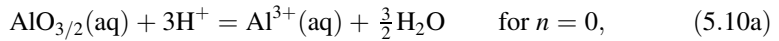


For $x = 2$, $n = 2$, reaction 5.8 is

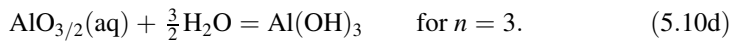


Reactions 5.9a, 5.9b and 5.9c occur in acidic, less acidic, and neutral solutions, respectively.

In a similar manner, for Al_2O_3 , and $x = 3$, reaction 5.8 is



and



Again, reactions 5.10a–c occur in acidic solutions, and reaction 5.10d in a neutral solution. For $\text{Al}(\text{OH})_3$, reaction 5.8 yields similar dissolution equations in alkaline regions.

Reaction 5.1 forms the basis for dissolution of an oxide for CBPC formation. It represents dissociation of metal oxides in which cations and anions are formed in an aqueous solution. In general, divalent metal oxides dissociate more easily than trivalent oxides, and quadrivalent oxides dissolve less easily than trivalent oxides, though some exceptions may be found to this general trend. The actual rate of dissolution will be discussed in detail as we develop a thermodynamic basis for these transformations.

In forming CBPCs, this dissociation is essential. The cations formed by dissociation react with phosphate anions that are present in the aqueous solution and form phosphate salt molecules. These salt molecules connect to each other and form a network and consolidate into a crystalline phosphate ceramic. Thus, success in forming CBPCs lies mainly in successfully dissociating sparsely soluble oxides in acidic solutions and precipitating salt in crystalline form. We will discuss the fundamentals of this dissociation in the next several chapters and present methods of dissociating various oxides in phosphate solutions to form ceramics.

5.3.

BORN EQUATION

As was discussed in Section 5.2, ionization of the solids in an aqueous solution is followed by aquosol formation by screening of charged ions. This screening prevents them from recombining. The free charges formed during dissociation interact with the water molecules locally. Water being polar, its molecule may be considered as a small rod with positive charge at one end and negative at the other. Thus, if there is a cation in the vicinity, the elongated water molecules orient themselves such that their negatively charged ends are attracted by the positive charge of the cation and, hence, will be closer to it. Conversely, their positively charged ends will be repelled away from the cation. Similar rearrangement will occur with anions, in which the positively charged ends of the water molecules will be attracted towards the anion, and the negatively charged ends will be repelled away from it. This reorientation of the polar molecules will reorient other polar water molecules in their vicinity, and there will be a short-range order around each of the cations and anions. The net result of this reorientation is screening or shielding of the charged ions and reduction of their field at comparatively longer distances. As a result of the reduction of this field, each screened ion along with the rearranged polar molecules will behave like a neutralized cluster in water. In addition, due to this screening, a cation will be separated from the anion, as they will not attract each other any more. Thus, one may visualize the entire solution to be full of screened clusters of molecules within a sea of polar water molecules.

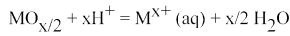
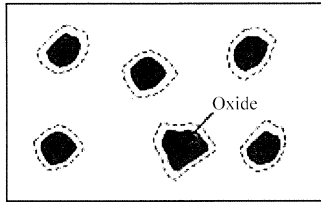
Such a situation has been thoroughly reported in solid state physics books on dielectrics subjected to external electric fields [3] and may be applied directly here to aqueous solutions. Consider, for example, a pair consisting of a cation and an anion (each of charge $+q$ and $-q$) that are freshly formed in vacuum. Suppose their centers are separated by a distance r . Then, Coulomb's law of electrostatics gives the change in electrostatic energy of attraction as

$$\Delta G_0 = -\frac{q^2}{4\pi\epsilon r}. \quad (5.11)$$

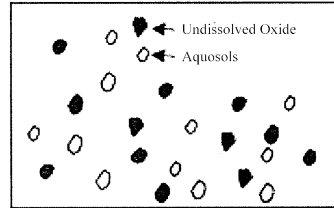
Here, ϵ ($= 1$) is the dielectric constant in vacuum. If these ions are in an aqueous solution, because of the rearrangement of the polar molecules around these ions, one needs to assign a new dielectric constant (ϵ_2) that is characteristic of this new medium. The net

Fig. 5.1.

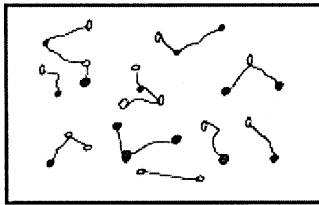
a. Dissolution of oxide



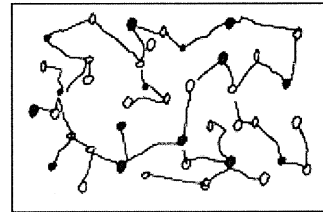
b. Formation of aquosols



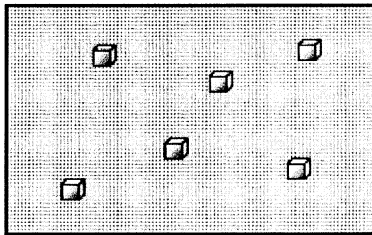
c. Acid-base reaction and condensation



d. Percolation and gel formation



e. Saturation and crystallization



Pictorial representation of formation of chemically bonded phosphate ceramic.

electrostatic energy change due to transfer of an ion from a medium of dielectric constant ϵ_1 to a medium of ϵ_2 is given by the Born equation:

$$\Delta G_0 = \frac{q^2}{4\pi r} \left(\frac{1}{\epsilon_2} - \frac{1}{\epsilon_1} \right) = \frac{q^2}{4\pi r} \left(\frac{1}{\epsilon} - 1 \right). \quad (5.12)$$

For the last expression in Eq. 5.12, $\epsilon_1 = 1$ and $\epsilon_2/\epsilon_1 = \epsilon$ for the second medium. In this case, the dielectric constant for water is 78, and Eq. 5.12 becomes

$$\Delta G_{\text{hydr}} = \frac{q^2}{4\pi r} \left(\frac{1}{78} - 1 \right) = -0.987 \frac{q^2}{4\pi r}. \quad (5.13)$$

Equation 5.13 implies that the electrostatic energy of an ion is reduced by 0.987 in an aqueous medium. In other words, an ion surrounded by rearranged polar molecules of water is equivalent to a new particle in water whose charge has been screened by the surrounding polar molecules of water, and as a result, its electrostatic energy is reduced by 0.987.

The Born equation for the solvation of ions provides a means of determining the hydration energy of a charge in an aqueous medium. When two ions in an aqueous medium react (as in the case of cations and anions in an acid–base reaction), the reaction may be considered as occurring between the dissociated ions whose energy is modified due to this hydration.

Equation 5.12 represents the simple case of screening of two point-charge ions. For a large number of molecules distributed in an aqueous medium, it is difficult to provide a detailed expression for the hydration energy. Nevertheless, Eq. 5.12 leads to the following useful conclusions:

1. For bigger ions, r is larger, and the hydration energy becomes less favorable.
2. For media such as organic liquids, ϵ is small compared to that of water. This implies that the energy in organic media is not as favorable as in water. Therefore, water is one of the most favorable media for acid–base reactions.

Though theoretically it is possible to use different solvents to dissolve oxides, we will consider only the formation of ceramics in an aqueous medium. For this reason, in our subsequent discussion, we assign the notation (aq) to the aqueous ions, implying that the electrostatic energy between the ions is to be reduced by the factor given in Eq. 5.13, and that single particles are to be treated with this modified electrostatic energy.

5.4.

KINETICS OF FORMATION OF CBPCs

Wagh and Jeong [4] have reported that, once the metal ions are dissociated and screened in an acid solution that is rich with phosphate anions, the kinetics of transformation to a CBPC is very similar to that of the conventional sol–gel process of fabricating ceramics of nonsilicates [4] with the major difference here being that the acid–base reaction used in forming CBPCs carries the mixture all the way to the formation of ceramics, while in the sol–gel process the sols are ultimately sintered to form superior ceramics. Figure 5.1 illustrates the step-by-step kinetics of the formation of CBPCs.

- (a) *Aquosol formation by dissociation.* When metal oxides are stirred into an acid solution, they dissolve slowly, and release cations and oxygen-containing anions (Fig. 5.1a, dissolution step). The cations react with water molecules and form positively charged “aquosols” by hydrolysis (Fig. 5.1b, hydration step). The dissolution and hydrolysis are the controlling steps in forming CBPCs and, hence, are discussed in detail in Section 5.5.

- (b) *Acid–base reaction and the formation of gel by condensation.* As illustrated in Fig. 5.1c, the sols subsequently react with the aqueous phosphate anions to form the hydrophosphate salts, while the protons and oxygen react to form water. As the oxide powder is stirred in water, more aquosols are formed in the solution and they start connecting to each other (Fig. 5.1c). This leads to the formation of a gel of loosely connected salt molecules (Fig. 5.1d).
- (c) *Saturation and crystallization of the gel into a ceramic.* As the reaction proceeds, this process introduces more and more reaction products into the gel, and it thickens. At this point, it becomes difficult to mix the slurry. The gel now crystallizes around the unreacted core of each grain of the metal oxide into a well-connected crystal lattice that grows into a monolithic ceramic (Fig. 5.1e).

The dissolution is the controlling step in the formation of the ceramic. It determines which oxides will form a ceramic and which will not, while the hydration step determines the pH range in which the ceramics will be formed. Formation of a well-crystallized ceramic or a poorly crystallized precipitate will depend on how slowly or rapidly the dissolution of the oxides occurs in the acid solution.

As stated before, the overall acid–base reaction is exothermic and heats the reaction slurry. To avoid excessive heating of the slurry, the reaction rate of the dissolved species should be slow. Thus, following are the two requirements for forming a well-crystallized CBPC.

1. The solubility of the oxides in the solution should be sufficiently high for the formation of a saturated gel, but at the same time, sufficiently low to allow slow crystallization of the gel.
2. The rate of exothermic heat production and hence dissolution rate of oxides should be sufficiently slow to allow the phosphate gel to crystallize slowly into a well-ordered crystal lattice without interruption, and grow into a monolithic ceramic.

These two requirements provide upper and lower limits on the solubility of the oxides. They are quantitatively formulated by using the thermodynamic properties of the oxides in the phosphate solution, which is discussed in Section 5.5.

5.5.

SOLUBILITY PRODUCT CONSTANT AND ITS pH DEPENDENCE

In Chapter 4, the ionization constant (i.e., the reaction constant of dissolution) for weak acids and acid phosphates was defined. The concept of the ionization constant is very general and useful while discussing dissolution of sparsely soluble oxides in acid–base reactions. We assign the symbol K for this constant.

Below we will discuss this constant when a sparsely soluble oxide is dissolved in a phosphoric acid solution. The same discussion may then be generalized to other phosphate solutions.

When an alkaline oxide such as MgO is stirred in phosphoric acid, the pH of the solution rises slowly due to the neutralization of this acid. Initially, the phosphoric acid has pH 0, but initial dissolution of the oxide and reaction with phosphate anions precipitate phosphate salts. This neutralization of the acid raises the pH of the solution to >2 . Even in this pH range, the acid dissolves sufficiently, and protons and H_2PO_4^- anions are readily available to react with the ions produced by the dissolution of metal oxides. Subsequently, consolidation of the precipitate in the neutral solution leads to the formation of ceramics.

Consider the dissolution of a metal M as given by reaction 5.3. The ionization constant K for this reaction is defined as

$$K_x = \frac{\langle \text{M}^{2x+}(\text{aq}) \rangle \langle \text{H}^+ \rangle^{2x}}{\langle \text{H}_2\text{O} \rangle^x \langle \text{MO}_x \rangle}. \quad (5.14)$$

As before, angle brackets indicate molar concentration of individual species. In Eq. 5.14, K_x is a quantitative measure of the amount of dissolution of a particular oxide and, hence, the extent of its ionization. This quantity determines whether a particular oxide satisfies the condition of slow dissolution and will form CBPC in a given pH range. We will explore K_x in detail using the thermodynamics of dissolution reactions in Chapter 6, but here we will study its pH dependence.

To determine the pH dependence of K_x , take the logarithm of both sides of Eq. 5.14. We obtain

$$\log K_x = \log \left[\frac{\langle \text{M}^{2x+}(\text{aq}) \rangle}{\langle \text{MO}_x \rangle} + x \log \frac{\langle \text{H}^+ \rangle^2}{\langle \text{H}_2\text{O} \rangle} \right]. \quad (5.15)$$

As was done before with the ionization constant, we can start with one mole of the oxide, so that Eq. 5.15 can be normalized to $\langle \text{MO}_x \rangle = 1$. Furthermore

$$-\log[\langle \text{H} \rangle / \langle \text{H}_2\text{O} \rangle^{1/2}] = \text{pH}. \quad (5.16)$$

Thus, we obtain from Eqs. 5.15 and 5.16

$$\log K_x = \log \langle \text{M}^{2x+} \rangle - 2xp\text{H}. \quad (5.17)$$

For a given reaction in equilibrium, K_x is a constant. It is customary to express Eq. 5.17 as

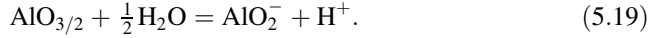
$$-\log \langle \text{M}^{2x+} \rangle = pK_{\text{sp}} - 2xp\text{H}, \quad (5.18)$$

where $pK_{\text{sp}} = -\log K_x$, that is the negative logarithm of the solubility product of the oxide. Equation 5.18 gives the pH dependence of the oxide solubility.

The quantity pK_{sp} is called “solubility product constant” or simply “solubility product”. It indicates the extent of dissolution of a particular chemical species in a given solution. Appendix C gives values of pK_{sp} for many useful oxides and minerals.

In several oxides, such as MgO, the solubility decreases as the pH increases and it eventually becomes insignificant in an alkaline region. However, oxides such as Al_2O_3 have significant solubility in both acidic and alkaline regions. Such oxides are called “amphoteric.” For these oxides, it is necessary to extend the definition of pK_{sp} even in an alkaline region. For example, in the case of Al_2O_3 , the following dissolution reaction in

the highly alkaline region yields AlO_2^-



The corresponding ionization constant is

$$K'' = \frac{\langle \text{AlO}_2^- \rangle \langle \text{H}^+ \rangle}{\langle \text{AlO}_{3/2} \rangle \langle \text{H}_2\text{O} \rangle} \quad (5.20)$$

or

$$-\log \langle \text{AlO}_2^- \rangle = \text{p}K'_{\text{sp}} - \text{pH}. \quad (5.21)$$

This relation is for one mole of $\text{AlO}_{3/2}$.

In the acid–base reactions that form ceramics, this alkaline region is of little interest to us, because the reaction products that constitute the ceramic are neutral, and hence, the reaction is not driven to the alkaline side. We will not elaborate on the reactions in alkaline regions, except in waste management applications in Chapters 16 and 17, where we discuss the stability of CBPC products in highly alkaline waters.

Table 5.1 displays dissolution reactions for oxides and hydroxides whose ceramics have potential practical applications. Also included is the pH range in which these reactions are valid. The pH range can be derived by the method described above, or as was done in Chapter 4, it can be calculated by equating the two subsequent equations at the transition boundary where these equations are equally valid. This table shows only the dissolution equations that are valid in acidic and neutral pH. For details covering the entire pH range and general discussions, the reader is referred to Ref. [5].

As noted during the discussion on the ionization constant of soluble phosphates in Chapter 4, the reactions provided in Table 5.1 are valid for all pH ranges for a given oxide, but the concentration of only one ionic species dominates in a given pH range. Thus, different ions in varying concentrations commonly coexist at any pH. In practice, in a given pH range, the lower concentrations are so small that, for practical applications, one may simply ignore them and consider only the dominant one.

Using the relations given in Table 5.1, along with similar equations for FeO and ZnO in the alkaline regions, the ionic concentrations are plotted as a function of pH in Fig. 5.2 for the major oxides of practical interest. The choice of these oxides (and similarly hydroxides) is dictated by the fact that they are starter powders in syntheses of common commercial CBPC products. One may make the following observations from Fig. 5.2:

1. Solubility of MgO, CaO, and Fe_2O_3 decreases as the pH increases, while the rest of the oxides show an amphoteric nature, i.e., their solubility has a minimum in between the entire pH range and increases at lower as well as higher pH.
2. Oxides are less soluble than hydroxides, but their solubility differs only slightly when compared with corresponding oxides.
3. Trivalent oxides are far more insoluble than divalent oxides. Quadrivalent oxides have negligible solubility. Exceptions exist to this rule, but this is a general trend.

Several inferences may be drawn from Eq. 5.18 and the data given in Table 5.1 as well as Fig. 5.2. For example, for $\text{p}K'_{\text{sp}} - (2n)\text{pH} > 0$, $\langle \text{M}^{2n+}(\text{aq}) \rangle$ will be very large, implying

Table 5.1.

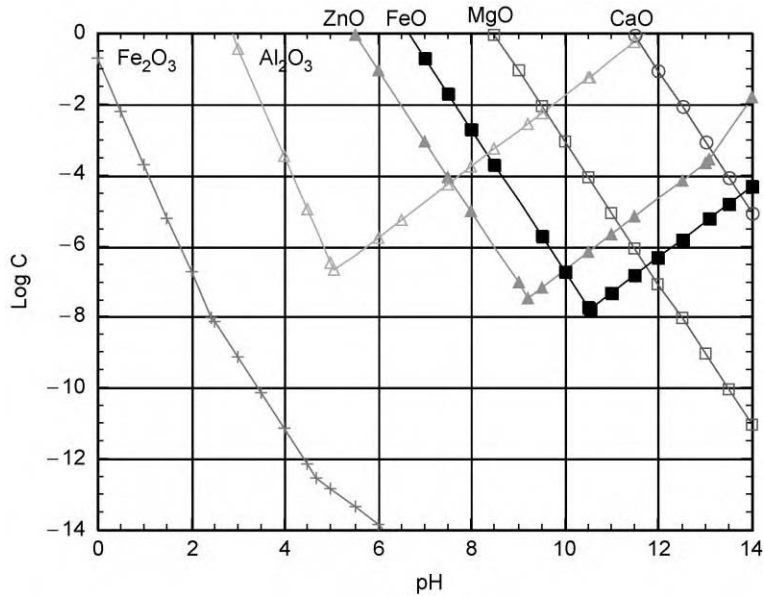
Dissolution Reactions and Related Constants for Oxides of Interest.

Oxide	Dissolution Equation	pH Range for Dominance of Ions
MgO	$\log[\text{Mg}^{2+}(\text{aq})] = 16.93 - 2\text{pH}$	Alkaline ^a
$\text{Mg}(\text{OH})_2$	$\log[\text{Mg}^{2+}(\text{aq})] = 21.68 - 2\text{pH}$	
CaO	$\log[\text{Ca}^{2+}(\text{aq})] = 22.91 - 2\text{pH}$	Highly alkaline ^a
$\text{Ca}(\text{OH})_2$	$\log[\text{Ca}^{2+}(\text{aq})] = 32.63 - 2\text{pH}$	
Al_2O_3 (Corundum)	$\log[\text{Al}^{3+}(\text{aq})] = 8.55 - 3\text{pH}$	$\text{pH} < 5.055$
$\text{Al}_2\text{O}_3 \cdot 3\text{H}_2\text{O}$ (hydrargillite)	$\log[\text{Al}^{3+}(\text{aq})] = 5.7 - 3\text{pH}$	$\text{pH} < 5.055$
$\text{Al}_2\text{O}_3 \cdot 3\text{H}_2\text{O}$ (bayerite)	$\log[\text{Al}^{3+}(\text{aq})] = 6.48 - 3\text{pH}$	$\text{pH} < 5.055$
$\text{Al}_2\text{O}_3 \cdot 3\text{H}_2\text{O}$ (boehmite)	$\log[\text{Al}^{3+}(\text{aq})] = 7.98 - 3\text{pH}$	$\text{pH} < 5.055$
$\text{Al}(\text{OH})_3$	$\log[\text{Al}^{3+}(\text{aq})] = 9.66 - 3\text{pH}$	$\text{pH} < 5.055$
Al_2O_3 (Corundum)	$\log[(\text{AlO}_2)^-(\text{aq})] = -11.76 + \text{pH}$	$\text{pH} > 5.055$
$\text{Al}_2\text{O}_3 \cdot 3\text{H}_2\text{O}$ (hydrargillite)	$\log[(\text{AlO}_2)^-(\text{aq})] = -14.6 + \text{pH}$	$\text{pH} > 5.055$
$\text{Al}_2\text{O}_3 \cdot 3\text{H}_2\text{O}$ (bayerite)	$\log[(\text{AlO}_2)^-(\text{aq})] = -13.82 + \text{pH}$	$\text{pH} > 5.055$
$\text{Al}_2\text{O}_3 \cdot 3\text{H}_2\text{O}$ (boehmite)	$\log[(\text{AlO}_2)^-(\text{aq})] = -12.32 + \text{pH}$	$\text{pH} > 5.055$
$\text{Al}(\text{OH})_3$	$\log[(\text{AlO}_2)^-(\text{aq})] = -10.64 + \text{pH}$	$\text{pH} > 5.055$
FeO	$\log[\text{Fe}^{2+}(\text{aq})] = 13.29 - 2\text{pH}$	$0 < \text{pH} < 10.53$
Fe_2O_3 (hematite)	$\log[\text{Fe}^{3+}(\text{aq})] = -0.72 - 3\text{pH}$	$\text{pH} < 2.53$
$\text{Fe}(\text{OH})_3$	$\log[\text{Fe}^{3+}(\text{aq})] = 4.84 - 3\text{pH}$	
Fe_2O_3 (hematite)	$\log[\text{FeOH}^{2+}(\text{aq})] = -3.15 - 2\text{pH}$	$2.53 < \text{pH} < 4.69$
$\text{Fe}(\text{OH})_3$	$\log[\text{FeOH}^{2+}(\text{aq})] = -2.41 - 2\text{pH}$	
Fe_2O_3 (hematite)	$\log[\text{Fe}(\text{OH})_2^+(\text{aq})] = -7.84 - \text{pH}$	$\text{pH} > 4.69$
$\text{Fe}(\text{OH})_3$	$\log[\text{Fe}(\text{OH})_2^+(\text{aq})] = -2.28 - \text{pH}$	
ZnO	$\log[\text{Zn}^{2+}] = 10.96 - 2\text{pH}$	$\text{pH} < 9.21$
$\text{Zn}(\text{OH})_2$	$\log[\text{Zn}^{2+}] = 12.26 - 2\text{pH}$	$\text{pH} < 9.21$

^a Dissolution for these compounds is spontaneous in acidic range.

rapid dissolution of the oxide. For controlled dissolution of the oxide and formation of a ceramic, $(2n)\text{pH}$ must be $> \text{p}K_{\text{sp}}$. Thus, the minimum pH (pH_{min}) for the formation of a ceramic is $\text{pH}_{\text{min}} = \text{p}K_{\text{sp}}/2n$. Note that CaO in the third equation in Table 5.1 does not satisfy this condition in the acidic region, because $\text{pH}_{\text{min}} = 11.45$ and lies in the highly alkaline region. It is thus not possible to form ceramics of Ca by an acid–base reaction. For this reason, ceramics have not been produced by using CaO, though successful ceramics have been produced with compounds such as CaSiO_3 . In the case of MgO, $\text{pH}_{\text{min}} = 8.46$, which is still in the alkaline region. Thus, MgO cannot be used to produce ceramics at least in a significantly large size. However, calcined MgO exhibits lower solubility even in the acidic region, and has been used to produce ceramics. Detailed discussion of calcination of MgO and its effect can be found in Chapter 9. For ZnO, $\text{pH}_{\text{min}} = 5.48$, which is in the mild acidic range. This oxide is the most suitable for forming a ceramic, and it may be for this reason, that zinc phosphate ceramic was the first dental cement. Details of zinc phosphate ceramics are provided in Chapter 10.

Fig. 5.2.



Solubility versus pH of several candidate oxide materials.

Trivalent oxides, such as Al_2O_3 and Fe_2O_3 , satisfy the condition that $(2n)\text{pH} \geq \text{p}K_{\text{sp}}$, but the solubility of Al_2O_3 or Fe_2O_3 is too low to form a ceramic. Chapters 11 and 12 will describe methods of enhancing the solubility of these oxides, either by mild heat treatment or by partially reducing the oxide to its lower oxidation state, such as FeO , and forming the ceramic.

REFERENCES

1. J. Wescott, R. Nelson, A. Wagh, and D. Singh, "Low Level and Mixed Radioactive Waste In-Drum Solidification," *Practice Periodical of Hazardous, Toxic, and Radioactive Waste Management*, Am. Soc. Civil Eng. Reston, VA. 2 [1] (1998) 4–7.
2. C.J. Brinker and G.W. Scherer, *Sol–Gel Science* (Academic Press, London, 1989), Chapters 1 and 4.
3. C. Kittel, *Introduction to Solid State Physics*, 7th ed. (Wiley, New York, 1996), Chapter 13.
4. A.S. Wagh and S.Y. Jeong, "Chemically bonded phosphate ceramics. I. A dissolution model of formation," *J. Am. Ceram. Soc.*, **86** (2003) 1838–1844.
5. M. Pourbaix, *Atlas of Electrochemical Equilibria in Aqueous Solutions* (NACE (Houston) and Cebelcor, Brussels, 1974).

Thermodynamic Basis of CBPC Formation

Thermodynamics is the basis of all chemical transformations [1], which include dissolution of chemical components in aqueous solutions, reactions between two dissolved species, and precipitation of new products formed by the reactions. The laws of thermodynamics provide conditions in which these reactions occur. One way of determining such conditions is to use thermodynamic potentials (i.e., enthalpy, entropy, and Gibbs free energy of individual components that participate in a chemical reaction) and then apply the laws of thermodynamics. In the case of CBPCs, this approach requires relating measurable parameters, such as solubility of individual components of the reaction, to the thermodynamic parameters. Thermodynamic models not only predict whether a particular reaction is likely to occur, but also provide conditions (measurable parameters such as temperature and pressure) in which ceramics are formed out of these reactions. The basic thermodynamic potentials of most constituents of the CBPC products have been measured at room temperature (and often at elevated temperatures) and recorded in standard data books. Thus, it is possible to compile these data on the starter components, relate them to their dissolution characteristics, and predict their dissolution behavior in an aqueous solution by using a thermodynamic model. The thermodynamic potentials themselves can be expressed in terms of the molecular behavior of individual components forming the ceramics, as determined by a statistical–mechanical approach. Such a detailed study is beyond the scope of this book.

A thermodynamic model of dissolution is presented in this chapter, which relates the solubility product constant to the thermodynamic potentials and measurable parameters, such as temperature and pressure of the solution. The resulting relations allow us to develop conditions in which CBPCs are likely to form by reactions of various oxides (or minerals) with phosphate solutions. Thus, the model predicts formation of CBPCs.

6.1.

REVIEW OF BASIC THERMODYNAMIC RELATIONS

Consider a collection of one mole of particles of chemical species completely isolated from its surroundings (clearly an idealized situation) and hence maintained at an absolute scale temperature T and pressure P . These particles may themselves be in motion, as happens with gas particles. In the case of a crystalline solid, the molecules of individual particles that are at the lattice points may be vibrating with respect to a mean lattice point or might even be rotating about some axis. Each linear, vibrational, and rotational motion contributes to the kinetic energy of individual particles and hence to the total energy of the collected particles. The sum of this energy is the internal heat energy assigned to the collection of the particles and is measured in joules per mole. If such an isolated system of particles is brought in contact with its surroundings, heat will exchange between the system and the surroundings. This exchange will result in mechanical work on the system or by the system. The heat exchange, Q , the internal energy, U , and the work, W , are related by the second law of thermodynamics

$$dQ = dU - dW. \quad (6.1)$$

In gases, dW is due to volume (V) expansion of the gas that occurs against the pressure P on the system. Hence, one may write $dW = -P dV$. In liquids and solids, this volume change is negligible, and much of the energy supplied will be stored in the substance as the internal energy. Depending on the heat stored in the system, the temperature will change. This temperature (T) in absolute scale is given by

$$T = \frac{dS}{dQ}, \quad (6.2)$$

where S represents entropy, a measure of disorder within the system and its interacting surroundings. Chemical reactions, such as dissolution of oxides, either convert the chemical species into their constituent ions, or the number of moles of a particular species (N) within the system. To incorporate such chemical changes, the second law of thermodynamics (Eq. 6.1) may be generalized as

$$T dS = dU + P dV - \mu dN, \quad (6.3)$$

where μ is the chemical potential. Equation 6.3 is the basis for discussion of solubility and chemical reactions that form CBPCs. To facilitate this discussion, the thermodynamic potentials are defined as follows: enthalpy,

$$H = U + PV = TS + \mu N \quad (6.4)$$

and Gibbs free energy

$$G = H - TS. \quad (6.5)$$

These definitions must be consistent with the second law of thermodynamics given by Eq. 6.3, and thus the second law imposes conditions on Eqs. 6.4 and 6.5. These conditions

are derived by differentiating both sides of Eq. 6.4:

$$dH = dU + P dV + V dP = T dS + S dT + \mu dN + N d\mu. \quad (6.6)$$

Substituting Eq. 6.3 into Eq. 6.6, we have the condition

$$V dP - S dT - N d\mu = 0. \quad (6.7)$$

Equation 6.7 is one of the Gibbs–Duhem relations. Substituting for dH from Eq. 6.6 in the equation obtained by differentiating both sides of Eq. 6.5, we can show that

$$G = \mu N. \quad (6.8)$$

Thus, G is the product of molar concentration of a component participating in the reaction and its chemical potential.

The thermodynamic potentials G , H , S , and U are further supplemented by properties of the system that are measurable. These are given by the following: specific heat at constant pressure

$$C_p(T) = \left(\frac{\partial H(T)}{\partial T} \right)_P, \quad (6.9)$$

compressibility

$$\kappa_T = - \left(\frac{1}{V} \right) \left(\frac{\partial V}{\partial P} \right)_P, \quad (6.10)$$

and thermal expansion coefficient

$$\alpha = \left(\frac{1}{V} \right) \left(\frac{\partial V}{\partial T} \right)_P. \quad (6.11)$$

For CBPCs, we deal with solids and liquids for which both α and κ_T are very small. Therefore, both of these parameters are negligible in most of our discussions.

It is now necessary to decide a proper scale for these thermodynamic potentials. According to the third law of thermodynamics, at absolute zero ($T = 0$ K), all the thermodynamic parameters are zero and hence the terms defined above have meaning only when they are measured as changes that occur between $T = 0$ K and the temperature of the system. In practice, we are concerned about the change in the state of a system in a chemical reaction, i.e., before and after the reaction, and hence need to determine changes in Gibbs free energy (ΔG), enthalpy (ΔH), and internal energy (ΔU). It is convenient to measure these quantities at standard pressure, P_0 (1 atm), and temperature, T_0 (25°C or 298 K). Data books report these thermodynamic parameters at T_0 and P_0 . For some of the important oxides, phosphates, and ions that are useful for discussions of CBPCs, values for ΔG_0 , ΔH_0 , and $C_p(T_0)$ are given in Appendix B.

The definitions given above are for a single species. Consider now a chemical reaction, such as any of the reactions discussed in previous chapters, that involves several species as reactants and form several reaction products. The net change in the Gibbs free energy in the entire reaction (ΔG) is given by the difference between the sum of Gibbs free energies

of reaction products (ΔG_f) and sum of Gibbs free energies of the reactants (ΔG_i). Thus

$$\Delta G = \Delta G_f - \Delta G_i. \quad (6.12)$$

We represent the net change of a thermodynamic parameter in a chemical reaction by, say, ΔG and individual component by subscripted letters.

6.2.

THERMODYNAMICS OF SOLUBILITY REACTIONS

As may be seen from Eq. 6.8, the Gibbs free energy, G , is the most important thermodynamic parameter in describing chemical reactions, because it represents the moles of the constituents participating in the reaction, and how a chemical reaction changes the number of moles. Dependence of a chemical reaction on thermodynamic parameters, such as the temperature and pressure, is best represented by ΔG in an Arrhenius type of equation for the dissolution constant K

$$K = \exp \beta(-\Delta G), \quad (6.13)$$

where $\beta = (RT)^{-1}$. R is the gas constant, given by $R = 8.31 \text{ J/mol}$. Following the notation used in Chapter 5 for the solubility product constant, pK_{sp} (see Eq. 5.18), we can now write

$$pK_{sp} = -\log K = \left(\frac{\beta}{2.301} \right) \Delta G. \quad (6.14)$$

Thus, Eq. 5.18 for an acidic medium becomes

$$-\log \langle M^{2+x}(\text{aq}) \rangle = \left(\frac{\beta}{2.301} \right) \Delta G + (2x)\text{pH}. \quad (6.15)$$

Using Eqs. 6.12 and 6.5, we can write

$$\Delta G = \Delta G_f - \Delta G_i = \Delta H - T\Delta S = \Delta H_f - \Delta H_i - T(\Delta S_f - \Delta S_i), \quad (6.16)$$

where ΔG determines the direction of a chemical reaction. For example, if ΔG is negative, or the total Gibbs free energy of the reaction products is smaller than that of the reactants, the reaction will go forward or the reactants will react and form products. On the other hand, if it is greater, then the reaction will go in the reverse direction. In the event that the total Gibbs free energy of both sides is the same, the reaction is in chemical equilibrium in which the reactants and reaction products will react equally such that there is no net gain or loss of the components on either side. Mathematically, we may write these conditions as

$$\Delta G < 0 \quad \text{for a spontaneous reaction}, \quad (6.17)$$

$$\Delta G > 0 \quad \text{for a nonspontaneous reaction}, \quad (6.18)$$

and

$$\Delta G = 0 \quad \text{for a chemical equilibrium}. \quad (6.19)$$

These relations reveal the nature of chemical reactions involved in formation of CBPCs, which include dissolution of oxides and acid phosphates, and their subsequent acid–base reaction to form ceramics. Therefore, the Gibbs free energy plays an important role in determining which reactions (and hence which components) are most suitable in forming ceramics.

Another important thermodynamic parameter implicit in the above relations is the net change in the enthalpy, ΔH . It is a measure of the heat generated or absorbed during a chemical reaction. Following the notation of Eq. 6.12, we can write it as

$$\Delta H = \Delta H_f - \Delta H_i. \quad (6.20)$$

In most CBPC fabrication processes, the pressure is a constant, but the temperature of the system changes due to evolution or absorption of heat. In such cases, following Eq. 6.9, we obtain

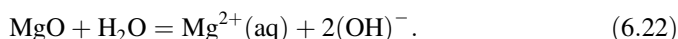
$$\Delta C_p = \left(\frac{\partial \Delta H}{\partial T} \right)_p, \quad (6.21)$$

where ΔC_p represents the net difference in the specific heat at constant pressure between the reaction products and the reactants in a given chemical reaction. This equation is useful in estimating heat generated during an exothermic reaction in formation of CBPCs.

6.3.

APPLICATIONS OF THERMODYNAMIC PARAMETERS TO CBPC FORMATION

Because the CBPC process is based on slow dissolution of the components, spontaneous dissolution of oxides is not desirable in the ceramic formation. This implies that Eq. 6.18 is a requirement for a dissolution reaction that is useful in forming a ceramic. Consider, for example, dissolution of MgO in a neutral medium given by Eq. 5.9c



The ΔG values of individual components participating in these reactions may be obtained from Appendix B, and are -569.57 , -238.59 , -456.01 , and -157.3 kJ/mol for MgO, H₂O, Mg²⁺(aq), and (OH)[−], respectively. These values yield $\Delta G = 37.55$ kJ/mol, a nonspontaneous reaction. For this reason, MgO can be directly used to form a ceramic in a near neutral medium. If, however, the same is calculated in an acidic medium using Eq. 5.9a, we obtain a spontaneous reaction, because $\Delta G = -125.03$ kJ/mol. For this reason, one cannot use phosphoric acid for making CBPC products of Mg without some neutralization. The same is true for most divalent metal oxides.

Note that dissolution of acid phosphates is an endothermic reaction that cools the slurry, while the subsequent reaction between dissolved ions is an exothermic reaction. The net acid–base reaction is, however, exothermic and generates heat. In the case of formation of MgKPO₄·6H₂O, for example, the initial cooling of the ceramic is significant and aids in

reducing the total heat generated in forming the ceramic. Consider the dissolution equation for KH_2PO_4 as given in Table 4.2



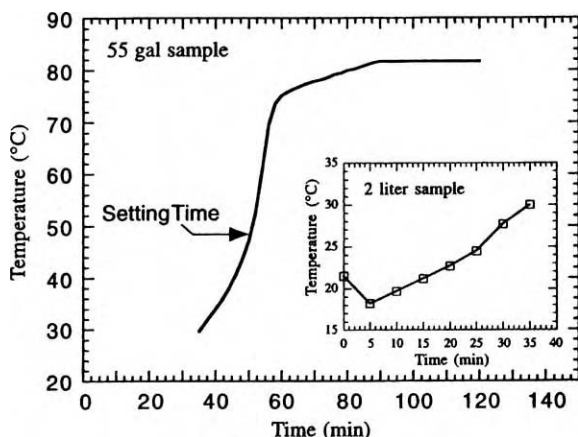
The ΔH values for KH_2PO_4 , K^+ , and H_2PO_4^- are -1570.7 , -252.4 , and -1292.1 kJ/mol, respectively (see Appendix B). With these values, ΔH equals 26.2 kJ/mol, a positive quantity implying that heat is needed for this reaction to proceed, or heat is absorbed from the surroundings. In contrast, consider the complete reaction given by



The ΔH values for MgO , KH_2PO_4 , H_2O , and $\text{MgKPO}_4 \cdot 6\text{H}_2\text{O}$ are -601.6 , -1570.7 , -236.73 , and -3724.3 kJ/mol, yielding $\Delta H = -368.35$ kJ/mol. Hence, heat is rejected during this reaction, implying an exothermic reaction process. This total exothermic quantity is much higher than the endothermic heat absorbed during the dissolution, but during the process, a small amount of cooling helps in extending the process time, and that increase is important in terms of rapid-setting.

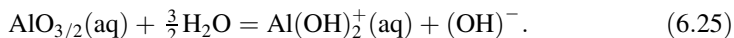
To evaluate the extent of the cooling during the dissolution of KH_2PO_4 , the temperature of the mixture of MgO , KH_2PO_4 , and H_2O was monitored at the 55-gal drum scale [2]. Figure 6.1 shows the temperature as a function of time during mixing of the slurry. Initially, the slurry cools by $\approx 3^\circ\text{C}$ in 10 min, during which KH_2PO_4 dissolves and makes the slurry slightly acidic. The acidic solution dissolves MgO partially, and the acid–base reaction takes off. During this time, as evident from Fig. 6.1, the temperature rises and reaches to $\approx 82^\circ\text{C}$. The entire slurry, however, sets at 55°C , and the ceramic heats up afterwards. Because of this setting behavior, this process can be used to make large products without boiling the slurry.

Fig. 6.1.



Temperature variation with time during setting of soil in magnesium potassium phosphate-based ceramic at 55-gal scale. The inset shows the same at 2-L volume.

In addition to the direction of reaction, ΔG also indicates whether the solubility of a given oxide will be adequate. Consider, for example, the case of dissolution of alumina. Its dissolution reaction in a neutral region is given by Eq. 5.10d



Calculations show that ΔG for this reaction is 188.02 J/mol, which is considerably larger than that for the dissolution of MgO. This calculation implies that a significant amount of heat will be required to dissolve alumina; hence, it will not dissolve on its own. Therefore, it may not be possible to develop a ceramic with alumina unless its solubility is enhanced by providing heat. A method of solubility enhancement at warm temperatures ($< 200^\circ\text{C}$) is discussed in Chapter 11.

The conditions under which spontaneous reactions can occur are listed below:

- 1) $\Delta H < 0$, $\Delta S > 0$, spontaneous at all temperatures.
- 2) $\Delta H > 0$, $\Delta S > 0$, spontaneous at high temperatures, where $\Delta G < 0$; otherwise, nonspontaneous.
- 3) $\Delta H < 0$, $\Delta S < 0$, spontaneous at low temperatures, where $\Delta G < 0$; otherwise nonspontaneous.
- 4) $\Delta H > 0$, $\Delta S < 0$, nonspontaneous at all temperatures.

The first condition implies that for a dissolution reaction to be useful, ΔH cannot be negative, and at the same time ΔS cannot be positive, and the fourth condition should be satisfied.

Consider the case of dissolution of MgO given by Eq. 6.22. ΔH and ΔS in this case are, respectively, -77.67 kJ/mol and -272.2 J/mol/K. These numbers will satisfy the third condition, so dissolution will be nonspontaneous at low temperatures, but can be spontaneous at higher temperatures. To form a good ceramic at a large scale, the temperature for Eq. 6.22 needs to be controlled such that it will not only maintain a nonspontaneous dissolution reaction but will also prevent water from boiling. As mentioned before, the whole ceramic sets at 55°C , and hence this condition is easily satisfied.

The example of MgO represents most of the candidate oxides because they have negative ΔS_0 and exhibit an exothermic dissolution reaction. Exceptions include oxides of the monovalent alkaline metals such as Na, K, and Cs, and a few higher valent metals. Since the hydroxyl ion also has a negative ΔS_0 , the dissolution reactions of the MgO-like oxides satisfy $\Delta S < 0$ and conform to the third condition; and hence, these oxides will exhibit nonspontaneous dissolution at low temperatures but may be spontaneous at high temperatures.

6.4.

TEMPERATURE DEPENDENCE OF SOLUBILITY PRODUCT CONSTANT

During the formation of CBPCs, because of the exothermic acid–base reaction, the temperature of the reacting aqueous solution rises. This subsequently increases the dissolution

of additional oxides into the solution and affects the overall formation of the ceramics. In certain cases, such as alumina, a heat treatment is, in fact, used to enhance the dissolution rate of the oxide (see Chapter 11). In addition, as described in Chapter 15, when CBPCs are used as drilling cements, they are pumped in oil and gas wells where the downhole temperature can be as high as 150°C. In geothermal wells, the temperature can be even higher. Thus, certain applications of CBPCs require ceramic formulations that set at higher temperatures. To gain an insight into such formulations, one needs to know the temperature dependence of the solubility product constant of the dissolving oxides.

Consider first the temperature dependence of the Gibbs free energy. We can write from Eq. 6.5

$$\left(\frac{\partial \Delta G}{\partial T}\right)_P = -\Delta S = \frac{\Delta G - \Delta H}{T}. \quad (6.26)$$

This equation, known in thermodynamics as one of the Gibbs–Helmholtz equations, allows us to calculate the temperature dependence of pK_{sp} . Differentiating K in Eq. 6.13 with T , we obtain at constant pressure

$$\left(\frac{\partial K}{\partial T}\right)_P = \frac{K}{R} \left[-\frac{1}{T} \left(\frac{\partial \Delta G}{\partial T}\right)_P + \frac{\Delta G}{RT^2} \right] = \frac{K\Delta H}{RT^2}. \quad (6.27)$$

Eq. 6.27 implies that K will increase or decrease with temperature depending on the sign of ΔH , i.e., if $\Delta H > 0$ (endothermic dissolution reaction), K will increase, while for $\Delta H < 0$ (exothermic dissolution reaction), K will decrease.

For divalent oxides, the dissolution reaction is exothermic, and hence K decreases as the temperature increases. As we shall see later, oxides such as MgO conform to this behavior in the acidic region. For Al_2O_3 , however, K initially increases and then decreases; thus there is a K maximum at a certain temperature. That temperature, T_m , may be calculated as follows:

$$\left(\frac{\partial K_{sp}}{\partial T}\right)_P = 0 \quad \text{at } T = T_m. \quad (6.28)$$

From Eq. 6.27,

$$\Delta H = 0 \quad \text{at } T = T_m. \quad (6.29)$$

Equation 6.28 implies that pK_{sp} is a maximum at $T = T_m$. As a result, if the reaction slurry is heated to T_m , the solubility of the oxide in the slurry will reach a maximum. As we shall see in Chapter 11, ceramics of some trivalent oxides, such as alumina, can be formed by reacting them at T_m .

The actual dependence of pK_{sp} on the temperature is rather complicated because of the dependence of the specific heat C_p on T , which is given by Debye's theory of specific heat for the reacting oxides and corresponding lattice dynamical model for crystalline solids. Simple assumptions regarding the net change in specific heats of the components involved in the dissolution reactions, however, allow one to avoid these complications [3].

The enthalpy and the entropy change for a system not subjected to any external forces, such as electrical or magnetic forces, and not undergoing any significant volume change,

are given in terms of the specific heat by

$$\Delta H(T) = \int_0^T \Delta C_p(T) dT, \quad (6.30)$$

and

$$\Delta S(T) = T \int_0^T \frac{\Delta C_p(T)}{T} dT. \quad (6.31)$$

Since for most solids and ions, the thermodynamic parameters at standard temperature ($T_0 = 298$ K) and pressure ($P_0 = 1$ MPa) are listed in data books, it is convenient to express Eqs. 6.30 and 6.31 in terms of T_0 and P_0 . For T_0 ,

$$\Delta H(T) = \Delta H_0 + \Delta T \int_{T_0}^T \Delta C_p(T) dT, \quad (6.32)$$

and

$$\Delta S(T) = \Delta S_0 + \int_{T_0}^T \frac{\Delta C_p(T)}{T} dT. \quad (6.33)$$

Here, ΔH_0 and ΔS_0 are changes in the standard enthalpy and entropy, respectively. For ceramics synthesized at warm temperature ranges (typically $T < 200^\circ\text{C}$ or 473 K), we can assume that

$$\Delta C_p(T) \approx \Delta C_p(298) = \text{constant}. \quad (6.34)$$

Integrating the right-hand sides of Eqs. 6.32 and 6.33, we obtain

$$\Delta H(T) = \Delta H_0 + \Delta C_p(T - 298), \quad (6.35)$$

and

$$\Delta S(T) = \Delta S_0 - \Delta C_p \ln\left(\frac{T}{298}\right). \quad (6.36)$$

Combining Eqs. 6.28, 6.29, and 6.35, we conclude that the solubility will be a maximum at

$$\Delta H(T) = \Delta H_0 + \Delta C_p(T - 298) = 0$$

or

$$T_m = 298 + \frac{\Delta H_0}{\Delta C_p(298)}. \quad (6.37)$$

This equation may be used to determine the temperature of maximum solubility. At this temperature, it should be possible to dissolve trivalent oxides in a phosphate solution and form a ceramic.

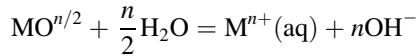
Substituting $\Delta H(T)$ and $\Delta S(T)$ from Eqs. 6.35 and 6.36 into Eq. 6.16, one can now write the Gibbs free energy as

$$\Delta G = \Delta G_0 - 298\Delta C_p + \Delta C_p T - \Delta C_p \ln\left(\frac{T}{298}\right). \quad (6.38)$$

This equation can be used to write the temperature dependence of the solubility product constant pK_{sp} . Thus, ΔH_0 , ΔS_0 , and the specific heats from the data books can be used to calculate the thermodynamic parameters as well as the solubility product constant. Consequently, by manipulating the processing temperature of a CBPC, one can solubilize the starter oxides.

The above discussion emphasizes the importance of the thermodynamic parameters of metal oxides and their cations in forming CBPCs. In general, the thermodynamic parameters of the metal oxides are easily available in data books, while those of the solvated ions may be found with some literature search. Those relevant to this book are listed in Appendix A.

The specific heats of aqueous ions of several metals are not readily available in the literature. As a result, it is difficult to determine the temperature dependence of the thermodynamic quantities and, hence, that of the solubility product constants for these metal oxides. This dependence can be roughly determined from the general dissolution equation



and

$$\Delta C_p = nC_p(OH^-) - \frac{n}{2}C_p(H_2O) + C_p(M^{n+}) - C_p(MO^{n/2}). \quad (6.39)$$

Since the specific heat of the hydroxyl ion $(OH)^-$ is very high as compared to the expected specific heats of the metal oxides or ions, and the specific heat of water is also comparatively high, the last two terms of the right-hand side of Eq. 6.39 can be ignored; thus

$$\Delta C_p = nC_p(OH^-) - \frac{n}{2}C_p(H_2O) = -185.175n \text{ (J/mol/K)}. \quad (6.40)$$

This equation works best for trivalent ($n = 3$) and quadrivalent ($n = 4$) oxides in the acidic region when CBPCs are formed by a thermal treatment. Substituting for ΔC_p from Eq. 6.40 in Eqs. 6.35 and 6.36, we obtain

$$\Delta H(T) = \Delta H_0 - 185.175n(T - 298), \quad (6.41)$$

$$\Delta S(T) = \Delta S_0 + 185.175n \ln\left(\frac{T}{298}\right). \quad (6.42)$$

Hence,

$$\Delta G = \Delta G_0 + 55,182n - 185.175nT + 185.175n \ln\left(\frac{T}{298}\right). \quad (6.43)$$

Substituting Eq. 6.43 into Eq. 6.14 gives the temperature dependence of K

$$pK_{sp} = -\log K = -\frac{\Delta G_0}{19.12T} - 2883.14n + 9.68nT - \frac{9.68n}{T} \ln\left(\frac{T}{298}\right). \quad (6.44)$$

Equation 6.44 provides the temperature dependence of the solubility product constant for a solubilization reaction valid in a highly acidic region for trivalent and quadrivalent oxides.

6.5.

PRESSURE DEPENDENCE OF SOLUBILITY PRODUCT CONSTANTS

The pressure dependence of the solubility product constant should arise from the enthalpy dependence on the pressure:

$$\Delta H = \Delta U + P\Delta V. \quad (6.45)$$

Hence

$$\Delta G = \Delta H - T\Delta S = \Delta U + P\Delta V - T\Delta S, \quad (6.46)$$

where ΔV is the change in the volume of the slurry during solubilization reactions. In practice, solubilization of metal oxides or that of acid phosphates does not increase the volume of the slurry significantly; thus, ΔV is always negligibly small. An exception occurs when there is a gas evolution due to simultaneous acid–base reactions, such as decomposition of carbonates. Such cases are irrelevant to the discussion of CBPC formation, however, because gas evolution interrupts homogeneous CBPC formation. For this reason, we may conclude that the pressure effects are negligible in CBPC formation. More detailed discussion of the pressure effect is provided in Chapter 15.

REFERENCES

1. D.W. Oxtoby, N.H. Nachtrieb, and W.A. Freeman, *Chemistry of Change* (Saunders Publishers, London, 1990).
2. J. Wescott, R. Nelson, A. Wagh, and D. Singh, “Low-level and mixed radioactive waste in-drum solidification,” *Practice Periodical Hazardous, Toxic, Radioactive Waste Mgmt*, **2** [1] (1998) 4–7.
3. A.S. Wagh, S. Grover, and S. Jeong, “Chemically bonded phosphate ceramics. II. Warm-temperature process for alumina ceramics,” *J. Am. Ceram. Soc.*, **86** [11] (2003) 1845–1849.

This page is intentionally left blank

Oxidation and Reduction Mechanisms

As was discussed in Chapter 5, the solubility of oxides, in general, decreases with the oxidation state. Monovalent alkali metal oxides are highly soluble, and most of the divalent oxides are sparsely soluble. Trivalent oxides such as alumina and hematite (Fe_2O_3) exhibit very low solubility but are more soluble than quadrivalent oxides containing titanium, lanthanides, and actinides. Fortunately, some of the metals have more than one oxidation state. For example, iron oxide is found as divalent wüstite (FeO), as trivalent hematite (Fe_2O_3), or as a combination of the two as magnetite (Fe_3O_4). Uranium oxide is found as U_2O_3 and UO_2 . Likewise, cerium is found as Ce_2O_3 and CeO_2 . If one can reduce the oxides of higher oxidation states into lower ones and dissolve them in acidic aqueous solution, one may be able to produce CBPCs of these oxides.

As was mentioned in Chapter 2, attempts to reduce oxides in forming phosphate glues were reported in the early literature. For example, Fedorov *et al.* [1] used a mixture of copper oxide (CuO) and metallic copper and developed a phosphate bonding agent for metals, where metal copper must have acted as the reductant. They also cite formation of phosphate glues with ZrO_2 and with CaZrO_3 in combination with Ni, Cr, and Ti.

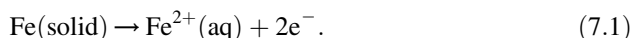
Some hazardous metals such as chromium (Cr) and radioactive fission products such as technetium (Tc) exhibit exactly opposite solubility characteristics as compared to the metals discussed above. These metals in higher oxidation states, e.g., chromates (Cr^{6+}) and pertechnetate (Tc^{7+}), are more soluble than their counterparts, e.g., chromium and technetium oxide (Cr^{3+} and Tc^{5+}). Chromium is a hazardous metal and technetium (^{99}Tc) is a radioactive isotope. As we shall see in Chapters 16 and 17, one way to reduce their dispersibility is to reduce their solubility in ground water and reduce them into their lower oxidation state, and then encapsulate them in the phosphate ceramic. Thus, the reduction approach is also useful in stabilization of hazardous metal oxides of high oxidation states. Because of these reasons, a good understanding of the reduction mechanism of oxides

within high oxidation states is needed. This chapter deals with the thermodynamic basis behind the oxidation and reduction mechanisms.

7.1.

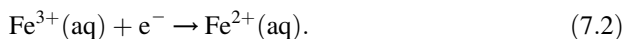
OXIDATION AND REDUCTION (REDOX) REACTIONS

As we noted in Chapter 5, release of protons (H^+) by an acid in a dissociation reaction makes the aqueous solution acidic. Often, such reactions may also involve electrons (e^-). For example, dissolution of a metal such as iron is accompanied by release of electrons in the solution. The reaction is given by

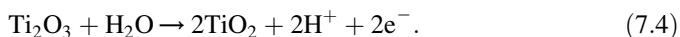
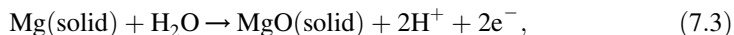


Such a reaction, where electrons are released, is called an oxidation reaction. This is one of the reactions that governs rusting of iron in humid environment.

It is also possible to reduce metals of higher oxidation states to lower ones. These are called reduction reactions. In the case of iron, such a reduction is given by



Such reactions are reduction reactions. The general term for reactions involving both production and absorption of an electron is a redox reaction. Following are some additional examples:



In reaction 7.3, oxidation of metallic magnesium results in liberation of both protons and electrons that is still an oxidation reaction. Similar is the case in reaction 7.4 except that this reaction represents oxidation of Ti_2O_3 that is in a lower oxidation state and is converted into TiO_2 that is now in a higher oxidation state.

Equations 7.1–7.4 contain neutral molecules as well as charged ions, and in addition, free electrons. In the absence of electrons, these equations represent simple chemical reactions. On the other hand, they represent electrochemical reactions in presence of free electrons, because they are most useful in electrochemistry, i.e., chemistry dealing with production of electric charges in devices such as batteries.

In chemical reactions, there is always a mass balance, i.e., number of atoms of any species on the left-hand side of an equation is the same as that of the species on the right-hand side. In an electrochemical reaction, in addition to the mass balance, there is also a charge balance in which the total charge on the left-hand side of an equation is the same as that on the right-hand side. Thus, mass and charge balance are two basic requirements of an electrochemical equilibrium.

As we have used the basic concepts of thermodynamics in a chemical reaction to predict formation of new products and to predict the direction of a reaction, the same can

be said for an electrochemical reaction also. Following Pourbaix's notation [2], equations representing very general electrochemical reactions may be written as

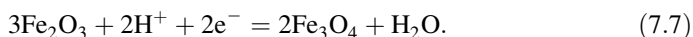
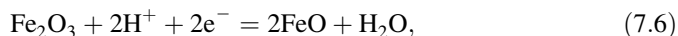
$$\sum \nu_i M_i + n e^- = 0. \quad (7.5)$$

In Eq. 7.5, n represents number of electrons either released or absorbed in an electrochemical reaction. If $n = 0$, it is a simple chemical reaction of the type discussed in previous chapters in which ν stands for stoichiometric coefficients and M for specific chemical species that are either reactants or the reaction products. For example, ν_1 and ν_2 in Eq. 7.1 would be $+1$ and -1 , M_1 and M_2 would be Fe , and $\text{Fe}^{2+}(\text{aq})$, while n will be equal to -2 . Similarly, $\nu_1 - \nu_4$ in Eq. 7.4 would be $1, 1, -2$, and -2 , while $M_1 - M_4$ would be $\text{Ti}_2\text{O}_3, \text{H}_2\text{O}, \text{TiO}_2$, and 2H^+ , and $n = -2$.

If $n < 0$, the electrons will be liberated. Such a reaction is an oxidation reaction because one of the components involved in such a reaction will lose an electron and reach into a higher oxidation state. Examples of reactions with $n < 0$ are those represented by Eqs. 7.1, 7.3 and 7.4. On the other hand, if $n > 0$, the reaction is a reduction reaction in which the electrons are absorbed by one of the components and this component will reach into a lower oxidation state. Reaction given by Eq. 7.2 is an example of this reduction.

If electrons are liberated, they will not remain as free charges. They will be absorbed somewhere else in a complete reaction. Thus in a complete chemical reaction, oxidation and reduction reactions are coupled as in the case of a galvanic cell where electrons are liberated by an anode and are subsequently absorbed by a cathode. Thus, these coupled reactions are redox reactions.

A good example of such redox reactions is a complete reaction of a mixture of iron (Fe) and hematite (Fe_2O_3). When this mixture is mixed with an acidic solution, Fe is ionized by the oxidation reaction given by Eq. 7.1. The liberated electrons are now captured by hematite. The reactions that represent capture of electrons are given by



In reactions 7.6 and 7.7, the protons are obtained from the dissolution of the acid in the aqueous solution. In highly acidic solutions, reaction 7.6 occurs while reaction 7.7 is more probable in less acidic solutions. Reaction 7.1 and either reaction 7.6 or 7.7 represent a complete redox reaction.

7.2.

REDOX POTENTIALS

As argued earlier, by coupling redox and dissolution reactions, it should be possible to form phosphate ceramics of certain insoluble oxides by reducing them to a lower oxidation state that is more soluble, or to convert contaminants of lower oxidation states and stabilize them as phosphates. For example, a mixture of insoluble hematite and elemental

iron, when mixed in phosphoric acid, reduces hematite first into wüstite (FeO) by the reaction given in Eqs. 7.1 and 7.6, and then dissolves the resulting FeO in the acidic solution to form phosphates of Fe. Similarly, technetium, when mixed with a reductant such as tin chloride (SnCl₂), is reduced from its highly soluble oxidation state of 7+ to a lower oxidation state of 5+. It is then dissolved in an acidic phosphate solution and stabilized and reacted with the phosphates to form a nonleachable phosphate compound. To discuss such applications of redox reactions in the formation of CBPCs, we must first develop a suitable thermodynamic basis for these reactions. This understanding will allow us to predict the redox reaction as a function of the pH and temperature of the medium in a manner similar to the discussions on dissolution reactions presented in Chapters 5 and 6.

To achieve this, we recognize that, in a complete chemical reaction, no free charges will be left. This implies that every reduction reaction will be coupled with an oxidation reaction. Thus, Eq. 7.5 will be coupled with another reaction given by

$$\sum \nu_j M_j - n e^- = 0, \quad (7.8)$$

so that Eqs. 7.5 and 7.8 together will form a complete chemical reaction

$$\sum \nu_i M_i + \sum_j \nu_j M_j = 0. \quad (7.9)$$

Equation 7.9 represents an imaginary galvanic cell, where the electrochemical reaction given by Eq. 7.5 represents reaction at one electrode, while Eq. 7.8 represents the reaction at the other electrode, and together the total chemical reaction of the entire cell is represented by Eq. 7.9. Transfer of the charges from one electrode to the other will build an electromotive potential difference ϕ measured in volts. This electromotive force may be related to the net change in Gibbs free energy as follows.

The chemical potential (μ) of individual chemical species such as those participating in the chemical reactions given by Eqs. 7.5 and 7.8 is defined as the Gibbs free energy per unit mole of the particular species:

$$\mu_i = \Delta G_i / \nu_i. \quad (7.10)$$

The net change in the Gibbs free energy in reactions 7.5 and 7.8 is given by

$$\Delta G_1 = \sum \nu_i \mu_i + \Phi_1, \quad \text{and} \quad \Delta G_2 = \sum \nu_j \mu_j - \Phi_2, \quad (7.11)$$

where Φ_1 and Φ_2 represent the corresponding contributions to the Gibbs free energy due to liberation and absorption of n number of electrons. The total reaction given by Eq. 7.9 will produce a net change in Gibbs free energy of

$$\Delta G = \Delta G_1 + \Delta G_2 = \sum \nu_i \mu_i + \sum \nu_j \mu_j + (\Phi_1 - \Phi_2). \quad (7.12)$$

The electromotive potential difference (E_h) measured in volts may be related to the corresponding contribution to the Gibbs free energy ($\Phi_1 - \Phi_2$) by

$$-nE_h = \frac{\Phi_1 - \Phi_2}{F}, \quad (7.13)$$

where F is the Faraday constant defined as the charge of 1 mol of electrons (96,485.3 C/mol).

Using Eqs. 7.12 and 7.13 we obtain the following equilibrium relation, i.e., when $\Delta G = 0$,

$$E_0 = \frac{\sum \nu_i \mu_i + \sum \nu_j \mu_j}{nF}. \quad (7.14)$$

Here E_0 is the equilibrium electrode potential difference between the two electrodes of the galvanic cell. It is now possible to choose the standard reference electrode as the hydrogen electrode, for which the chemical potentials μ_j of the constituents H^+ and H_2 are taken to be zero at standard temperature and pressure. The equilibrium condition 7.14 then becomes

$$E_0 = \frac{\sum \nu_i \mu_i}{nF}. \quad (7.15)$$

Equation 7.15 implies that, for an electrochemical reaction involving a redox reaction, there exists an electrode potential that is related to the chemical potentials of the reactants and the reaction products and is calculated by this equation. This electrochemical potential is called the “redox potential”. This potential is positive for an oxidation reaction, where a constituent involved will gain in valency, while it is negative for a reduction reaction, where the valency is reduced for the constituent. In the standard thermodynamic state (i.e., for an ideal condition where each of the species is 1 mol at standard temperature and pressure), the standard redox potential is

$$E_0^0 = \frac{\sum \nu_i \mu_{i0}}{nF}. \quad (7.16)$$

Here, μ_{i0} is the standard chemical potential of the i th species. For a given reaction, E_0 is listed in data books or can be determined from the standard values of μ_{i0} .

Consider, for example, Eq. 7.1. For this reaction, the standard redox potential E_0 may be obtained from Eq. 7.15. We have

$$E_0^0 = -\frac{\mu(\text{Fe}^{2+}) - \mu(\text{Fe(solid)})}{nF} = -\frac{[-84,854 - 0]}{96,485.3} = 0.88. \quad (7.17)$$

This positive quantity indicates that Eq. 7.1 is an oxidation reaction. On the other hand, for the reduction reaction given by Eq. 7.2, we have

$$E_0^0 = -\frac{\mu(\text{Fe}^{2+}) - \mu(\text{Fe}^{3+})}{nF} = -\frac{[-(84,854) - (-10,575.4)]}{96,485.3} = -0.77, \quad (7.18)$$

which is negative. Using E_0^0 as the zero of the measure of E , we define the redox potential E_h as

$$E_h = E - E_0^0. \quad (7.19)$$

Substituting Eq. 7.16 into Eq. 7.19 gives

$$E_h = E - \frac{\sum \nu_i \mu_i}{nF}. \quad (7.20)$$

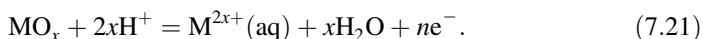
Since μ_i is a function of pH as well as temperature in Eq. 7.20, E_h will also depend on the pH of the medium and the temperature. This dependence is discussed in the next two sections.

7.3.

E_h -pH DIAGRAMS

In Chapter 5, we discussed the pH dependence of ionic concentration for dissolution reactions using the concentration-pH diagrams. In a similar manner, the pH dependence of E_h can be represented by the E_h -pH diagrams at standard temperature and pressure. These diagrams provide domains of occurrence for a given ionic or oxide species. They are constructed for a given metal such as Fe, in which equations representing all reactions at various pH are written first and are drawn on a E_h -pH graph for given ionic concentrations.

Consider Eq. 7.3, for example. It describes a general dissolution reaction for an oxide in an acidic medium. Similar to this equation, the dissolution reaction involving a redox reaction is



Here, as before, M is a metal of valency $2x$, (aq) means the particular ion is dissolved. In addition, n is the number of electrons released in the redox reaction. The ionic concentration of $\text{M}^{2x+}(\text{aq})$ is given by

$$\frac{\langle \text{M}^{2x+}(\text{aq}) \rangle}{\langle \text{MO}_x \rangle} = \frac{\langle \text{H}^+ \rangle^{2x}}{\langle \text{H}_2\text{O} \rangle} \exp[-\beta \Delta G], \quad (7.22)$$

where $\beta = 1/RT$, R being the gas constant and T , the absolute temperature. Taking logarithm to the base 10 of both sides of Eq. 7.22, we obtain

$$\log \left[\frac{\langle \text{M}^{2x+}(\text{aq}) \rangle}{\langle \text{MO}_x \rangle} \right] = -xp\text{H} - \frac{\beta}{2.301} \Delta G. \quad (7.23)$$

Since, $\Delta G = -nF(E_h - E_0^0)$, we obtain

$$E_h = E_0^0 + \frac{2.302RT}{nF} \left[xp\text{H} + \log \frac{\langle \text{M}^{2x+}(\text{aq}) \rangle}{\langle \text{MO}_x \rangle} \right]. \quad (7.24)$$

Equation 7.24 represents the electrode potential as a function of the cation concentrations in a solution of given pH. This relation may be used to determine conditions in which one can either reduce or oxidize given oxides to change their solubility and thereby dissolve them so that they will react with phosphate anions and form CBPCs. At room

temperature, substituting the values of all constants, we obtain

$$E_h = E_0^0 + \frac{0.0591}{n} \left[xpH + \log \frac{\langle M^{2x+}(aq) \rangle}{\langle MO_x \rangle} \right]. \quad (7.25)$$

Using Eq. 7.25, one can represent the general conditions of dissolution of metals and oxide in terms of E_h -pH diagrams by plotting E_h vs. pH for given cation concentrations. These diagrams provide graphical representations of occurrence of cation species for given thermodynamic conditions.

To draw these diagrams, one needs the E_0^0 values. These are listed in data books or may be determined by the standard potentials for each of the components of the reactions using Eq. 7.16. The dissolution and chemical reaction equations are then written for all possible oxidation states with suitable values of x as a function of pH. Using different values of $\langle M^{2x+}(aq) \rangle / \langle MO_x \rangle$, one can then calculate E_h and plot the results vs. pH.

Such diagrams are extensively used in electrochemistry and can be borrowed from reference books such as the *Atlas on Electrochemical Equilibria* [2]. We will use these diagrams in redox reactions that form CBPCs, such as that of Fe_2O_3 (see Section 7.5, and also Chapter 12), and also for redox conditions used to stabilize contaminants such as technetium (see Chapter 17). In addition, these diagrams provide limits on use of the redox reactions because of limits on water stability. This point is discussed below.

7.4.

E_h -pH DIAGRAM OF WATER

Because CBPCs are formed in an aqueous solution, the stability of water at different E_h and pH is an important consideration. E_h -pH diagrams provide a graphical representation of the stability regions of water in which CBPCs can be synthesized. As we shall see below, outside the region of this stability, water will decompose and produce either hydrogen or oxygen gases, which will result in formation of porous and weak CBPCs. The liberated hydrogen or oxygen may also react with dissolved cations or anions and will interfere with phosphate-forming reactions. For these reasons, detailed discussion of the redox reactions of water and its E_h -pH diagrams is important.

The equations that are relevant to the stability of water are given by



For the reaction given by Eq. 7.26 we have already shown (see Eq. 4.6) that

$$\log \langle OH^- \rangle = -14.00 + pH. \quad (7.29)$$

For Eqs. 7.27 and 7.28, we can derive the E_h -pH relations by following the procedure described in the last section. For the components involved in these two equations, the

standard Gibbs free energies are given by $\Delta G_0(\text{H}_2\text{O}) = -236.7 \text{ kJ/mol}$, $\Delta G_0(\text{OH}^-) = -157.3 \text{ kJ/mol}$, and $\Delta G_0(\text{H}_2)$, $\Delta G_0(\text{H}^+)$, $\Delta G_0(\text{O}_2)$, and $\Delta G_0(\text{e}^-)$ are all zero. These values yield E_0 for the reaction given by Eq. 7.27:

$$E_0^0 = \frac{2\Delta G_0(\text{H}^+) + 2\Delta G_0(\text{e}^-) - \Delta G_0(\text{H}_2)}{2 \times 96,485.3} = 0. \quad (7.30)$$

Since $x = 2$ and $n = 2$ in Eq. 7.27, we derive the following from Eq. 7.25:

$$E_h = 0 - 0.0591 \text{ pH} - 0.0295 \log p_{\text{H}_2}, \quad (7.31)$$

where p_{H_2} denotes partial pressure of hydrogen. For the reaction given by Eq. 7.28,

$$\begin{aligned} E_0^0 &= \frac{\Delta G_0(\text{O}_2) + 4\Delta G_0(\text{H}^+) + 4\Delta G_0(\text{e}^-) - 2\Delta G_0(\text{H}_2\text{O})}{4 \times 96,485.3} \\ &= \frac{0 + 4 \times 0 + 4 \times 0 - 2(-236,700)}{4 \times 96,485.3} = 1.227 \text{ V}. \end{aligned}$$

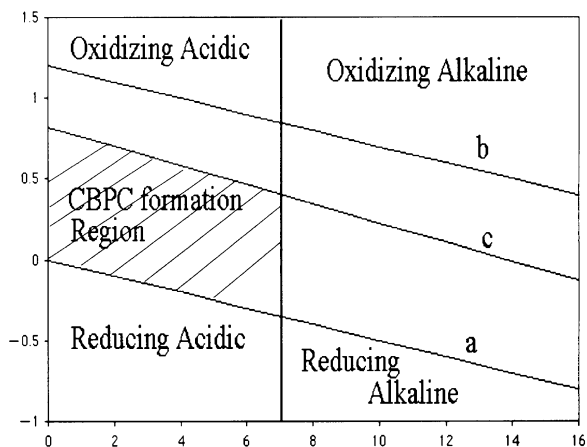
Recognizing that $x = 4$ and $n = 4$ in Eq. 7.28, we obtain Eq. 7.25 for this reaction as

$$E_h = 1.228 - 0.0591 \text{ pH} - 0.0147 \log p_{\text{O}_2} \quad (7.32)$$

p_{O_2} in Eq. 7.32 denotes the partial pressure of oxygen. As we may recall from Chapter 4, Eq. 7.29 provides the definition of pH for water ($= 7$).

We have plotted Eqs. 7.31 and 7.32 in Fig. 7.1. The vertical pH line divides the entire region into acidic and alkaline regions. The two parallel lines denoted by a and b correspond to Eqs. 7.31 and 7.32 with a slope -0.0591 . They divide the graph into a region of stability of water and a region of decomposition of water. Between lines a and b is the

Fig. 7.1.



E_h -pH diagram of water.

region of stability of water in which CBPCs are formed. Above line b, water will decompose into oxygen and hydrogen, while below the line a, hydrogen will ionize into H^+ .

Similar to the definition of pH that denotes the acidity and alkalinity of a solution, the definition of r_H and r_O indicates the reduction and oxidation states of a solution, where r_H and r_O are defined by

$$r_H = -\log p_{H_2} \quad \text{and} \quad r_O = -\log p_{O_2}. \quad (7.33)$$

This is done by combining Eqs. 7.27 and 7.28 and eliminating e^- . We obtain the decomposition reaction for water:



Corresponding to this decomposition reaction, $2H_2$ and O_2 will be in equilibrium when the corresponding partial pressures are equal. This gives

$$p_{H_2} = 2p_{O_2}, \quad \text{or} \quad \log p_{H_2} = \log 2 + \log p_{O_2}. \quad (7.35)$$

This results in the redox potential given by

$$E_0 = 0.819 - 0.0591 \text{ pH}. \quad (7.36)$$

Equation 7.36 divides the entire E_h -pH diagram in Fig. 7.1 into oxidation and reduction regions. Above the line c which represents Eq. 7.36, we have the oxidation region, while below is the reduction region. Thus, Eqs. 7.32 and 7.36 together divide the entire diagram into four quadrants: (1) oxidizing alkaline, (2) oxidizing acidic, (3) reducing acidic, and (4) reducing alkaline.

For acid-base reactions that produce CBPCs, since the pH of the reaction slurry is mainly in the acidic region, the second and third quadrants are most important. Within these quadrants the reduction mechanism is represented by the region between line c and a as shown by the shaded area in Fig. 7.1. For this reason, much of the discussion of subsequent chapters will focus on this region.

7.5.

REDUCTION OF IRON OXIDE AND FORMATION OF CBPC

An important oxide used in the reduction mechanisms discussed in the previous sections is Fe_2O_3 . This oxide is one of the most common and low cost raw materials used in forming inexpensive CBPCs. This oxide is very stable and cannot be dissolved sufficiently in an acid solution to produce $Fe^{2+}(aq)$ or $Fe^{3+}(aq)$ to form CBPC by the conventional dissolution method. If, however, the Fe_2O_3 could be converted to more soluble FeO , or Fe_3O_4 that is a combination of FeO and Fe_2O_3 , it can then be dissolved in the reduced state [3]. As will be discussed in this section, the reduction may be achieved simply by adding a small amount of elemental iron. We will now discuss how CBPC of Fe_2O_3 can be formed by this reduction mechanism.

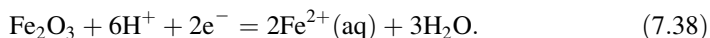
Consider a mixture of Fe_2O_3 and a small amount of Fe mixed with phosphoric acid solution such that the initial pH of the solution is near zero. In this solution, the elemental

iron will dissolve by releasing electrons and forming cations of iron according to reaction 7.1. Either by using Eq. 7.25 or allowing Pourbaix's treatment of iron oxide [2], the electrochemical potential may be expressed as

$$E_1 = -0.44 + 0.0295 \log \langle \text{Fe}^{2+}(\text{aq}) \rangle. \quad (7.37)$$

The notation $\langle \text{Fe}^{2+}(\text{aq}) \rangle$ represents the molar concentration of $\text{Fe}^{2+}(\text{aq})$ in the aqueous state.

In the acidic and reduced environment of this slurry, reduction of Fe_2O_3 is represented by the following reaction:



The corresponding E_h -pH relation is given by

$$E_2 = -0.728 + 0.1773\text{pH} + 0.0591 \log \langle \text{Fe}^{2+}(\text{aq}) \rangle. \quad (7.39)$$

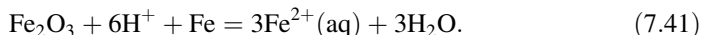
Equations 7.37 and 7.39 provide bounds on the compositions for dissolution of Fe_2O_3 at low pH.

At higher pH, similar reaction occurs through formation of magnetite, Fe_3O_4 given by Eq. 7.7.

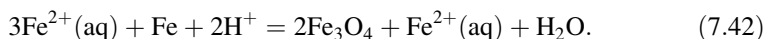
The corresponding electrode potential is given by

$$E_2 = 0.221 - 0.0591\text{pH}. \quad (7.40)$$

Combining Eqs. 7.1 and 7.38 and eliminating e^- , we obtain



Similarly, from Eqs. 7.1 and 7.7 we obtain



Equations 7.41 and 7.42 imply that it is possible to produce $\text{Fe}^{2+}(\text{aq})$ by using Fe as reductant of Fe_2O_3 in an acidic region (or in presence of protons). Wagh and Jeong [3] used this procedure to form ceramics of iron oxide and also that of wastes containing iron oxide as a major constituent. Details of forming such ceramics are presented in Chapter 12. The treatment presented here, however, illustrates the advantage of reduction mechanisms in forming CBPCs. In addition, the reduction process discussed here is also very useful in stabilization of most difficult contaminants such as radioactive technetium in CBPCs. That will be discussed in Chapter 17.

REFERENCES

1. N.F. Fedorov, L.V. Kozhevnikova, and N.M. Lunina, Current-conducting phosphate cements, UDC 666.767.
2. M. Pourbaix, Atlas of Electrochemical Equilibria in Aqueous Solutions (National Association of Corrosion Engineers, Houston, TX, 1974).
3. A.S. Wagh and S.Y. Jeong, "Chemically bonded phosphate ceramics. Part III: reduction mechanism and its application to iron phosphate ceramics," *J. Am. Ceram. Soc.*, **86** [11] (2003) 1850–1855.

Mineralogy of Orthophosphates

As discussed in Chapter 3, though phosphates exist in three structural forms, orthophosphates, pyrophosphates and metaphosphates, they are found in nature mainly as orthophosphates. The acid phosphates used in the synthesis of CBPCs, as well as the resulting products that constitute CBPCs are also orthophosphates, and therefore, this chapter is focused on orthophosphate minerals. Readers interested in other types of phosphates are referred to the excellent review by Corbridge *et al.* [1].

The interatomic bonds that produce the crystalline structures of minerals are briefly discussed first. This is followed by general rules used in constructing models of crystal structures of phosphate minerals, then the crystal structures of orthophosphate mineral forms. The discussion is brief because the emphasis of the book is on practical aspects of novel phosphate ceramics and cements. Readers interested in more details are referred to Corbridge *et al.* [1] and Kanazawa [2].

The basic building block of the orthophosphates is the PO_4 unit, which is briefly discussed here. This helps us to better understand various mineral forms that constitute the orthophosphate ceramics and cements. For additional discussion on crystal chemistry and crystal structures, see Refs. [1–3].

8.1.

NATURE OF INTERATOMIC BONDS

Atoms and even the PO_4 unit in a phosphate crystal may be considered as spherical balls and stacked in various configurations. The PO_4 unit is held together in solids by five types of bonds. These bonds, which hold the atoms at definite distances from each other, are formed by the electronic configuration of the atoms. The equilibrium distance between

these imaginary balls and the packing order determine the crystal form and the mineral properties. For this reason, these bonds and configurations are briefly discussed.

8.1.1. Ionic Bonds

As seen in Chapters 4 and 5, aqueous cations and anions are formed by the dissolution of metal oxides and acid phosphates. Electrostatic (Coulomb) force attracts the oppositely charged ions to each other and stacks them in periodic configurations. That results in an ionic crystal structure. Thus, the ionic bond is one of the main mechanisms that is responsible for forming the acid–base reaction products.

The crystals formed by ionic bonds are not very hard. Compared to other forms of crystal structures, they are more soluble in water and not very stable in a heat treatment. Most of the acid phosphates fall into this category.

8.1.2. Covalent Bonds

Often, one or more electrons are shared between two atoms in such a manner that these electrons are attracted by the nuclei of both. This sharing creates a bond between the two atoms. The force of attraction is strong and leads to the formation of crystals that are hard, insoluble, and thermally stable.

The bonding mechanism in most phosphate minerals is partly ionic and partly covalent, and depending on which bond is dominant, the mineral properties vary. Thus, the minerals with more covalent bonds, such as anhydrous phosphates are less soluble in water and are thermally stable.

8.1.3. Metallic Bonds

These bonds are found mainly in metals and do not occur in the products formed by the acid–base reactions. Metal structures are considered to be positive ions embedded in a cloud of electrons. The electrons move freely, and, hence, metals conduct electricity. The CBPCs are invariably poor conductors, and any small conductivity that is exhibited mostly from the ionic conductivity.

8.1.4. van der Waals Bonds

The hardball structure of atoms or molecules is only an approximation. When they are very close to each other, the charge distribution in them may not be uniform, and each atom or molecule may behave as if it is a dipole with a small amount of positive charge concentrated at one end and negative charge at the other end. The positive charge of one atom or molecule will now attract the negative charge of the neighbor, and this force holds them together while the negative charge of the first will be attracted by the positive charge of another atom or molecule. This creates a configuration where the atoms and molecules are attracted by the dipole attraction between each other, and a structure is formed.

Because dipole forces are only secondary, the forces are very weak. Thus, the properties that they impart on the crystal are much weaker than in the covalent and ionic crystals. For this reason, van der Waals bonds do not significantly influence the crystal properties of phosphate ceramics.

8.1.5. Hydrogen Bond

The hydrogen bond results from an electrostatic attraction between a positively charged hydrogen ion with negatively charged ions such as O^{2-} or N^{2-} . The hydrogen atom may lose its sole electron to any of its neighbors with equal probability. This results in hydrogen bonding to its neighbors of opposite charge and holds them together. The hydroxyl ion is a good example of hydrogen bonding, where one negative charge of O^{2-} is attracted by the positive charge of hydrogen to form the unit $(OH)^-$. This unit, due to its net negative charge, will then form a component of the phosphate crystal structures.

The hydrogen bond is not as strong as the ionic and covalent bonds, but is stronger than the van der Waals bond.

8.2.

RULES FOR CRYSTAL STRUCTURE FORMATION

Though the different bonds explain whether a particular crystal is hard or not, soluble or insoluble, thermally stable or unstable, the crystal structure itself may be visualized by considering the atoms and molecules as hard balls of different radii. Thus, the atomic and ionic radii are important factors in constructing crystal structures. Once these radii are known, one may consider hard balls of the sizes of these radii and construct physical models by stacking the balls in layers. While arranging the structures, however, the following rules apply.

8.2.1. Charge Balance and Coordination Principle

Generally, a crystal is electrically neutral. This implies that the crystal should have an equal number of positive and negative charges. Thus, when oppositely charged ions come together to form a neutral crystal structure, each ion coordinates with as many ions of opposite charge as the size permits. This coordination principle dictates both electrical neutrality of the crystal structure and compact packing of the atoms within the structure.

8.2.2. Effect of Relative Ionic Size

The number of the nearest neighbors that an atom can accommodate in a given crystal is called the “coordination number”, and the shell formed by the nearest neighbors is called

Table 8.1.

Radius Ratios of Nearest Neighbors and Crystal Structure.

Range of Radius Ratio	Coordination Number	Stable Crystal Structure
1	12	Hexagonal close packed or cubic close packed
0.732–1	8	Cubic
0.414–0.732	6	Octahedral
0.225–0.414	4	Tetrahedral
0.155–0.225	3	Triangular
<0.155	2	Linear

the “first coordination shell”. Apart from the charge balance, the coordination number will also depend on the relative size of the neighboring atoms. Simply by arranging the solid spherical balls of different sizes, one can determine the coordination number and the crystal structure, which are presented in Table 8.1 for different radius ratios of neighboring atoms.

8.2.3. Rules for Ionic Substitutions

Pure crystals that are formed by the above rules are rare, and in most crystals, the minerals exhibit wide-ranging compositional variation. In these minerals, a given ion at a given site is substituted by another similar ion, and hence, a mineral is characterized by percent substitution of impurities or atomic percentage of one metal for another. The resulting mineral forms are called “solid solutions”.

The ionic substitutions are again governed by definite criteria known as Hume–Rothery rules. Size of the atoms is the most important factor in these rules. Substitution of one atom by another in a crystal structure is most likely when their ionic radii are within 15%; it is less likely when sizes differ by 15–30%, and unlikely beyond that range. Note that these substitutions must also maintain overall charge balance, because the crystal structure must be neutral.

These rules not only allow us to understand the phosphate mineral structures, but also help us in predicting the acid–base reaction products in the syntheses of novel CBPCs. The following discussion focuses on such products, which are the building blocks of phosphate minerals in CBPCs.

8.3.

MAJOR PHOSPHATE CRYSTAL STRUCTURES

The main building block of orthophosphate crystals is the PO_4 polyhedron. It is possible to construct more complex phosphate structures using this unit.

8.3.1. Structure of PO_4 Polyhedron

The radius of P^{5+} is 0.035 nm, while that of O^{2-} is 0.14 nm. Thus, their ratio is 0.25. According to Table 8.1, this gives a coordination number of 4 and hence the structure is a tetrahedron.

Figure 8.1 shows this tetrahedral crystal structure of $(\text{PO}_4)^{3-}$. Because P is a pentavalent element, it needs five negative charges from the four oxygen ions to bond. Therefore, it forms single bonds with each of the three oxygen ions and a double bond with the fourth ion. The first three oxygen ions also bond to the neighboring atoms in the orthophosphate crystal structure, and the PO_4 tetrahedron acts like a trivalent ion. For this reason, for all subsequent discussions, we will picture the PO_4 tetrahedron as a spherical ball in the stacking of atoms.

8.3.2. Structure of Acidic Orthophosphates of Alkali Metals

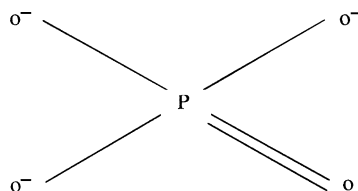
Acid phosphates of alkali metals, used in the acid–base reaction in forming a CBPC are represented by the formula $\text{A}_2\text{H}_2\text{PO}_4 \cdot n\text{H}_2\text{O}$, where A represents a monovalent element, such as Na, K, and Cs, from Group 1a of the Periodic table. The symbol A can also represent $(\text{NH}_4)^+$, the ammonium ion. The integer n denotes the number of water molecules of hydration that are bonded by the van der Waal forces in the crystal structure.

Some alkali orthophosphates have been well studied. The most important among these are KH_2PO_4 and $\text{NH}_4\text{H}_2\text{PO}_4$. In the KH_2PO_4 structure, hydrogen bond links the PO_4 tetrahedron to four others in a continuous three-dimensional network, while the K^+ ion is coordinated 8-fold by oxygen atoms. In the case of $\text{NH}_4\text{H}_2\text{PO}_4$, the structure is similar, but a system of N–H–O bonds exists instead of coordination of the K^+ ion. These bonds are mostly ionic, and hence, acid phosphates are soluble and used as such in the acid–base reaction to form CBPCs.

8.3.3. Alkaline Earth Orthophosphates

Next to the acidic alkali phosphates, alkaline earth orthophosphates are of interest, because they represent many CBPC products, such as $\text{CaH}_2\text{PO}_4 \cdot \text{H}_2\text{O}$ and $\text{MgH}_2\text{PO}_4 \cdot 2\text{H}_2\text{O}$. They are also the result of an acid–base reaction between an acid phosphate and an oxide containing an alkaline earth metal, such as Ca and Mg. They exhibit the same structure

Fig. 8.1.



Structure of $(\text{PO}_4)^{3-}$.

as that of a very wide class of minerals called “apatites” and also that of anhydrous phosphates of alkaline earth metals, such as $\text{Mg}_3(\text{PO}_4)_2$. Especially because calcium phosphates cover numerous phosphate minerals found in nature, the human body, fertilizers, etc., alkaline earth phosphates are of considerable interest. Different forms of these phosphates are discussed below.

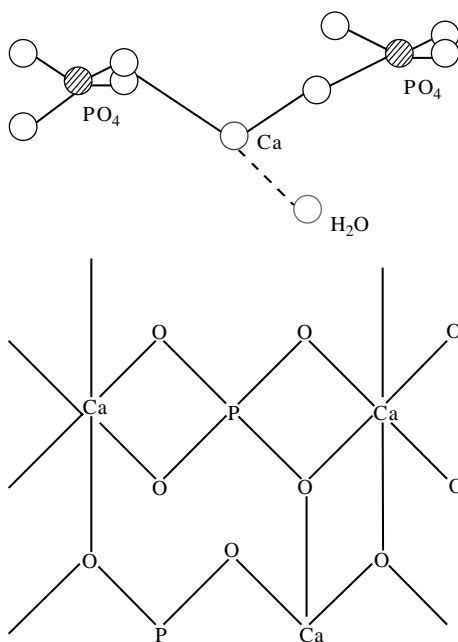
8.3.3.1. ALKALINE EARTH ACID ORTHOPHOSPHATES

Mono- and di-hydrogen phosphates of alkaline earth metals fall into this category. Both exhibit layered structures with $-\text{Ca}-\text{PO}_4-\text{Ca}-\text{PO}_4-$ chains as shown in Fig. 8.2. In the case of monohydrogen phosphates such as $\text{CaHPO}_4 \cdot 2\text{H}_2\text{O}$, the link between the layers is through hydrogen bonds to the water molecules, while in the case of dihydrogen phosphates, one of the water molecules is replaced by PO_4 ions.

8.3.3.2. HYDROXYAPATITE AND RELATED COMPOUNDS

When acidic alkali phosphates are reacted with alkaline earth oxides such as CaO and MgO , we obtain CBPCs of Ca and Mg and most common structures of the reaction products fall into the category of apatites. Apatites are most common in natural minerals,

Fig. 8.2.



Structure of calcium acid orthophosphate.

especially apatites of calcium. Because apatites are also found in bones, they have been extensively studied [4].

A whole series of apatite structures can be derived from the formula

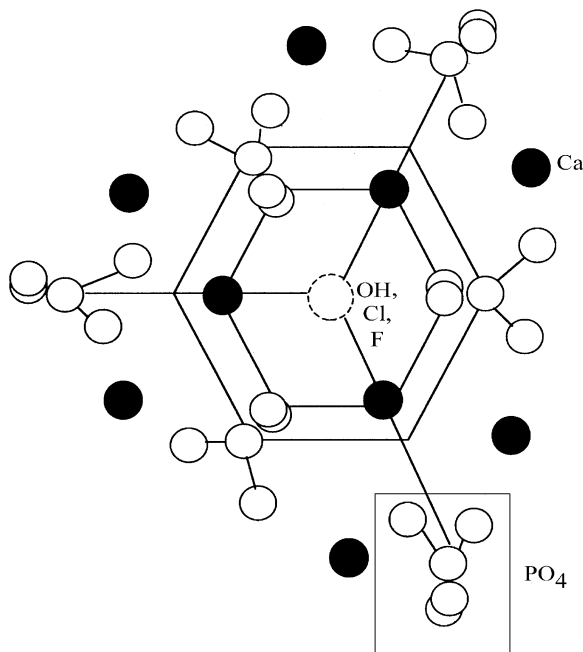


where M is a metal and Z is an anion (OH, Cl, F, and even CO₃). Apatite structures also exist with arsenates, chromates, silicates, etc., which are isostructural with phosphate apatites. Here, we will focus on phosphates, and in particular on alkaline earth apatites, because they are part of many CBPCs.

The most common apatite is Ca₅(PO₄)₃OH and is called hydroxyapatite. Other forms include chloroapatite (Ca₅(PO₄)₃Cl), fluoroapatite (Ca₅(PO₄)₃F) and carbonate apatite or dahllite (Ca₅(PO₄)₃CO₃). These minerals are in pure forms, but it is also possible to generate them by partial replacement of one anion by another or one cation by another. For example, Ca may be replaced by Pb by ionic substitution, yielding pyromorphites [Pb₅(PO₄)₃(OH,Cl,F)]. As we shall see in Chapter 16, this mineral is very important in stabilizing the hazardous metal Pb. Also as discussed in Chapter 2 and shall be seen in later chapters, Mg-based CBPCs have many applications, and hence minerals such as Mg₅(PO₄)₃(OH,Cl,F) are also very common.

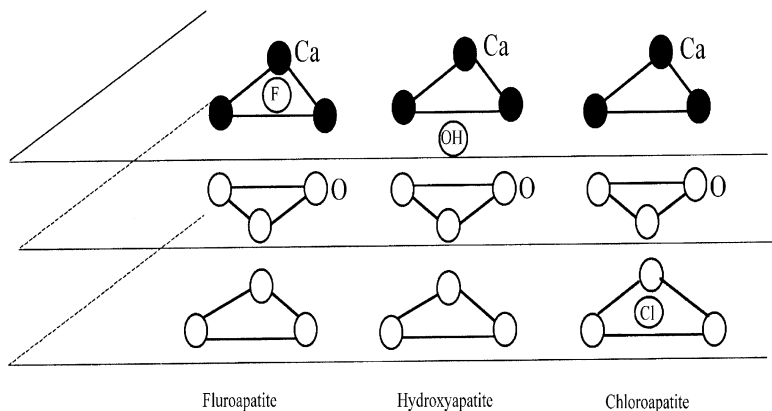
Figure 8.3 illustrates the hexagonal apatite structure. One set of calcium ions is in 6-fold coordination with oxygen atoms belonging to the PO₄ tetrahedra. Thus, as

Fig. 8.3.



Apatite structure. The solid circles are Ca, shaded ones are OH, Cl, F etc., and the tetrahedra are PO₄.

Fig. 8.4.



Layered structure of hydroxy-, chloro-, and fluoroapatites.

shown in Fig. 8.3, for every two layers of oxygen, there is one layer of calcium. The anions (OH, Cl, F, etc.) lie in the channels formed by the three calcium atoms as well as oxygen. Their placement is shown in detail in Fig. 8.4. In fluoroapatites, F atoms are placed in between three ions of Ca; in hydroxyapatites, OH ions are placed between the layers of Ca and oxygen; and in chloroapatites, Cl ions are in between three oxygen ions. Thus, the entire structure is hexagonal close packed or a layered structure.

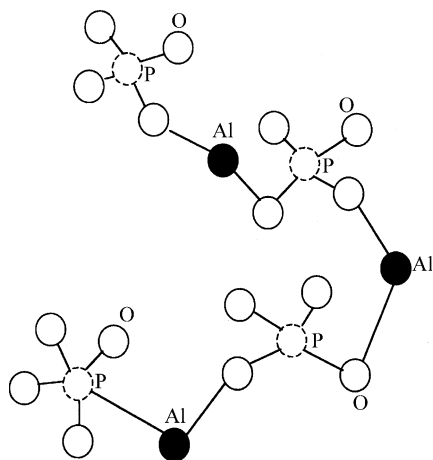
8.3.3.3. $M_3(PO_4)_2$ -TYPE PHOSPHATES

The tri-calcium, barium, and strontium phosphates are members of an isostructural series $M_3(PO_4)_2$, where $M = Ca, Ba, Sr$, etc. The minerals formed by Ca are very important in bioceramics, and because Ba and Sr are fission products (i.e., formed as by-products in nuclear reactions), apatite minerals play a major role in their stabilization for disposal (see Chapter 17). Within these common structures, however, calcium phosphate goes through several phase changes at different temperatures. These phases are labeled as β , α , α' , etc. The reader is referred to Refs. [1,2] for details.

8.3.3.4. SILICA-TYPE COVALENT PHOSPHATE STRUCTURES

$AlPO_4$ is a classic example of the SiO_2 type covalent phosphate structure. In this structure, Al and P atoms share one bond with each oxygen and each of them forms a tetrahedron. Through the common oxygen atom, the tetrahedra are linked to each other and form a three-dimensional covalent structure that is similar to silica

Fig. 8.5.



Bonding in covalent silica-type structures.

structures in which a basic SiO_2 unit hosts other atoms in alternate sites of Si and forms various silicates. Therefore, AlPO_4 shares many of the chemical and physical properties of silica, though as a CBPC it is synthesized at a much lower temperature (see Chapter 12).

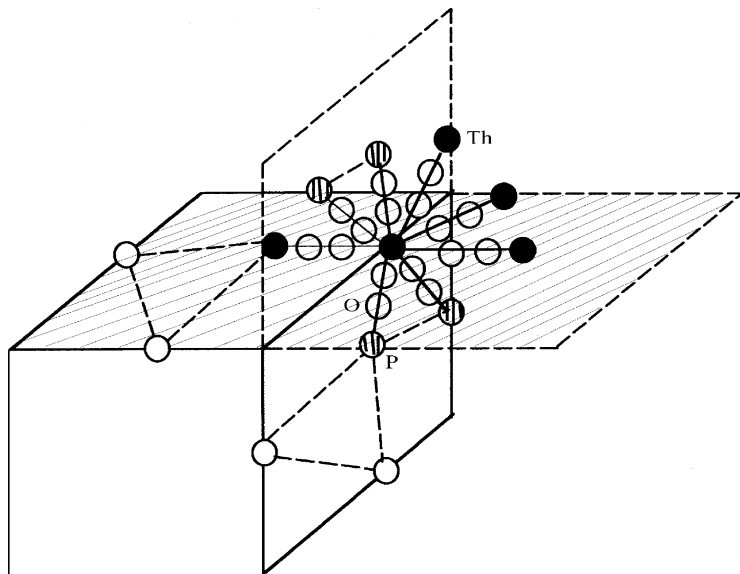
Bonding in the silica-type covalent phosphate structure is illustrated in Fig. 8.5. Because this bonding is covalent, the resulting minerals are very hard and their aqueous solubility is extremely low. These properties make them attractive for the disposal of radioactive barium and strontium isotopes formed during nuclear reactions. These two isotopes may be converted to their covalent phosphate structures as $\text{Sr}_3(\text{PO}_4)_2$ and $\text{Ba}_3(\text{PO}_4)_2$ and can be disposed or stored in repositories safely.

8.3.3.5. HEAVY METAL ORTHOPHOSPHATES

Many lanthanide and actinide minerals in nature are phosphates. Examples are monazite (CePO_4), LaPO_4 , NdPO_4 , and ThPO_4 . In monazite, substitution of radioactive elements is possible, e.g., Ce can be replaced partially by Th, and that makes the material radioactive. Phosphates of other actinides, such as plutonium phosphate (PuPO_4), fall into the same category.

The crystal structure of these phosphates consists of metal ion coordinated with eight phosphate tetrahedrons, as illustrated in Fig. 8.6. One may imagine a metal ion placed at the center of one of the edges of a cube. As shown in the figure, this ion coordinates with two metal ions placed in four neighboring planes. Thus, the metal ion is coordinated with eight tetrahedra.

Fig. 8.6.



Coordination of metal ions with neighbors through phosphate tetrahedra in heavy metal phosphate minerals.

8.4.

RELEVANCE TO MINERALS CONSTITUTING CBPC

Appendix C contains the chemical formulae for the minerals used in this book. There are very few minerals that have the ideal crystalline structures discussed above. There are sufficient substitutional impurities, crystal defects, and distortions that make the CBPC structure significantly different from the models discussed above. Several well-established minerals exhibit these features, as are many of those listed in Appendix C. For example, $\text{Ca}(\text{UO}_2)_2(\text{PO}_4)_2 \cdot 10\text{H}_2\text{O}$ is formed by the substitution of Ca in autunite by uranyl (UO_2) ions, making the autunite a mineral of radioactive uranium. Similarly, $(\text{Ce}, \text{Th})\text{PO}_4$ is formed by the substitution of the Ce in monazite by Th. Numerous minerals can be formed by substitutions and provide a researcher sufficient degree of freedom to synthesize very complex minerals to produce useful CBPCs.

The CBPC structure is a mixture of both crystalline and noncrystalline material. The crystalline phases are detectable by X-ray diffraction, but noncrystalline phases are difficult to identify, even though their presence is indicated by a broad hump in the X-ray diffraction pattern. We shall see such complex structures in almost all CBPC formations in the subsequent chapters.

The modification of mineral structure by substitutions is, in fact, the strength of practical CBPCs. With substitution, one can trap radioactive and hazardous contaminants in

the CBPC structure. Hazardous contaminants (Pb, Cd, Cr, etc.) or radioactive contaminants (Tc, Cs, Th, etc.) that are found in waste streams in small quantities can be trapped within a crystalline matrix. This capability makes CBPCs a highly versatile matrix for immobilizing radioactive and hazardous contaminants. Chapters 16 and 17 will shed more light on this topic.

REFERENCES

1. D. Corbridge, M. Pearson, and C. Walling, *Topics in Phosphorous Chemistry*, vol. **3**. (Interscience, New York, 1966), pp 437.
2. *Inorganic Phosphate Materials*, ed. T. Kanazawa (Elsevier, New York, 1989), p. 288.
3. C. Klein, and C. Hurlbut, Jr., *Manual of Mineralogy*, 20th ed. (Wiley, New York, 1977), p. 596.
4. R.B. Martin, Bone as a ceramic composite material, in *Bioceramics*, ed. J.F. Shackelford (Trans Tech Pub, Brandrain, 1999), p. 9.

This page is intentionally left blank

Magnesium Phosphate Ceramics

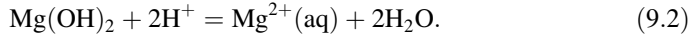
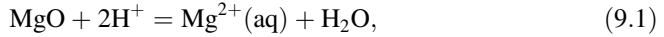
As the review in Chapter 2 indicates, Mg-phosphate ceramics are the most developed and studied CBPCs and also have found several commercial applications.

In the early stage of development of these materials, attempts were made to react MgO with H_3PO_4 and form ceramics. Such reactions were rapid and highly exothermic and formed inhomogeneous mass [1]. The phases formed in this rapid reaction included a precipitate of magnesium dihydrogen phosphate ($\text{Mg}(\text{H}_2\text{PO}_4)_2 \cdot n\text{H}_2\text{O}$); this product is consistent with the solubility analyses presented in Chapter 4. This compound is soluble in water, and hence the entire product was not stable in water. Patents have been issued to Sherif *et al.* on some of these products [2–6]. Subsequently, because of the high solubility of the phases formed in these products, attempts were made to use less acidic components, such as ammonium dihydrogen and monohydrogen phosphates [7,8], sodium tripolyphosphate [9,10], potassium dihydrogen phosphate [11,12], aluminum hydrophosphate [13], and even $\text{Mg}(\text{H}_2\text{PO}_4)_2$ itself [14], as the acid phosphates, and to form ceramics by reacting them with MgO. Reactions of MgO with these phosphates were comparatively slow, generated less exothermic heat, and produced ceramic products of very low solubility. The mineral compositions of most of these ceramics have been well studied [1,15–17]. Several papers provide microstructures, mechanical properties, and chemical compositions [11,18,19] on these ceramics. Though these materials were developed during the last two decades, their applications have surpassed the zinc phosphate dental cement that was developed during the early part of the last century. Mg-phosphate based materials are finding application as quick-setting cements for repair of roads [20], industrial floors, and runways [20,21], and for stabilization and solidification of low-level radioactive and hazardous waste streams [22].

9.1.

SOLUBILITY CHARACTERISTICS OF MgO AND ITS REACTION WITH ACID PHOSPHATES

As discussed in Chapter 3 (also see Ref. [23]), MgO and Mg(OH)₂ are sparsely soluble and their dissolution reactions are given by



Correspondingly, as we have seen in Table 5.1, the pH dependence of the ionic concentration of Mg²⁺ in an acidic solution, i.e., $\langle \text{Mg}^{2+}(\text{aq}) \rangle$, is given by

$$\log \langle \text{Mg}^{2+}(\text{aq}) \rangle = 16.95 - 2\text{pH}, \quad \text{for MgO}, \quad (9.3)$$

$$\log \langle \text{Mg}^{2+}(\text{aq}) \rangle = 21.68 - 2\text{pH}, \quad \text{for Mg}(\text{OH})_2. \quad (9.4)$$

These equations were used to plot the pH dependence of $\log \langle \text{Mg}^{2+}(\text{aq}) \rangle$ in Fig. 5.2.

The plots in Fig. 5.2 show that $\langle \text{Mg}^{2+}(\text{aq}) \rangle$ decreases linearly as the pH increases. Thus, its solubility in H₃PO₄ solution is high, but will be significantly less if acid phosphate solutions of higher pH are used to form the ceramics. For this reason, as stated above, acid phosphate salts are used in fabrication of almost all Mg-phosphate ceramics.

9.2.

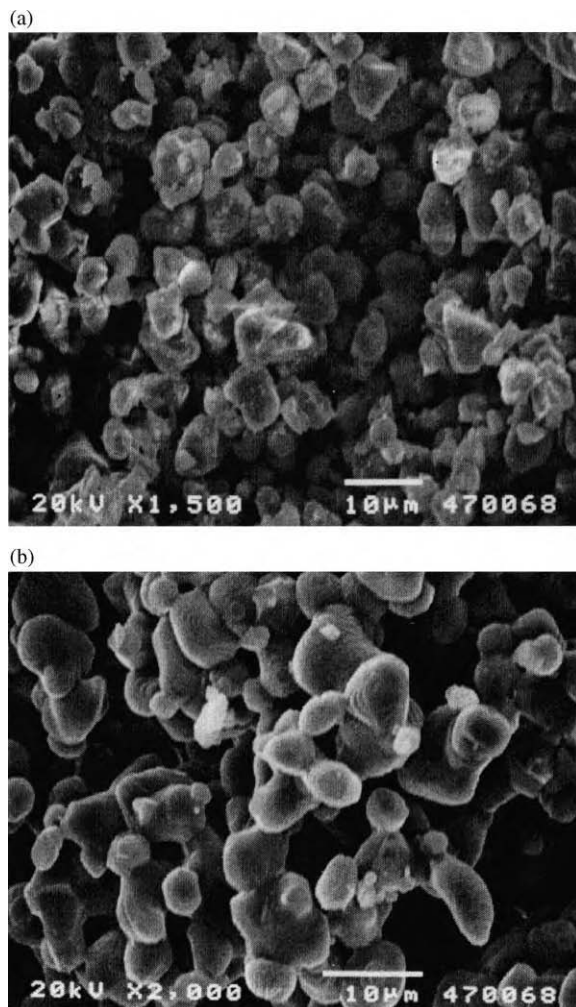
CONTROLLING REACTION RATES DURING FORMATION OF Mg-PHOSPHATE CERAMICS

For the reason given above, fabrication of ceramics of small size of typically a few tens of cubic centimeters, using acid phosphates, works adequately. To fabricate large ceramics, however, even this reduced rate of dissolution of MgO in acid phosphate solutions is not low enough. The exothermic heat generated during the acid–base reaction is not dissipated adequately in large ceramics and that leads to heating of the reaction slurry. Therefore, to form practical ceramics, one must decrease this rate further either by pretreatment of MgO or by reduction of the dissolution rate by other chemical means. The standard pretreatment of MgO involves its calcination at high temperature, and the chemical method involves addition of a small amount of boric acid in the mixture of MgO and acid phosphate. These two methods are discussed next.

9.2.1. Effect of Calcination on the Solubility of MgO

Eubank [24] showed that calcination of MgO at 1300°C reduces the porosity of individual grains and also increases the particle size. To confirm his findings, Wagh and Jeong [25]

Fig. 9.1.



Scanning electron micrographs of (a) uncalcined MgO, (b) calcined MgO.

explored the effect of calcination of technical-grade MgO. As shown in Fig. 9.1(a), technical-grade MgO particles, when observed under an electron microscope, have a porous structure. After its calcination at 1300°C for 3 h, the powder agglomerated into a hard mass. It was returned to the original particle size (average $10\mu\text{m}$) with light crushing. Its scanning electron micrograph is shown in Fig. 9.1(b) for comparison with uncalcined powder shown in Fig. 9.1(a). The grain surface of the uncalcined powder appears to be covered with a powdery or microcrystalline substance, while the particle surface of the calcined powder is smooth, indicating reduction of the amorphous coating on individual

grains that resulted from crystallization. Porosity is absent from individual particles. At high resolution, some striations were observed on the surface of individual grains of the calcined powder. The particles of calcined powder also appear bigger in Fig. 9.1(b), indicating that some grain growth had occurred during the calcination. The density of the powder increased by calcination from 3.36 to 3.57 g/cm³, while the surface area decreased from 33.73 to 0.34 m²/g. This significant reduction in the surface area is possibly the main reason for the reduced solubility of the calcined MgO powder.

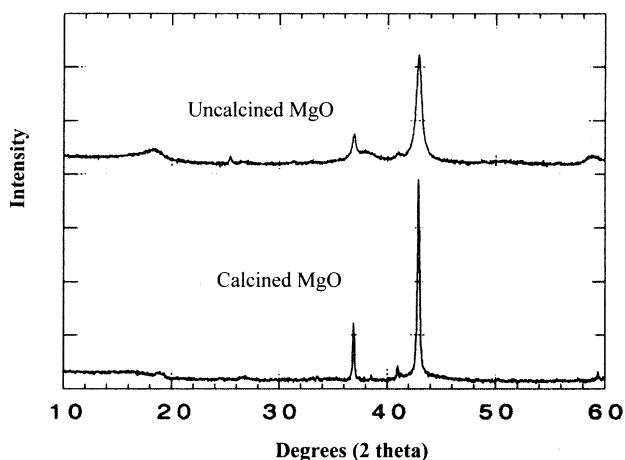
The X-ray diffraction patterns of the uncalcined and calcined powders are shown in Fig. 9.2. After calcination, MgO peaks are taller and sharper, suggesting an improvement in crystallization of the powder.

The above observations imply that calcination reduces the MgO powder solubility by reducing the porosity, increasing the grain size, and recrystallizing the amorphous coatings on individual grains.

Wagh and Jeong [25] compared the rate of dissolution of MgO in H₃PO₄ solution before and after calcination. They titrated a measured small amount of MgO in 50 wt% concentrated solution of H₃PO₄ and periodically monitored the pH resulting from the neutralization of the acid. The observed pH is plotted in Fig. 9.3 as a function of time (MgO added).

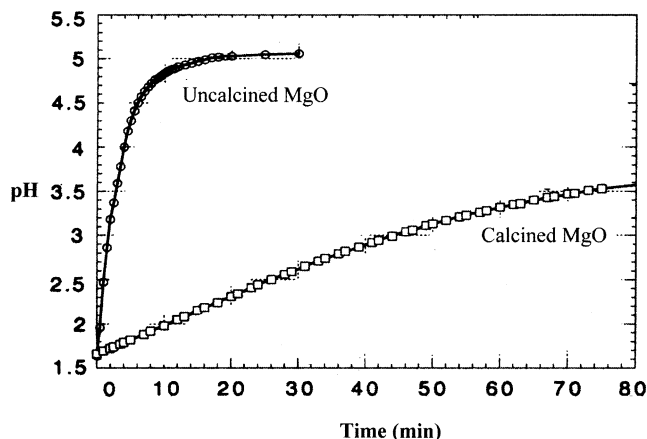
The curves show that, before calcination of the powder, the pH rise is very steep but tapers off at pH \approx 10. In contrast, the pH of the calcined powder increases very slowly at a constant rate. This constant rate of increase in the pH helps to produce Mg-based phosphate ceramics in large sizes and makes the process practical. Most commercially available MgO exhibits very high dissolution rates in acid solutions, and its calcination becomes a necessity for production of ceramics at a commercial scale. The titration test provides a good method for testing these powders for their suitability for CBPC formation.

Fig. 9.2.



X-ray diffraction pattern of uncalcined and calcined MgO.

Fig. 9.3.

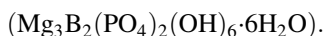
Dissolved content of uncalcined and calcined MgO as a function of pH of H_3PO_4 solution.

9.2.2. Reduction of MgO Solubility Using Boric Acid

Precalcination reduces the rate of dissolution of MgO substantially, and as we shall see later in this chapter, a slurry of MgO and H_3PO_4 or an acid phosphate can be mixed for several minutes before the exothermic acid–base reaction kicks off. Often, large-scale production of ceramics, such as oil well cements, requires hours of pumping time (see Chapter 15) or long setting times. Even in a production line of refractories that produce castables of consistent quality, the reaction slurry must have a storage life of a few hours. In such cases, chemicals are added to retard the reactions in the slurry.

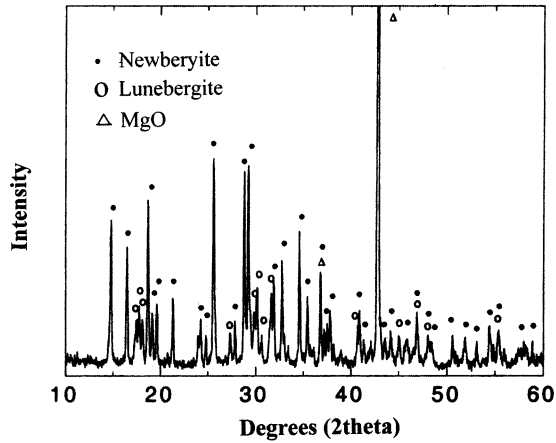
Literature on the formation of magnesium–potassium and magnesium–ammonium phosphate ceramics reports addition of several retardants, including boric acid and borates [15,25]. Sarkar [25] studied the kinetics of retardation of MgO and ammonium phosphate with boric acid; he reported that boric acid develops a polymeric coating on MgO grains and thus retards the setting rate. Addition of only 1% of boric acid in a powder mixture of MgO and KH_2PO_4 can retard the mixing and setting time of the slurry from 1.5 to 4.5 h (see Chapter 15 for a controlled test for this retardation).

Figure 9.4 shows the X-ray diffraction output of a magnesium–potassium phosphate ceramic in which boric acid was added as a retardant. The amount of boric acid was 1 wt% of MgO in the powder blend. The X-ray diffraction pattern indicated that the polymeric coating on the MgO particles was a low-solubility magnesium–boron–phosphate compound, called “lünebergite”



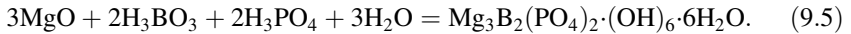
Sengupta *et al.* [26] studied the crystal structure of this mineral and established the X-ray diffraction patterns that were used in identifying it.

Fig. 9.4.



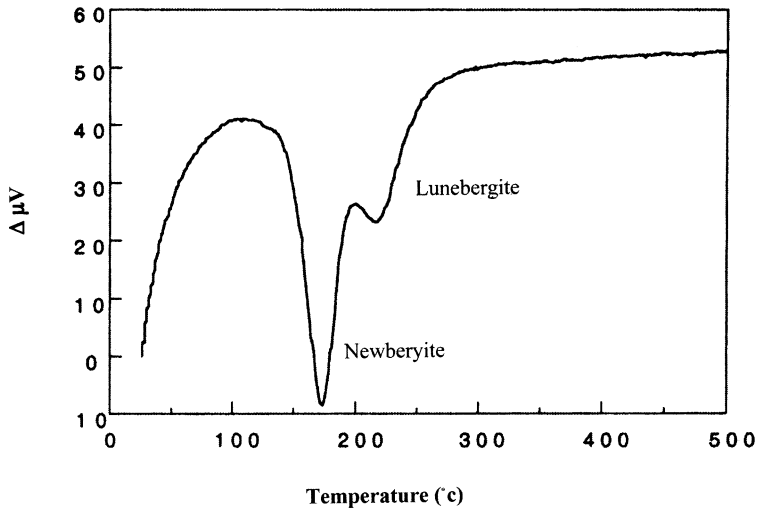
X-ray diffraction output of $\text{MgKPO}_4 \cdot 6\text{H}_2\text{O}$ ceramic with boric acid.

Figure 9.5 shows the differential thermal analysis (DTA) output from the ceramic. The endotherms confirm formation of newberyite and lünebergite. Lünebergite is formed by the reaction



The general concept of the kinetics of retardation of this reaction is as follows. When MgO-containing H_3BO_3 is mixed in the phosphate solution, lünebergite is formed on the

Fig. 9.5.



Differential thermal analysis output of $\text{MgKPO}_4 \cdot 6\text{H}_2\text{O}$ ceramic with boric acid.

surface of individual grains of MgO, and that compound coats the individual particles. This less soluble compound prevents the grains from dissolving in the acid solution. Subsequently, as the pH of the solution rises, the coating dissolves slowly into the solution exposing the grains back to the acid solution. Because dissolution of MgO is delayed, the rates of dissolution and the acid–base reaction are reduced.

Calcined MgO is a requirement for forming practical Mg-based ceramics, while boric acid addition is not essential in several systems such as formation of $\text{MgKPO}_4 \cdot 6\text{H}_2\text{O}$, unless the mixing and pumping times of the slurry need to be extended for several hours. We will be discussing various Mg-based ceramics that have been developed using these methods.

9.3.

FABRICATION AND PROPERTIES OF Mg-BASED PHOSPHATE CERAMICS

As indicated in Chapter 2, the major products formed in various Mg-phosphate ceramics can be represented by the formulae, $\text{Mg}(\text{X}_2\text{PO}_4)_2 \cdot n\text{H}_2\text{O}$ or $\text{MgXPO}_4 \cdot n\text{H}_2\text{O}$, where X is hydrogen (H), ammonium (NH_4), or an alkali metal. Compounds represented by $\text{Mg}(\text{X}_2\text{PO}_4)_2 \cdot n\text{H}_2\text{O}$, however, are intermediate products and are soluble in water. In the presence of additional MgO, they react and form the more stable $\text{MgXPO}_4 \cdot n\text{H}_2\text{O}$. For example, H_3PO_4 produces a ceramic containing soluble $\text{Mg}(\text{H}_2\text{PO}_4)_2 \cdot \text{H}_2\text{O}$. This intermediate product itself may be used to react with additional MgO to produce insoluble newberyite ($\text{MgHPO}_4 \cdot 3\text{H}_2\text{O}$) ceramic. Similarly, one may use dihydrogen acid phosphates of NH_4 , Al, and K to produce corresponding ceramics.

Table 9.1 summarizes the various magnesium phosphate ceramics that have been produced using either H_3PO_4 or an acid phosphate. These acid phosphates are produced by neutralizing H_3PO_4 partially with NH_4 , Al, or K ions. Because of the increased use of CBPCs during the last decade, some manufacturers are now producing these acid phosphates and supply them commercially. While ceramics formed by NH_4 - and Al-hydrogen phosphates are produced only in small quantities (typically less than a gallon), Mg–K-hydrogen phosphate may be formed in any size. This is because KH_2PO_4 has the highest pH in the acidic range, and the least amount of heat is generated during formation (see Table 4.2).

One common characteristic of these ceramics is that a significant amount of MgO is unreacted and left behind in the final product. Thus, in addition to the phases given in Table 9.1, one finds a large amount of MgO, and to a small extent, brucite [$\text{Mg}(\text{OH})_2$] in the ceramic.

9.3.1. Magnesium Phosphate Ceramics

Reaction between even well calcined MgO and H_3PO_4 solution is highly exothermic, and only small-size ceramics can be formed by this reaction. Rapid reaction gives a soluble $\text{Mg}(\text{H}_2\text{PO}_4)_2$ product, but the same reaction in the presence of boric acid slows down, and

Table 9.1.

Mg-Phosphate Ceramics Produced by Using Acid or Acid Phosphates.

Principal Reaction	Equation Number	Starting pH (size)	Reaction Product	Reference
$MgO + Mg(H_2PO_4)_2 \cdot 2H_2O = 2MgHPO_4 \cdot 3H_2O$	9.6	2.3 (small)	Newberyite	[14]
$MgO + (NH_4)H_2PO_4 + 5H_2O = MgNH_4PO_4 \cdot 6H_2O$	9.7	3.8 (any size)	Struvite	[18]
$MgO + 2NH_4H_2PO_4 + 3H_2O = Mg(NH_4)_2(HPO_4)_2 \cdot 4H_2O$	9.8	3.8 (small size)	Schertelite	[7]
$MgO + (NH_4)_2HPO_4 + 5H_2O = MgNH_4PO_4 \cdot 6H_2O + NH_3 \uparrow$	9.9	7.2 (any size)	Struvite	[8]
$2MgO + Al(H_2PO_4)_3 + (n + 1)H_2O = 2MgHPO_4 \cdot 3H_2O + AlPO_4 \cdot nH_2O$	9.10	<1	Newberyite	[13]
$MgO + KH_2PO_4 + 5H_2O = MgKPO_4 \cdot 6H_2O$	9.11	4.3–8 (any size)	Magnesium potassium phosphate hexahydrate (MKP)	[11,12]

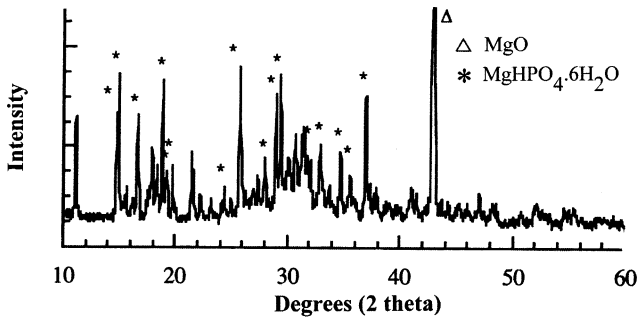
newberyite is formed by the reaction



Though newberyite is a very useful product and appears in several rapid-setting commercial cements, only small quantities of the cement can be mixed at a time. As a result, this product has not found wide use.

Recently, Wagh and Jeong [27] reacted MgO with H₃PO₄ solution and formed Mg(H₂PO₄)₂-rich powder, which they reacted with MgO and dye-casted the mixture to form ceramic forms. The reaction is represented by Equation 9.6 in Table 9.1. Dye casting is suitable for forming ceramics with highly exothermic reactions that set rapidly. As evident from the X-ray diffraction pattern in Fig. 9.6, the major product is newberyite, and

Fig. 9.6.



X-ray diffraction pattern of ceramic formed by the reaction between MgO and Mg(H₂PO₄)₂·2H₂O.

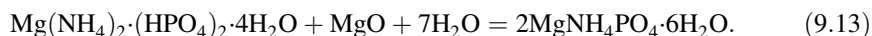
as usual, some MgO remains unreacted. The strength of such products is moderate. For example, the compressive strength of dye-cast specimens with equimolar product in which class F ash was added at 60 wt% loading was found to be 14 MPa (≈ 2000 psi) [28]. The process may be the most suitable for dye casting of refractory products in which ash may be replaced by refractory materials, such as alumina.

9.3.2. Magnesium Ammonium Phosphate Ceramics

Magnesium ammonium phosphates are formed by reacting calcined MgO with either diammonium hydrogen phosphates $((\text{NH}_4)_2\text{HPO}_4)$ [7] or ammonium dihydrogen phosphate $(\text{NH}_4\text{H}_2\text{PO}_4)$ [8], both being components of common fertilizer. The resultant products have been extensively developed for use as mortars. The main problem with these mortars is that during formation and even after, they tend to release ammonia. Hence, though they are comparatively inexpensive, their use is limited to outdoor applications.

9.3.2.1. MORTARS WITH AMMONIUM DIHYDROGEN PHOSPHATE

Formation of mortars and ceramics using ammonium dihydrogen phosphate has been studied by several investigators (Kato *et al.* [28], Takeda *et al.* [29], Abdelrazig and Sharp [17], Popovics *et al.* [21], Abdelrazig *et al.* [19], and El-Jazairi [20]). As shown in Table 9.1, the main products of reaction of calcined MgO with ammonium dihydrogen phosphate are struvite and schertelite. In the presence of sufficient water, the latter converts to struvite by the reaction



Often formed in addition to these two phases are dittmarite $(\text{MgNH}_4\text{PO}_4 \cdot \text{H}_2\text{O})$ and stercorite $(\text{MgNH}_4\text{PO}_4 \cdot 4\text{H}_2\text{O})$, which differ in composition from struvite in the amount of hydration. Formation of struvite from these phases will depend on the amount of water that is available for the complete reaction [17–19].

Abdelrazig *et al.* [19] provided snapshots of the microstructure of magnesium ammonium phosphate cement while it is curing. Initially, the structure starts with poorly crystalline grains and hanger into one containing platy crystals, which were identified as dittmarite and struvite. As the mass cures further, rod-like struvite crystals grow, indicating that struvite is the final crystal structure in this cement. Detailed study by Abdelrazig *et al.* [18] showed several typical characteristics of these rapid-setting cements:

1. The compressive strength depends on water content and curing time. Mortars with less water showed higher strength. For example, a solid-to-water ratio of 8 gave a compressive strength of 19.5 MPa (2790 psi) in 24 h, while the mortar made with a solid-to-water ratio of 16 attained a strength of 27.4 MPa (3910 psi).
2. Strengths increased rapidly with curing time initially, and then slowly with longer curing duration. Compressive strengths of a typical sample were 20 MPa (2900 psi)

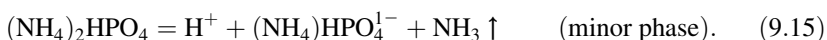
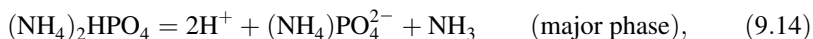
after 1 h, 30 MPa (4286 psi) after 3 h, and approached 50 MPa (7143 psi) after 24 h. The moduli of rupture were more than 6 MPa (857 psi) in 1 h and 9 MPa (1286 psi) after 24 h. After 1 day these values changed very little.

3. The overall pore volume decreased with time from 27.4 mm³/g in 1 h to 20.3 mm³/g in 28 days.

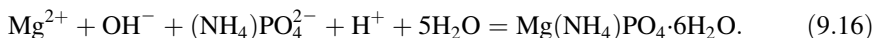
Overall, these characteristics demonstrate that ammonium dihydrogen phosphate makes excellent rapid-setting grouts for outdoor applications such as road-repair materials in winter time in cold countries, because cold weather retards the initial setting, release of ammonia does not affect the workers and users in an open atmosphere, and the high strength makes these cements superior to conventional Portland cement. Products based on this material have been marketed commercially.

9.3.2.2. CEMENT WITH DIAMMONIUM HYDROGEN PHOSPHATE

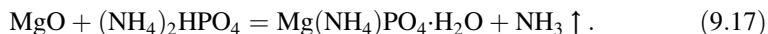
Sugama and Kukacka [7] reported formation of struvite-rich cements by reacting diammonium hydrogen phosphate solution with calcined magnesium oxide. They also reported a magnesium phosphate phase (Mg₃(PO₄)₂·4H₂O) in it. Abdelrazig and Sharp [17] and Wilson and Nicholson [1], however, do not believe that such a phase could exist in these cements. We would agree with these latter authors, because the starting pH of the diammonium hydrogen phosphate is 3.8, and the pH of the cement when formed is nearly 8. In this pH range, according to the discussion presented in Chapter 4, the dissolution of (NH₄)₂HPO₄ is given by



The dissolved MgO will produce Mg²⁺ and OH⁻, which will react with the diammonium phosphate ions to form struvite by the reaction



To form Mg₃(PO₄)₂·4H₂O, ionization of (NH₄)₂HPO₄ will yield PO₄³⁻, which does not occur in the pH range of 3.8–8 in which these ceramics are formed. However, other hydrated phases such as dittmarite or schertelite could be formed by the reactions 9.8 and 9.17, which follow from the dissolution reactions



The cement formed by these reactions showed all the characteristics of rapid-setting cements. The strengths after 30 and 60 min were 5.65 MPa (820 psi) and 6.75 MPa (980 psi), respectively. After 15 h, the strength seemed to have leveled off at 19.3 MPa (2800 psi). These strengths are not as high as those obtained from ammonium dihydrogen phosphates, but the rapid-setting characteristics are similar. It is likely that mortars of these cements will also exhibit higher strengths.

Like cements made from ammonium dihydrogen phosphates, these are also very porous cements (porosity of 52%). The high porosity must be due to evolution of ammonia during cement formation.

One interesting feature of Sugama and Kukacka's study [7] is that the strength kept rising as they heated this cement up to 1300°C. The strength reached 48.23 MPa (7000 psi). Struvite appears to be very stable, even at high temperature, and probably decomposes only at 930°C. The stability of these phosphate cements at high temperature is an important characteristic because conventional Portland cements are not stable at high temperatures and, hence, cannot be used for refractory applications. Phosphate cements can be very useful in this respect because they can be cast into required shapes at room temperature and sintered at high temperatures.

9.3.3. Cement with Aluminum Acid Phosphate

Aluminum acid phosphate ($\text{Al}(\text{H}_2\text{PO}_4)_3$) was first studied by Abdelrazig *et al.* [30] and Ando *et al.* [31]. Subsequently, a detailed study was also conducted by Finch and Sharp [13]. The basic reaction governing cement formation with aluminum acid phosphate is given by Eq. 9.10 presented in Table 9.1. The first term on the right-hand side of Eq. 9.10 is newberyite, a crystalline product. The second term represents hydrated aluminum orthophosphate, an amorphous product. Finch and Sharp [13] argued, on the basis of stoichiometry and energy-dispersive X-ray analyses of fractured surfaces of these cements, that the latter cannot be in pure form and must contain some MgO, thus forming a phase of $\text{Al}_2\text{O}_3\text{--MgO--P}_2\text{O}_5\text{--H}_2\text{O}$.

Because of the low pH of $\text{Al}(\text{H}_2\text{PO}_4)_3$, the reaction given in Eq. 9.10 is highly exothermic and, hence, only small batches can be made of this cement. In this respect, the reaction imitated that of MgO with H_3PO_4 solution, in which newberyite is formed at a very low pH and only in small batches. Finch and Sharp [13] found that the molar ratio given by Eq. 9.10 yielded a cement that set slowly, but when the molar ratio of MgO to $\text{Al}(\text{H}_2\text{PO}_4)_3$ was raised to 4 : 1, the cement set with maximum content of newberyite. The overall structure of the cement may be considered as newberyite crystals bonded by the amorphous phase of $\text{Al}_2\text{O}_3\text{--MgO--P}_2\text{O}_5\text{--H}_2\text{O}$.

9.3.4. Magnesium Potassium Phosphate Ceramic (Ceramicrete)

In an effort to develop stronger and denser encapsulating material for radioactive and hazardous waste streams in large sizes, Wagh and his group [11,12,32] developed magnesium potassium phosphate ceramic by reacting calcined magnesium oxide with monopotassium phosphate in an aqueous solution. The reaction between these components is given by Eq. 9.11 in Table 9.1. The reaction product is highly crystalline. Because this ceramic sets at room temperature like concrete, it was named Ceramicrete. The product is formed by reacting a blend of 1 mol each of MgO and KH_2PO_4 powders with 5 mol of water. In small scale (a liter size), the slurry is mixed for ≈ 25 min till it forms a thick but pourable paste. It is then allowed to set. The setting time is approximately

an hour. In larger scale, this mixing time is reduced significantly. The product has superior properties when it is mixed with fly ash or wollastonite (CaSiO_3) [3,11]. Compressive strengths range from 55 to 83 MPa (8000–12,000 psi).

Apart from the high strength of the composites of this material, its major advantage lies in forming large castings. The reaction given by Eq. 9.11 is less exothermic. KH_2PO_4 has a solubility that is lower than ammonium phosphates (see Chapter 3) and hence dissolves slowly. This helps in reducing the reaction rate as well as exothermic heat release. Bulk-scale applications of this material will be discussed in subsequent chapters.

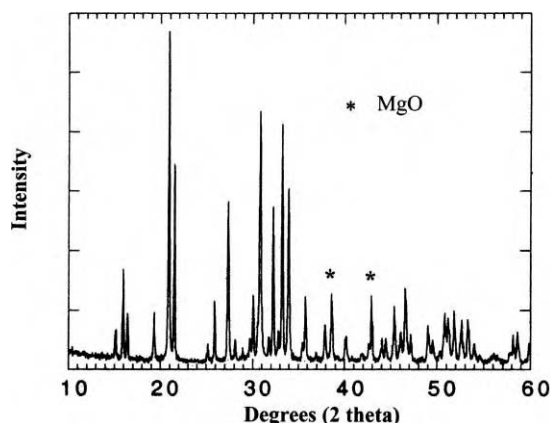
The X-ray diffraction output of this ceramic and its microstructure is shown in Figs. 9.7 and 9.8, respectively. The X-ray diffraction pattern does not contain any peaks other than those of MKP and unreacted MgO . Similarly, the scanning electron microphotographs show only crystals of MKP. Thus, unlike other cements such as those formed by ammonium phosphates in which reaction products contain more than one phase, this product is comparatively phase pure.

The literature on MKP mineral is scarce. Sivaprasad *et al.* [33] and Wagh *et al.* [34] consider this material as an analog of struvite, in which NH_4 is replaced by K, and have determined its crystalline structure. Differential thermal analysis (DTA) and thermogravimetric analysis (TGA) indicated that the 6 mol of water in the crystal are loosely bound and escape upon heating at 120°C (Fig. 9.9), after which anhydrous MKP is formed.

9.3.5. Other Magnesium Phosphate Ceramics

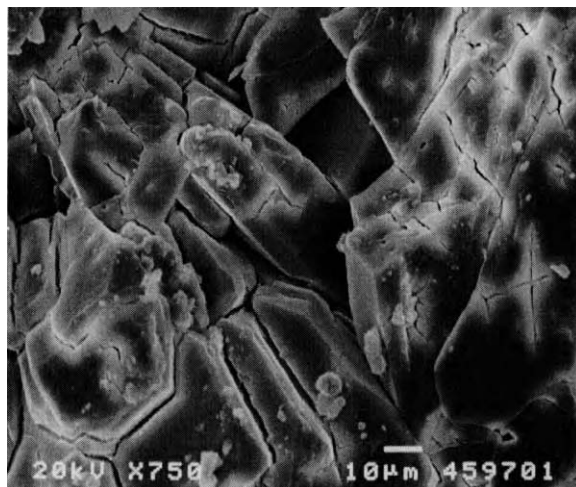
The literature cites several other Mg-based phosphate ceramics or cements that use different acid phosphates or salts of magnesium. Connaway-Wagner *et al.* [9] reacted ammonium triphosphosphate with calcined MgO and formed a hard cement with strength of 13,000 psi (90 MPa). The reaction product was an amorphous phase of magnesium

Fig. 9.7.



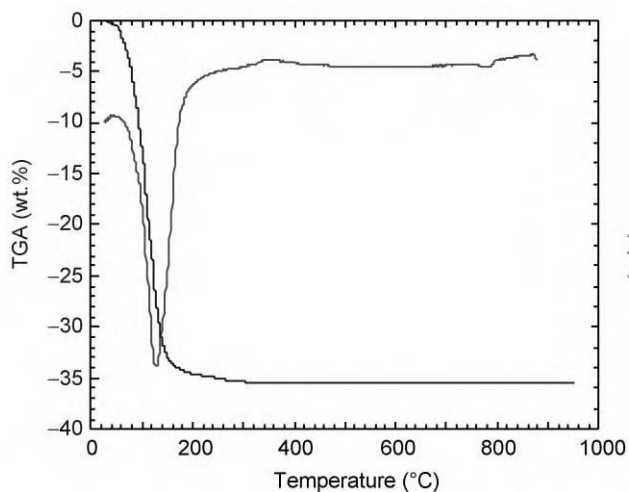
X-ray diffraction output of Ceramicrete.

Fig. 9.8.



Scanning electron micrograph of Ceramicrete.

Fig. 9.9.



DTA and TGA outputs of Ceramicrete.

ammonium triphosphosphate when made in small batches, while it also formed orthophosphates and pyrophosphates when made in large batches.

Magnesium titanates have also been used to form such cements. Mg_2TiO_4 , MgTiO_3 , and $\text{Mg}_2\text{Ti}_2\text{O}_5$ have been reacted with phosphoric acid by Sychev *et al.* [35] and Sudakas *et al.* [36]. Newberyite is formed when Mg_3TiO_4 is used, but in other cases, amorphous phases are formed that are difficult to identify.

REFERENCES

1. A.D. Wilson and J.W. Nicholson, *Acid-Base Cements* (Cambridge University Press, Cambridge, 1993).
2. F.G. Sherif and E.S. Michaels, Fast-setting cements from liquid waste phosphorous pentoxide containing materials, U.S. Patent No. 4,487,632, 1984.
3. F.G. Sherif and E.S. Michaels, Fast-setting cements from solid phosphorous pentoxide containing materials, U.S. Patent No. 4,505,752, 1985.
4. F.G. Sherif and A.G. Ciamei, Fast-setting cements from superphosphoric acid, U.S. Patent No. 4,734,133, 1988.
5. F.G. Sherif and F.A. Via, Production of solid phosphorous pentoxide containing materials for fast-setting cements, U.S. Patent No. 4,755,227, 1988.
6. F.G. Sherif, F.A. Via, L.B. Post, and A.D.F. Toy, Improved fast-setting cements from ammonium phosphate fertilizer solution, EP Patent No. EP0203485, 1986.
7. T. Sugama and L.E. Kukacka, "Magnesium monophosphate cements derived from diammonium phosphate solutions," *Cem. Concr. Res.*, **13** (1983) 407–416.
8. T. Sugama and L.E. Kukacka, "Characteristics of magnesium polyphosphate cements derived from ammonium polyphosphate solutions," *Cem. Concr. Res.*, **13** (1983) 499–506.
9. M.C. Connaway-Wagner, W.G. Klemperer, and J.F. Young, "A comparative study of magnesia-orthophosphate and magnesia tripolyphosphate cements," *Ceram. Trans.*, **16** (1991) 679–688.
10. E.D. Demotakis, W.G. Klemperer, and J.F. Young, "Polyphosphate chain stability in magnesia-polyphosphate cements," *Mater. Res. Symp. Proc.*, **45** (1992) 205–210.
11. A.S. Wagh, S.Y. Jeong, and D. Singh, High-strength phosphate ceramic (cement) using industrial by-product ash and slag. *Proc. of Int. Conf. on High-Strength Concrete, Kona, HI*, July 1997.
12. A.S. Wagh, D. Singh, and S.Y. Jeong, Method of waste stabilization via chemically bonded phosphate ceramics, U.S. Patent No. 5,830,815, 1998.
13. T. Finch and J.H. Sharp, "Chemical reactions between magnesia and aluminium orthophosphate to form magnesia-phosphate cements," *J. Mater. Sci.*, **24** (1989) 4379–4386.
14. S.Y. Jeong and A.S. Wagh, Formation of chemically bonded ceramics with magnesium dihydrogen phosphate binder, U.S. Patent pending.
15. A.K. Sarkar, "Hydration/dehydration characteristics of struvite and dittmarite pertaining to magnesium ammonium phosphate cement system," *J. Mater. Sci.*, **26** (1991) 2514–2518.
16. O.S. Krylov, I.N. Medvedeva, G.N. Kas'yanova, Yu.P. Tarlakov, and S.A. Mertsalova, Characteristics of magnesium phosphates formed during hardening of magnesium phosphate cements, UDC 546.46'185, Translated from *Isvestia Akademii Nauk SSSR, Neorganicheskie Materialy*, **12** [3] (1976) 566–568.
17. B.E.I. Abdelrazig and J.H. Sharp, "Phase changes on heating ammonium magnesium phosphate hydrates," *Thermochim. Acta*, **129** (1988) 197–215.
18. B.E.I. Abdelrazig, J.H. Sharp, and B. El-Jazairi, "The microstructure and mechanical properties of mortars made from magnesia-phosphate cement," *Cem. Concr. Res.*, **19** (1989) 247–328.
19. B.E.I. Abdelrazig, J.H. Sharp, and B. El-Jazairi, "The chemical composition of mortars made from magnesia-phosphate cement," *Cem. Concr. Res.*, **18** (1988) 415–425.
20. B. El-Jazairi, "Rapid repair of concrete pavings," *Concrete*, **16** [9] (1982) 12–15.
21. S. Popovics, N. Rajendran, and M. Penko, "Rapid hardening cements for repair of concrete," *ACI Mater. J.*, **84** (1987) 64–73.
22. A.S. Wagh and S.Y. Jeong, Chemically bonded phosphate ceramics for stabilization and solidification of mixed waste, in *Handbook of Mixed Waste Management Technology* (CRC Press, Boca Raton, FL, 2000), Chapter 6.3.
23. M. Pourbaix, *Atlas of Electrochemical Equilibria in Aqueous Solutions*, 2nd English ed. (National Association of Corrosion Engineers, Houston, TX, 1974), pp. 139–145.
24. W.R. Eubank, "Calcination studies of Mg oxide," *J. Am. Ceram. Soc.*, **34** [8] (1951) 225–229.
25. A.S. Wagh and S.Y. Jeong, "Chemically bonded phosphate ceramics: I. A dissolution model of formation," *J. Ceram. Soc.*, **86** [11] (2003) 1838–1844.
26. P. Sengupta, G. Swihart, R. Dimitrijevic, and M. Hossain, "The crystal structure of lunebergite," *Am. Mineral.*, **76** (1991) 1400–1407.

27. A.S. Wagh and S. Jeong, Argonne National Laboratory, unpublished data.
28. K. Kato, M. Shiba, M. Nakamura, and T. Ariyoshi, Report of the Institute of Medical and Dental Engineering (Tokyo Medical and Dental University), **10** (1976) 45–61.
29. S. Takeda, S. Kawahara, M. Nakamura, K. Sogawa, S. Machara, H. Mori, M. Yokoyama, H. Takahashi, and A. Yata, *Shika Igaku*, **42** (1979) 429.
30. B.E.I. Abdelrazig, J.B. Sharp, P.A. Siddy, and B. El-Jazairi, “Chemical reactions in magnesia-phosphate cement,” *Proc. Br. Ceram. Soc.*, **35** (1984) 141–154.
31. J. Ando, T. Shinada, and G. Hiraoka, “Reactions of monoaluminum phosphate with alumina and magnesia,” *Yogyo-Kyokai-Shi*, **82** (1974) 644–649.
32. A.S. Wagh and S.Y. Jeong, Chemically bonded phospho-silicate ceramics, U.S. Patent No. 6,518,212, 2003.
33. P. Sivaprasad, K. Ramesh, and Y.P. Reddy, “Optical absorption spectrum of nickel doped $\text{MgKPO}_4 \cdot 6\text{H}_2\text{O}$,” *Solid State Commun.*, **73** [3] (1990) 239–241.
34. A.S. Wagh, R. Strain, S.Y. Jeong, D. Reed, T. Krause, and D. Singh, “Stabilization of rocky flats Pu-contaminated ash within chemically bonded phosphate ceramics,” *J. Nucl. Mater.*, **265** (1999) 295–307.
35. M.M. Sychev, I.N. Medvedeva, V.A. Biokov, and O.S. Krylov, “Effect of reaction kinetics and morphology of neoformation on the properties of phosphate cements based on magnesium titanates,” *Chem. Abstr.*, **96**, 222252e.
36. G.L. Sudakas, L.I. Turkina, and A.A. Chernikova, “Properties of phosphate binders,” *Chem. Abstr.*, **96**, 202,472.

This page is intentionally left blank

Zinc Phosphate Ceramics

As mentioned in Chapter 2, zinc phosphate dental cements were discovered over a century ago, and their development has continued since then [1–9]. A brief history of this development is given in that chapter. For a detailed history of these cements and properties of contemporary formulations, the reader is referred to the book by Wilson and Nicholson [10]. Because, the kinetics of formation of these cements has not been discussed in these earlier publications, we will emphasize it in this chapter and present the earlier work in light of the solubility characteristics of zinc oxide and its products in an acid phosphate solution.

Roastaing's patents [1] and Rollins's article [2], published in the late 19th century, are the first documents that provide formulations in which zinc oxide is reacted with phosphoric acid to produce dental cements. The purpose behind much of the following research was to find ways to retard the fierce reaction between these components so that practical cements could be developed. It was accomplished by the calcining of zinc oxide and neutralizing phosphoric acid partially with zinc and/or aluminum hydroxide. Combination of these two methods yielded good dental cements [11,12] that allowed dentists sufficient time to mix and apply them. The resulting phases in these cements were crystalline. The major phases depended on time of curing and the presence of water during curing. These phases were also influenced by other components, such as aluminum oxide, in the mixture. However, in simple systems of zinc oxide and phosphoric acid, investigations revealed that zinc hydrophosphates ($\text{Zn}(\text{HPO}_4)_2 \cdot 2\text{H}_2\text{O}$ and $\text{ZnHPO}_4 \cdot 3\text{H}_2\text{O}$) are formed first and these partially soluble hydrophosphates are gradually converted to hopeite, $\text{Zn}_3(\text{PO}_4)_2 \cdot 4\text{H}_2\text{O}$ [7,9,13–17], which is the ultimate form of the cement.

The role of aluminum in the zinc phosphate cements was considered very important. Aluminum oxide greatly moderated the reaction of zinc oxide and phosphoric acid, and this effect was attributed to the formation of an aluminum phosphate gelatinous coating on zinc oxide particles. In fact, Wilson and Nicholson [10] believe that the gelatinous

substance may even be zinc aluminophosphate phase, which subsequently crystallizes into hopeite and aluminophosphate amorphous gel ($\text{AlPO}_4 \cdot n\text{H}_2\text{O}$).

The final cement is an opaque solid that consists of excess zinc oxide coated and bonded by possibly aluminum phosphate and zinc phosphate gels. The cement is porous and permeable to dyes [10].

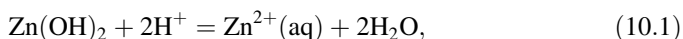
Another major development in zinc phosphate cement is zinc silicophosphate [18]. Mixing aluminosilicate glass and zinc oxide and then reacting the mixture with phosphoric acid produced this cement. Its properties lie between those of zinc phosphate and silicate cements. For example, the compressive strength is 99–1681 MPa (14,300–24,400 psi) [19], which is lower than that of silicate dental cement but higher than that of zinc phosphate cement. Fluorides are added in these cements, and hence, their main advantage is the sustained release of fluorine, which is invaluable in dentistry [20]. After being absorbed by the tooth enamel, this fluorine protects the tooth from caries-producing debris and plaque.

10.1.

SOLUBILITY CHARACTERISTICS OF ZINC OXIDE

Like calcium oxide, zinc oxide readily forms zinc hydroxide in water. Thus, the solubility of zinc hydroxide is more relevant with regard to the formation of zinc ceramics that are formed in an aqueous solution.

Five different phases of zinc hydroxides have been identified [21]. Amorphous $\text{Zn}(\text{OH})_2$ is the most soluble species, while less soluble phases are denoted by Greek letters α , β , γ and ϵ with $\epsilon\text{-Zn}(\text{OH})_2$ being the least soluble phase. The corresponding solubility equations may be derived from first principles, as discussed in Chapter 5, or may simply be reproduced from Ref. [21]:



Corresponding to these three solubility equations, the dissolved ionic concentrations are given by

$$\log\langle\text{Zn}^{2+}(\text{aq})\rangle = 10.96 - 2\text{pH}, \quad (10.1a)$$

$$\log\langle\text{Zn}^{2+}(\text{aq})\rangle = 12.26 - 2\text{pH}; \quad (10.1b)$$

$$\log\langle\text{HZnO}_2^-(\text{aq})\rangle = -16.68 + \text{pH}, \quad (10.2a)$$

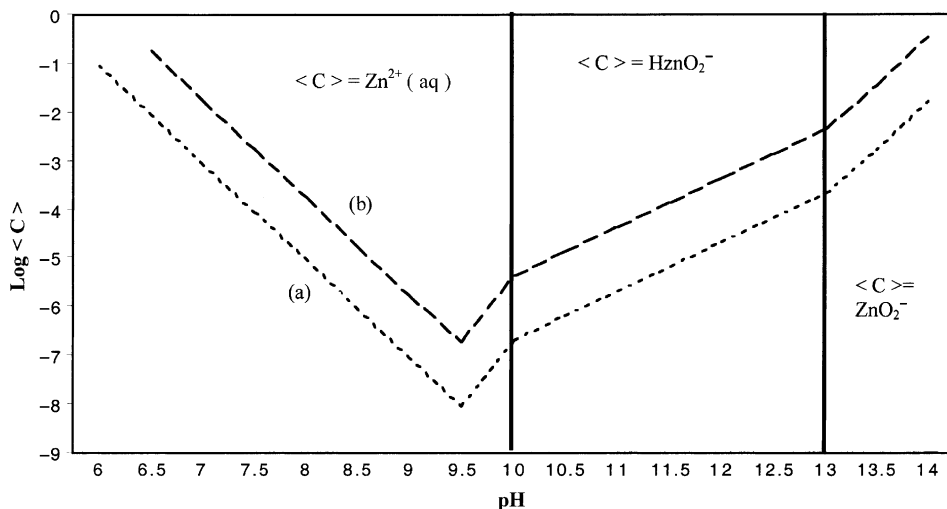
$$\log\langle\text{HZnO}_2^-(\text{aq})\rangle = -15.37 + \text{pH}; \quad (10.2b)$$

$$\log\langle\text{ZnO}_2^{2-}(\text{aq})\rangle = -29.78 + 2\text{pH}, \quad (10.3a)$$

$$\log\langle\text{ZnO}_2^{2-}(\text{aq})\rangle = -28.48 + 2\text{pH}. \quad (10.3b)$$

In the equations given above, “a” stands for the most stable phase $\epsilon\text{-Zn}(\text{OH})_2$, while “b” stands for the amorphous phase that is most soluble.

Fig. 10.1.



Solubility of various phases of zinc oxide as a function of pH.

Figure 10.1 is drawn from Eqs. (10.1a)–(10.3b) and shows the solubility curves of these two most common phases of zinc hydroxide. In these curves, $\text{Zn}(\text{OH})_2$ is amphoteric and has a solubility minimum at pH 9.3. Because the CBPCs are formed within the acidic pH range, the amphoteric nature of $\text{Zn}(\text{OH})_2$ is of little significance during the formation of the ceramic. However, once the ceramic is formed and the pH is ≈ 7 , the excess oxide that remains will be nearly insoluble, and that condition makes the ceramic nonleachable, and hence, more durable in an aqueous environment. In addition, comparing this curve with that of $\text{Ca}(\text{OH})_2$, MgO , and Al_2O_3 , one can see that the solubility of $\text{Zn}(\text{OH})_2$ is lower than that of MgO and $\text{Ca}(\text{OH})_2$ but higher than that of Al_2O_3 (see also Fig. 5.2). Thus, the solubility of $\text{Zn}(\text{OH})_2$ is in the most desirable range for the formation of ceramics. The solubility is not too high, like that of MgO and $\text{Ca}(\text{OH})_2$, and hence the ceramic is not too rapid setting, and at the same time, it is not too low, like that of Al_2O_3 , by which a ceramic could not be formed at room temperature. This feature may be why zinc phosphate was the first successful phosphate cement.

10.2.

FORMATION OF ZINC PHOSPHATE CERAMIC

The literature review summarized in Chapter 2 and discussed in Ref. [10] indicates that zinc phosphate ceramics have been synthesized only in small sizes as dental cements, and no attempt has been made to cast large forms of these cements. In spite of this,

the process of formation has been extensively studied, and properties have been optimized.

The process of fabrication of zinc phosphate cements is very similar to that of magnesium phosphate ceramics. Direct reaction with phosphoric acid is fierce and needs to be slowed down. This is done by the following methods.

10.2.1. Neutralization of Phosphoric Acid

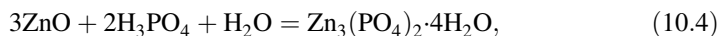
Unlike magnesium oxide, zinc oxide is seldom used in its pure form. It is blended with MgO and often with Al₂O₃ to initiate some neutralization of phosphoric acid [10]. MgO will form its dihydrogen phosphate (see Chapter 9), and as shown in Chapter 11, Al₂O₃ will also form its hydrophosphate. This partial neutralization of the acid aids in reducing the fierce reaction between the base ZnO and the acid. Typically, 3–10 wt% MgO and <1% Al₂O₃ are used.

10.2.2. Precalcination

As in the case of MgO, the powder is precalcined at temperatures of 1000–1350°C to reduce the surface area of the particles [22]. The surface area is reduced by partial elimination of porosity of individual grains and by grain growth resulting from consolidation of amorphous content. The presence of MgO and silica in zinc oxide promotes densification by forming a solid solution of ZnO with these oxides [7,23]. In addition to this densification, compounds of lower solubility formed by the solid solutions, such as zinc silicates, are likely to reduce the overall solubility of zinc oxide.

As described in Ref. [10], in spite of the partial neutralization of the acid and the precalcination of the powder, the ceramic formation is extremely rapid. Accordingly, these cements gain half of their strength in the first 10 min and 80% within an hour [24,25]. As a result, this product is most suitable for dental applications, where the dentist will produce slurry in a small scale within a few minutes, apply it to the patient, and expect its solidification within a reasonable waiting time.

The reaction during the formation of these cements is highly exothermic. From the enthalpies of formation presented in the Appendices, the extent of energy evolution during the reaction,



is $\Delta H = -241.17$ kJ/mol of the product formed. This energy is expended in a short time and may heat the slurry. Therefore, the heat must be dissipated during ceramic formation. When a dentist prepares only a few grams of the sample, the heat dissipates easily, but if one were to prepare large samples, in spite of the partial neutralization of the acid and precalcination of the powder, the heat is too much, and boils the entire slurry. Thus, only small-sized zinc phosphate ceramics can be made.

10.3.**PHASE FORMATION IN ZINC PHOSPHATE CEMENTS AND THEIR MICROSTRUCTURE**

When zinc oxide is reacted with phosphoric acid, ZnO will form its hydroxide first, and then the acid–base reaction will go through several steps forming intermediate acid phosphates:



This step-by-step neutralization of ZnO is similar to other acid–base cements (and ceramics), such as MgO-containing cement. There is one difference between cement formation with MgO and ZnO. In the case of MgO, as we have noted in Chapter 9, the reaction stops when monohydrogen phosphate ($\text{MgHPO}_4 \cdot 3\text{H}_2\text{O}$, newberyite) is formed, while in the case of zinc phosphate cements, the ultimate phosphate product is a neutral orthophosphate, $\text{Zn}_3(\text{PO}_4)_2 \cdot 4\text{H}_2\text{O}$ (hopeite) [10]. The reason for this difference is the higher solubility of ZnHPO_4 as compared to that of newberyite. The solubility, calculated by the procedure described in Chapter 5.5, is 9.93 g/l for ZnHPO_4 and 0.0026 g/l for MgHPO_4 . Because of its much greater solubility, ZnHPO_4 will dissolve during curing and form hopeite after its reaction with excess ZnO. On the other hand, the less soluble MgHPO_4 will remain as the final phase in the ceramic.

Like Mg-phosphate cements discussed before, all ZnO will not react and form its phosphate. The reaction with phosphoric acid and subsequently the acid phosphates (such as $\text{Zn(H}_2\text{PO}_4)_2$ and ZnHPO_4) occurs only on the surface of individual grains, while the core of the grains, at least for large grains, remains unreacted and acts like the nucleus for the phosphate crystallite growth. Initially, the grains are bonded by the amorphous phosphate gel, which consists of hydrophosphates of zinc and aluminum. Over a long curing time, these amorphous phases may further react with ZnO and form ultimate phases or crystallize. Thus, like other phosphate-bonded ceramics and cements, zinc phosphate cement may also be considered as a two phase material, containing randomly distributed unreacted ZnO that is bonded by either amorphous or crystalline phosphate phases or by both.

10.4.**PROPERTIES OF ZINC PHOSPHATE CEMENTS**

Wilson and Nicholson [10] have provided a thorough discussion on the properties of commercial zinc phosphate cements that contain either magnesium oxide or aluminum oxide. The compressive and tensile strengths of cements are in the range 69–127 MPa (10,000–18,500 psi) and 4.1–8.3 MPa (600–1200 psi), respectively. These strengths are several times higher compared to the strengths of conventional portland cement, which has corresponding strengths of 28 MPa (4000 psi) and 1 MPa (140 psi). Unlike magnesium

phosphate cements that take a long time to attain full strength, these cements attain their full strength within 24 h. This rapid gain of ultimate strength is due to the higher solubility of the intermediate product $\text{ZnHPO}_4 \cdot 3\text{H}_2\text{O}$. Such a rapid gain of strength does not occur in magnesium phosphate cements because of the insolubility of the intermediate product $\text{MgHPO}_4 \cdot 3\text{H}_2\text{O}$.

The ultimate compressive strength of zinc phosphate cements is higher than that of magnesium phosphate cements. This difference may not be because magnesium phosphate cements are weaker than zinc phosphate cements, but it may be a size effect. As we discussed before, zinc phosphate samples are cast in a very small size as dental cements, while magnesium phosphate cements are used in bulk scale. Because large ceramics and cement casts tend to have more flaws, their strength is expected to be lower. As was discussed in Chapter 18, other phosphate-based dental cements also exhibit higher strength because they are cast in small sizes.

REFERENCES

1. C.S. Roasting di Rostagni, Verfahren zur Darstellung von Kitten für zahnärztliche und ähnliche Zwecke, bestehend von Gemischen von Pyrophosphaten des Calciums oder Bariums mit den Pyrophosphaten des Zinks oder Magnesiums, German Patent 6015 (Berlin), 1878. Also in *Correspondenz-Blatt für Zahnärzte*, **10** (1881) 67–69.
2. W.H. Rollins, "A contribution to the knowledge of cements," *Dent. Cosmos*, **21** (1879) 574–576.
3. E.S. Gaylord, "Oxyphosphates of zinc," *Arch. Dent.*, **33** (1889) 364–380.
4. W.B. Ames, "Oxyphosphates," *Dent. Cosmos*, **35** (1893) 869–875.
5. H. Fleck, "Chemistry of oxyphosphates," *Dent. Items Interest*, **24** (1902) 906.
6. W. Souder and G.C. Paffenbarger, Physical properties of dental materials, Natl. Bur. Standards (US) Circ. No. C433, 1942.
7. W.S. Crowell, "Physical chemistry of dental cements," *J. Am. Dent. Assoc.*, **14** (1927) 1030–1048.
8. E.W. Skinner, *Science of Dental Materials*, 3rd ed. (Saunders, Philadelphia, 1947).
9. N.E. Eberly, C.V. Gross, and W.S. Crowell, "System zinc oxide, phosphorous pentoxide, and water at 25 degrees and 37 degrees," *J. Am. Chem. Soc.*, **42** (1920) 1433.
10. A.D. Wilson and J.W. Nicholson, *Acid-Base Cements* (Cambridge University Press, Cambridge, UK, 1993).
11. G.C. Paffenbarger, S.J. Sweeney, and A. Isaacs, "A preliminary report on zinc phosphate cements," *J. Am. Dent. Assoc.*, **20** (1933) 1960–1982.
12. A.B. Wilson, G. Abel, and B.G. Lewis, "The solubility and disintegration test for zinc phosphate dental cements," *Br. Dent. J.*, **137** (1974) 313–317.
13. B.W. Darwell, "Aspects of chemistry of zinc phosphate cements," *Aust. Dent. J.*, **29** (1984) 242–244.
14. F. Halla and A. Kutzeilnigg, "Zür Kennetnis des Zinkphosphatzements," *Zeitschrift für Stomatologie*, **31** (1933) 177–181.
15. D.F. Vieira and P.A. De Arujo, "Estudo a Cristizacao de Cimento de Fosfato de Zinco," *Revista da Faculdade Odontologia da Universidade de Sao Paulo (~ on a in Sao)*, **1** (1963) 127–131.
16. J. Komarska and V. Satava, "Die Chemischen Prozesse bei der Abbindung von Zinkphosphatzementen," *Deutsche Zahnärztliche Zeitschrift*, **25** (1970) 914–921.
17. A.D. Wilson, "Zinc oxide dental cements," in *Scientific Aspects of Dental Materials*, ed. J.A. von Fraunhofer (Butterworths, Boston, 1975), Chapter 5.
18. P.J. Wisth, "The ability of zinc phosphate and hydrophosphate cements to seal space bands," *Angle Orthodont.*, **42** (1972) 395–398.
19. A.D. Wilson, S. Crisp, and B.G. Lewis, "The aqueous erosion of Silicophosphate cements," *J. Dent.*, **10** (1982) 187–197.

20. K.R. Anderson and G.C. Paffenbarger, "Properties of silicophosphate cements," *Dent. Prog.*, **2** (1962) 72–75.
21. M. Pourbaix, *Atlas of Electrochemical Equilibria in Aqueous Solutions* (National Association of Corrosion Engineers, Houston, 1974).
22. D. Dollimore and P. Spooner, "Sintering studies on zinc oxide," *Trans. Faraday Soc.*, **67** (1971) 2750–2759.
23. V.F. Zuravlev, S.L. Volfson, and B.I. Sheveleva, "The processes that take place in the roasting of zinc-phosphate dental cement," *J. Appl. Chem. (USSR)*, **23** (1950) 121–128.
24. C.G. Plant and H.J. Wilson, "Early strength of lining materials," *Br. Dent. J.*, **129** (1970) 269–274.
25. P.D. Williams and D.C. Smith, "Measurement of the tensile strength of dental restorative materials by use of a diametral compressive strength test," *J. Dent. Res.*, **50** (1971) 436–442.

This page is intentionally left blank

Aluminum Phosphate Ceramics

High alumina ceramics are preferred materials for a number of reasons. Their strength is valuable for high load bearing applications, and they are resistant to corrosion in high temperature environments such as steam and CO atmospheres [1,2]. Alumina ceramics are also well known for their low electrical and thermal conductivity. Therefore, they are the most useful materials in refractory bricks and electrical insulating components. Because of their technological importance, their low-temperature processing by chemical bonding has considerable technological significance.

As discussed in Chapter 2, use of alumina in CBPCs has a long history. Alumina and silicates have been used as moderators of acid–base reactions in dental cements. As mentioned in Chapter 2, van Dalen [3] moderated the reaction of zinc oxide and phosphoric acid using aluminum oxide, and attributed the moderation effect to the formation of an aluminum phosphate gelatinous coating on zinc oxide particles. Wilson and Nicholson [4] suspect that the gelatinous substance may even be zinc aluminophosphate phase that subsequently crystallizes into hopeite $((\text{Zn})_3(\text{PO}_4)_2 \cdot 4\text{H}_2\text{O})$ and aluminophosphate amorphous gel $(\text{AlPO}_4 \cdot n\text{H}_2\text{O})$. The resulting cement, in spite of some porosity, has compressive and tensile strengths of 70–31 MPa (10,000–18,600 psi) and 4.3–8.3 MPa (600–1186 psi), respectively [5]. These very high strengths are typical of aluminophosphate products.

Porcelain dental cements were developed by Steenbock [6] who produced silico-phosphate dental material using 50 wt% concentrated phosphoric acid solution and an aluminosilicate glass. Wilson *et al.* [7] showed that various brands of commercial cements consist of powdered alumina–lime–silica glass mixed with phosphoric acid, which form a hard and translucent product. The phosphoric acid used in these cements is partially neutralized by aluminum oxide.

Unlike magnesium phosphate ceramics, phosphate bonded alumina ceramics consist of particles, whose surfaces are coated with berlinite (AlPO_4) , a crystalline orthophosphate. The bonding phase AlPO_4 [8] is formed by the chemical reaction between the phosphoric

acid and alumina. This phase is a solid formed by covalent network of oxygen-bridged alternating PO_4 and AlPO_4 tetrahedra [9]. This structure is isomorphous with that of various forms of silica. Consequently, aluminum phosphate shares many chemical and physical properties of silica, yet AlPO_4 is formed at a much lower temperature [10]. This lower temperature formation of AlPO_4 , possibly with less internal stresses in it than sintered counterparts, may translate into an economic advantage in producing ceramics suitable for high temperature service at low processing costs.

Early studies by Kingery [11] in phosphate bonding involved room temperature bonding of oxide-phosphoric acid mixtures, including alumina. Subsequently, studies were conducted concerning the kinetics of formation of aluminum phosphate from solutions of phosphoric acid or monoaluminum phosphate [12–14]. Bothe and Brown [12] and Lukasiewicz and Reed [13] studied the kinetics of formation of AlPO_4 at low temperatures. O'Hara *et al.* [14] identified the intermediate phases formed during hydrothermal treatment of alumina with phosphoric acid. They observed formation of monoaluminum phosphate ($\text{AlH}_3(\text{PO}_4)_2 \cdot \text{H}_2\text{O}$) at 100–150°C and its conversion to berlinite above 150°C. The exact temperature of formation of intermediate phases may depend on the forms of alumina, with the most reactive ones reacting at lower temperatures [15]. Singh *et al.* [16] formed alumina ceramics by boiling a mixture of alumina and phosphoric acid and then pressing the dried powder. When the mixture was boiled, some reaction of alumina must have occurred that produced an intermediate phase of $\text{AlH}_3(\text{PO}_4)_2 \cdot \text{H}_2\text{O}$, which transformed into a berlinite bonding phase upon curing. Wagh *et al.* [17] conducted a detailed study to understand the kinetics of formation of berlinite bonded alumina ceramics so that a reproducible process may be developed to form such ceramics.

One may recall from Chapter 9 that newberyite has also been found in ceramics formed by reaction of MgO and $\text{Al}(\text{H}_2\text{PO}_4)_3$. Detailed study by Finch and Sharp [18] showed that, when the ratio of $\text{MgO}/\text{Al} : \text{H}_2\text{PO}_4)_3$ is 4:1, newberyite content is maximum in the matrix. In addition, they have also found AlPO_4 and suspect phases of Al-Mg-PO_4 within the ceramic.

Unlike divalent oxides, the solubility of alumina is low and hence some warm temperature treatment is required. In addition, rather than using lower solubility phosphate solutions such as ammonium and potassium phosphate solutions, phosphoric acid solution is directly used. Wagh *et al.* [17] employed a thermodynamic analysis to study the effect of the temperature on the solubility of individual phases of alumina on the formation of its phosphate phases during heat treatment where solubility of hydrated aluminum oxide, viz., hydrargillite ($\text{Al}_2\text{O}_3 \cdot 3\text{H}_2\text{O}$) is enhanced, and that contributes further to the formation of berlinite phase. They confirmed this by differential thermal analysis (DTA) and X-ray diffraction (XRD) analysis on samples heated beyond 118°C.

Production of alumina aquosols from alumina has been well researched in sol-gel science [19]. Yoldas [20] was the first one to show that monolithic alumina gels could be formed by hydrolysis and condensation of aluminum alkoxide. As discussed in Chapter 5, formation of aquosols and their gel is an intermediate step in the formation of chemically bonded phosphate ceramics. Condensation of the hydrated alumina sols by reaction with phosphoric acid to form $\text{Al}(\text{H}_2\text{PO}_4)_3 \cdot \text{H}_2\text{O}$ gel is the first step toward synthesis of a berlinite-bonded alumina ceramic. When this gel is heated to 150°C, this gel reacts with additional alumina and releases water, and crystalline berlinite is produced. This Chapter

details the kinetics of formation of alumina ceramics through these intermediate transformations and also provides the basic physical and mechanical properties of the ceramic.

11.1.1.

SOLUBILITY ENHANCEMENT WITH TEMPERATURE, AND FORMATION OF BERLINITE PHASE

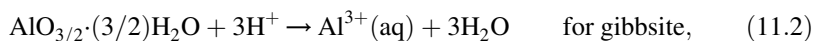
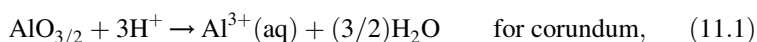
Dissolution of alumina at high pH is well recognized in the Bayer process used to extract alumina from its mineral, bauxite. Bauxite is digested in a very high pH (>13) solution at 150–250°C and 20 atm, and the dissolved alumina is separated from the rest of the insoluble bauxite minerals. The hydrothermal dissolution of alumina is also used in forming calcium aluminate cement by partially dissolving alumina and calcium oxide [21]. These examples indicate that the process may also be used to form phosphate bonded alumina ceramic by dissolving alumina in phosphoric acid solution. The difference between the above two examples and the formation of CBPC of alumina is that, the dissolution in the latter case is in an acidic medium, while in the former two, it is in an alkaline medium. Because alumina is amphoteric, and exhibits higher solubility at both extremes of the pH range, it has been possible to dissolve it at low as well as high pH. An extensive discussion on the solubility of alumina has already been given in Chapter 5. The thermodynamic tools developed in Chapter 6 may be used to predict an enhancement of the solubility of various alumina phases at slightly elevated temperatures. The dissolved alumina should react subsequently with phosphate ions to form aluminum phosphate phases.

Aluminum oxides are found in various forms; alumina (corundum, Al_2O_3), gibbsite ($\text{Al}_2\text{O}_3 \cdot 3\text{H}_2\text{O}$), and boehmite (AlOOH) are the most important crystalline forms among these. In addition, aluminum hydroxide ($\text{Al}(\text{OH})_3$) may also exist in an amorphous form. Depending on which oxide is used to form a ceramic, the solubility varies and so do the conditions in which it dissolves. This phenomenon is similar to the dissolution of alumina from the mineral bauxite. Depending on whether the bauxite is gibbsitic or boehmitic, different temperatures are used to digest the bauxite in caustic soda solution.

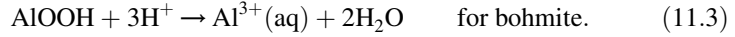
Roy *et al.* [8] reported ceramic reactions between various forms of alumina and phosphoric acid when the mixtures were subjected to an ultrasound signal. Though this method by itself did not produce a solid phosphate ceramic, the reactions themselves were an important step towards the formation of the ceramics.

Dissolution of various forms of alumina in an acidic, neutral, and basic conditions is given by the following reactions.

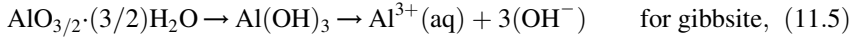
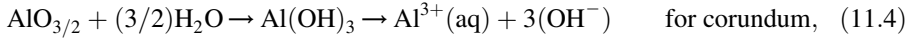
(a) *Reactions in acidic conditions:*



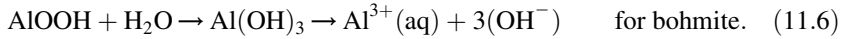
and



(b) *Reactions in neutral conditions:*

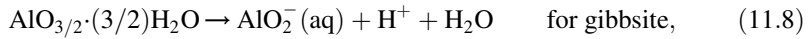
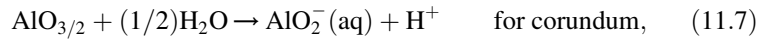


and

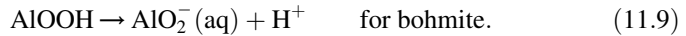


The intermediate reaction that yields $\text{Al}(\text{OH})_3$ arises in all these cases because it is in near thermodynamic equilibrium with alumina phases in water.

(c) *Reaction in alkaline region:*



and



The corresponding solubility equations (11.10)–(11.17) for the above reactions for various forms of alumina are given in Table 11.1. The numbers in these equations have

Table 11.1.

Solubility Equations for Various Forms of Alumina.

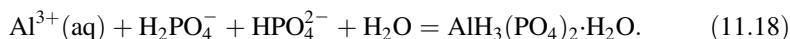
Form of Alumina	Solubility Equation
Corundum	$\log(\text{Al}^{3+}(\text{aq})) = 8.55 - 3\text{pH}$ in acidic and neutral ^a regions, (11.10) $\log(\text{Al}^{3+}(\text{aq})) = -11.76 + \text{pH}$ in alkaline region, (11.11)
Gibbsite or hydrargillite ($\text{Al}_2\text{O}_3 \cdot 3\text{H}_2\text{O}$)	$\log(\text{Al}^{3+}(\text{aq})) = 5.7 - 3\text{pH}$ for acidic and neutral ^a regions, (11.12) $\log(\text{AlO}_2^-) = -13.2 + \text{pH}$ in alkaline region, (11.13)
Bohmite ($\text{Al}_2\text{O}_3 \cdot \text{H}_2\text{O}$)	$\log(\text{Al}^{3+}(\text{aq})) = 7.98 - 3\text{pH}$ in acidic and neutral ^a regions, (11.14) $\log(\text{AlO}_2^-) = -12.32 + \text{pH}$ in alkaline region, (11.15)
Aluminum hydroxide ($\text{Al}(\text{OH})_3$)	$\log(\text{Al}^{3+}(\text{aq})) = 9.66 - 3\text{pH}$ in acidic and neutral ^a regions, (11.16) $\log(\text{AlO}_2^-) = -10.64 + \text{pH}$ in alkaline region, (11.17)

^aThe general convention for neutral regions is to start from Eqs. 11.4–11.6 and obtain solubility equations as $\log(\text{Al}^{3+}(\text{aq})) = K_0 - 3\text{pH}$, where K_0 for the four phases above is $K_{\text{sp}} - 3 \times 14$, because 14 is the maximum pH. This arises from the fact that $\log(\text{OH}^- \times \text{H}^+) = 14$, and the conventional solubility product constant K_0 is defined as $\log(\text{Al}^{3+}(\text{aq})) \times (\text{OH}^-)^3$, which when substituted for $\langle \text{OH}^- \rangle$ gives $K_0 = K_{\text{sp}} - 3 \times 14$.

been calculated using the procedure discussed in Chapter 5 and the Gibbs free energy given in Appendix A (see also Ref. [21] for details).

Figure 11.1 shows the plots of ionic concentrations $\langle \text{Al}^{3+}(\text{aq}) \rangle$ and $\langle \text{AlO}_2^-(\text{aq}) \rangle$ as functions of pH for various forms of alumina. These have been drawn using the equations in Table 11.1. These curves in this figure imply that the solubility has a minimum at $\text{pH} \sim 5$ and increases in both acidic and alkaline regions, exhibiting amphoteric behavior of alumina.

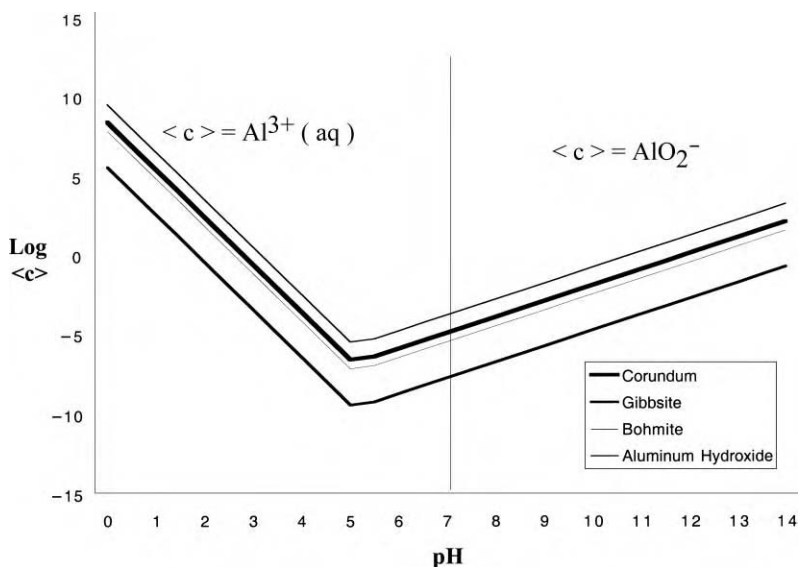
The pH range of formation of CBPCs is 2–8, as in this region there is abundance of dissolved phosphate species such as H_2PO_4^- , and HPO_4^{2-} . The cationic concentration $\langle \text{Al}^{3+}(\text{aq}) \rangle$ in the acidic range is high at the pH 2, but rapidly decreases as the pH is increased (see Fig. 11.1). The neutralization of the acid in this range occurs due to the reaction



Because of this neutralization, the solubility of alumina decreases till the solution attains the neutral pH, in which as noted by Pourbaix [22], there is abundance of $\text{Al}_2\text{O}_3 \cdot 3\text{H}_2\text{O}$ which has a very low solubility. $\text{Al}_2\text{O}_3 \cdot 3\text{H}_2\text{O}$ forms a passivation layer on the surface of individual particles, and consequently, further solubilization is hindered by this coating and formation of the ceramic is obstructed. At this point, it is necessary to enhance the solubility of $\text{Al}_2\text{O}_3 \cdot 3\text{H}_2\text{O}$ by other means.

The required dissolution of $\text{Al}_2\text{O}_3 \cdot 3\text{H}_2\text{O}$ is carried out by a mild heat treatment by enhancing the solubility of this layer. The temperature of maximum solubility of $\text{Al}_2\text{O}_3 \cdot 3\text{H}_2\text{O}$ may be determined thermodynamically.

Fig. 11.1.



Solubility curves of alumina as a function of pH.

As we have seen in Chapter 6, the solubility product dependence on temperature is given by

$$K_{sp}(T) = -\frac{\beta}{2.301}(\Delta G) = -\frac{\beta}{2.301} \left[\Delta G_0 - T_0 \Delta C_p + \Delta C_p T - \frac{\Delta T}{T_0} (\Delta H_0 - \Delta G_0) + \Delta C_p T \ln \left(\frac{T}{298} \right) \right]. \quad (11.19)$$

The temperature for maximum solubalization of $\text{Al}_2\text{O}_3 \cdot 3\text{H}_2\text{O}$ can be easily calculated by differentiating K given by $K = \exp\beta[-\Delta G]$. We obtain

$$d(K_{\max})/dT = 0 = (-1/kT^2)\Delta G + (1/kT)d/dT(\Delta G). \quad (11.20)$$

Invoking the second Gibbs–Helmholtz relation, i.e.,

$$d/dT(\Delta G) = -\Delta S = (\Delta G - \Delta H)/T \quad (11.21)$$

we obtain from Eq. 11.20,

$$K_{\max}(\Delta H/RT^2) = 0. \quad (11.22)$$

The solubility product constant is maximized when the temperature $T = T_{\max}$, given by

$$\Delta H(T_{\max}) = 0. \quad (11.23)$$

Equation 11.23 may be used to maximize the solubility of Al_2O_3 . When calculated for acidic and alkaline regions, however, T_{\max} is very large, but in neutral region, it gives only a warm temperature. Thus, if we assume that the specific heats of the individual components in Eq. 11.3 do not vary appreciably with temperature in the temperature range of T_0 and T_{\max} , we write using Eq. 11.23

$$\Delta H(T_{\max}) = \Delta H(T_0) + \Delta C_p(T_{\max} - T_0) = 0, \quad (11.24)$$

where ΔC_p is the net change in C_p in the solubility reaction. The condition for maximizing K_{sp} becomes

$$T_{\max} = T_0 - \Delta H(T_0)/\Delta C_p. \quad (11.25)$$

Using the values of ΔH_0 and C_p for the individual components in Eqs. 11.4–11.6 from the tables in Appendix B, we obtain the net changes ΔH_0 and ΔC_p and substitute them in Eq. 11.25 to obtain T_{\max} for each of the alumina phases. The corresponding values of $\log\langle\text{Al}^{3+}(\text{aq})_{\max}\rangle$ are then calculated using the following equation derived in Section 5.4.

$$\log(\text{Al}^{3+}(\text{aq})_{\max}) = pK_{sp_{\max}} - 3\text{pH} \quad (11.26)$$

Table 11.2 provides T_{\max} and $\log\langle\text{Al}^{3+}(\text{aq})_{\max}\rangle$ in the neutral region for the different phases of alumina.

The numbers in Table 11.2 show the temperatures of maximum solubility differ for each of the phases and also the extent of solubility enhancement is different for each of the species. Gibbsite, though starts with a lower solubility, picks up as the temperature is increased.

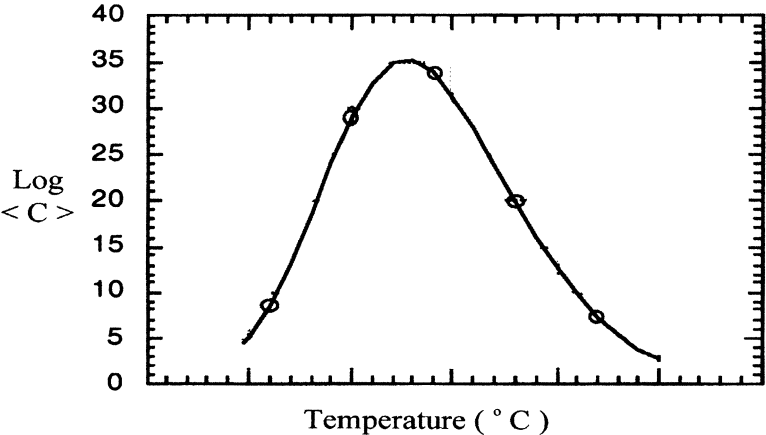
Table 11.2.
Temperature (T_{\max}) at Maximum Solubility, and $\langle \text{Al}^{3+}(\text{aq}) \rangle$ at T_{\max} .

Parameters	Corundum	Gibbsite	Bohmite	Aluminum Hydroxide (Amorphous)
T_{\max} ($^{\circ}\text{C}$)	106.36	169.8	125.68	132.5
$\langle \text{Al}^{3+}(\text{aq}) \rangle$	4.47×10^{-13}	5.16×10^{-16}	2.51×10^{-13}	1.78×10^{-13}
$\frac{\langle \text{Al}^{3+}(\text{aq})_{\max} \rangle}{\langle \text{Al}^{3+}(\text{aq}) \rangle}$	8.3	13.8	22.9	22.39

Several conclusions may be drawn from these numbers. To make a chemically bonded phosphate ceramic, it is necessary that we have undissolved nuclei, around which phosphate phases will grow and connect to each other. Amorphous alumina, though has a higher solubility at room temperature, is not a suitable material because it cannot provide such nuclei, but being amorphous, is a very good dissolving material when mixed with other phases. Gibbsite is the only one that has a $T_{\max} > 150^{\circ}\text{C}$. At 150°C berlinite is formed. This implies that solubility will not have reached to a maximum for gibbsite prior to phosphate conversion and formation of ceramic. Therefore, use of any other phase is preferred to form a ceramic, where the powders dissolve first and then the phosphate reaction occurs.

Figure 11.2 shows the variation of $\langle \text{Al}^{3+}(\text{aq}) \rangle$ as a function of the temperature for alumina. The broad maximum indicates near maximum dissolution can occur in a wide range of temperature. This observation is important from practical standpoint because so often the temperature in ovens is not constant and not the same in the entire space in an oven.

Fig. 11.2.



Variation of solubility product constant in neutral regions for alumina with temperature.

Overall, once the oxide phase dissolves, it forms $\text{AlH}_3(\text{PO}_4)_2 \cdot \text{H}_2\text{O}$, which subsequently reacts with the remaining oxide components on the surface of their grains to form berlinite and binds them. For example, in the case of corundum, the reaction may be written as



AlPO_4 (berlinite) is the bonding phase that binds individual particles and forms the ceramic.

11.2.

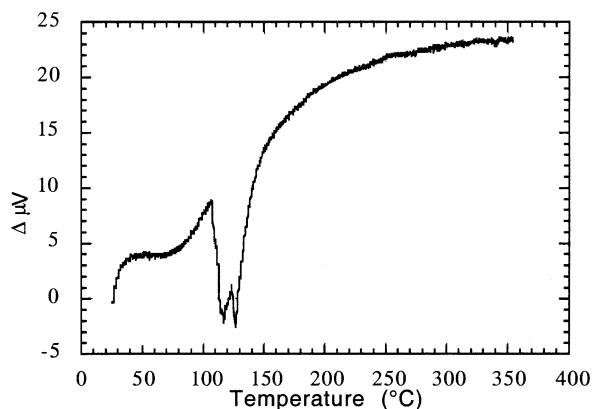
FORMATION OF BERLINITE BONDED ALUMINA CERAMIC

To test the validity of the theoretical analyses of the kinetics of formation of alumina ceramics, Wagh *et al.* [17] conducted an experimental investigation of alumina and phosphoric acid slurry. They used a mixture of coarser and finer alpha-alumina to obtain good packing. The coarser alumina was supplied by Reynolds Chemical Company. Its mean particle size was 0.96 mm. Alumina from Fisher Scientific, sieved to a mean particle size of 0.08 mm, was combined with this powder and 50 wt% phosphoric acid solution to produce a mixture of Al_2O_3 and H_3PO_4 with a weight ratio of five.

To test the effect of the temperature on the reaction kinetics, DTA was employed at a rate of $50^\circ\text{C}/\text{h}$ up to 400°C and phase changes were noted at different temperatures. The output is given in Fig. 11.3. The endotherm slightly above 100°C indicates evaporation of water, but the one near 118°C indicates a phase transformation.

To identify phases formed above T_{max} , the slurry was heated in an oven at 130°C and cured at that temperature for 1, 2 and 4 days in a closed container to avoid evaporation of water. Much of the water seemed to have reacted with alumina as the product in the

Fig. 11.3.



DTA of the slurry of alumina without curing.

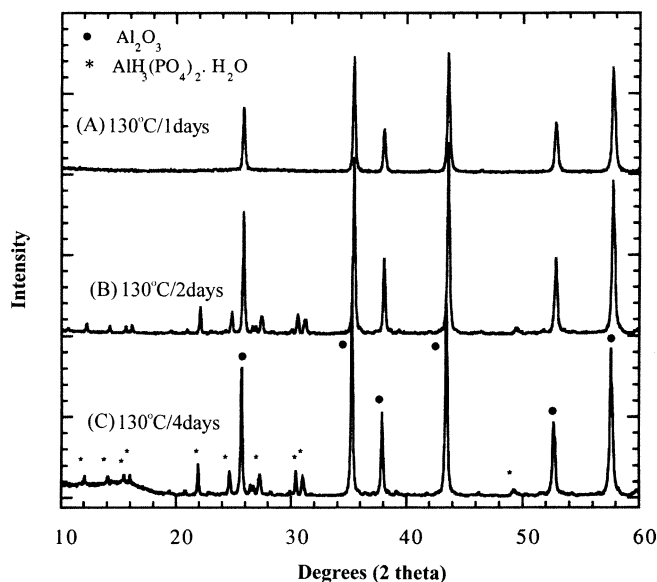
container was thick putty. It was kept at ambient temperature for a week, so that some crystalline growth would occur in the gel. Crystalline phases in the gel were then identified using XRD analysis. The output is shown in Fig. 11.4.

The XRD output in Fig. 11.4 shows clear peaks of unreacted Al_2O_3 and the reaction product, $\text{AlH}_3(\text{PO}_4)_2 \cdot \text{H}_2\text{O}$. Formation of this reaction product is consistent with the observations made by earlier investigators [14]. Sharper and taller peaks in the X-ray patterns of samples cured for longer time indicate that their concentration in the gel is time dependent. This implies that in order to form a chemically bonded ceramic, sufficient hydrothermal curing is necessary to allow the water–alumina reactions to occur, and the dissolution of alumina to take place. This confirms the importance of the role of water in these reactions as noted by Bothe and Brown [12].

The samples, cured at 130°C , when dried, are hard monoliths indicating that $\text{AlH}_3(\text{PO}_4)_2 \cdot \text{H}_2\text{O}$ has acted as the binding phase between the alumina particles. However, these samples also disintegrated when placed in water. This indicates that there was no significant formation of durable insoluble phases such as berlinite. On the other hand, same samples cured at or above 150°C , were durable in water immersion tests. This observation is consistent with the findings of Gonzalez and Halloran [15] who note that berlinite phase is formed at approximately 150°C . Considerable porosity was found in these monoliths indicating release of bound water. The XRD patterns of the resulting ceramics are shown in Fig. 11.5.

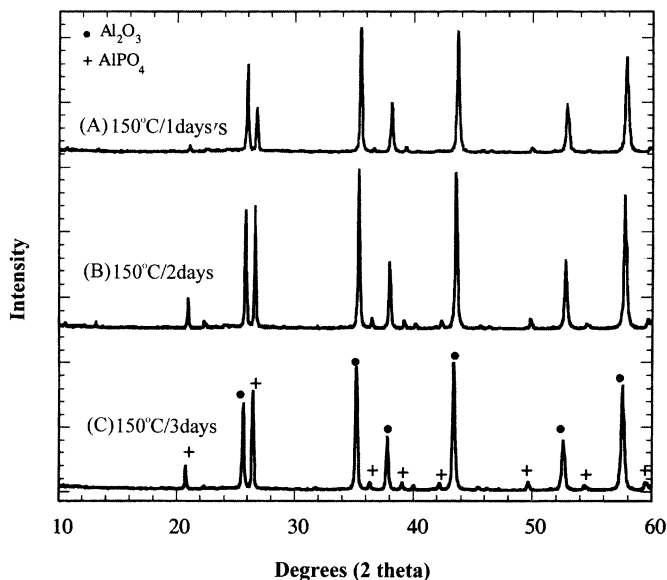
The X-ray pattern of sample heated at 150°C for different periods of time show emergence of berlinite peaks. These peaks are taller in samples heated for 2 and 3 days.

Fig. 11.4.



X-ray diffraction patterns of the dried slurry cured at different temperatures.

Fig. 11.5.



X-ray diffraction patterns of slurry cured at 150°C.

No peaks of $\text{AlH}_3(\text{PO}_4)_2 \cdot \text{H}_2\text{O}$ are visible. This indicates that there has been a transformation of $\text{AlH}_3(\text{PO}_4)_2 \cdot \text{H}_2\text{O}$ to berlinite according to Eq. 11.27.

The product ceramic in each case appeared to be a very hard monolith, with dense phases separated by large pores. The top portion of each monolith was covered with a thin soft layer of acid phase that precipitated during heating. When this layer was sliced off using a diamond saw, the samples did not dissolve in water, nor did they lose any significant weight when soaked in water for several days. Also, the pH of the water remained near neutral indicating lack of any soluble acid phosphates.

The SEM in Fig. 11.6 shows a typical micrograph of a fractured surface. The photograph reveals that the individual particles are glued together by a binding phase that may be berlinite. Due to the small grain size of individual particles, energy dispersive X-ray analysis (EDX) could not be employed to distinguish between the phases of Al_2O_3 and AlPO_4 . However, EDX patterns clearly revealed homogenous distribution of AlPO_4 , given by a constant ratio of aluminum and phosphorous content over the entire specimen surface. This indicates that all of the particles have been coated with AlPO_4 .

The authors [17] also have reported an average strength of 6824 psi on samples of 20.9 vol% open porosity. Ignoring the berlinite phase and using the density of alumina (3.97 g/cm^3) the authors estimated the total porosity in the sample to be 37.3 vol%. Subtracting the measured open porosity, they estimate 16.4 vol% as the closed porosity. The fact that in spite of the large porosity, the strength is high in these materials. Therefore, if one were to find methods of producing dense samples, the strength can be very high. Better methods of producing berlinite bonded ceramics are needed.

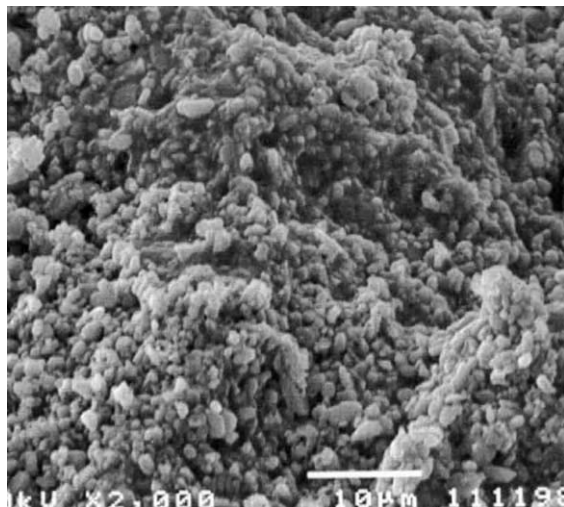
11.3.

CONSOLIDATION MODEL OF CBPC FORMATION

As we have discussed before, a chemically bonded alumina ceramic is formed by bonding individual particles of alumina by berlinite that is formed by chemical reaction. Initially, the oxide particles are packed to the maximum density of the powders and the voids between the particles are filled by the phosphate solution. This phosphate solution reacts with the surface of the particles and forms the reaction products that crystallize or form glassy phases and join the particles. The maximum consolidation is achieved by selecting suitable particle size distribution of the powder as is normally done in any ceramic processing. However, if the reaction products have a lower density than the original oxide, an additional advantage is gained. Due to the higher volume that the reaction products will occupy, the product will fill the void space and produce a denser CBPC. If its expansion after the reaction is more than the total void space, then the volume of the ceramic will be larger than the original closed-packed powder. If it is equal, the ceramic will be fully dense with no volume change. On the other hand, if the reaction product is denser than the oxide, some void space will be left, and as a result, a porous ceramic will be produced. These considerations are demonstrated in a consolidation model given by Wagh *et al.* [17].

To start with, for simplicity, let us assume that all particles are of equal size in the oxide powder. If the radius of individual particles is $2r$ and if we take n^3 particles and pack them in a cube of each side $2rn$, then the total volume of the cube will be $8r^3n^3$. The actual volume occupied by the particles is $\frac{4}{3}\pi n^3r^3$, and hence the void space between the particles will be $8r^3n^3 - \frac{4}{3}\pi n^3r^3$. The net porosity will be the ratio of this difference and the volume of the cube is $1 - \pi/6$ or equal to 47%. Thus if the increase in volume due to phosphate

Fig. 11.6.



SEM microphotograph of a fully reacted berlinite bonded alumina ceramic.

formation is more than this amount, then the entire volume of the ceramic will be more than the original powder. Generally, 47% volume is too large to be exceeded by the reaction products and hence it is very unlikely that the entire ceramic will expand significantly if the oxide particles are of one size. However, this is possible when particles are at least bimodal and well packed.

The net amount of reaction product that would be formed is governed by the solubility of the particular product. As we have noted before, the reaction products that are responsible for bonding are formed between pH 2 and 8. As we have noted before, dissolved fraction of the oxide at a given pH is given by

$$\langle M(\text{aq}) \rangle = 10^{pK_{\text{sp}}(T) - npH} \quad \text{for the acidic region.} \quad (11.28)$$

In the case of corundum, for example, first hydrargillite ($\text{AlO}_{3/2} \cdot \frac{3}{2} \text{H}_2\text{O}$) is formed at pH 5, which then converts into berlinite bonding phase. Thus, the total fraction of the oxide dissolved between pH 5 and 8 is given by

$$\langle M_{\text{tot}}(\text{aq}) \rangle = \int_5^8 (10^{pK_{\text{sp}}(T) - npH}) dpH. \quad (11.29)$$

Since $\int b^{ax} dx = b^{ax}/a \ln b$, we can integrate right-hand side of Eq. 11.29 and obtain,

$$\langle M_{\text{tot}}(\text{aq}) \rangle = \frac{10^{pK_{\text{sp}}(T)}}{n \ln 10} (10^{-2n} - 10^{-8n}). \quad (11.30)$$

Therefore,

$$\langle M_{\text{tot}}(\text{aq}) \rangle = \frac{10^{K_0(T)}}{6.9} (10^{-15} - 10^{-24}) = \frac{10^{K_0(T)}}{6.9} 10^{-15}. \quad (11.31)$$

Here we have used K_0 instead of pK_{sp} for the reason given in the footnote of Table 11.1. When explicitly calculated, we obtain

$$\langle M_{\text{tot}}(\text{aq}) \rangle = 4 \times 10^{-7}. \quad (11.32)$$

Equation 11.32 indicates that a very small fraction of alumina is converted into berlinite. For each mole of corundum, we need only 7.7×10^{-7} g of phosphoric acid for this conversion. Excess phosphoric acid added into the solution is simply used for reaction with corundum which will partially neutralize the acid solution.

From Eq. 11.32, one may also calculate the amount of AlPO_4 formed as a bonding phase. It gives us 1.87×10^{-8} g for each gram of alumina. This is a very small fraction that forms a thin layer on each particle of alumina and holds adjacent particles together. Thus, conversion of alumina needed to form a berlinite bonded alumina ceramic is very small, and therefore, berlinite bonding is possible even when the solubility of alumina is very small.

REFERENCES

1. W.V. Ballard and D.E. Day, "Stability of the refractory-bond phases in high alumina refractories in steam-CO atmospheres," *Ceram. Bull.*, **57** [7] (1978) 660–666.
2. W.V. Ballard and D.E. Day, "Corrosion resistance of refractory bond phases to steam-CO at 199°C," *Ceram. Bull.*, **57** [4] (1978) 438–439, 443.
3. E. van Dalen, *Oriënterende Onderzoekingen over Tandcementen*, Thesis, Delft University, Netherlands, 1933.
4. A.D. Wilson and J.W. Nicholson, *Acid-Base Cements* (Cambridge University Press, Cambridge, 1993), 398pp.
5. P.J. Wisth, "The ability of zinc phosphate and hydrophosphate cements to seal space bands," *Angle Orthodont.*, **42** (1972) 395–398.
6. P. Steenbock, Improvements in and relating to the manufacture of a material designed to the production of cement, British Patent 15,181, 1904.
7. A.D. Wilson, B.E. Kent, D. Clinton, and R.P. Miller, "The formation and microstructure of the dental silicate cement," *J. Mater. Sci.*, **7** (1972) 220–228.
8. R. Roy, D.K. Agrawal, and V. Srikanth, "Acoustic wave stimulation of low temperature ceramic reactions. The system $\text{Al}_2\text{O}_3\text{-P}_2\text{O}_5\text{-H}_2\text{O}$," *J. Mater. Res.*, **6** [11] (1991) 2412–2416.
9. J.E. Cassidy, "Phosphate bonding then and now," *Ceram. Bull.*, **56** [7] (1977) 640–643.
10. K.B. Babb, D.A. Lindquist, S.S. Rooke, W.E. Young, and M.G. Kleeve, *Porous Solids of Boron Phosphate, Aluminum Phosphate, and Silicon Phosphate*, eds. S. Komarneni, D.M. Smith, and J.S. Beck, *Advances in Porous Materials*, vol. 371. (Materials Research Society, 1995), pp. 279–290.
11. W.D. Kingery, "Fundamental study of phosphate bonding in refractories. I–III," *J. Am. Ceram. Soc.*, **33** [8] (1950) 239–250.
12. J.V. Bothe, Jr. and P.W. Brown, "Low temperature synthesis of AlPO_4 ," *Ceram. Trans.*, **16** (1991) 689–699.
13. S.J. Lukasiewicz and J.S. Reed, "Phase development on reacting phosphoric acid with various bayer-process aluminas," *Ceram. Bull.*, **66** [7] (1987) 1134–1138.
14. M.J. O'Hara, J.J. Duga, and H.D. Sheets, Jr., "Studies in phosphate bonding," *Am. Ceram. Soc. Bull.*, **51** [7] (1972) 590–595.
15. F.J. Gonzalez and J.W. Halloran, "Reaction of Orthophosphoric Acid with Several Forms of Aluminum Oxide," *Ceram. Bull.*, **59** [7] (1980) 727–731.
16. D. Singh, A.S. Wagh, and L. Knox, *Low-temperature setting phosphate ceramics for stabilizing DOE problem low-level mixed waste*, eds. M. Wacks and R. Post, *Proceedings WM94* (WM Conferences, Inc., Tucson, AZ, 1994), pp. 1853–1857.
17. A.S. Wagh, S. Grover, and S.Y. Jeong, "Chemically bonded phosphate ceramics. Part II. Warm temperature process for alumina ceramics," *J. Am. Ceram. Soc.*, **86** [11] (2003) 1845–1849.
18. T. Finch and J.H. Sharp, "Chemical reactions between magnesia and aluminum orthophosphate to form magnesia-phosphate cements," *J. Mater. Sci.*, **24** (1989) 4379–4386.
19. C.J. Brinker and G.W. Scherer, *Sol-Gel Science* (Academic Press, London, 1989), pp. 59–78.
20. B.E. Yoldas, *Am. Ceram. Soc. Bull.*, **54** (1975) 286–290.
21. T. Sugama and N. Carciello, "Hydrothermally synthesized aluminum phosphate cements," *Adv. Cem. Res.*, **5** [17] (1993) 31–40.
22. M. Pourbaix, *Atlas of Electrochemical Equilibria in Aqueous Solutions* (Pergamon Press, New York, 1974), 644pp.

This page is intentionally left blank

Iron Phosphate Ceramics

Next to silica and alumina, iron oxide is the most abundant mineral on the earth's crust. It is found in three main forms: wüstite (FeO), hematite (Fe_2O_3), and magnetite (Fe_3O_4). Among these oxides, hematite is the most common and the most stable. It is a bright red mineral. Magnetite, on the other hand, is generally black and exhibits magnetic properties. Because of the abundance of iron oxides, it is attractive to explore methods of forming their CBPCs.

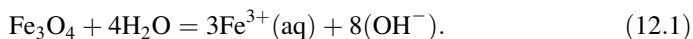
Wüstite and hematite correspond to oxidation states 2 and 3, while magnetite is an equimolar combination of these two. Hematite is an intimate component in lateritic soils (tropical soils rich in alumina and iron oxide), which are very common building materials in the tropics, and this mineral makes the soil red. Iron mine tailings, a very high-volume waste stream, are rich in this oxide. Next to alumina, hematite is the major component in bauxitic soils and is the major component in the highly alkaline waste called "red mud" that is generated when alumina is extracted from these soils by the Bayer process [1]. Due to high alkalinity, red mud is an environmental nuisance and, hence, needs to be treated suitably and recycled. Large-scale industrial use of iron and steel also has produced a significant amount of machining waste streams (swarfs) [2,3]. Swarfs contain iron fines that oxidize into hematite or magnetite. Because swarfs also contain residual machining oil, this oxidation makes them pyrophoric (self-igniting) and hence a fire hazard, especially when these wastes are stored in large dumps.

Iron phosphate CBPCs may provide inexpensive means to recycle these waste streams. Iron mine tailings and red mud may be recycled in building components by fabricating ceramics from them at ambient temperature. Iron-rich swarfs may be recycled if a way is found to solidify these fines into pellets and feed them back into a blast furnace. Thus, iron phosphate CBPCs facilitate solidification of iron-rich waste streams and recycling.

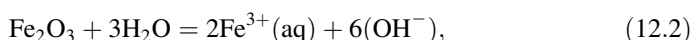
Kingery [4] and, independently, Turkina *et al.* [5] showed that magnetite can be reacted with H_3PO_4 to form a ceramic with an exothermic reaction at room temperature. Kingery

also found that hematite takes ≈ 72 h to set into a tacky product. Golynko-Wolfson *et al.* [6] reported that it is possible to calcine hematite at 600°C and react the product with H_3PO_4 to form a ceramic. Wagh *et al.* [7] also reported reacting magnetite directly with phosphoric acid and forming ceramic.

Formation of a ceramic with magnetite is possible because it is sparsely soluble. This may be seen by calculating the $\text{p}K_{\text{sp}}$ of magnetite using its Gibbs free energies and that of dissolution products (listed in Appendix B), and the aqueous solubility equation



This calculation gives ΔG as -107.71 kJ/mol, and $\text{p}K_{\text{sp}} = 18.8$. The $\text{p}K_{\text{sp}}$ for hematite, calculated by the following solubility equation



is 43.9. Thus, hematite is far less soluble than magnetite, and it is understandable that Kingery [4] could not form a ceramic with this oxide but ended with a tacky product. However, as discussed in Chapter 7, solubilization of hematite in an acidic solution is possible by partially reducing it to magnetite, which can then lead to the formation of a ceramic. It is quite likely that Golynko-Wolfson *et al.* [6] achieved partial reduction of hematite when they heated hematite in a furnace; the furnace probably had a slightly reduced environment due to the lack of supply of oxygen, and heating hematite in it produced some magnetite. Subsequently, when this partially reduced hematite was reacted with phosphoric acid [1], ceramic must have formed. The method of reduction is explored below in detail, and a method of ceramic formation from hematite is presented.

12.1.

REDUCTION AS THE BASIS FOR ENHANCED SOLUBILITY

The reduction of hematite was discussed in Section 7.6. We will use those results in describing methods of formation of ceramics here.

The required solubility equations and the corresponding potential–pH relations of FeO , Fe_2O_3 , and Fe_3O_4 in an acidic solution are summarized in Table 12.1 (see also Ref. [8]).

Equations (12.3)–(12.14) govern dissolution of the oxides and, hence, formation of their phosphate ceramics. Equations (12.3) and (12.4) indicate that iron itself may be used as a reductant in the process. Equations (12.7) and (12.8) indicate that FeO is sufficiently soluble in an acidic solution that it may be dissolved directly in phosphoric acid to form a ceramic. In contrast, Fe_2O_3 , being insoluble in water, will require reduction, and Eqs. (12.9) and (12.10) or Eqs. (12.11) and (12.12) provide means to reduce this oxide to produce $\text{Fe}^{2+}(\text{aq})$ ions. In fact, adding each side of Eq. (12.3) and (12.9), we obtain

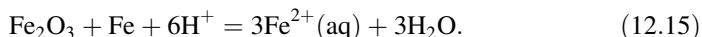


Table 12.1.

Solubility Equations and Corresponding Potential–pH Relations.

Oxide, Metal	Solubility Equation	Potential–pH Relation
Fe	$\text{Fe} = \text{Fe}^{2+}(\text{aq}) + 2\text{e}^- \quad (12.3)$	$E = -0.44 + 0.0295 \log(\text{Fe}^{2+}(\text{aq})) \quad (12.4)$
	$2\text{Fe} + 3\text{H}_2\text{O} = \text{Fe}_2\text{O}_3 + 6\text{H}^+ + 6\text{e}^- \quad (12.5)$	$E = -0.051 - 0.0591\text{pH} \quad (12.6)$
FeO	$\text{FeO} + 2\text{H}^+ = \text{Fe}^{2+}(\text{aq}) + \text{H}_2\text{O} \quad (12.7)$	$\log(\text{Fe}^{2+}(\text{aq})) = 13.29 - 2\text{pH} \quad (12.8)$
Fe_2O_3	$\text{Fe}_2\text{O}_3 + 6\text{H}^+ + 2\text{e}^- = 2\text{Fe}^{2+}(\text{aq}) + 3\text{H}_2\text{O} \quad (12.9)$	$E = -0.728 + 0.1773\text{pH} + 0.0591 \log(\text{Fe}^{2+}(\text{aq})) \quad (12.10)$
	$3\text{Fe}_2\text{O}_3 + 2\text{H}^+ + 2\text{e}^- = 2\text{Fe}_3\text{O}_4 + \text{H}_2\text{O} \quad (12.11)$	$E = 0.221 - 0.0591\text{pH} \quad (12.12)$
Fe_3O_4	$\text{Fe}_3\text{O}_4 + 8\text{H}^+ + 2\text{e}^- = 3\text{Fe}^{2+}(\text{aq}) + 4\text{H}_2\text{O} \quad (12.13)$	$E = -0.98 - 0.2364\text{pH} - 0.0886 \log(\text{Fe}^{2+}(\text{aq})) \quad (12.14)$

Similarly, from Eqs. (12.3) and (12.11), we obtain



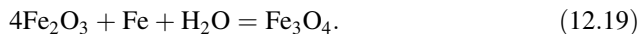
Equations (12.15) and (12.16) exhibit the stoichiometry to use elemental iron as a reductant and produce aquosols of $\text{Fe}^{2+}(\text{aq})$ in an acidic environment. These sols will subsequently react with phosphate anions H_2PO_4^- or HPO_4^{2-} and form the hydrophosphate bonding phases $\text{Fe}(\text{H}_2\text{PO}_4)_2$ and FeHPO_4 . The complete reactions are given by



and



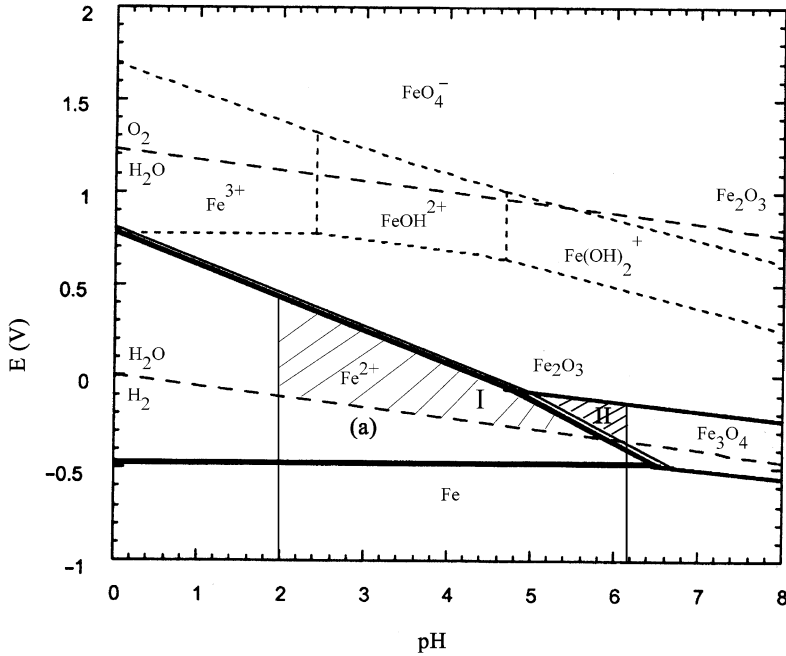
Because $\text{Fe}(\text{H}_2\text{PO}_4)_2$ is more soluble than FeHPO_4 , it is likely that it will eventually convert into the latter during curing, and the final binder product will be FeHPO_4 . From Eqs. (12.3) and (12.9), we obtain



According to Eq. (12.16), using elemental iron, it is possible to reduce hematite into magnetite and aquosols of $\text{Fe}^{2+}(\text{aq})$. Fe_3O_4 produced this way will again result in aquosols of $\text{Fe}^{2+}(\text{aq})$ (Eq. 12.13). Either way, elemental iron helps us in producing $\text{Fe}^{2+}(\text{aq})$. Figure 12.1 shows the E_h –pH diagram of iron. Several inferences may be drawn from this figure and the equations in Table 12.1.

1. Equation (12.3) indicates that 1 mol of Fe will reduce 1 mol of Fe_2O_3 and produce 3 mol of $\text{Fe}^{2+}(\text{aq})$. Subsequent reaction of $\text{Fe}^{2+}(\text{aq})$ with phosphate anions, such as HPO_4^{2-} , will produce 3 mol of the ceramic binder phase FeHPO_4 . In terms of

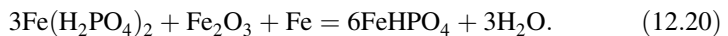
Fig. 12.1.



Region of formation of CBPCs of iron oxide within the E_h -pH diagram (see Ref. [9] for details).

weights, this means that a gram of Fe will convert to 8–13.5 g of the binder, depending upon whether it forms FeHPO_4 or $\text{Fe}(\text{H}_2\text{PO}_4)_2$. Similarly, Eq. 12.16 indicates that 1 mol of Fe reacts with 3 mol of Fe_2O_3 and produces 2 mol of Fe_3O_4 . In terms of weight, 1 g of Fe will react with 8.58 g of Fe_2O_3 and produce 8.29 g of Fe_3O_4 . In each case, reduction of a small amount of iron oxide produces a significant amount of binder.

- When the powder is added to a solution of H_3PO_4 , the initial partial conversion of Fe_2O_3 to the binder will be in region I (light shade) in the diagram because of the reduction of Fe_2O_3 [see Eq. (12.15)]. This raises the pH of the slurry, and further conversion of Fe_2O_3 to the binder will occur in region II (dark shade) of diagram due to the reduction of Fe_2O_3 to Fe_3O_4 (see Eq. 12.16).
- In region I, the majority of the binder at low pH will likely be $\text{Fe}(\text{H}_2\text{PO}_4)_2$ because $\text{H}_2\text{PO}_4^{2-}$ is the major anion resulting from the dissolution of H_3PO_4 . As the pH increases, $\text{Fe}(\text{H}_2\text{PO}_4)_2$ will convert to FeHPO_4 by the reaction



Thus, a fully cured ceramic will form FeHPO_4 as the final binder phase, provided that a reducing environment is maintained.

12.2.

CERAMIC FORMATION WITH IRON OXIDES

The triangular shaded region in Fig. 12.1 is the most relevant for forming ceramics by hematite reduction. It is bounded by the vertical line on the left at pH 2. Below this pH, dissolution of phosphates does not occur, and hence phosphate anions are not available for reaction. Line (a) ensures that the reduction reaction does not fall below the stability region of water. The third side ensures dissolution of Fe_2O_3 . Within this triangular region, one can select compositions that allow maximum loading of Fe_2O_3 (75–80 wt% solids).

Wagh and Jeong [9] tested three compositions within this region, which are listed in Table 12.2. The acid was neutralized using K_2CO_3 to pH 2 and then the powders were mixed in the solution. The reaction was exothermic and spontaneous, but all pastes set well. During setting, a considerable amount of water was expelled from the samples. This water condensed on the surface of the samples.

The samples were cured for 3 weeks, and their open porosity was measured by the water immersion method. The pH of the water was ≈ 6 , indicating that no substantial unreacted acid remained in the samples. As evident in Table 12.2, the compressive strength and the open porosity of the ceramic are very similar to those of Portland cement concrete used in the construction industry [9]. The high porosity may be due to rapid setting of the ceramic and high exothermic reaction. Due to this heating, water will evaporate and create open pores. It is necessary to slow down the rate of reaction to make practical ceramics. Fractured surfaces of these ceramics exhibited trapped isolated pores. Again, these pores must have been generated by rapid evaporation of water that could not escape.

Visual observation showed that the samples contained a considerable amount of a glassy phase. Because of the lack of crystalline phases, X-ray diffraction was not very useful in determining the phase composition. Figure 12.2 shows the X-ray diffraction pattern of the ceramic formed with the first composition given in Table 12.2. As expected, the peaks show only the presence of residual Fe_2O_3 and a broad hump in the middle of the pattern representing the glassy phase. As the theoretical predictions indicate, this amorphous phase must be a result of the formation of $\text{Fe}(\text{H}_2\text{PO}_4)_2$ and FeHPO_4 , the latter being

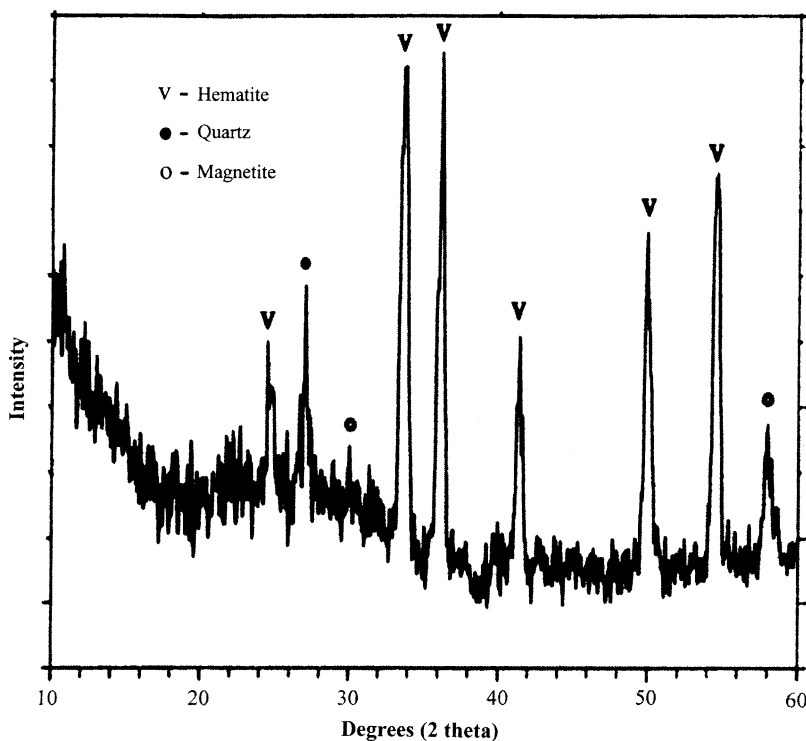
Table 12.2.

Compositions and Properties of Hematite Ceramics with 50 wt% fly ash.

Composition (wt%)	Density (g/cm^3)	Open Porosity (vol%)	Compressive Strength	
			MPa	psi
$\text{Fe}_2\text{O}_3 : \text{Fe} = 49 : 1$	1.7	19.9	25 ± 4	3699 ± 524
$\text{Fe}_2\text{O}_3 : \text{Fe} = 48 : 2$	1.7	18.6	22 ± 3	3237 ± 460
$\text{Fe}_2\text{O}_3 : \text{Fe} = 47 : 3$	1.52	21.2	22 ± 4	3263 ± 517
Portland Cement ^a	2.4	≈ 15	21	3000

^a Given for comparison.

Fig. 12.2.



X-ray diffraction pattern of iron phosphate ceramic.

converted from the former as the sample cures over time. Figure 12.3 shows the scanning electron microphotograph of a fractured surface of the sample. Again one notices a considerable featureless region that is probably the glassy phase in the sample, confirming observations of the X-ray diffraction pattern.

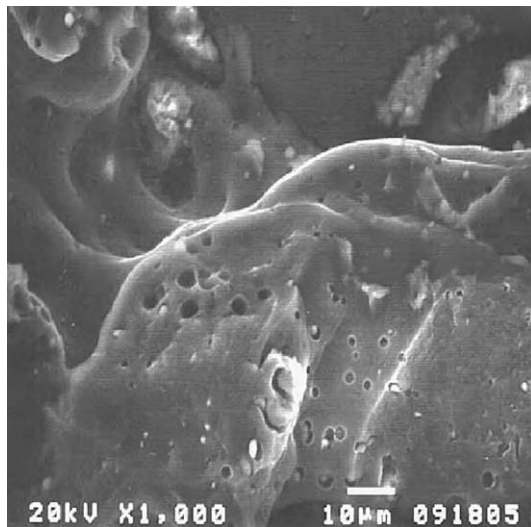
Note that the ratios $\text{Fe}_2\text{O}_3 : \text{Fe}$ given in Table 12.2 yield $\langle \text{Fe}^{2+}(\text{aq}) \rangle = 0.1, 0.2, \text{ and } 0.3$. These numbers are close to the theoretically predicted range of 0–0.15 (Section 12.2). When a larger percentage of Fe was selected, the mixtures were hot due to the reaction of Fe, but did not set into ceramics. This implies that Fe content of only within or near the theoretically predicted range will form ceramics.

12.3.

CONCLUSIONS

The example of iron phosphate demonstrates applications of reduction mechanisms in forming ceramics of oxides that occur in higher oxidation states. There is only a very

Fig. 12.3.



Scanning electron photomicrograph of iron phosphate ceramic.

narrow region in the E_h –pH diagram in which such a method can be used. Outside this region, either decomposition of water may occur, or the oxides are not reduced into proper lower oxidation phases. Thus, generalizing this approach to forming ceramics is difficult. Possibly, this method may be used for manganese oxide that also exhibits an E_h –pH diagram similar to iron oxide.

In spite of this limitation, the method is very useful, because it provides a means of forming a ceramic of one of the most common and inexpensive oxides. As discussed before, iron oxide is a component of lateritic soils and red mud, high-volume iron mine tailings, and machining swarfs. Thus, useful products of several mineral waste streams can be formed by the process described in this chapter. Development of ceramics using red mud and swarfs is discussed in Chapter 14.

REFERENCES

1. A.S. Wagh and V. Douse, "Silicate bonded unsintered ceramics of Bayer process waste," *J. Mater. Res.*, **6** [9] (1991) 1094–1102.
2. M.J. Hess and S.K. Kawatra, "Environmental beneficiation of machining wastes. Part I. Materials characterization of machining swarf," *J. Air Waste Mgmt*, **49** (1999) 207–212.
3. S.K. Kawatra and M.J. Hess, "Environmental beneficiation of machining wastes. Part II. Measurement of the effects of moisture on the spontaneous heating of machining swarf," *J. Air Waste Mgmt*, **49** (1999) 477–481.
4. W.D. Kingery, "Fundamental study of phosphate bonding in refractories. II. Cold-setting properties," *J. Am. Ceram. Soc.*, **33** [5] (1950) 242–250.
5. L.I. Turkina, L.G. Sudakas, V.A. Paramonova, A.A. Chernikova, *Inorganic Materials*, vol. 26. (Plenum Press, New York, 1990), 1680–1685; Translated from Russian Original.

6. S.L. Golynko-Wolfson, M.M. Sychev, L.G. Sudakas, and L.I. Skoblo, *Chemical Basis of Fabrications and Applications of Phosphate Binders and Coatings* (Khimiya, Leningrad, 1968).
7. A. Wagh, S. Jeong, D. Singh, A. Aloy, T. Kolytcheva, and Y. Macheret, *Iron-Phosphate-Based Chemically Bonded Phosphate Ceramics For Mixed Waste Stabilization*, Proceedings of the Waste Management Annual Meeting, Session 29, Tuscon, March 2–6, 1997).
8. M. Pourbaix, *Atlas of Electrochemical Equilibria in Aqueous Solutions* (Pergamon Press, New York, 1974).
9. A.S. Wagh and S.Y. Jeong, “Chemically bonded phosphate ceramics. Part III. Reduction mechanism and its application to iron phosphate ceramics,” *J. Am. Ceram. Soc.*, **86** [11] (2003) 1850–1855.

Calcium Phosphate Cements

As discussed in Chapter 5, calcium oxide has the highest solubility among the candidate divalent metal oxides, and its reaction with phosphoric acid is highly exothermic. As a result, it is difficult to use this oxide directly to form a phosphate ceramic. In addition, the phosphate chemistry of calcium is complicated because calcium forms a range of phosphate salts, which are often difficult to identify within the reaction products. Historically, calcium oxide has been used as an additive in zinc oxide dental products. Wilson *et al.* [1] report various brands of commercial cements containing calcium. These cements consist of powdered alumina–lime–silica glass mixed with phosphoric acid that formed a hard and translucent product. The starter glass powder consists of 7.7–9.0 wt% calcium oxide. Wilson and Kent [2] showed that calcium precipitates rapidly within a setting time of 5 min after mixing the slurry, forms its compounds, and provides an early strength to the cements. The ultimate product of calcium is probably a silico-phosphate glass.

Naturally occurring phosphate cements are also known. Krajewski [3] cites calcium-based phosphate cements in the Albeian condensed Glauconitic Limestone of the Tatra Mountains in Western Carpathians. In recent years methods have been developed to fabricate calcium phosphate ceramics by direct reaction of calcium compounds and either phosphoric acid or an acid phosphate. The mineralogy of the products has also been well studied. Most of these efforts are directed towards development of calcium-based bioceramics containing calcium phosphate compounds, such as hydroxyapatite. These developments are discussed below.

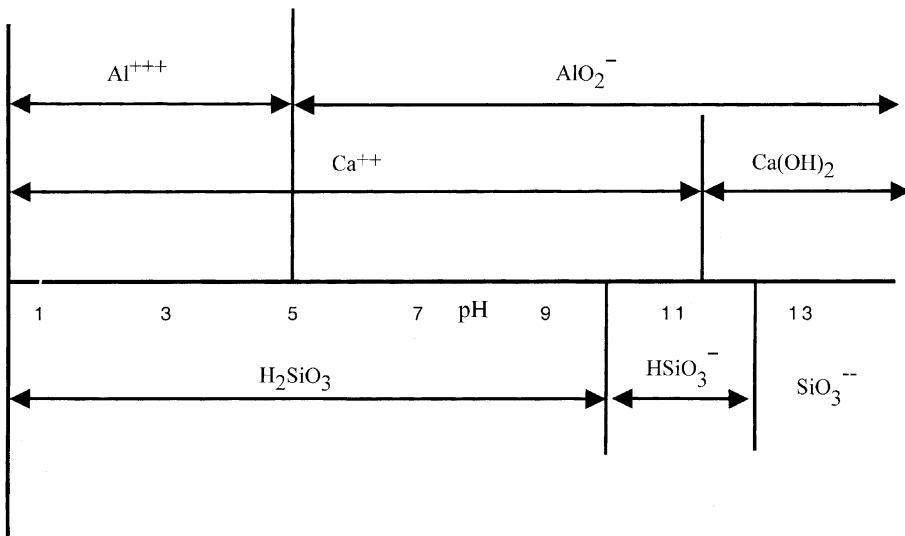
13.1.

CHEMISTRY OF CALCIUM PHOSPHATES

Since calcium oxide is more than sparsely soluble and its reaction with phosphoric acid or a soluble phosphate is highly exothermic, researchers have used less soluble salts of calcium to react with the phosphates and form a phosphate ceramic [4–12]. In the acidic medium of the phosphate solutions, the salts of calcium dissolve slowly and release $\text{Ca}^{2+}(\text{aq})$ into the solution, which subsequently reacts with phosphate anions and forms calcium phosphates. The best calcium minerals for forming CBPCs are combination of oxides of calcium and insoluble oxides such as silica or alumina, e.g., calcium silicate (CaSiO_3) and calcium aluminates (CaAl_2O_4), or even a phosphate of calcium such as tetracalcium phosphate ($\text{Ca}_4(\text{PO}_4)_2\cdot\text{O}$). These minerals are reacted with acid phosphate salts to form phosphate cements.

Consider, for example, CaSiO_3 as a combination of CaO and SiO_2 or CaAl_2O_4 as a combination of CaO and Al_2O_3 . We have discussed the solubility characteristics of CaO and Al_2O_3 in the previous chapters. Pourbaix [13] has also provided the solubility characteristics of SiO_2 , which is mostly insoluble except in a highly alkaline region. The thermodynamic approach used previously to discuss the solubility characteristics may also be employed to develop stability regions of various ionic species related to the dissolution of calcium silicates and aluminates. These regions are presented in Fig. 13.1. The figure has been constructed by assuming that calcium silicates and aluminates are in near equilibrium with their respective components CaO and SiO_2 or Al_2O_3 . This assumption

Fig. 13.1.



Stability regions of ionic species of calcium silicate and aluminates.

Table 13.1.Stability Regions of CaO and SiO₂.

Dissolved Aqueous Phases	Dissolution Reaction and Ionic Concentration	Equation No.	pH Range
Ca ²⁺ (aq) and H ₂ SiO ₃	CaSiO ₃ + 2H ⁺ = Ca ²⁺ (aq) + H ₂ SiO ₃	13.1a	0–10
	log⟨Ca ²⁺ (aq)⟩ = 1.315 – pH	13.1b	
Ca ²⁺ (aq) and HSiO ₃ [–]	CaSiO ₃ + H ⁺ = Ca ²⁺ (aq) + HSiO ₃ [–]	13.2a	10–11.45
	log⟨Ca ²⁺ (aq)⟩ = –3.61 – 0.5pH	13.2b	
Ca ²⁺ (aq) and Al(aq) ³⁺	CaAl ₂ O ₄ + 8H ⁺ = Ca ²⁺ (aq) + 2Al ³⁺ (aq) + 4H ₂ O	13.3a	0–5
	log⟨Ca ²⁺ (aq)⟩ = 9.24 – 4pH	13.3b	
Ca ²⁺ (aq) and AlO ₂ [–]	CaAl ₂ O ₄ = Ca ²⁺ (aq) + 2AlO ₂ [–] , stable	13.4a	5–11.45
	log⟨Ca ²⁺ (aq)⟩ = –11.13	13.4b	

may be verified by calculating the total Gibbs free energy (ΔG) of the oxides and comparing the total with that of the respective mineral.

Among the four stability regions (Table 13.1), the first and second regions are of interest for formation of CBPCs, because they fall partially in the acidic region. In these regions, H₂PO₄[–] and HPO₄^{2–} are readily available for acid–base reaction (see Chapter 4). Therefore, the dissolution reactions given by Eqs. 13.1a and 13.2a are suitable for forming ceramics of CaSiO₃. For these, we can determine the solubility dependence with pH derived by methods described in Chapters 5 and 6.

Consider, for example, Eq. 13.1a. Following the notations of Chapters 4 and 5, we relate the concentrations of individual species and the net change in Gibbs free energy that occurs during the reaction by the following relation. We obtain from Eq. 13.1a,

$$-\log \left[\frac{\langle \text{Ca}^{2+}(\text{aq}) \rangle \langle \text{H}_2\text{SiO}_3 \rangle}{\langle \text{H}^+ \rangle^2} \right] = \text{p}K_{\text{sp}} = \frac{\Delta G}{2.301RT_0}. \quad (13.5)$$

To calculate ΔG in the last term of Eq. 13.5, we recognize that

$$\langle \text{Ca}^{2+}(\text{aq}) \rangle = \langle \text{H}_2\text{SiO}_3 \rangle \quad (13.6)$$

and that $-\log \langle \text{H}^+ \rangle^2 = 2\text{pH}$. This gives us $\Delta G = 14,980 \text{ kJ/mol}$. Hence, Eq. 13.5 now yields

$$\log \langle \text{Ca}^{2+}(\text{aq}) \rangle = 1.315 - \text{pH} \quad \text{for } 0 < \text{pH} < 10. \quad (13.7)$$

Equation 13.7 provides the ionic concentration $\langle \text{Ca}^{2+}(\text{aq}) \rangle$ in the pH range of 0–10. One may follow a similar approach to derive the pH dependence of $\langle \text{Ca}^{2+}(\text{aq}) \rangle$ for other pH regions.

Equations 13.1b and 13.2b indicate that $\log \langle \text{Ca}^{2+}(\text{aq}) \rangle$ is a monotonically decreasing function of pH. In highly acidic regions, $\langle \text{Ca}^{2+}(\text{aq}) \rangle$ is high, but becomes low in the regions of formation of CBPCs, especially in the regions of the pH of phosphate salts such as KH₂PO₄.

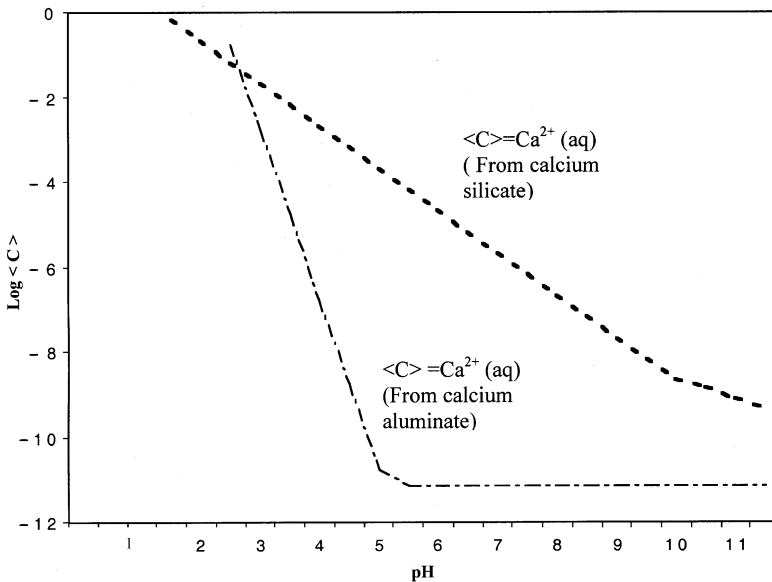
With the procedure given above, one may also calculate the pH dependence of $\langle \text{Ca}^{2+}(\text{aq}) \rangle$ from dissolution of calcium aluminates. The results of such calculations are summarized in Table 13.1. Figure 13.2 shows the solubility diagram for $\langle \text{Ca}^{2+}(\text{aq}) \rangle$ as a function of pH for both silicates and aluminates drawn from the equations given in Table 13.1.

Beyond pH 7, as Pourbaix [13] has stated, dissolution of Al_2O_3 (and hence that of aluminate) will lead to the precipitation of $\text{Al}(\text{OH})_3$ gel. As a result, dissolution of Al_2O_3 will not lead to the formation of a phosphate ceramic.

Note in Fig. 13.2 that the solubility of monocalcium silicate is higher than that of the corresponding aluminate at any $\text{pH} > 3$. In the acidic region that is of interest for forming CBPCs, both may be considered as sparsely soluble, and if they are reacted with a phosphate salt, ceramics may be formed. Thus, monocalcium silicate and aluminate are starter minerals to form calcium phosphate ceramics.

There exist other calcium compounds such as dicalcium and tricalcium silicates and aluminates, as well as monocalcium disilicate or dialuminate. To represent such minerals in simple notations, hereafter, we will use the cement chemistry notations for calcium silicates and aluminates. In these notations, CaO is represented by **C**, Al_2O_3 by **A**, SiO_2 by **S**, and H_2O by **H**. Thus, CaSiO_4 ($\text{CaO} \cdot \text{SiO}_2$) will become **C·S**, and Ca_2SiO_4 ($2\text{CaO} \cdot \text{SiO}_2$) will be represented by **C₂·S**. In general, the methods used above to calculate $\langle \text{Ca}^{2+}(\text{aq}) \rangle$ may be generalized to calculate the same from any combination of **C**, **A**, and **S** that has a mineral form **C_m·S_n** or **C_m·A_n**. In these cases, the solubility of **C** is much higher than that of **S** or **A**. As a result, as the content of CaO in a mineral decreases relative to the second

Fig. 13.2.



Solubility dependence of calcium silicate and aluminate as a function of pH.

component (i.e., as the ratio m/n decreases), the solubility decreases and vice versa. For example, $\langle \text{Ca}^{2+}(\text{aq}) \rangle$ formation due to dissolution of $\text{C}_2\cdot\text{S}$ and $\text{C}_3\cdot\text{S}$ within $0 < \text{pH} < 10$ is given, respectively, by

$$\log\langle \text{Ca}^{2+}(\text{aq}) \rangle = 1.66 - 0.67\text{pH}, \quad (13.8)$$

$$\log\langle \text{Ca}^{2+}(\text{aq}) \rangle = 11.42 - 2\text{pH}. \quad (13.9)$$

Comparison of Eqs. 13.8 and 13.9 with Eqs. 13.1a and 13.2a, respectively, indicates that the solubility of $\text{C}_2\cdot\text{S}$ and $\text{C}_3\cdot\text{S}$ is much higher than that of $\text{C}\cdot\text{S}$. On the other hand, by similar calculations, one may also show that the solubility of minerals such as $\text{C}_m\cdot\text{S}_n$, where $m < n$, is lower than that of $\text{C}\cdot\text{S}$. In fact, $\text{C}\cdot\text{S}$ and $\text{C}\cdot\text{A}$ have the right combination to form ceramics at room temperature, and the rest of the minerals are either too soluble or insoluble.

13.2.

CALCIUM PHOSPHATE CEMENTS FROM CALCIUM SILICATES AND ALUMINATES

Table 13.2 lists phosphate cements developed using $\text{C}\cdot\text{S}$ and $\text{C}\cdot\text{A}$ as the starter powders. Semler [4] used a naturally occurring mineral, wollastonite ($\text{C}\cdot\text{S}$), as the source of $\text{Ca}(\text{aq})^{2+}$ and reacted it with H_3PO_4 solution that was buffered with Al and Zn to produce a calcium phosphate quick-setting cement that hardened within 3–8 min and provided

Table 13.2.

Calcium Phosphate Cements Made from Calcium Silicates and Aluminates.

Starter Ingredients	Composition and Physical Properties	Reference
Wollastonite and H_3PO_4 buffered with Zn and Al	50% P_2O_5 , 6% Zn, 1% Zn. Liquid to powder ratio of 0.4. Set in 8 min. Comp. strength of 73 MPa (10,645 psi). Comp. strength after 45 freeze-thaw cycles or 43 thermal cycling was > 52 MPa (7500 psi). Thermal expansion, 4.6×10^{-6} in. 2 /F. Tensile strength 3 MPa (450 psi).	[4]
$\text{C}\cdot\text{A}$, $\text{C}_3\cdot\text{A}$, $\text{C}\cdot\text{A}_2$ each reacted with ammonium polyphosphate solution (poly-N acid)	Acid contained (in wt%) 11.1 l N from ammonia, 37 P_2O_5 , 0.16 Fe, 0.11 MgO, 0.12 each of Al_2O_3 and F, 0.6 S, and 50.79 water	[5]
Commercial calcium aluminate cements reacted with polybasic Na-phosphate reagent	Reagent solution contained 30 wt% ($-\text{NaPO}_3-$) $_n$. One of the aluminate cements contained $\text{C}\cdot\text{A}$, $\text{C}_2\cdot\text{A}\cdot\text{S}$ (gehlenite), and $\text{C}\cdot\text{A}_2$. The second cement had $\text{C}\cdot\text{A}$, $\text{C}\cdot\text{A}_2$, corundum, and $\text{C}_2\cdot\text{A}\cdot\text{S}$ as the minor phase	[6]
Wollastonite within magnesium potassium phosphate	A mixture of MgO, $\text{C}\cdot\text{S}$, and KH_2PO_4 reacted with water	[12]

a compressive strength between 60 and 73 MPa (8650 and 10,645 psi). The freeze-thaw and thermal cycling resistance was >52 MPa (>7500 psi). The thermal expansion coefficient was $8.2 \times 10^{-6} \text{C}^{-1}$, and the tensile strength was 3 MPa (450 psi). X-ray diffraction pattern showed only the presence of crystalline $\text{C}\cdot\text{S}$, implying that the reaction products were amorphous and hence were not detectable by X-ray diffraction.

Sugama and Allan [5] used calcium aluminates (tricalcium aluminate, $\text{C}_3\cdot\text{A}$, monocalcium aluminate, $\text{C}\cdot\text{A}$, or calcium dialuminate, $\text{C}\cdot\text{A}_2$) as the cation donors and reacted them with an ammonium polyphosphate fertilizer solution and formed quick-setting cements. The purpose of this study was to develop cements that are not affected by the CO_2 environment and are useful as downhole cements in geothermal wells (see Chapter 15). The composition of the fertilizer was 11.1 wt% N as ammonia, 37.0 wt% P_2O_3 , 50.79 wt% water, and the rest trace elements. Differential scanning calorimetry (DSC) showed that the reaction rates of the three minerals are in the decreasing order:

$$\text{C}\cdot\text{A} > \text{C}_3\cdot\text{A} > \text{C}\cdot\text{A}_2.$$

This observation by Sugama and Allan is contrary to the conclusion of the solubility analysis discussed in Section 13.1. According to that analysis, as the relative content of C increases, the solubility should increase, while Sugama and Allan observe that tricalcium silicate has a lower solubility than calcium silicate. Their analysis using X-ray photoelectron spectroscopy (XPS), in fact, seems to confirm the conclusions of the solubility analyses. They find that within the interfacial zone between the calcium silicates and the poly-N solution, the uptake of Ca was higher for higher molar ratio of Ca/Al. Furthermore, they also analyzed the filtrate solutions of the three calcium aluminates in the poly-N solution and found that the ionic concentration of Ca was higher in the $\text{C}_3\cdot\text{A}$ solution than in the $\text{C}\cdot\text{A}$ solution. Thus, there appears to be a discrepancy between their DSC and XPS analyses, but our solubility analyses agree with the latter.

The solubility analyses presented above seem to support the findings of Sugama *et al.* [6] on commercial calcium aluminate cements given in Table 13.2. The authors use two commercial cements, one containing more calcium and the other containing a comparatively higher amount of alumina (or low calcium). The thickening times determined by consistency measurements (see Chapter 15) at 125°C show that setting started after 40 and 120 min, respectively, for high and low calcium cements.

The data in Table 13.3 show that the onset temperature of reaction for the three minerals becomes higher as the relative content of C becomes lower. As evident from the third column in Table 13.3, this trend is supported by the calculated temperature of maximum solubility. The second column reflects the experimentally observed temperature where the solubility is significant enough that the acid–base reaction starts. Thus, the numbers in the second column should be slightly lower than those in the third column, but they should be in the same range. The exception is $\text{C}_2\cdot\text{S}$, where the calculated T_{max} is lower than the experimentally observed value for the onset of reaction. This anomaly may simply be because the measurements started at room temperature, and if they had been done from 0°C , one would have obtained a temperature closer to the theoretical calculations.

Table 13.3.

Approximate Temperatures of Reaction for Calcium Silicate and Aluminates.

Mineral	Temperature of Onset of Reaction (°C)	T_{\max} from Solubility Analyses (°C)	Max. Exothermic Heat Rate (mcal/s)
C_2S	23	0	4.5
$C\cdot A$	30	42.66	5
$C\cdot A_2$	70	98.2	4.5

Sugama and Carciello [11] studied the degree of reactivity of C_2S , $C\cdot A$, and $C\cdot A_2$ in poly-N acid solution as a function of temperature by DSC. Their temperatures for the onset of reaction and the maximum reaction are given in Table 13.3.

Semler [4] demonstrated that wollastonite based phosphate cements can have very high compressive strengths, in the order of 69 MPa (10,000 psi). However, that is when small sized samples are made. Making large samples with even partially neutralized H_3PO_4 is difficult because of excessive exothermic heat evolution during formation of these cements. Sugama and Allan [5] and Sugama *et al.* [6] used an ammonium phosphate salt to replace phosphoric acid as the acid component and overcame the difficulty of excessive heat generation. Even then, the compressive strengths of the cements they produced were comparatively low, in the order of 7–20 MPa (1000–3000 psi). Probably due to the evolution of ammonia, their porosity was also high, and that condition led to poorer strengths. Furthermore, even with the use of ammonium phosphate, it has not been possible to produce large products.

Recently, Wagh *et al.* [12] used wollastonite as an additive to their magnesium potassium phosphate (Ceramicrete) blend to produce a composite ceramic. They call it “phospho-silicate Ceramicrete.” The advantage of using Ceramicrete as the matrix for wollastonite is that even at very high loading of wollastonite, the exothermic reaction rate is minimal, and large casts can be made. Table 13.4 lists properties of this Ceramicrete after curing for 21 and 15 days.

As shown in Table 13.4, the loading of wollastonite may be very high. Typically, the compressive and flexural strengths of conventional portland cement are ≈ 27 and 5 MPa

Table 13.4.

Physical and Mechanical Properties of Wollastonite-Filled Ceramicrete.

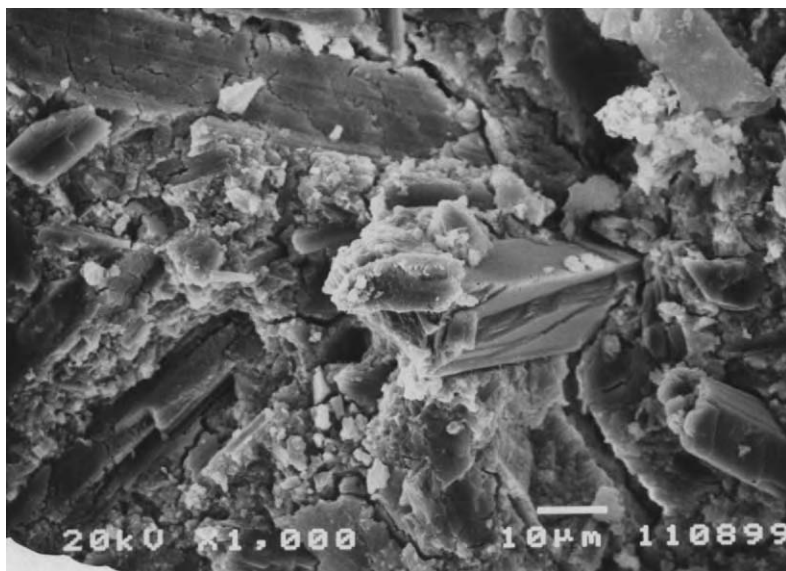
Loading and Properties	Measured Value	
Curing (days)	21	15
Loading of wollastonite (wt%) in powder blend	50	60
Compressive strength, MPa	53 (7755 psi)	58 (8426 psi)
Flexural strength, MPa	8.5 (1236 psi)	10 (1474 psi)
Fracture toughness ($MPa\cdot m^{\frac{1}{2}}$)	0.63	0.66
Water absorption (wt%)	2	2

(≈ 4000 and 700 psi). The same properties for wollastonite-based Ceramicrete are nearly twice that of conventional portland cement. The fracture toughness is also high. The superior mechanical properties coupled with the ability to fabricate large forms make this product practically a superior cement.

The superior mechanical properties of phospho-silicate Ceramicrete may be attributed to the whisker form of the grains of wollastonite. As a result, the composite becomes a whisker-reinforced ceramic. Figure 13.3 shows the scanning electron micrograph of a fractured surface of this ceramic. Each whisker in this case was ≈ 200 μm in length. These whiskers act as a second phase in the phospho-silicate Ceramicrete and deflect cracks during fracture of the ceramic, thus raising the fracture energy. This deflection of cracks may be seen in the figure. The result is an increase in the fracture toughness and the flexural strength.

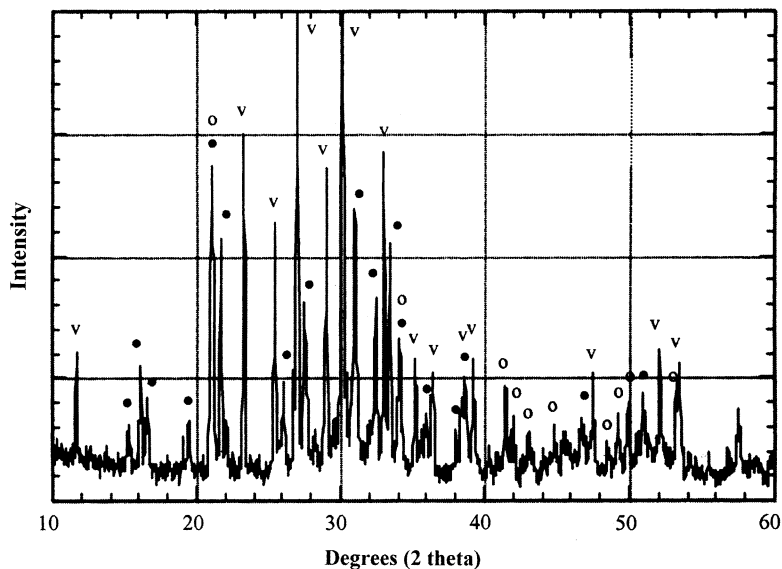
As the solubility analysis presented in this section indicates, wollastonite is reactive in a phosphate solution. Therefore, even though the structure of its whiskers is retained in the ceramic, a reaction occurs between the surface of the whiskers and the matrix. Very fine powders of wollastonite may completely react losing their shape. One of the products of this reaction is calcium hydrophosphate. Figure 13.4 shows the X-ray diffraction pattern of the ceramic formed at 50 wt% wollastonite loading. It shows distinct peaks of wollastonite and magnesium potassium phosphate, as well as small peaks of calcium hydrophosphate (CaHPO_4). This last mineral must have been formed due to the reaction between wollastonite and KH_2PO_4 . If this is true, the same reaction will also produce metastable silicic acid (H_2SiO_3) as a byproduct that will produce silicates such as K_2SiO_3 . We do not

Fig. 13.3.



Scanning electron micrograph of fractured surface of the phospho-silicate Ceramicrete.

Fig. 13.4.



X-ray diffraction pattern of calcium phospho-silicate Ceramicrete. The symbols are, (●) $\text{MgKPO}_4 \cdot 6\text{H}_2\text{O}$, (v) CaSiO_3 , and (○) $\text{CaHPO}_4 \cdot 2\text{H}_2\text{O}$.

see a peak corresponding to these silicates, but there is a broad hump in the middle of the pattern. This hump may be due to the amorphous or glassy nature of the silicate. Formation of such glassy reaction products is a positive attribute of this reaction. The glassy phase makes this material dense by filling in connected porosity. As noted in Table 13.4, the result is higher compressive strength.

13.3.

ADHESION OF PORTLAND CEMENT AND CBPCs

In several applications of CBPCs, one encounters a need for bonding hardened portland cement concrete with CBPCs. Examples include repairing cracks within cement concrete structures such as buildings, geotechnical structures, and utility supply lines; filling potholes on roads; and recycling debris of portland cement concrete by making products of CBPC binders. In fact, use of CBPCs for encapsulating radioactively contaminated cement debris for safe disposal during decontamination and decommissioning work at several DOE sites in the US, as well as sites in Europe and Russia, is one of the key applications (see Chapter 17) of CBPCs. Thus, the bonding characteristics of CBPCs with conventional cements need to be evaluated.

The analyses given in Chapter 13.2 predict that due to the presence of calcium silicates or aluminates in conventional cements, the cement particles will react with the phosphate

solutions. The main mineral components of portland cement are β -dicalcium silicate (β - C_2S) and tricalcium silicate (C_3S). Both of these minerals react instantaneously with phosphate solutions. The same analyses, and work by Sugama and his group cited in this chapter, show that calcium aluminates also react with phosphate solutions. This implies that the surface of conventional cement particles will react with phosphate solutions. Therefore, it should be easy to develop an intimate bond between conventional silicate or aluminate cement products and CBPCs. A methodical study is needed in this area. The analysis in Section 13.2 provides insight into the kinetics of bond formation between portland and aluminate cements and CBPCs.

13.4.

CALCIUM PHOSPHATE CEMENTS WITH BIOMEDICAL APPLICATIONS

The major interest in calcium phosphate cements has always been in their potential for biomedical applications. This is because bone contains hydroxyapatite ($Ca_5(PO_4)_3OH$), a calcium phosphate mineral. Any material that could be used to bond bone or produce an artificial graft should contain this mineral for compatibility. In fact, much of the research in producing calcium phosphate-based cements or sintered ceramics was motivated by their biomedical applications. We will discuss applications of calcium phosphate cements in detail in Chapter 18. This section describes their materials development.

Brown and Chow [7] have listed the important calcium phosphate compounds arranged in the order of increasing basicity (Ca to P ratio). This list is reproduced in Table 13.5 along with a short form notation for each compound in the first column. We have also included in the list an additional mineral, dahllite, recently synthesized by Constantz *et al.* [14], because this mineral is an important compound found in bones.

Table 13.5.

Calcium Phosphate Compounds and their Solubility Product Constants (pK_{sp}).

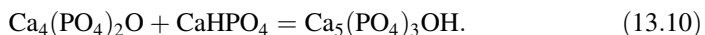
Compound	Formula	pK_{sp}
Monocalcium phosphate monohydrate (MCPM)	$Ca(H_2PO_4)_2 \cdot H_2O$	Soluble
Monocalcium phosphate anhydrous (MCPA)	$Ca(H_2PO_4)_2$	Soluble
Dicalcium phosphate dihydrate (DCPD)	$CaHPO_4 \cdot 2H_2O$	6.59
Dicalcium phosphate anhydrous (DCPA)	$CaHPO_4$	6.9
Octacalcium phosphate (OCP)	$Ca_8H_2(PO_4)_6 \cdot 5H_2O$	23.48
α -Tricalcium phosphate (α -TCP)	α - $Ca_3(PO_4)_2$	25.5
β -Tricalcium phosphate (β -TCP)	β - $Ca_3(PO_4)_2$	28.9
Hydroxyapatite (OHAP or simply HAP)	$Ca_5(PO_4)_3 \cdot OH$	58.4
Fluorapatite (FAP)	$Ca_5(PO_4)_3 \cdot F$	60.5
Carbonated hydroxyapatite (dahllite)	$Ca_5(PO_4 \cdot CO_3)_3(OH_1F)$	NA
Tetracalcium phosphate (TTCP)	$Ca_4(PO_4)_2 \cdot O$	≈ 6.9

As evident from the list, the increasing basicity almost coincides with the decreasing solubility of these compounds as indicated by their pK_{sp} . The exception is the compound with the greatest basicity, TTCP. This compound has a much higher solubility than most of the preceding compounds; its pK_{sp} is almost the same as that of DCPD.

Brown and Chow [7] studied the solubility of these compounds extensively. Using the pK_{sp} given in Table 13.5 and the dissociation constants of H_3PO_4 (discussed in Chapter 4), and following the procedure given in Ref. [13], Chow [8] has developed a ternary diagram for most of the compounds given in Table 13.5. This diagram shows the solubility of these compounds as a function of concentration of phosphorus and pH of the solution at body temperature of 37°C.

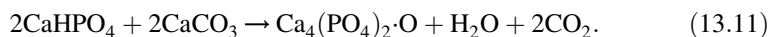
In addition to body temperature, the condition of a neutral pH is important because these materials are implanted in a human body, which has a near neutral pH, and extreme acidity or basicity can affect the soft tissues within the body. Brown and Chow's [7] analysis reveals that the most stable compound in the near neutral pH region is HAP, which is the major component of bones.

As pointed out by Chow [8], TTCP is the only compound in Table 13.5 that has a Ca/P ratio higher than that of apatites. As a result, TTCP is the only compound that could be reacted with other calcium phosphates with a lower Ca/P ratio to form HAP. For example, reaction of TTCP and DCPA will produce HAP without producing any acidic or basic byproducts. The reaction is as follows:



The first component on the left-hand side of Eq. 13.10 is alkaline, and the second one is acidic. Thus, this reaction is an acid–base reaction that yields HAP at a near neutral pH in an aqueous environment, where both reacting components are sparsely soluble.

TTCP is first prepared by reacting commercially available DCPA and $CaCO_3$ by heating the mixture at 1500°C for 6 h and then quenching it at room temperature in a desiccator [8]. The reaction is represented by



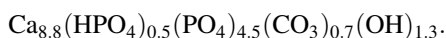
To prepare HAP, an equimolar mixture of TTCP and DCPA, each of average grain size of 15 μm , and $CaCO_3$ of average grain size of 1 μm are reacted. These powders are then mixed in water to form an aqueous paste that sets into a hard mass by Eq. 13.11.

Fucase *et al.* [9] reported that setting of this cement in a physiological environment (pH 8 and temperature, 37°C) occurred in 4 h. The compressive strength increased linearly during these 4 h, then tapered off to 36 MPa (5100 psi) thereafter. Chow *et al.* [10] have shown that the compressive strength of the cement samples prepared under a moderate pressure of 0.7 MPa (100 psi) and cured in water for 20 h can be as high as 66 MPa (9400 psi). The tensile strengths of such samples are 9.97–10.84 MPa (1430–1550 psi). Fucase *et al.* [9] also used the intensity of the HAP phase in the X-ray diffraction patterns to show that the only reaction product formed was HAP, and its formation was complete within 4 h.

The microstructure of the cement was highly crystalline [9]. Initially, the crystals were petal-shaped and extremely small ($\approx 0.05 \mu m$ in width and 1 μm in length). Subsequently,

they grew into rod-like structures. Within the first hour of formation of the cement, the crystals were very small, and the structure appeared to be amorphous, but after 24 h of curing, the structure grew into a well-crystallized matrix.

Recently, Constantz *et al.* [14] reacted a mixture of monocalcium phosphate monohydrate ($\text{Ca}(\text{H}_2\text{PO}_4)_2 \cdot \text{H}_2\text{O}$), α -tricalcium phosphate ($\text{Ca}_3(\text{PO}_4)_2$), and calcium carbonate (CaCO_3) with a solution of trisodium phosphate (Na_3PO_4) to produce dahllite with the stoichiometric formula,



The result was fast-setting cement with a high compressive strength of 55 MPa (8000 psi) in one day and an ultimate tensile strength of ≈ 2.1 MPa (300 psi). Applications of this cement are discussed in Chapter 18.

13.5.

CONCLUSIONS

Calcium oxide is the main ingredient in conventional portland cements. Since limestone is the most abundant mineral in nature, it has been easy to produce portland cement at a low cost. The high solubility of calcium oxide makes it difficult to produce phosphate-based cements. However, calcium oxide can be converted to compounds such as silicates, aluminates, or even hydrophosphates, which then can be used in an acid–base reaction with phosphate, forming CBPCs. The cost of phosphates and conversion to the correct mineral forms add to the manufacturing cost, and hence calcium phosphate cements are more expensive than conventional cements. For this reason, their use has been largely limited to dental and other biomedical applications. Calcium phosphate cements have found application as structural materials, but only when wollastonite is used as an admixture in magnesium phosphate cements. Because calcium phosphates are also bone minerals, they are indispensable in biomaterial applications and hence form a class of useful CBPCs that cannot be substituted by any other.

REFERENCES

1. A.D. Wilson, B.E. Kent, D. Clinton, and R.P. Miller, "The formation and microstructure of the dental silicate cement," *J. Mater. Sci.*, **7** (1972) 220–228.
2. A.D. Wilson and B.E. Kent, "Dental silicate cements. IX. Decomposition of the powder," *J. Dent. Res.*, **49** (1970) 21–26.
3. K.P. Krajewski, "Early diagenetic phosphate cements in the Albeian condensed glauconitic limestone of the Tatra mountains, Western Carpathians," *Chem. Abst.*, **10** (1984) 114382.
4. C.E. Semler, "A quick-setting wollastonite phosphate cement," *Am. Ceram. Soc. Bull.*, **55** (1976) 983–988.
5. T. Sugama and M. Allan, "Calcium phosphate cements prepared by acid–base reaction," *J. Am. Ceram. Soc.*, **75** [8] (1992) 2076–2087.
6. T. Sugama, N.R. Carciello, T.M. Nayberg, and L.E. Brothers, "Mullite microsphere-filled lightweight calcium phosphate cement slurries for geothermal wells: setting and properties," *Cem. Conc. Res.*, **25** [6] (1995) 1305–1310.

7. W.E. Brown and L.C. Chow, *A new calcium phosphate water-setting cement*, in *cements research progress*, ed. P.W. Brown (American Ceramic Society, Westerville, OH, 1986), pp. 352–379.
8. L.C. Chow, “Calcium phosphate cements: chemistry, properties, and applications,” *Mat. Res. Soc. Proc.*, **599** (2000) 27–37.
9. Y. Fucase, E.D. Eanes, S. Takagi, L.C. Chow, and W.E. Brown, “Setting reactions and compressive strengths of calcium phosphate cements,” *J. Dent. Res.*, **December** (1990) 1852–1856.
10. L.C. Chow, S. Hirayama, S. Takagi, and E. Perry, “Diametral tensile strength and compressive strength of a calcium phosphate cement: effect of applied pressure,” *J. Biomed. Mater.*, **53** [5] (2000) 511–517.
11. T. Sugama and N. Carciello, “Hydrothermally synthesized aluminum phosphate cements,” *Adv. Cem. Res.*, **5** [17] (1993) 31–40.
12. A.S. Wagh, S.Y. Jeong, D. Lohan, and A. Elizabeth, Chemically bonded phospho-silicate ceramics, US Patent No. 6,518,212 B1, 2003.
13. M. Pourbaix, *Atlas of Electrochemical Equilibria in Aqueous Solutions* (Pergamon Press, New York, 1974).
14. B.R. Constantz, I.C. Ison, M.T. Fulmer, R.D. Poser, S.T. Smith, M. VanWagoner, J. Ross, S.A. Goldstein, J.B. Jupiter, and D.I. Rosenthal, “Skeletal repair by in situ formation of the mineral phase of bone,” *Science*, **267** (1995) 1796–1799.

This page is intentionally left blank

Chemically Bonded Phosphate Ceramic Matrix Composites

Sintered ceramics have been in use as structural products since the beginning of human culture. Archeological findings such as pottery and rudimentary tools produced over thousands of years tell us a great deal about the human culture of those times. Ceramics are also modern technological materials, especially in high temperature applications, and hence ceramic science is an active field of research even today. Sintering of these ceramics, however, is energy intensive and expensive, when large sizes are sintered. The alternative is chemical bonding.

Portland cement is such an alternative. Formed by chemical reactions, it is an inexpensive product and is used in large volumes. There is a wide gap between the attributes of ceramics and Portland cement, however. Ceramics exhibit superior mechanical properties compared to cements. Ceramics are far more stable in acidic and high temperature environments, but cements are not. Thermal stability of cements is poor, while ceramics are refractory and are used at very high temperature, such as linings in furnaces. Cements are porous, but ceramics can be very dense.

The modern technological needs of structural materials are not fulfilled entirely by these two types of materials. There is also a need for materials that exhibit properties in between cement and sintered ceramics. That need can be met by CBPC matrix composites—materials that are produced like cements at ambient or at slightly elevated temperatures, but exhibit properties of ceramics. These composites are attractive for many structural applications, including architectural products, oil-field drilling cements, road repair materials that set in very cold environments, stabilization of radioactive and hazardous waste streams, and biomaterials.

CBPC matrix composites are formed by incorporating a small amount of CBPC binder in a much greater amount of a second-phase material. These components are then mixed with water to form a slurry that will react and form the composite. Varying the properties of the additive alters the composite so that one obtains a range of products with tailored

properties. For example, mechanical properties can be virtually doubled by adding fly ash to the mixture. Adding insulating particles such as ash, sawdust, or hollow microspheres of silica can reduce the thermal conductivity. The ability of CBPCs to bind a range of materials (“extenders”) and to form composites makes them promising for niche applications that cannot be fulfilled by conventional cement.

The ever-increasing industrial activity is depleting natural resources worldwide, and at the same time, producing wastes that need disposal. Much of the solid waste that is produced is nonhazardous and can be recycled as CBPC structural products. For example, statistics published in 1986 [1] revealed that ≈ 40 ton of waste was generated per person in the US that year. Most of it was nonhazardous. CBPCs can incorporate much of this high volume benign waste into value-added products. When benign waste streams, especially fly ash, are incorporated in CBPCs at high loadings, the mechanical properties of CBPCs are enhanced several fold. Conventional cement does not have this advantage. While CBPCs are expensive, a high loading of waste streams can be incorporated in them. This high loading reduces the cost of CBPC products and makes them cost effective. As a result, CBPCs are finding niche applications in other areas. These include road repair in winter seasons in cold countries, novel architectural products, construction material for low cost housing, and structural material in permafrost regions. CBPC matrix composites are especially useful in extreme cold climate and corrosive environments. This chapter describes attributes of these structural materials for different applications.

14.1.

RECYCLING OF BENIGN WASTE STREAMS IN CBPC VALUE-ADDED PRODUCTS

CBPC matrix composites can incorporate a high volume of industrial waste streams such as fly ash, mineral waste such as iron tailings and Bayer process residue from the aluminum industry (red mud), machining swarfs from the automobile industry, and forest product waste such as saw dust and wood chips. Table 14.1 lists some of these waste streams and potential products or applications.

As noted in Chapters 9, 11–13, CBPCs made with the room-temperature binders of Mg, Fe, Zn, and Ca exhibit physical properties similar to those of conventional cement, but suitable extenders can enhance them at very high loading. This improvement is not possible in conventional cement. Figure 14.1 illustrates the main difference between CBPCs and conventional cement. This difference is partly because the CBPC process is based on an acid–base reaction, while conventional cement is formed only in an alkaline region. Therefore, one can add acidic, neutral, or alkaline components in CBPCs at a high load factor. Cement, on the other hand, can accept only neutral and alkaline streams, even those at a modest load factor, as discussed below.

Wagh and Singh [2–4] have incorporated a range of waste streams and other extenders in Ceramicrete and shown that desired properties can be obtained in Ceramicrete matrix composites. Table 14.2 compares typical properties of Ceramicrete and cement. It also lists the extenders used and niche applications.

Table 14.1.
Industrial Waste Streams Incorporated in CBPCs and Potential Applications.

Waste Stream	Loading (wt%)	Potential Applications
Class C and F fly ash from power plants, steel slag, other combustion products [2]	40–80	Structural ceramics, superior cements, waste management
Red mud [3]	50–60	Structural products
Iron mine tailings [3]	50–80	Structural materials products
Swarfs, machining waste from steel and automobile industry [3]	≈50	Recycling metal values
Wood chips, saw dust [4]	≈50	Thermally insulating structural products
Shredded Styrofoam [4]	10–15	Superior insulation

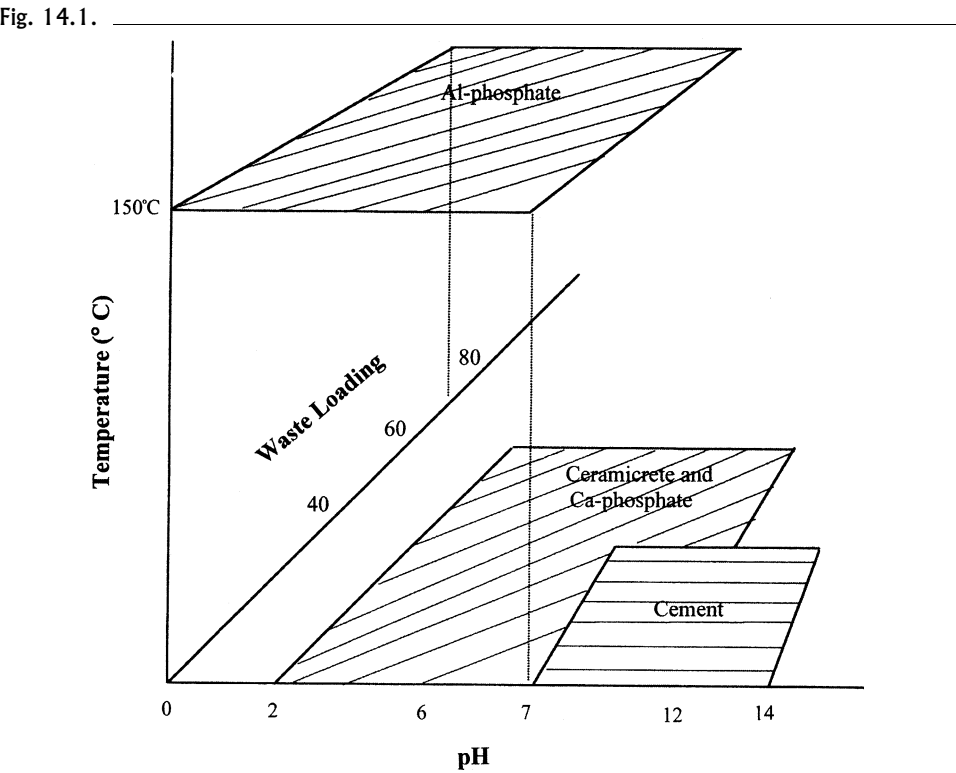


Figure illustrating difference between CBPC and conventional cement.

Table 14.2.

Typical Properties of Ceramicrete Matrix Composites and their Applications.

Property	Additive	Ceramicrete	Cement	Application
Delayed setting time (h)	Boric acid	1–7	6 h	Structural ceramics, oil well cements, waste encapsulation
Accelerated setting time	Excess MgO	Minutes	6 h	Sprayable coatings for construction, dental cements
Setting pH	Most fillers	7–8	11–13	Most
Density (g/cm ³)	Fly ash	1.7–2.0	2.4	Lightweight grout for all applications. Density is varied with suitable aggregates
Volume change during setting	Most fillers	Slight expansion	Slight contraction	Architectural moldings, oil well cements
Compressive strength, psi (MPa)	Fly ash, wollastonite	6000–12,000 (42–84)	4000 (28)	Structural ceramic, waste management
Flexural strength, psi (MPa)	Fly ash, wollastonite, and 1–3% glass fiber	1300–1700 (9–12)	≈700 (4.9)	Macro-encapsulation of radioactive objects, structural ceramics
Shear bond strength, psi (MPa)	Fly ash and aggregates	5922 (42) after 7 days		Road-based applications [6]
Fracture toughness (MPa√m)	Wollastonite	0.3–0.7	≈0.3	Range of structural materials applications
Increasing thermal conductivity (W/m K)	Iron oxide	0.8	0.54	Radioactive waste encapsulation
Decreasing thermal conductivity (W/m K)	Styrofoam, wood chips, cenospheres	0.37	0.54	Permafrost and other insulating cements
Linear expansion coeff. (°C ⁻¹)	Fly ash	≈10 ⁻¹⁰	1.2 × 10 ⁻⁵	Macro-encapsulation of contaminated equipment
Expansion in water (%)	Fly ash and aggregates	0.358		Road-based applications [6]
γ-ray absorption	Fe ₂ O ₃ , UO ₂			Encapsulation of radioactive materials
Neutron absorption coefficient (cm ⁻¹)	Boric acid, boron carbide	3.08	0.06	Encapsulation of nuclear materials
Water absorption (wt%)	Fly ash and aggregates	<2	5–20	Most applications
Freeze-thaw durability factor	Fly ash and aggregates	89.7% after 300 cycles		Road-based and permafrost applications
Durability in pH of water	Any filler	Stable between pH 3 and 11	In pH > 7	Stabilization of acids and alkalis, resistance to acid rain

Properties of cement are listed for comparison [4].

Though the data given in Table 14.2 are for Ceramicrete matrix composites, similar properties in other CBPC matrix composites are possible with different extenders. Therefore, overall CBPC matrix composites are versatile materials and have the potential for varied applications as structural and nuclear materials, as well as civil engineering applications in general. In this chapter, we discuss some common CBPC matrix composites and their applications in the construction industry. Additional applications are presented in subsequent chapters.

14.1.1. CBPC Matrix Composites Based on Fly Ash

Fly ash is one of the biggest industrial wastes. It is produced in the utility industry by burning fossil fuels during energy production. Incinerator ash from municipal solid waste, volcanic ash, and slags from the iron industry are other combustion products that along with fly ash pose disposal problems due to their high volume. At present, approximately one-third of the fly ash produced by utility plants is recycled in cement-based products, which can incorporate $\approx 15\text{--}20\%$ ash in them. Efforts are underway to improve this loading [5], but have not been successful at a commercial scale for several reasons:

- (1) Cement chemistry is sensitive to the components of the combustion products. Some contain chlorides. Chlorides and other anions hinder the setting of cement.
- (2) The carbon content of ash is also a major factor. High carbon ash hinders setting of cement. In particular, ash produced by low- NO_x burners contains a high proportion of carbon. To meet the Clean Air Act requirements, future industries may opt for low- NO_x burners that will produce ash unsuitable for cement.
- (3) At low loading of ash in cement, the process is not very economical.

CBPC products do not have these drawbacks. The CBPC chemistry is not very sensitive to the waste components, and ash itself seems to participate in the setting reaction. The end product has low open porosity, yet is a lightweight material of high strength.

A range of ash types may be incorporated in a CBPC matrix. These include utility-industry fly ash, high carbon ash, and steel industry slag. The CBPC provides a means to manufacture ash products with high ash loading. The most voluminous ash is fly ash collected from the exhaust of power plants using electrostatic precipitators. In the US, this ash is well classified according to its content and its commercial availability. For this reason, we next discuss CBPC products formed with this ash. A typical fly ash composition was given in Table 3.2

Particulates of fly ash are very fine. Some of the silica in the ash is found in the form of small silica spheres, called cenospheres or extensospheres, which make ash a very flowable material. This property not only makes ash miscible in a CBPC slurry, but it reduces the viscosity of the slurry and makes the slurry smooth, easily pumpable, and pourable. This property is a great advantage with CBPC-based drilling cements (Chapter 15).

Figure 3.3 is a typical SEM micrograph of ash cenospheres in Class F ash. Figure 3.2 shows sharp peaks in the XRD output from various minerals, such as silica and alumina, that are present in ash in crystalline form. In addition, the broad hump in the XRD pattern

possibly represents amorphous silica and alumina. This amorphous material is reactive and makes the ash pozzalanic, i.e., it exhibits some hardening when mixed with water. The amorphous material is also important in a CBPC matrix composite because, as we shall see later, it enhances the physical and mechanical properties of CBPCs and forms superior cement.

Typical ash loading in a CBPC matrix composite is $\approx 50\text{--}70$ wt%. This loading is significantly higher than in conventional cement systems where 25 wt% is considered very good. High loading offsets some of the high cost of the CBPC binder materials. Because of the superior properties and lower cost, a blend of CBPC binders and ash is ideal for most applications.

Wagh *et al.* [2] conducted a systematic study of incorporating Class C and Class F ash with compositions described in Table 14.1, and their mixture in the Ceramicrete matrix. Table 14.3 provides the properties of the resulting ceramics.

The density of the class C fly ash product is slightly higher than that of class F. This difference may be because class F ash contains more carbon and, hence, is slightly lighter. Since the ash and the binder powders have nearly the same density, the ash loading has hardly any effect on the density. Overall, the ash products are approximately 25% lighter than the corresponding cement products.

The open porosity, which affects water absorption in the ceramic, is lower in the Ceramicrete products than in the portland cement products. It is $\approx 20\%$ for cement products and $<5\%$ (typically, 2–3%) for CBPC products.

Though the open porosity in the ash-containing Ceramicrete is very low, the matrix has a significant amount of closed or isolated pores. Estimates, based on the densities of individual minerals formed in the final products, show that the closed porosity is ≈ 20 vol%. Coupled with this closed porosity, a significant amount of bound water (typically 15 wt%) in the binder component makes this cement lightweight.

The major advantage of the ash-based CBPC matrix composite, as a structural material, is the high compressive strength. As shown in Table 14.3, the compressive strength of the binder is only 3337 psi (23.4 MPa), but incorporating even 30 wt% of class F fly ash increases its strength to 5651 psi (39.5 MPa). Higher loading increases the strength further, reaching a maximum between 50 and 60%. The strength of conventional cement products is ≈ 4000 psi (28 MPa), while the maximum strength of CBPC is $\approx 75\%$ higher with class F fly ash and three times higher with class C. A CBPC matrix composite with a mixture of class F and class C fly ash exhibits a strength between the composites with class F and class C. This strength is more than twice that of conventional cement products.

It is interesting to see how the strength evolves during the setting period of the ash-based phosphate-cement products. Figure 14.2 shows the compressive strength evolution over time when Class C fly ash is incorporated in Ceramicrete. The material attains compressive strength equal to that of conventional cement products within a day of curing. Subsequently, the strength more than doubles in 5 days and keeps increasing, though less rapidly afterwards. In 45 days, the strength is slightly less than three times that of conventional cement, and then it tapers off. Thus, long-term curing has a significant effect on the compressive strength, though the product itself is ready for use after a day.

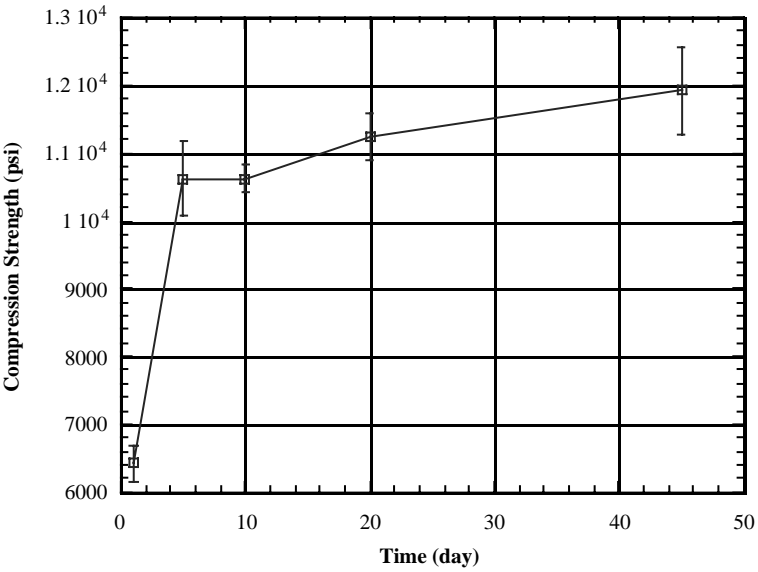
Table 14.3.

Physical and Mechanical Properties of Ceramicrete with Class F and C Ash at Different Loadings.

Ash Loading (wt%)	Density (g/cm ³)	Open Porosity (vol%)	Compression Strength, psi (MPa)
0	1.73	2.87	3337 (23.4)
<i>Class F loading</i>			
30	1.67	5.22	5651 (39.6)
40	1.77	4.09	6207 (43.4)
50	1.80	2.31	7503 (52.5)
60	1.63	8.15	5020 (35)
70	Not measured	Not measured	2177 (15.2)
<i>Class C loading</i>			
50	1.966	4.79	8809 (61.6)
60	2.069	3.4	11,924 (83.3)
70	2.058	5.34	7608 (53.2)
80	1.918	8.025	4753 (33.3)
<i>Class C + F loading</i>			
60	1.78	6.58	9665 (67.7)

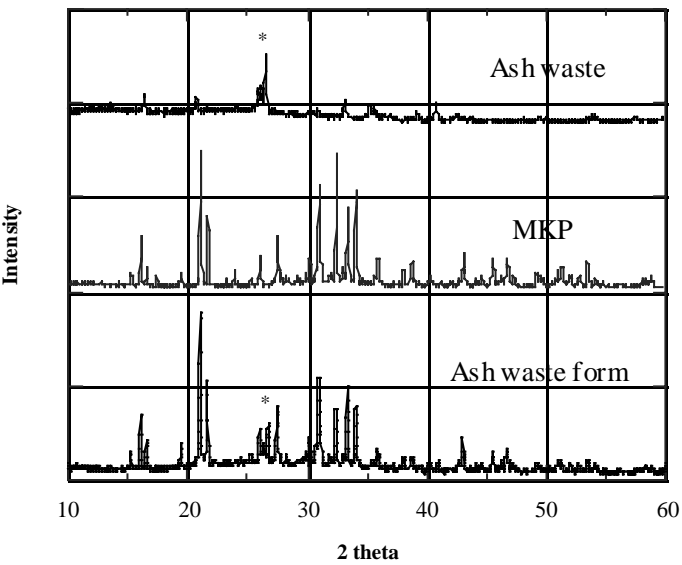
Generally, CBPC products with Class C fly ash set faster than with Class F ash. This behavior is understandable since Class C fly ash contains much higher levels of CaO (see Table 3.2). Since solubility of CaO is high, this fly ash reacts faster in the acidic phosphate solution. Class F fly ash is low in CaO and contains residual carbon and silica that are less soluble, and hence, this ash is less reactive. The exothermic reaction between CaO and the acid phosphate generates considerable heat during setting of the ceramic. As a result, in spite of the higher strength of the end product, incorporating Class C fly ash alone is generally not suitable while forming large-size ceramics. The exception is the drilling cements for deep wells that are described in Chapter 15. Therefore, a blend of Class C and F ash is preferred in most CBPC construction materials. Figure 14.3 shows the X-ray diffraction output of Ceramicrete at 60 wt% Class F ash. All the peaks in the binder (see Fig. 9.8) and ash (Fig. 14.3) are also present in the ash product. No new peaks are apparent in Fig. 14.3, implying that no new crystalline minerals are formed by the interaction between ash and the binder components. However, a broad hump occurs in the middle in Fig. 14.3. This hump corresponds to an amorphous or noncrystalline phase that cannot be identified by X-ray diffraction. However, some insight may be gained into these amorphous phases from the differential thermal analysis (DTA) output shown in Fig. 14.4 for the class F fly ash and the corresponding Ceramicrete matrix composite. In the same figure, the DTA output of the binder from Fig. 9.10 is reproduced for the sake of comparison. As noted in Chapter 9, the endotherm of the binder at 120°C is due to the escape of the bound water from the matrix. A similar loss of bound water is also apparent in the ash product. No new endotherms are noticeable in the ash product. This finding suggests that the new amorphous phases are thermally stable.

Fig. 14.2.



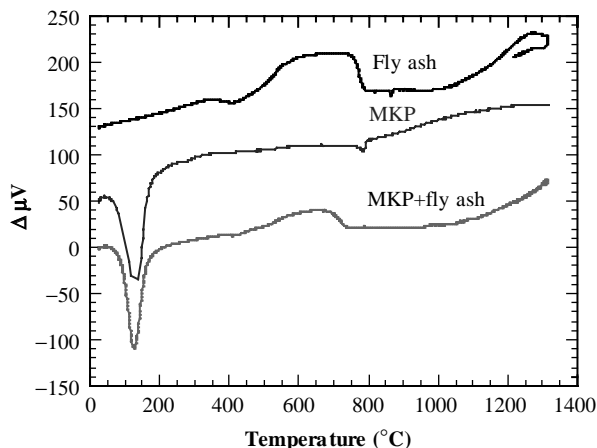
Compressive strength of Ceramicrete with 60 wt% Class C fly ash, as a function of curing time.

Fig. 14.3.



X-ray diffraction output of Ceramicrete with 60% Class F fly ash.

Fig. 14.4.

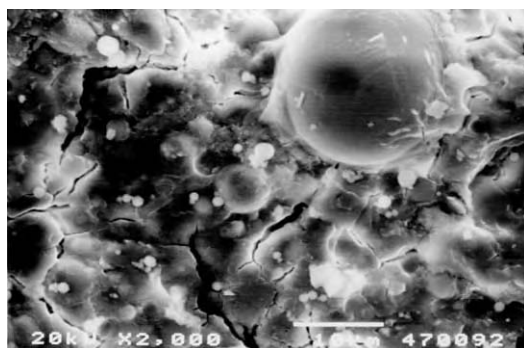


Differential thermal output of Ceramicrete with 60% Class F fly ash.

The SEM micrograph of the ash product in Fig. 14.5 reveals these new amorphous phases as a coating of continuous glassy phase on cenospheres. Commercially, such spheres are separated from ash and are used in cement composite to reduce the product density. Likewise, in CBPC matrix composites they help to reduce the overall product density.

The amorphous content in ash is suspected to be silica and a silicophosphate. The latter may be responsible for the low open porosity and high strength of the ash-containing CBPC product. Work in dental cements [7] has revealed the possibility of silicophosphate bonds that are very strong. It is likely that similar phases also contribute to the strength and low porosity of the ash-containing CBPC product.

Fig. 14.5.



SEM micrograph of Ceramicrete with 60% Class F fly ash.

14.1.2. Industrial and Mining Waste Streams

As listed in Table 14.1, various other waste streams can be incorporated in Ceramicrete to produce useful ceramic matrix composites. In addition to those listed in the table, Wagh and his group have explored incorporating drill cuttings from oil fields, slags from iron industry, wood chips, saw dust, and many other waste streams [8]. Most of these studies were limited to proof of concept, and more work is needed to demonstrate concept usefulness. Here, we discuss case studies on swarfs and red mud in which detailed work has been done.

The most common metal swarfs are iron-based [9,10] and produced by the machine tool and automobile industries. The resulting fine Fe particles oxidize in storage and form magnetite and hematite. Because they also contain flammable machine oils, this oxidation makes them pyrophoric and hence a liability. Because the particle surfaces are coated with oil, they cannot be incorporated in conventional cement. As demonstrated by Wagh and Jeong [3], the acid phosphate in the CBPC process acts like a detergent and exposes the surface of these particles to the acid–base reaction and binds them.

The ingredients given in Table 14.4 were mixed for only a few minutes, and the resulting thick putty-like mass was transferred into a rigid plastic mold. The samples were pressed with pressure ≈ 1000 psi (7 MPa) for 10 min. When removed from the mold, the samples were hard. The composition used to make each set of samples and their strength are also given in Table 14.4. The strength given in the table is an average for three samples. The strengths, except for Sample 1, are ≈ 2000 psi (14 MPa). In Sample 1, addition of pure Fe does not enhance the strength. This is because the swarf contains some Fe. More Fe lowers the redox potential below the stability line of water (see Chapter 7). The water will partially decompose and form hydrogen, which will hinder the setting reaction.

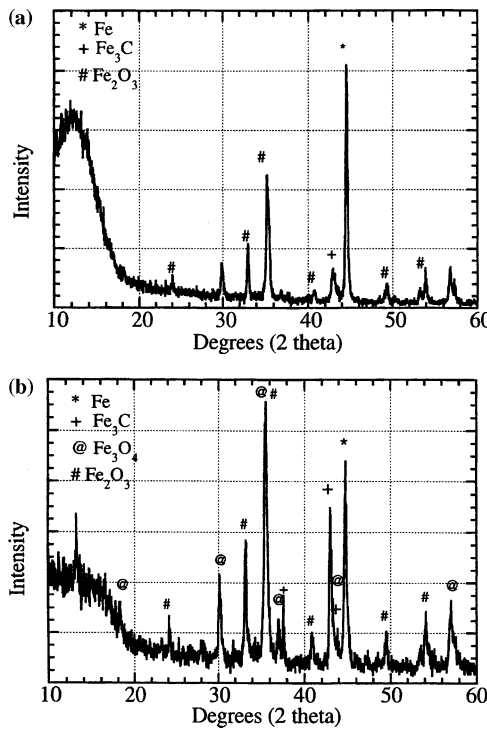
The X-ray diffraction patterns of the swarf material and its ceramic are given in Fig. 14.6. This swarf contains Fe_2O_3 , iron carbide (FeC), and some Fe. Evidence of reduction of Fe_2O_3 to Fe_3O_4 by Fe during the acid–base reaction is evident in Fig. 14.6, where, in addition to the swarf peaks, peaks of Fe_3O_4 are also present; thus, Fe_3O_4 must have been formed by Fe_2O_3 reduction. The hydrated phosphate phase, however, is amorphous, and hence, it would not be visible in the X-ray diffraction pattern. This study [3],

Table 14.4.

Compositions Used in Swarf Solidification and Corresponding Compressive Strengths [3].

Component (wt%)	Sample 1	Sample 2	Sample 3	Sample 4
Swarf	69.6	69.6	74	78.3
Fe_2O_3	7.8	8.7	0	0
Fe	0.9	0	0	0
85 wt% H_3PO_4	10.2	10.2	15.2	10.2
H_2O	11.5	11.5	10.8	11.5
Compressive strength, psi (MPa)	972 ± 2 (6.8 ± 0.01)	2345 ± 311 (16.4 ± 2)	1937 ± 92 (13.6 ± 0.6)	1800 ± 459 (12.6 ± 3)

Fig. 14.6.



X-ray diffraction pattern of (a) Fe-based swarf and (b) its phosphate ceramic.

though limited, demonstrates that it is possible to take advantage of the iron present in the waste itself and produce a hardened ceramic.

As mentioned before, red mud is a residue produced during Bayer process extraction of alumina from bauxite [11]. In this process, the ore is digested at a very high pH in caustic soda, and alumina is dissolved in the solution. The pregnant liquor is then separated, and a residue rich in iron oxide is disposed or stored. This residue contains 1–3 wt% caustic soda and is highly alkaline. Table 14.5 provides the composition of the red mud used in the study by Wagh and Jeong [3]. The Fe₂O₃ content in this waste was high; other significant oxides were those of aluminum, silicon, titanium, and calcium

Table 14.5.

Typical Composition (wt%) of Alcoa (Point Comfort) Red Mud.

Al ₂ O ₃	Fe ₂ O ₃	Na ₂ O	CaO	SiO ₂	TiO ₂	Loss on Ignition
18	40	2.7	7.6	9.6	8.5	10.3

oxide. The loss on ignition was as much as 10 wt%, possibly due to evolution of carbon dioxide from calcium and sodium oxides. Because of the 2.7 wt% of Na_2O in the waste, the residue had a $\text{pH} > 13$.

The “as-received” mud was in the form of sludge, with water content of 30 wt%. This low content of water is due to the dry stacking method used during storing [12]. The mud is disposed on slopes of $\approx 4^\circ$, which is the angle of repose for the mud. Much of the caustic water flows down the slope, leaving thick sludge on the stacks. Additional drying occurs in the sun, and the mud becomes a thick sludge.

Bricks were made from this mud by dye casting. To that end, 250 g of sand and 250 g of wet red mud were added to 30 wt% water and mixed for 10 min in a Hobart cement mixer. To this mixture, 62.5 g of 85 wt% concentrated H_3PO_4 solution was added and mixed for another 5 min when the pH of the solution became 3.11. At this point, 1 g of reagent grade Fe was added, and the slurry was mixed for 25 min; it formed a thick mass, which was then pressed at 1000 psi (7 MPa) in a brick mold of size $8 \times 4 \times 2.5 \text{ in.}^3$ ($20 \times 10 \times 6 \text{ cm}^3$). The resulting brick was cured in a closed container at room temperature; it hardened sufficiently after one day.

In this example, no extra water was added, except for a few drops while dye casting. Use of the in situ water from the red mud avoided dewatering and still made a useful product. Dewatering is expensive, and the method presented here avoids it.

During Ceramicrete formation using H_3PO_4 , the caustic soda reacts with the acid-phosphate and forms amorphous $\text{MgNaPO}_4 \cdot n\text{H}_2\text{O}$. The neutralized waste is micro-encapsulated in the Ceramicrete matrix, in which the $\text{MgNaPO}_4 \cdot n\text{H}_2\text{O}$ also acts like a binding phase.

The examples of swarfs and red mud may be used to compare costs of fabricating products from iron phosphate ceramics and conventional portland cement products. The main material cost in the former is for H_3PO_4 , sold at ≈ 20 cents per pound, while elemental iron is available at ≈ 5 cents a pound. Assuming $\approx 10 \text{ wt\%}$ H_3PO_4 is used in either swarf or red mud products, the material costs of producing one pound of a product is ≈ 3 cents. The cost of portland cement is ≈ 4 cents a pound, and portland cement products contain $\approx 15 \text{ wt\%}$ of cement; therefore, the materials cost in the concrete products amounts to ≈ 0.6 cents. This calculation suggests that cement products are cheaper than the iron phosphate ceramics, even though the latter use industrial waste streams that are inexpensive. However, some costs are offset by the advantages of the phosphate ceramic products. For example, phosphate ceramics are quick setting and do not need to be hydrated or steam cured. They expand slightly during curing (1–2 vol%) and, hence, capture intricate features of the molds. They bond to any material except plastics with smooth surfaces and bond well to set themselves. Furthermore, on islands and in some third world countries (Jamaica, Guyana), while portland cement is expensive because of energy-related costs, industrial waste material such as red mud is readily available at no cost. Thus, to fabricate value-added products such as terra cotta molded forms or construction products in areas where conventional cement is scarce and expensive but where industrial waste containing iron is readily available, the CBPC process can be very useful and could help to clean up industrial waste dumps in these regions.

14.2.

FIBER REINFORCEMENT OF CBPC PRODUCTS

In Section 13.2, we mentioned that whisker reinforcement aids in increasing the flexural strength and fracture toughness of CBPCs. Acicular crystals of wollastonite act like whiskers. In this section, the effect of fiber reinforcement is discussed.

Because the CBPC processes are carried out at room or slightly elevated temperatures, natural fibers, man-made glass, or polymer fibers may be added in the product. Jeong and Wagh [13] have demonstrated this capability by incorporating glass fibers in ash-containing Ceramicrete. They used chopped glass fibers of length 0.25 in. (0.6 cm) and 0.5 in. (1.3 cm). A small amount (1–3%) of fibers was added to the Ceramicrete and ash powder blend. When water was added, the slurry was thin enough to mix and form a thick paste that was poured into molds. The distribution of the fibers was found to be very uniform throughout the sample, and no agglomeration of fibers occurred during mixing. Monopotassium phosphate is a dispersant, and though fibers were added as a bunch of strands, they dispersed well in the slurry. Figure 14.7 shows the increase in flexural strength with fiber content for 40 and 60 wt% ash-containing Ceramicrete. The initial strength of ≈ 900 psi (6.3 MPa) has been increased to 1300 (9.1 MPa) and 1700 psi (11.9 MPa) with fibers of length 0.25 in. (0.6 cm) and 0.5 in. (1.3 cm), respectively. The longer fibers give higher flexural strength. Similar is the case with fracture toughness (Fig. 14.8). The initial fracture toughness of $0.35 \text{ MPa m}^{1/2}$ has been increased to $0.65 \text{ MPa m}^{1/2}$ in both cases.

The scanning electron micrograph in Fig. 14.9 gives some insight into the mechanism behind this increase in strength. This micrograph was taken on a fractured surface. It shows that the matrix covers all around individual fibers, which can be pulled out clean. This property implies considerable enhancement in the fracture energy. Chemical damage (corrosion) did not occur on the fiber surface because the Ceramicrete matrix is neutral; in highly alkaline cement systems, glass fibers are damaged.

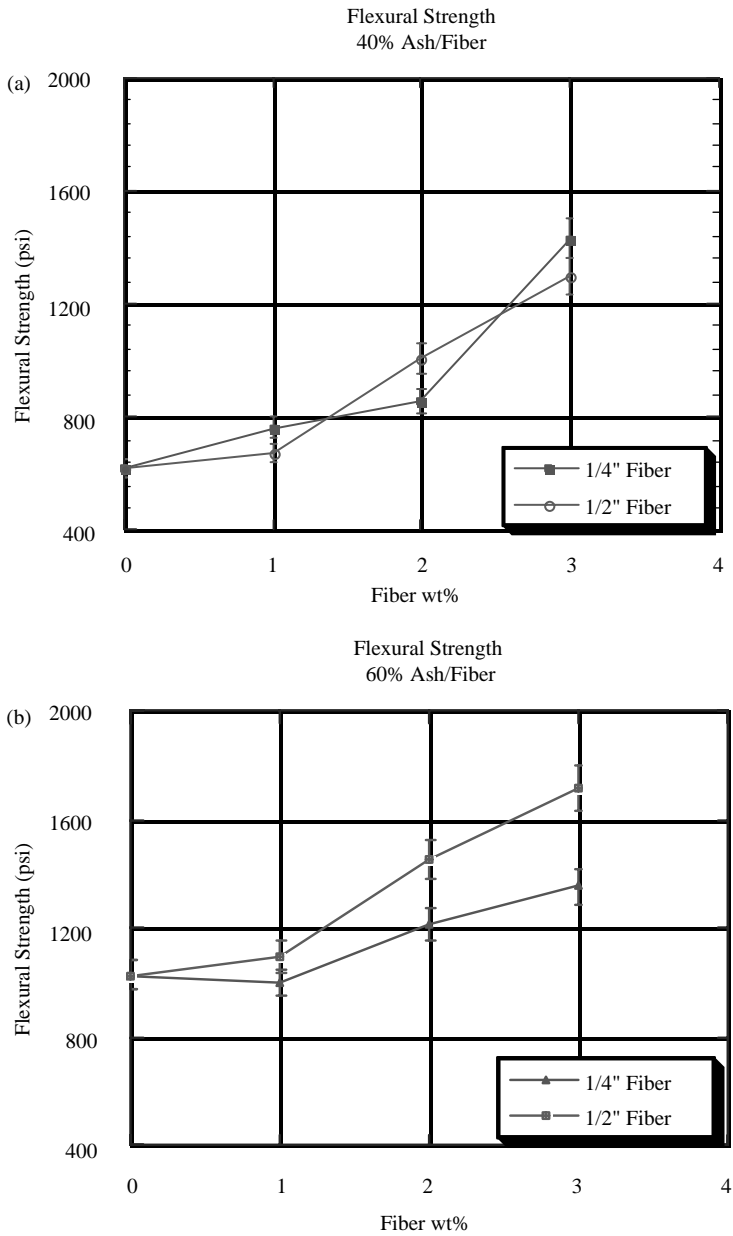
These studies by Wagh and coworkers with glass fibers are only an indication of how fiber-reinforced composites may be developed using CBPCs. Because of neutrality of the CBPC matrix and its formation at room temperature, a range of fibers may be added in the matrix that include natural fiber (such as wood, cellulose, and cotton) and artificial fibers (such as nylon). The greatest potential is in wood composites. Unlike the case of glass fibers, a bond should form between the natural fiber surface and the CBPC matrix. This bond should produce superior fiber-reinforced composites (cements). These areas are still open for research, and hardly any work has been reported in the literature.

14.3.

NICHE APPLICATIONS

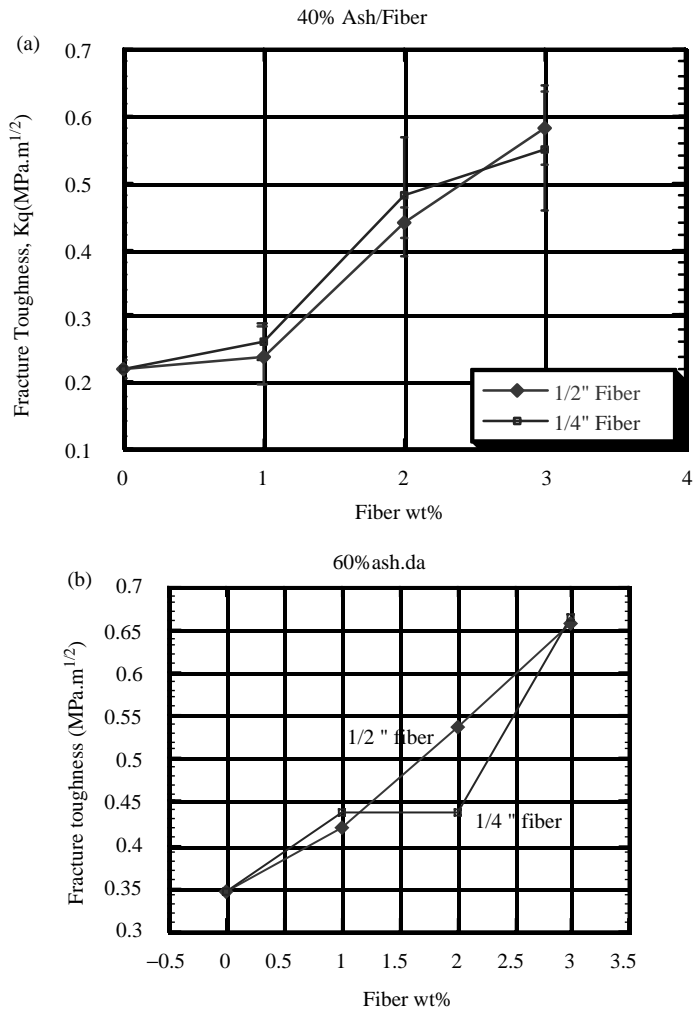
Wide-ranging applications of CBPCs are possible, because, as mentioned in the preceding section, CBPC matrix composites can be made with very high loading of either waste

Fig. 14.7.



Flexural strength as a function of glass fibers in ash containing Ceramicrete.

Fig. 14.8.

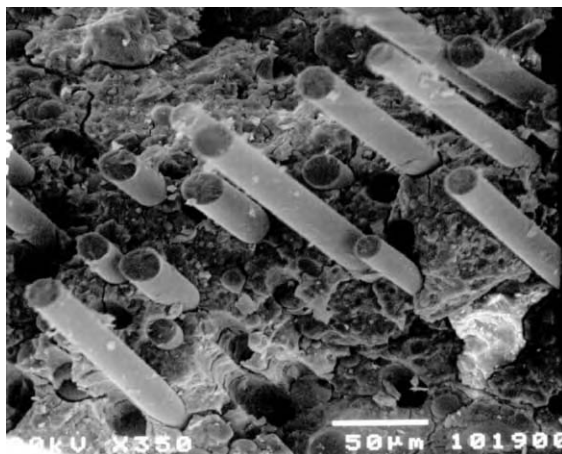


Fracture toughness as a function of glass fibers in ash containing Ceramicrete.

materials or other extenders. Waste materials with wide-ranging pH can also be incorporated in a CBPC matrix (see Table 14.1). As in cement, most of the CBPC matrix composites are formed at ambient temperature.

This versatility allows one to develop CBPC matrix composites with specific properties required for niche applications (see Table 14.2), such as heavy Ceramicrete with iron oxide or light-weight Ceramicrete with cenospheres, γ -ray shield with iron oxides or any other heavy metal oxide, neutron shield with light elements such as boron, insulators with cenospheres and ash, and comparatively better conductor with metals. The remaining chapters in this book address some of the niche applications where considerable scientific

Fig. 14.9.



SEM micrograph of fractured surface of fiber-reinforced ash containing Ceramicrete.

progress has been made. Below are some applications of CBPC matrix composites that have been pursued in the structural material area.

Producing rapid-setting cement for use in cold regions is a challenge in the cement industry. Conventional portland cement has limitations in its use on roads and bridges and other applications in cold climates. For example, road repairs are often done by first filling the potholes temporarily in winter, and then the final repair is completed with portland cement in the spring. In permafrost regions, such as Alaska and northern Canada, because of long winters, any cementing job is a great challenge whether it is building roads, or highways, or laying foundations for buildings. The drilling and completion industry in oil fields faces a similar problem in the Arctic region. Cementing without disturbing the permafrost formation surrounding the drilling area is a challenge because conventional cements neither set well, nor sufficiently insulate the surrounding ice formation when hot crude flows through the boreholes or pipelines. Even pipeline supports need insulating cement to avoid thawing of the supporting ground due to flow of hot crude in the pipes.

Portland cement-based variations currently in use do not provide a satisfactory solution. These variations still use the same cement chemistry (i.e., calcium silicate based) in that their basic properties such as setting characteristics and thermal properties do not change much. Thus, a novel solution is needed to address the cold climate problems in the cement industry.

Ceramicrete development has been pursued at Argonne National Laboratory (ANL) to help solve these cementing problems, and it is now being used for cold climate applications such as road repair and the construction industry, and may soon find use in Arctic oil fields. The oil-field applications are discussed in Chapter 15. Here, we will discuss the road and other structural materials applications.

Two road patches were repaired at ANL with Ceramicrete matrix composite containing 50 wt% class F fly ash on a trial basis in March 1999. The potholes are located on a road with heavy traffic from delivery trucks. The debris from the patches was not cleared, nor were the sides cut into smoother shapes as normally done. The temperature was 40 °F. After a few hours, it rained heavily, and the patches, being in low-lying areas, were under water till the next day. In spite of this weather, the patches set well the next day. They have not only withstood traffic for the last four years, but also the freeze-thaw cycles of the three winters have not affected patch integrity. At present, the intact patches show up well because the original asphalt road surrounding the patches is crumbling.

Bindan Corp. (Oak Brook, IL) sells several compositions of Ceramicrete matrix composite as commercial road-repair materials. The American Association of State Highway Transportation Officials (AASHTO) has tested one of these products [6]. Table 14.6 provides the results of their tests.

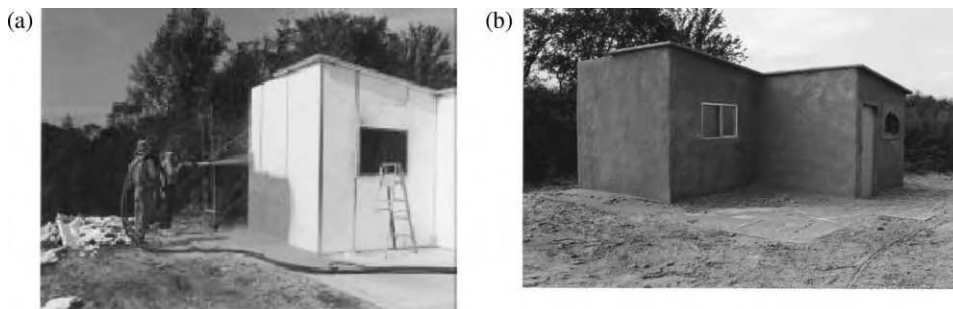
The Bindan Monopatch is a rapid-setting cement, and its 28-day strength shows that it is a high-strength product. The shear bond strength also confirms this conclusion. The slight shrinkage in air must be due to drying prior to setting, but this drying may be avoided by covering the sample during curing. AASHTO found that the freeze-thaw durability and scaled loss are nearly the same as most similar materials. Following this testing by AASHTO, roughly 15 states in the US conducted their own independent tests and have placed the product on their approval list. The Monopatch is being used not only

Table 14.6.

AASHTO Results on Bindan's Monopatch [6].

Acceptance Criteria	Results
<i>Time of set</i>	
Initial (≥ 10 min and ≤ 4 h)	26 min
Final (< 24 h)	30 min
<i>ASTM C 109 (2 in cube) Compressive strength, psi (MPa)</i>	
6 hr	2055 ± 89 (14 ± 0.6)
1 day	8066 ± 155 (56 ± 1)
7 days	8613 ± 537 (60 ± 3.5)
28 days	$10,202 \pm 427$ (71 ± 3)
<i>ASTM C 882 (3 × 6 cylinders with 45° interface 1 day shear bond strength (≥ 1000 psi)</i>	
1 day	7190 ± 270 (50 ± 1.5)
7 day	5910 ± 53 (41 ± 3.5)
<i>ASTM C 157 as modified in ASTM C 926 Section 8.3</i>	
Length change air storage ($\leq -0.15\%$ at 28 days)	0.103
Length change water storage ($\leq +0.15\%$ at 28 days)	0.358
<i>ASTM Freeze-thaw (neat material ≥ 80 durability)</i>	89.7/300 cycles
<i>ASTM C 672 Scaling (25 cycles)</i>	
Visual rating (< 2.5)	1
Scaled loss (< 1.0 lb/ft ²)	0.75

Fig. 14.10.



A low-cost home built by spraying Grancrete (photo: courtesy of Casa Grande, LLC).

as a road patching material but at important crossroads such as the Pennsylvania Turnpike (See the inset on the front cover of the book.)

The Ceramicrete process is based on the acid–base exothermic reaction. As a result, the exothermic heat evolution and its rate depend on the size of the waste forms produced. Larger forms generate more heat, which does not dissipate rapidly. Thus, the setting slurry heats up and accelerates the acid–base reaction, and the mixture is able to set even in cold surroundings.

Recently, ANL extended this concept and developed an insulating cement formulation as a construction material for large-size Dewars for storage of cryogenic fluids, such as liquid nitrogen.

Another US Company, Casa Grande, in collaboration with ANL, has developed a formulation, called Grancrete, which can be sprayed on vertically erected Styrofoam sheets to produce dwellings (see Fig. 14.10) in record time. Typically, a two-bedroom house of 1000 ft² can be built on a solid concrete foundation by two workers in two days. Apart from the low cost (a typical house sold for US \$12,000), the advantages of Grancrete include rapid construction, well-insulated dwelling, use of local materials such as sand and ash, and versatility of the formulation that allows construction in both hot and cold climates. If wollastonite is added instead of ash, one can color the formulation and obtain aesthetically pleasing dwellings. This company plans to build low-cost housing to meet third-world needs.

14.4.

ENERGY AND ENVIRONMENTAL ISSUES RELATED TO BINDER PRODUCTION

If phosphate binders were widely used for construction, very large volumes of them would replace conventional cement. It is, therefore, important to assess the effect of these binders on energy usage and the environment and to compare the results to the corresponding

Table 14.7.
Energy Consumed in Production of the Binders.

Binders	BTU/ton		Reference
Phosphate binders	MgHPO ₄	2.89	[14]
	CaHPO ₄	1.92	
	MgKPO ₄	2.27	
	Average	2.36	
Cement	Total	5.8	[14]

The author acknowledges help from Matt Aro of University of Minnesota, Duluth, in calculating these numbers.

energy and environmental effects from conventional cement. Table 14.7 provides the energy costs for the production of phosphate binders and portland cement. For the production of three common phosphate binders, the average energy is 2.36 million BTU/ton, compared to 5.8 million BTU for cement [14]. Thus, the production of the phosphate binders consumes about one-fourth the energy consumed during cement production. The low energy consumption of the phosphate binders is due to the less-energy-intensive chemical processes used in the extraction of the phosphate from ores, as compared to the energy-intensive clinkering process in cement production. Thus, phosphate binders reduce energy dependence as compared to conventional cement.

Coupled with the energy consumption is the environmental effect from production of these binders. For every ton of phosphoric acid, ≈5 ton of phosphogypsum (calcium sulfate) is produced [15]. This waste can be recycled into value-added products such as gypsum board, but often there is a radioactivity issue. Some phosphogypsum contains radium and emanates radon gas. At the present time, such waste can only be disposed in a landfill.

Clinkering of cement has its own environmental effects. Every ton of cement generates 2 ton of CO₂, one ton due to the limestone that is decomposed into calcium oxide and CO₂, and the other due to burning of fuel [16]. This gas releases to the environment and hence is not controlled. Thus, the choice is between land filling for phosphate ceramics and releasing CO₂ into the atmosphere without any control for cement.

REFERENCES

1. United Nations Environmental Program, *Wastes and waste management*, Environmental Data Report, Part 8, Washington, DC (1993–1994) pp. 329–333.
2. A. Wagh, S.Y. Jeong, and D. Singh, *High-Strength Phosphate Cement Using Industrial Byproduct Ashes*, eds. A. Azizinamini, D. Darwin, and C. French, Proceedings of the First International Conference on High Strength Concrete (American Society of Civil Engineers, Reston, VA, 1997), pp. 542–553.
3. A. Wagh and S. Jeong, “Chemically bonded phosphate ceramics. III. Reduction mechanism and its application to iron phosphate ceramics,” *J. Am. Ceram. Soc.*, **86** [11] (2003) 1850–1855.

4. D. Singh and A. Wagh, "A novel low-temperature ceramic binder for fabricating value-added products from ordinary wastes and stabilizing hazardous and radioactive wastes," *Mater. Technol.*, **12** [5/6] (1997) 143–157.
5. L. Lamarre, "Building from ash," *Electric Power Res. Inst. J.*, **April/May** (1994) 22–28.
6. American Association of State Highway Transportation Officials, *Laboratory evaluations of rapid set concrete patching materials*, Report 99 NTPEP 160, Washington, DC, 2000.
7. K.R. Anderson and G.C. Paffenbarger, "Properties of silicophosphate cements," *Dent. Prog.*, **2** (1962) 72–75.
8. D. Singh and A. Wagh, Phosphate bonded structural products from high volume wastes, US Patent No. 5,846,894, 1998.
9. M.J. Hess and S.K. Kawatra, "Environmental beneficiation of machining wastes. Part I. Materials characterization of machining swarf," *J. Air Waste Mgmt*, **49** (1999) 207–212.
10. S.K. Kawatra and M.J. Hess, "Environmental beneficiation of machining wastes. Part II. Measurement of the effects of moisture on the spontaneous heating of machining swarf," *J. Air Waste Mgmt*, **49** (1999) 477–481.
11. A. Wagh and V. Douse, "Silicate bonded unsintered ceramics of bayer process waste," *J. Mater. Res.*, **6** [5] (1991) 1094–1102.
12. M. Be'langer, "Red mud stacking," in *Light Metals*, ed. J. Angier (TMS Foundation, Warrendale, PA, 2001).
13. S. Jeong and A. Wagh, "Cementing the gap between ceramics, cements, and polymers," *Mater. Technol.*, **18** [3] (2003) 162–168.
14. BCS, Inc., *Energy and environmental profile of the US mining industry*, prepared for USDOE, 2002, pp. 8-10–8-15.
15. Florida Institute of Phosphate, *Proceedings of Phosphogypsum Fact-Finding Forum*, Research Publication No. 01-132-117, 1996.
16. Portland Cement Association *US Cement Industry Fact Sheet* (1990).

Chemically Bonded Phosphate Ceramic Borehole Sealant

Cementing operations in oil and gas wells place demanding requirements on cement properties. In spite of this challenge, the drilling and completion industry has relied exclusively on conventional portland cement with a few modifications for its cementing needs. The properties of portland cement and its modifications used in the oil industry are discussed in Chapter 3 of Ref. [1].

CBPCs could be used in many of the oil-field cementing needs, where conventional cements have limitations. Suitable CBPC formulations can be developed for wells, depending on their depth, to allow extended pumping time. CBPC slurry can be formulated for pumping in oil and natural gas wells in permafrost regions, geothermal wells with downhole temperatures $> 150^{\circ}\text{C}$ (300°F), or hot deep wells with downhole pressures $> 15,000$ psi (120 MPa). CBPCs can be formulated to provide sufficient pumping time for any of these temperature and pressure settings. When used as ceramic borehole sealants (CBS), they bond to earth materials and set rapidly under water (even in seawater). The slurry is smooth, has low viscosity, and can be pumped easily. It hardens into an impermeable barrier and can be an excellent seal to gas migration.

The worldwide cement composition is ≈ 1.6 billion metric tons per year [2], approximately 3% of which is consumed by the oil and natural gas industry. Thus, the annual cement consumption by this industry is ≈ 48 million metric tons. The industry, till now, has depended on modified portland cement, but there are niche areas where conventional cement is not reliable. Portland cement has several shortcomings for borehole sealant. It does not set easily in permafrost temperatures, because the water in it will freeze even before the cement sets. Its bonding to earth materials in the presence of oily surfaces is poor. Inherently porous, it cannot form a good seal. A major ingredient, calcium oxide, is affected by downhole gases such as carbon dioxide; as a result, cement performance can be poor. These problems can be overcome by a range of CBPC formulations because of their above-mentioned superior properties.

Besides borehole sealants for the oil industry, CBS may have other mining and civil engineering applications. These include reinforcement of mined out structures, water shut off, and underground and underwater construction, etc.

Argonne National Laboratory (ANL) and Brookhaven National Laboratory (BNL) have invested considerable efforts in developing CBS products. In collaboration with Halliburton Energy Services and Unocal Corp., BNL developed a product for use in geothermal wells called “ThermaLock.” In collaboration with Global Petroleum Research Institute (GPRI, a consortium of Exxon–Mobil, Chevron, BP-Amoco, and Shell), ANL focused on alternative oil well cements for the entire range of downhole temperature and pressure. This chapter provides a summary of key properties of CBS slurries and products resulting from the BNL and ANL efforts.

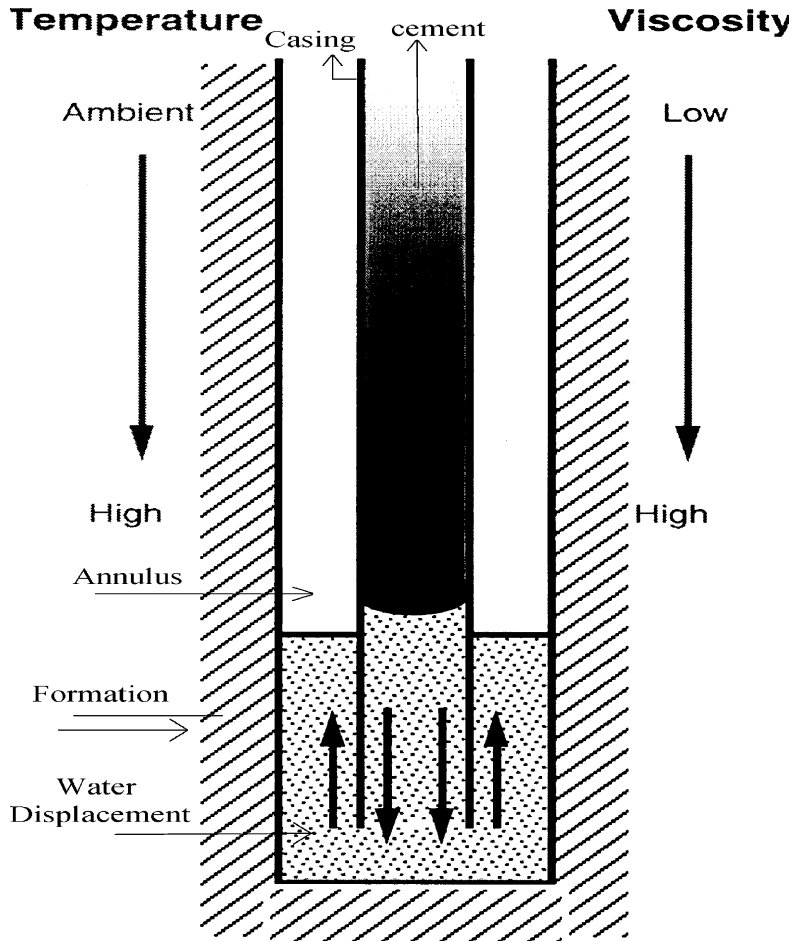
15.1.

PARAMETERS AFFECTING CBS SLURRY DESIGN

Drilling for oil and natural gas can be done in any region of the world: the permafrost region in the Arctic (e.g., in Northslope in Alaska), tropics and deserts where the surface temperature can be high $>80^{\circ}\text{F}$, or ocean beds in a saline environment. The downhole temperature depends also on the depth of a well. In most wells, it is $<250^{\circ}\text{F}$; only $<1\%$ of wells are hotter than that. Due to the water head, deeper wells have very high downhole pressure. Thus, there is a general correlation between the downhole temperature and pressure, except in geothermal wells, which are hot even at shallow depths. In general, CBPC materials for the borehole sealant application need to be designed for acceptable pumping time and setting temperature. In addition, unlike the CBPC slurries that set in air, CBS slurries have to set underwater in a borehole. This condition poses a design problem: the slurry, when pumped, must be sufficiently thick and particles in it must have developed sufficient cohesive forces between them so that the slurry does not disperse in water but displaces water through the annulus between the casing and the CBPC formation.

The main application of the cement in an oil well is to stabilize the casing in the borehole. The cement is pumped through the borehole and is pushed upwards through the annulus between the casing and the CBPC formation (see Fig. 15.1). The cement will be exposed to temperature and pressure gradients of the borehole. Therefore, the main parameters that affect the slurry design are downhole temperature and pressure, which vary according to the depth of the well. As the depth increases, the downhole temperature increases and reduces the thickening time of the cement. From a practical standpoint, it is necessary to retard the CBS slurry sufficiently to allow a typical pumping time of 3–5 h, and the slurry design must include retardants to reduce the dissolution rate of the oxide significantly. Alternatively, it is also possible to select oxides that exhibit good solubility at the elevated downhole temperatures but low solubility below that temperature. Such oxides will not dissolve during pumping at lower temperatures, but will dissolve once they experience the high static downhole temperature. Using the first approach, ANL developed Ceramicrete-based CBS slurries for most wells. Then using the second, ANL also developed aluminum-phosphate-based slurries for hot and deep wells.

Fig. 15.1.



Typical profile of an oil and gas well and pumping mode.

American Petroleum Institute (API) has developed standards for testing downhole cements that are described in API recommended practice 10 [3]. In API specifications (API Spec. 10), if one assumes an ambient temperature of 80 °F (25°C), then the depth dependence of the downhole temperature is approximately given by

$$T(\text{static}) = 80 + 0.015d. \tag{15.1}$$

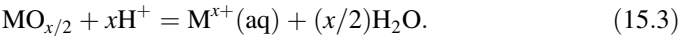
The temperature (T) is measured in Fahrenheit, and depth (d) in feet. This “static” temperature is that temperature, where the CBS will be placed and will set. The actual “circulating” temperature is considered to be the average of the downhole temperature and the surface temperature:

$$T(\text{circulating}) = 80 + 0.0075d. \tag{15.2}$$

Table 15.1 shows the ideal temperatures and pressures at varying depths used for testing candidate oil-well cements. As shown in Table 15.1, the temperature can be as high as 300 °F in deep wells (the temperature can reach 450 °F in geothermal wells). Also the pressures can be as high as 20,000 psi (140 MPa) in deep wells. In actual wells, the temperatures and pressures may vary according to the geographical location of the well, such as whether it is on- or off-shore, and the downhole conditions such as whether any low-pressure zones exist. While the profiles given in Table 15.1 are somewhat idealized, they are used by cement manufacturers and oil-field service companies to pretest cements in the laboratory, and they have become part of the API and International Standards Institute (ISI) procedures. These profiles are also very useful for cement manufacturers who are developing new formulations of oil-field cements.

As discussed in Chapters 4 and 5, CBPC formation is governed by the oxide solubility. The solubility, in turn, is related to the Gibbs free energy, which is a function of temperature and pressure. As a result, the CBS formulation depends on the downhole temperature and pressure. The effect of the temperature on the solubility has already been discussed in Section 6.4. The pressure effect can be assessed in a similar manner, but as we shall see, it is negligibly small and can be ignored for all practical purposes.

Consider a typical solubility equation of an oxide such as MgO or Al₂O₃ in the neutral region. For these metal oxides, where the metal valency is x , the solubility equation 5.3 is reproduced here:



The net change in the Gibbs free energy $\Delta G(T, P)$ in this reaction is given by

$$\Delta G(T, P) = \Delta G_f(T, P) - \Delta G_i(T, P), \quad (15.4)$$

where $\Delta G_f(T, P)$ and $\Delta G_i(T, P)$ are, respectively, the Gibbs free energies of the right-hand and left-hand side of Eq. 15.3, and T and P are the downhole temperature and pressure.

Table 15.1.

Ideal Temperature and Pressure Profiles in Oil Wells used in API Spec. 10 [3].

	Depth (ft)					
	1000	6500	9800	14,300	18,300	21,750
<i>Circulating temperature</i>						
in °F	80	120	150	200	250	300
in °C	25	49	66	93	121	149
<i>Static temperature</i>						
in °F	92	158	198	252	300	341
in °C	33	70	92	122	149	172
<i>Pressure</i>						
in psi	700	3850	6160	9655	13,285	16,650
in MPa	5	27	43	68	93	116

Expressing the right-hand side of Equation 15.4 in terms of the enthalpy ΔH and entropy ΔS , we obtain

$$\Delta G(T, P) = \Delta H_f(T, P) - \Delta H_i(T, P) - T[\Delta S_f(T) - \Delta S_i(T)]. \quad (15.5)$$

The subscripts in Eq. 15.5 have the same meaning as in Eq. 15.4. The entropy is an explicit function of T , while the enthalpy depends on both T and P . The explicit temperature dependence on ΔG has been discussed in Chapter 6 and used to study its effect on alumina solubility in Chapter 11. Here, because the downhole pressure is very high, we extend the discussion of dependence of ΔG on P .

When components of CBS slurry dissolve in water, their aqueous ions may have a different ionic size as compared to that in the unreacted crystal, and hence, the volume of the dissolved species may be different from that of the unreacted components. Thus, the total volume after dissolution V_f may be different from the total volume prior to dissolution V_0 . This volume change will occur against the downhole pressure, because the slurry components will be mixed during pumping and will dissolve when they are placed in downhole conditions. Thus, the change in enthalpy of an individual component is given by

$$\Delta H(T, P) = \Delta H_f(T, P) - \Delta H_i(T, P) = \Delta H_0 + \Delta C_p \Delta T + P_f \Delta V_f - P_0 \Delta V_0. \quad (15.6)$$

Equation 15.6 is a generalization of Eq. (6.15) and includes the pressure effects. ΔH_0 is the change in enthalpy if the dissolution were to take place at normal temperature, while the rest of the terms on the right-hand side of Eq. 15.6 correspond to the change in enthalpy when the dissolution occurs at downhole temperature and pressure.

If we assume in Eq. 15.6 that the volume change ΔV does not depend on the temperature and pressure, we can write $\Delta V_f = \Delta V_0$, and the last two terms on the right-hand side reduce to $(P_f - P_0)\Delta V_0$. Calculations from this equation, based on the ionic radii of the right-hand side and the molecular radii of the left-hand side (see Ref. [4] for these data) of Eq. 15.3, indicate that ΔV_0 is very small even at a high pressure difference $(P_f - P_0)$. Therefore, the pressure effects on the oxide solubility can be ignored, and the only variable one needs to consider while formulating the CBS slurry is the downhole temperature.

15.2.

CBS ENGINEERING PROPERTIES IN SIMULATED DOWNHOLE ENVIRONMENT

The CBS slurry must exhibit several pumping and setting characteristics to qualify for cementing oil and natural gas wells. These characteristics are given in API Spec. 10 [3] and include pumping time before the cement thickens at a given downhole temperature and pressure, slurry rheology, lost circulation, free water, gas permeability, and overall mechanical properties. Depending on the well conditions, there may be additional requirements such as heat of hydration for wells in the permafrost region, and durability of the cement against downhole gas environment. Each one of these characteristics is briefly described below. Consult Ref. [1] for details.

15.2.1. Pumping Characteristics

To pump cement slurry into a well and place it in the annulus between the casing and the formation, or at the desired depth, at least 3 h is required. Depending on the depth, even additional time may be needed. Therefore, the slurry should remain as low-viscosity fluid during that time and should harden rapidly when placed in the borehole. Operations on oil well platforms are expensive, and failures can be costly. For this reason, every cement composition is pretested in a laboratory before its use in the field to ensure its reliability.

Pretesting is done by using a consistometer (Fig. 15.2), in which the cement mixing slurry cup is placed in a bath of oil. The oil temperature and pressure can be raised or

Fig. 15.2.



Typical consistometer assembly.

lowered by controlled joule heating compression so that downhole temperature and pressure profiles can be generated.

In a typical consistometer, such as the one shown in Fig. 15.2, the temperature and pressures can be varied from ambient conditions to 400 °F (215°C) and 21,000 psi (147 MPa), but consistometers with higher temperatures and pressures are available. Freezing temperatures are simulated by connecting a chiller to the consistometer.

The slurry cup is fitted with a rotating vertical paddle. It rotates with a constant speed (150 rpm). The resistance on the paddle is measured by a pre-calibrated potentiometer. Consistency, which is a function of the nonlinear viscosity of the slurry, is measured in Bearden units (Bc). The downhole temperature and pressure and Bc are recorded by a chart recorder and also often on a computer.

Fully set cement is considered to have a consistency of 100 Bc. To avoid full setting of the cement and its bonding to the slurry cup and the paddle, the test is conducted only up to 70 Bc.

According to API Spec. 10, a Waring blender with only two speeds is used to blend the slurry. Water is added to the blender and then the cement powder is added in the first 15 s, after which the blender is run for 20 s at a slower speed. The blending is continued at the higher speed for the next 35 s so that the total time of this operation is above 1 min. The resulting slurry is transferred into the consistometer cup until this cup, with the paddle assembly in it, is completely filled. The cup is then closed and lowered into the pressure cell. The cell is sealed with a plug that allows insertion of a thermocouple into the axle of the paddle; otherwise, the entire assembly is sealed. The necessary pressure and temperature profiles are programmed as per the specifications given in Table 15.1. Satisfactory cement compositions are expected to attain 70 Bc in 3–5 h. The thickened slurry with this Bc is transferred to a curing chamber, which is maintained at the downhole temperature and pressure, and its hardening time is determined.

15.2.2. Slurry Rheology

For pumping ease, the initial Bc should be very low, preferably <30 Bc, which can be measured by the consistometer. The rheological behavior can be measured by means of a rotational viscometer, which consists of an outer sleeve and an inner drum, both rotating at different speeds. The outer sleeve is rotated at a constant speed, which causes a torque on the inner drum that can be measured on a dial. Starting from 600 rpm, the rotor speed is lowered successively at 20 s intervals, and the measurements of the torque are taken at the end of each period. Typically the speed is lowered in steps of 6 rpm, and the results are represented graphically.

15.2.3. Lost Circulation

If the formation has openings too large for the cement to plug them, much of the cement, pumped down the hole, may be lost. In such cases, it is necessary to first plug these openings by means of flash-setting cements. CBS formulations can be designed to flash set

at desired depths, because these are rapid-setting cements and may be tailored to set at a desired downhole temperature. Once they plug the large openings, the CBS formulations may be drilled through to open the borehole. In spite of the excellent potential of CBPC materials for this application, no systematic studies have been conducted on such sealants.

15.2.4. Free Water

The water in the slurry should be intimately mixed, and the solid particles in the slurry should not be segregated. For this reason, free water is measured immediately after the slurry is mixed in the blender and before it is placed in the slurry cup of the consistometer. It is poured in a graduated glass cylinder, and the cylinder is kept at an angle of 45° for 2 h. The free water standing above the slurry is then decanted and measured.

15.2.5. Permeability

Permeability is a measure of the amount of gas that will flow through the cement per unit area of its cross section per unit time. It is measured in darcies. One darcy is equal to the flow of 1 cm^3 per second of a fluid of 1 centipoise viscosity through an area of 1 cm^2 under a pressure gradient of 1 atmosphere per cm [5].

The permeability of the set sealant is measured by an API-recommended permeameter, which consists of a cylindrical sealant holder that is filled with the setting slurry. Once the slurry has set, the holder is fitted on a base. The base has an opening for gas connection, which can be attached to a nitrogen gas cylinder. Gas at different pressures is applied, and the pressure difference is measured by a mercury column. Knowing the pressure difference, the cross sectional area of the holder, and its length, one calculates the permeability in millidarcies. Details of such a permeameter and the procedure may be found in the API Spec. [3].

CBS formulations produce very dense cements, and as we shall see below, the permeability of hardened CBS is always an order of magnitude lower than that of conventional oil-well cements. This characteristic indicates that CBPCs make an excellent sealant against gas migration.

15.2.6. Heat of Hydration and Formation

By definition, heat of hydration is the heat generated during setting of the cement due to hydration. In the case of CBS, however, heat of hydration may not be an appropriate term, because CBS sets by acid–base reaction and not hydration. The most appropriate term would be heat of formation, which is the net change in the enthalpy during the reaction that is given out as heat.

The heat of formation may be measured with a calorimeter. The sealant slurry is poured in a well-insulated calorimeter fitted with a stirrer and a thermometer. The slurry is stirred constantly until it hardens and stirring is impossible. The temperature of the slurry is

monitored periodically to determine when the slurry reaches the maximum attainable temperature and starts cooling. Often, the CBS slurry continues to heat up even when it is hard and cannot be stirred. This is because the chemical reaction continues to occur between the particles, as do phase transformations within the reaction products. Knowing the maximum temperature, the slurry mass and its approximate specific heat, one can calculate the heat of formation.

15.2.7. Physical Properties

The compressive strength of the set sealant is measured with ASTM standard specimens of a ($2 \times 2 \times 2$ in.³) cube [6]. The slurry from the consistometer is poured in molds and is allowed to set in a curing chamber. It is then taken out after a desired period, and the strength is measured by applying a load on it in a uniaxial press. Knowing the total load and the area of the face on which the load is applied, one can calculate the compressive strength.

Unlike other applications of cements, a 500-psi (3.5 MPa) strength is considered to be adequate for downhole applications. This is because the major purpose of downhole cements is to hold the casing in place in a borehole. With a large surface area between the casing and the formation, the total bonding force is very large. In addition, the bond strength between the cement and the downhole rocks, such as limestone, shale, and dolomite, as well as between the cement and mild steel, should also be adequate so that good impermeable seals are formed.

15.2.8. Volume Change during Setting

If the cement shrinks during hardening, it will produce annular space between the casing and the formation, and that condition will destabilize the casing. It will also be a poor seal for prevention of lost circulation, water shut-off, or gas migration. For this reason, slight expansion of the cement while setting and hardening is desirable.

The extent of expansion or contraction of the sealant may be measured by determining the density difference between the slurry and the set sealant. As we shall see below, CBPCs are ideal for sealant application because they expand slightly during setting.

15.3.

CBS SLURRY DESIGNS

When the CBS slurry is pumped down a borehole and as it travels through the borehole, its temperature will increase with depth. The higher temperature will, in turn, increase the solubility of the oxide components in the slurry. If the solubility of the oxides becomes too high, the slurry may flash set within the borehole prematurely and clog it. To avoid this situation and to allow free flow of the slurry, one must control the solubility of the oxides. Alternatively, one may use components that have their maximum solubility only at the

downhole static temperature (and pressure), where the slurry is destined to be placed and does not excessively dissolve at the pumping temperatures. Equation 6.37 may be used to identify such slurry components for the desired downhole static temperature.

Using this logic, ANL and BNL scientists have developed a unique approach to develop novel slurry compositions [7,8]. It consists of the following steps:

- (a) The thermodynamic analysis and the solubility criterion given in Chapter 6 are used to identify suitable oxide or oxide minerals for a given well profile. The maximum solubility of the selected oxide or mineral should approximately lie in the dynamic temperature range of the well, and the actual reaction should occur near the static temperature.
- (b) An appropriate acid phosphate or phosphoric acid is then selected to react with the oxide or mineral that will form a ceramic at the selected temperature. The dissolution and setting reactions are confirmed by using differential thermal and thermogravimetric analyses (DTA, TGA) and differential scanning calorimetry (DSC).
- (c) The resulting ceramics are then tested at the selected pumping temperature in an oven. If needed, the reactions are retarded using boric acid to allow sufficient mixing (pumping) time.
- (d) The same formulations are then tested at the downhole temperatures and pressures for desired pumping and hardening time using the consistometer and a curing chamber.

Using this approach, ANL and BNL have identified slurry compositions for a range of depths and temperatures of relevant oil, gas, and geothermal wells. The pumping time and slurry compositions are presented in Table 15.2.

Because MgO has high solubility even at room temperature, Ceramicrete compositions are suitable for permafrost and shallow wells only. Boric acid is used to retard the reaction in these formulations. The amount of water used in these formulations is also higher than normally needed for the acid–base reaction. This excess water and a minimum amount of boric acid (0.125 wt% of the powder blend) are needed to reduce the initial Bc (or reduce the yield stress and the initial viscosity) of the slurry.

For permafrost well compositions, the binder content in the slurry is as high as 72.5 wt%, and the rest is wollastonite and boric acid. The high binder content provides sufficient KH_2PO_4 solution, which lowers the freezing point of the slurry and allows the acid–base aqueous reaction to continue. With low binder content, the water in the slurry freezes before it reacts. At ambient temperature, however, one may reduce the amount of binder and substitute it with suitable extenders. Wollastonite, because of its temperature of maximum solubility at 109 °F (43°C) is the preferred choice, but a combination of Class C and F ashes has also been used by researchers [9].

Figure 15.3 shows a typical time versus consistency graph for a permafrost-sealant test composition. The low initial Bc ensures a low yield stress and pumping viscosity. The increase in Bc is gradual, indicating slow dissolution of MgO and wollastonite in the solution. As the Bc increases, its rise to 70 is rapid, and the time versus Bc curve is almost vertical. Such behavior ensures that the slurry, once placed, will set rapidly.

Ceramicrete formulations with Class C fly ash are suitable for shallow wells. Though Class C fly ash reacts more rapidly due to its calcium content, it also responds favorably

Table 15.2.

CBPC Oil-Well Slurry Compositions Tested at ANL and BNL [7,9–10].

Well Conditions	Pumping, <i>T</i> (°F)	Slurry Components (g)	Pumping Time (h:min)
Permafrost and ambient	32 and 70	Ceramicrete binder (50–72.5) CaSiO ₃ (25–13.75) Class C fly ash (25–13.75) Boric acid (0.5–0.125) Water (37.5 ml)	5:30 and 4:40
Shallow	120–200	Ceramicrete binder (50–55) Class C fly ash (50–45) Boric acid (0.875–1.5) Water (29 ml)	5:10–3:40
Deep and geothermal	250–300	Calcined alumina (96.8) Aluminum hydroxide (2.2) Boric acid (0.97) 45% H ₃ PO ₄ solution (48.4 ml for 100 g of powder)	4:00–6:00
Geothermal	> 250	CaAl ₂ O ₄ (24) Sodium polyphosphate 40 Fly ash (36) Water sufficient	≈ 4:00

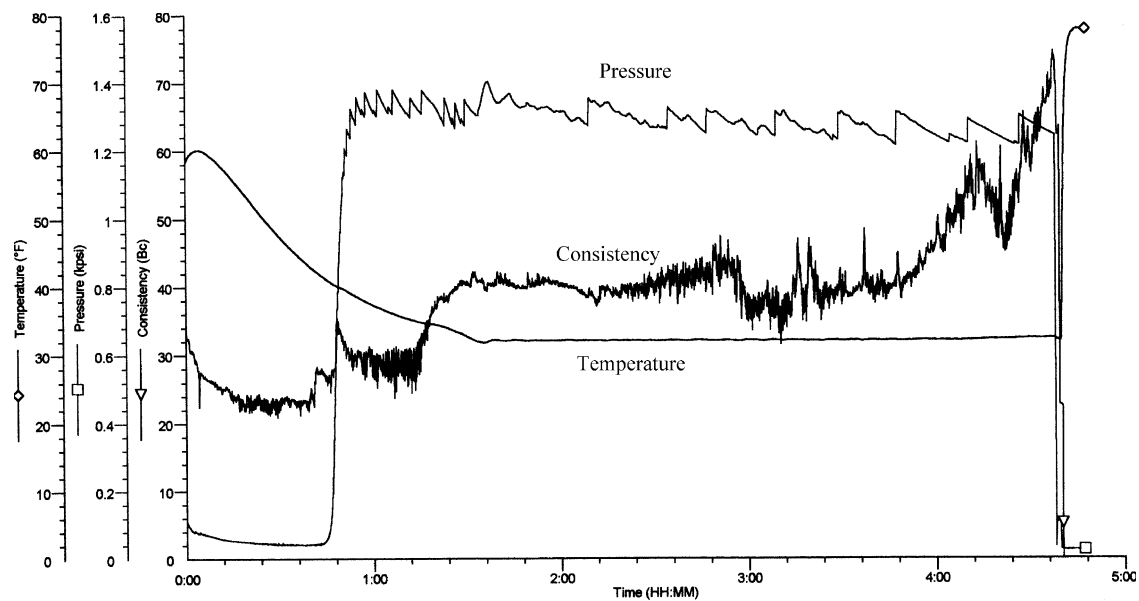
to boric acid, and the pumping time can be extended by increasing the boric acid content with temperature of the well. Wollastonite and Class F fly ash react too quickly at $T > 120^\circ\text{F}$ (43°C).

Studies have shown that boric acid is effective only up to 120°C (248°F). Increasing the boric acid content for wells with higher pumping temperature has little effect on the pumping time, but because of the initial retardation below this temperature, the pumping time can be extended somewhat.

Deep and geothermal wells are inherently hot and are well served by aluminum phosphate formulations (see Chapter 11). The dynamic temperature in these wells is 250°F (121°C) or higher, and the static temperature is $> 350^\circ\text{F}$ (235°C). For these wells, berlinite-based CBPC works well with its maximum solubility at 244°F (118°C) of alumina and phosphoric acid solution. As we have seen in Chapter 11, this reaction takes place at 302°F (150°C) that is in the range of the temperatures of deep and geothermal wells [7]. Even at these temperatures, the solubility of aluminum oxide is too low, but addition of a small amount of microcrystalline or amorphous aluminum hydroxide aids in increasing the soluble ions in the solution. With its large surface area, alumina provides the necessary solubility at the given downhole temperature.

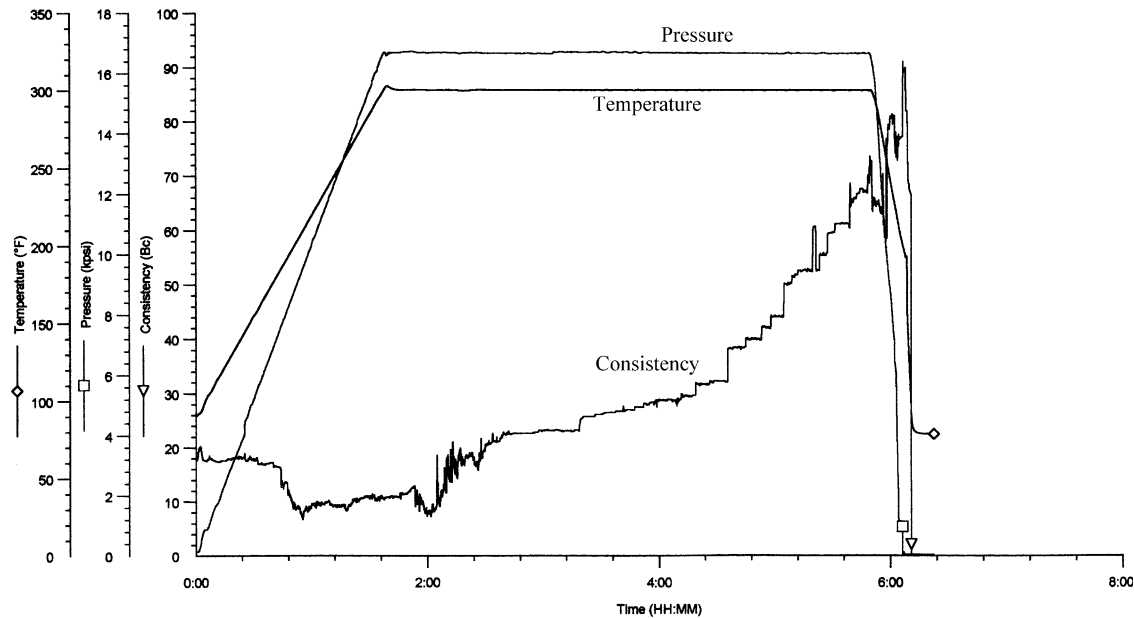
Figure 15.4 shows the time versus Bc curve for aluminum phosphate slurries for wells pumped at 300°F (200°C). The initial Bc is again very low, in fact, lower than that of magnesium-phosphate-based slurries. This initial low Bc is due to the formation of

Fig. 15.3.



Consistency versus time graph of Ceramcrete-based permafrost cement.

Fig. 15.4.



Time versus consistency graph of aluminum-phosphate-based deep well cement.

aluminum hydrophosphate [$\text{AlH}_3(\text{PO}_4)$] gel at lower temperatures. Thus, this gel provides a smooth slurry during pumping. Once placed, as we have seen in Chapter 11, the gel will react with additional alumina to form berlinite at the static temperature of 150°C (302°F). Thus, aluminum-phosphate-based slurries exhibit all the favorable characteristics of a deep well cement.

CBS formulations were investigated by Sugama and his group [10,11]. They developed phosphate cements that are suitable for geothermal wells, especially those with downhole temperature as high as 572°F (300°C) and with alkali carbonation. Under this environment, conventional portland cement is carbonated to form calcium bicarbonate that is soluble in water. The carbonation weakens the cement and also makes it porous. To overcome this difficulty, Sugama and his group tested two phosphate systems. The first one used the acid–base reaction between alumina and ammonium phosphate and cured it at high temperature [8]. This formulation was very similar to the aluminum-phosphate-based CBS developed at ANL and described above. Note that the BNL formulation used ammonium phosphate, while the ANL formulation contained phosphoric acid. The BNL formulation produced very porous and weak cement, and further development was not pursued. As the ANL work indicates, had the BNL researchers used phosphoric acid instead of ammonium phosphate, they would have probably developed a desired cement formulation that is stable in the carbonation downhole environment.

Sugama [10] pursued a different route to develop CBS for geothermal wells. Instead of orthophosphate as the acid component, they used sodium metaphosphate [$(\text{Na}_3\text{PO}_3)_n$, see Chapter 3 for the definition] and reacted it with a blend of 60 wt% Class F fly ash and 40 wt% calcium aluminate. The ratio of this blend and sodium metaphosphate solution was also 60 : 40. This approach is a major departure from all CBPC formulations that have been described in this book because metaphosphates themselves are inorganic polymers and appear to be ideal systems to produce cements that exhibit polymeric structures. These formulations, tested by Sugama *et al.*, gave a satisfactory thickening time of 4 h at 50°C (122°F) and produced cements that had a compressive strength of ≈ 5000 psi (34.86 MPa). In spite of having a high porosity of $\approx 30\%$, the cement strength was not affected by the curing environment of sodium carbonate solution to the same extent as conventional G-class portland cement. The authors attribute the resistance of this cement to a carbonation environment to the formation of hydroxyapatite and analcime ($\text{NaAlSi}_2\text{O}_6\text{H}_2\text{O}$) phases, which are not affected by a CO_2 environment; the formation of the latter phase was assisted by the Na_2CO_3 environment itself. Curing this cement for long periods converted the analcime phase into cancrinite [$\text{Na}_6\text{Ca}(\text{CO}_3)(\text{AlSiO}_4)\text{H}_2\text{O}$], and some of the CO_2 was captured in the mineral phase. However, such curing did not affect the strength of the cement, suggesting that this cement is very durable over a long period.

BNL, Halliburton Energy Services, and Unocal Corp. have developed cements suitable for geothermal wells with this formulation [11]. The brand name of this cement is “ThermaLock.” This cement was tested successfully in Unocal’s geothermal well in Sumatra, Indonesia, and its first use has been reported by Japan Petroleum Exploration Company for completion of geothermal wells in Kyushu, Japan.

The density of such cements is in the range of 15–17 lb per gallon. Such high-density cements tend to fracture the formations in geothermal wells in which the cement gets lost.

Recently, Halliburton Energy Services [12] developed a lightweight cement for such high temperature wells. A typical composition of this cement is 46 wt% Class F fly ash, 25 wt% calcium aluminate cement, 25 wt% sodium polyphosphate, 3 wt% alpha-olefinic sulfonate, and 1 wt% betaine. A gas is used to foam the cement sufficiently. Water is added to pump the slurry with ease. The inventors also used gluconic and citric acids successfully to extend the thickening time by more than 4 h. The density of the cement was reduced to 11.5–15 lb per gallon by using the organic additives described above.

15.4.

PROPERTIES OF CBS

In addition to their pumping characteristics, these cements should also satisfy several other conditions. For example, the permafrost phosphate sealant should be a good insulator; otherwise, the hot crude flowing through the pipe will melt the surrounding permafrost formation and destabilize the casing. The heat of formation of these sealants should be very low; otherwise, the heat generated during setting of the sealant may again thaw the permafrost formation. Sealants used in the gas hydrate region should exhibit very low permeability to the gas. The downhole gases should not affect the sealant performance. CBS has been suitably modified with additives to meet these requirements. These additives and the resulting properties along with the properties of conventional cements are listed in Table 15.3.

Table 15.3.

Comparison of Ceramicrete-based Permafrost and Conventional Portland Cement.

Property	Cement		Remarks
	Phosphate	Portland	
Density (g/cm^3)	1.7–1.9	2.4	CBS is lighter
Slurry density (g/cm^3)	1.5–1.7	1.8	CBS slurry is lighter and easier to pump
Open porosity (vol.%)	0.3	≈ 5	No pore fluids in CBS; therefore, stable in freeze-thaw cycles
Permeability (millidarcies)	0.004	≈ 0.1	CBS is impermeable
Room-temperature compressive strength (psi)	7000–8000	≈ 4000	High strength of CBS allows addition of cenospheres, etc., that improve thermal properties and reduce slurry weight
Thermal conductivity ($\text{W/m}\cdot\text{K}$)	0.27	0.53	CBS is a better insulator
Heat of fusion (J/cm^3)	347	514–640	Low heat of fusion ensures less thawing of permafrost region during CBS setting
Setting in hydrocarbon environment	Unaffected by CO_2	Flash-sets by carbonation	CBS is most useful in gas hydrate regions

15.4.1. General

As Table 15.3 indicates, CBS is lightweight cement in general, and its slurry is even lighter. As indicated in Table 14.2, the slurry density can be varied using suitable additives. For example, the density may be increased to $\approx 3 \text{ g}\cdot\text{cm}^{-3}$ by adding heavier minerals such as hematite; by adding cenospheres similarly, the density can be reduced to $< 1.5 \text{ g}\cdot\text{cm}^{-3}$. This composition allows one to produce slurries suitable to meet on-site pumping requirements and makes the sealant a versatile and user-friendly material. Such additions are feasible, because the strength of this CBS is high, and though these modifications lower the strength, the sealant still meets the 500 psi (3.5 MPa) strength requirement easily.

Adding cenospheres and Styrofoam up to 10 wt%, its thermal conductivity can be lowered to half that of conventional cement. When Ceramicrete-based permafrost sealant was cured in a CO_2 environment, it set well, and when stored in CO_2 for a week, it did not show any deterioration. Sugama and Carciello [8] predict that these sealants are durable up to 20 years in a downhole environment, compared to conventional cements that last for only a year. Unlike conventional cements, because CBS are neutral in pH and are not affected by downhole hydrocarbon gases, they are ideal for use in the gas hydrate regions in arctic climates.

As Table 15.3 indicates, the heat of formation of Ceramicrete-based permafrost cement is typically 50–60% of the heat of formation of conventional cement. Even though the acid–base reaction is highly exothermic, i.e., it releases a significant amount of heat during setting. In CBS compositions, the binder that produces heat is only a part of the entire CBS formulation, and the remaining components are extenders. Thus, the net amount of heat generated is about half that in the equivalent amount of conventional cement.

Once set, CBS exhibits negligibly small open porosity, making the sealant an impermeable barrier to gas migration. This is evident from the very low permeability of $\approx 0.004 \text{ md}$ (Table 15.3). Because it is pore free, CBS is also stable during freeze-thaw cycles. ASTM standard size cubes ($2 \times 2 \times 2 \text{ in.}^3$) of this cement were cured for one week, and then immersed in liquid nitrogen for 15 min. The results indicated no structural damage even when the procedure was repeated 15 times, while cubes of conventional cement cracked into large chunks in the first cycle. In another test, a small cup of 10 cm wall thickness and $\approx 100 \text{ ml}$ volume was made with the same composition. Liquid nitrogen was poured in it, and even after several minutes, one could hold the cup in bare hands without feeling the frost. This result shows that the phosphate-based permafrost cement is not only durable, but also a good insulating dewar for storage of cryogenic fluids, as discussed in Chapter 14.

15.4.2. Bond Strength

For the downhole cement to be effective, the bond between the cement and the casing steel as well as downhole rocks should be good. Wagh *et al.* [9] evaluated the Ceramicrete formulations given in Table 15.2 for bond strength. They used pipe sections made of mild steel API 5L for bond strength tests with the casing steel. The sections had an internal

diameter of 1.6 and 1 in. length. Three specimens each were filled with sealant slurry having deep and shallow well formulations. Some were cured in hot water, and some in air at ambient temperature. After curing for four days, the former were taken out from water, and cured in air along with the rest of the air-cured samples. After three days of drying in air, the specimens were subject to the bond strength test. In this test, one empty cylinder was placed coaxially below the specimen, and the set sealant was pushed in a compressive mode by an Instron machine. Even when a vertical stress of 10,000 psi (70 MPa) was applied, none of the sealants could be dislodged. This observation shows that the bond between the casing steel and the sealant is exceptionally strong.

Similar tests were also conducted with cylindrical rock core samples extracted from an oil well having diameters of 1.4–1.5 in. These rocks were cut at an angle 45° to the axis of the cylinder, and the slurry was sandwiched between them on the slanted surface. The bonded samples were cured at a downhole temperature of 170 °F under water in a consistometer cell. The bonding in sandstone and limestone was good, but poor in dolomite. In general, sandstone and limestones are porous, but dolomite is very dense. The cut surfaces of sandstone and limestone were rough, but the dolomite surface was very smooth. The bonding of the sealant with a porous object is good because the sealant enters the pores and adheres to the object, but no pores are available for bonding in dense dolomite. Because the downhole rock surfaces will not be as smooth as the dolomite specimen cut in the laboratory, bonding should be good with downhole rocks in general.

15.4.3. Extent of Expansion During Setting

Both shallow and deep well compositions underwent slight expansion during setting. The extent of this expansion may be evaluated from the densities of the slurries and hardened sealants (see Table 5.4). The difference in slurry and the sealant densities yields 1.57 vol% expansion for the shallow well and 2.61 vol% for the deep well compositions. This slight expansion in each case makes CBS excellent sealants because, during setting, the sealant will expand and fill any gap between rocks and casing and form an excellent plug (Table 15.4).

This expansion during setting is likely to be due to air trapped during rapid hardening. During mixing and pumping, air is mixed in the slurry and some of it dissolves in the slurry

Table 15.4.

Densities of the Ceramicrete Slurry and the Set Sealant.

Units	Slurry		Sealant	
	Shallow Well	Deep Well	Shallow Well	Deep Well
g/cm ³	1.91	1.91	1.88	1.86
lb/ft ³	119.3	119.3	117.4	116.2
%Expansion			1.57	2.61

and vaporizes during the setting reaction. It forms isolated micropores within the set sealant. The pores increase the total volume and cause the expansion.

15.5.

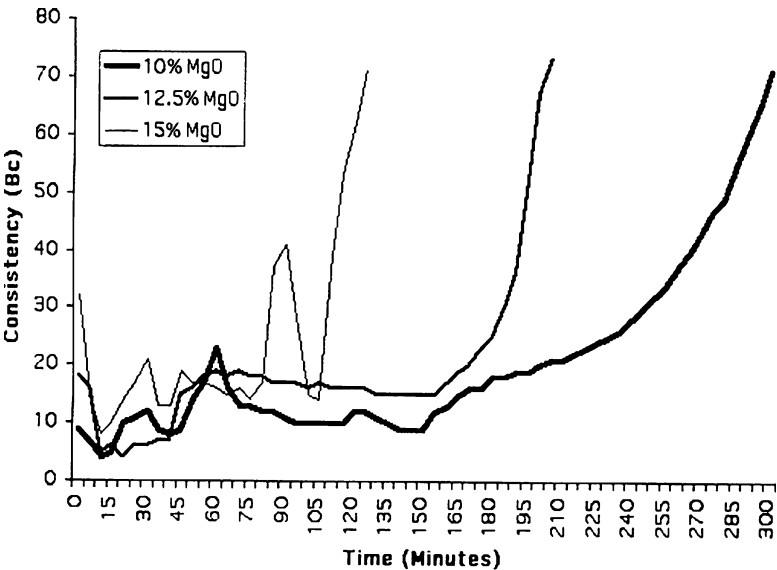
**EFFECT OF INDIVIDUAL COMPONENTS
ON SLURRY BEHAVIOR**

The pumping characteristics discussed above were measured in a controlled laboratory environment. In a field application, the mixing of the powders may not occur exactly as tested in the laboratory. In an offshore well, for example, the water may be saline. Setting of the slurry may need to be slowed down or accelerated during pumping. Such variations can be made by marginally varying the composition. The following addresses the versatility of the CBS to needs in the field.

15.5.1. Effect of Excess Oxides

The pumping time is very sensitive to MgO content in the Ceramicrete slurry. A slight increase in MgO accelerates the acid–base reaction, and the slurry sets faster. Figure 15.5 shows the effect of excess MgO on the pumping time at 200 °F (93°C). Excess MgO provides additional surface area for dissolution. It also provides additional nucleation sites

Fig. 15.5.



Effect of excess MgO on pumping time for a well at 200 °F.

Table 15.5.

Composition of the Simulated Seawater.

Component	Amount
Deionized water	5 l
NaCl	77.76 g
MgCl ₂	10.88 g
MgSO ₄	4.74 g
CaSO ₄	3.6 g
K ₂ SO ₄	2.46 g
MgBr ₂	0.22 g
CaCO ₃	0.34 g

during formation of the ceramic. As a result, dissolution and formation of the ceramic are rapid, and the pumping time is reduced significantly, even with a 10% increase in MgO content.

Alumina-based slurries behave similarly. A small increase in the aluminum hydroxide content will reduce the pumping time significantly.

In general, the same compositions used for onshore wells also work for the offshore wells. Saline water retards the setting rate, and longer pumping time is available for the same CBS formulation in offshore wells compared with onshore wells. In addition, because the saline water contains dissolved solids, one needs to add more water in the slurry to obtain the same low initial Bc. Results of the pumping time versus temperature are shown in Table 15.6 for formulations that are similar to those given in Table 15.5.

15.5.2. Effect of Saline Water in Offshore Wells

Wagh *et al.* [9] tested their Ceramicrete formulation for offshore wells by using simulated seawater. The composition of this water is given in Table 15.5, and the results are presented in Table 15.6.

Table 15.6.

Pumping Time for Offshore Well Formulations.

Temperature (°F)	MgO (g)	C Ash (g)	F Ash (g)	Saline H ₂ O (ml)	Boric Acid (g)	Setting Time (h:min)
80	100	200	200	240	4	>6
120	120	200	200	250	4	5:50
150	100	200	200	205	16	7:00
250	120	380	00	225	12	>6

15.6.

CONCLUSIONS

The ANL and BNL studies show that CBS has excellent potential in borehole applications. Except for the ThermaLock formulations, however, CBSs have not been field-tested. Nonetheless, because these cements were tested according to API procedures and have shown excellent results, one may conclude that they are more than likely to succeed in these applications.

REFERENCES

- 1 D.K. Smith, *Cementing*, Monograph, vol. 4. (Society of Petroleum Engineers, 1990), 254pp.
- 2 US Geological Survey, *Mineral Commodities Summaries*, (2002), pp. 43–44.
- 3 American Petroleum Institute, *Recommended Practice for Testing Oil Well Cements and Cement Additives*, API RP, 10, (1984).
- 4 N. Alcock, *Bonding and Structure*, (Ellis Hardwood, New York, 1990), pp. 315–317.
- 5 *McGraw Hill Dictionary of Physics*, ed. S. Parker (1985), p. 125.
- 6 American Society for Testing of Materials, *Standard test for compressive strength of hydraulic cement mortars*, C109/C109M-02, (2003).
- 7 A.S. Wagh, S. Jeong, and R. McDaniel, Chemically bonded phosphate ceramic sealant formulations for oil field applications, Argonne National Laboratory, Patent applied for.
- 8 T. Sugama and N. Carciello, “Hydrothermally synthesized aluminum phosphate cements,” *Adv. Cem. Res.*, **5** [17] (1993) 31–40.
- 9 A.S. Wagh, *Chemically bonded phosphate ceramic borehole sealants*, *Final Report to Global Petroleum Research Institute*, Argonne National Laboratory, Unpublished, 2002.
- 10 T. Sugama, “Hot alkali carbonation of sodium metaphosphate modified fly ash/calcium aluminate blend hydrothermal cements,” *Cem. Concr. Res.*, **26** [11] (1996) 1661–1672.
- 11 Brookhaven National Laboratory, News Release No. 00-56, August 2000.
- 12 L. Brothers, D. Brenneis, D. Chad, and J. Childs, Lightweight high temperature well cement compositions and methods, US Patent no. 5,900,053, granted to Halliburton Energy Services, Inc., 1999.

Applications of CBPCs to Hazardous Waste Stabilization

The ever-increasing production of waste is a direct result of increasing world population, and its appetite for a better life. Finding a suitable disposal strategy, one that will avoid contamination of air, water, and land, is essential. For a detailed discussion on types of wastes, including their production statistics, the reader is referred to Ref. [1]. These waste streams are produced by individual households, utilities, and a wide range of industries, including petrochemical and other chemical, medical and pharmaceutical, and electronics. Much of the waste is simply wastewater that is treated and recycled. A large amount is organic waste that is also either treated or destroyed. The inorganic waste, however, needs a case-by-case disposal strategy, and phosphate treatment plays a major role in disposal of these waste streams.

The waste streams may be disposed safely if they do not contain contaminants that are harmful to living beings. Several waste streams, however, contain harmful chemicals that enter the human body through the food chain via soil or water or the air that we breathe. These contaminants may be toxic chemicals or radioactive. The former is referred to as “hazardous”, and the latter as “radioactive”. Both need treatment to isolate the contaminants from the groundwater, air, and soil prior to disposal. Treatment of hazardous waste streams is the subject of this chapter, while treatment of radioactive wastes, or those containing both hazardous and radioactive contaminants (“mixed” wastes), is discussed in Chapter 17.

In most waste streams, either hazardous or radioactive, only a small amount of harmful contaminants is found in a large volume of otherwise harmless waste, and the treatment is aimed at reduction of the effect of these contaminants on the environment. Possible treatments include separation and recycling of the contaminants, destruction of the waste, and if these methods fail, isolation of the entire waste volume and disposal or safe storage. The decontamination and recycling of waste is a good strategy, provided it is economical. Where recycling is not economical, destruction of the wastes takes precedence over any

other remediation technology [2,3]. Typically, destruction involves incineration or some other chemical destruction method. This treatment produces secondary waste streams with reduced volume, such as ash or secondary waste chemicals. The concentration of contaminations in these secondary waste streams is higher than that of the original waste. Applying destructive methods to secondary waste, such as incineration, produces harmful gases that carry some of the contaminants and contaminate air. Thus, destruction is not always a good option. Also, decontamination technologies are not available for certain waste streams. In such cases, the waste must be treated so that the contaminants are isolated within the waste stream and cannot be released into the environment and, thereby, into the food cycle upon disposal. The waste treated in this way is called the “waste form”, and the treatment methods are grouped under the name “stabilization and solidification”. While there is some ambiguity as to the exact definition of this term, we will use the definition given by Conner [3]:

Stabilization is the process used for reduction of hazard potential of the waste by converting the contaminants into their least soluble, least immobile, or least toxic form. Other characteristics of the waste may not change in this treatment.

Solidification, on the other hand, physically binds or encapsulates the waste in a monolithic solid of high structural integrity. Thus, solidification may be of sludge, and liquids.

Stabilization processes chemically convert the contaminants into their least soluble form so that they do not dissolve in groundwater and, hence, are not dispersible. In addition, these processes may convert the contaminants into a nontoxic form so that they do not contaminate soil and air. By converting a powder into a monolithic solid of high structural integrity, solidification eliminates free liquid, increases load-bearing strength, and decreases the surface area of the waste materials that will come in contact with groundwater or soil.

Stabilization and solidification of waste streams (sludges, liquids, and powders) is needed during transportation as well as disposal. Transportation of the waste requires that the waste be packaged according to the regulations set by the Department of Transportation (DOT) or a similar authority in each state, so that the waste is not amenable to spillage, leakage, or release to the atmosphere during transportation and interim storage. In addition, proper disposal of the waste requires a stabilization procedure in which the waste form meets certain requirements to ensure that no release of the contaminants to soil, air, or groundwater will occur. Thus, while stabilization addresses chemical immobilization of individual contaminants, solidification is aimed at consolidating sludge, liquids, and powders into a solid form so that such waste streams are not dispersible during transportation, long-term storage, or disposal.

Waste may be stabilized or solidified by either thermal or nonthermal treatments. Thermal treatments are ideal for destruction of organic contaminants. They reduce the volume of the waste and, hence, disposal costs. They are, however, energy intensive and more expensive than nonthermal methods, and release volatile elements that need to be contained. If the waste stream contains inorganic contaminants, the residue left after the thermal treatment is often more concentrated in these contaminants because they cannot be destroyed by such treatment. They also contaminate equipment such as furnaces and filters used during the treatment, which also ultimately need proper disposal. Thus, there is

a trade-off between the high treatment cost and savings in the disposal cost due to volume reduction. In addition, because the secondary waste streams resulting from the thermal treatment also need to be stabilized for proper disposal, thermal destruction is not a final step for waste streams containing inorganic contaminants.

The typical approach to nonthermal stabilization for waste streams containing inorganic contaminants is chemical immobilization. In this approach, low-cost stabilizing chemicals are added to the waste stream, and contaminants are chemically treated to render them harmless. Such a treatment, if conducted at ambient temperature, is ideal for handling high waste volumes at low cost, provided the waste volume is not increased excessively during the treatment (higher volume may raise the transportation and disposal costs). Thus, the major constraint for nonthermal treatment is that the waste volume increase be kept to a minimum.

Inorganic contaminants are immobilized by “washing” the waste with soluble phosphates. This treatment uses a very small amount of phosphate, does not change other characteristics of the waste such as its granular nature or volume, and is relatively inexpensive. If the waste contains radioactive contaminants, phosphate washing is not sufficient because the dispersibility of the radioactive contaminant powders needs to be reduced, and hence, the waste needs to be solidified. Solidification requires generating phosphate ceramics of the waste in the form of a CBPC. In the case of radioactive waste, both stabilization and solidification are needed because they not only immobilize the contaminants, but also solidify the entire waste. As we will see in this and the next chapter, whether phosphate treatment is used only for stabilization or for both stabilization and solidification, it is very effective for a wide range of waste streams.

16.1.

TEST CRITERION FOR STABILIZATION

Based on toxicological studies, the US Environmental Protection Agency (EPA) has determined that, in addition to a large number of organic chemicals, the following metals are hazardous and need effective stabilization prior to disposal:

Cr, Ni, Zn, As, Ag, Cd, Ba, Hg, Pb

These metals are considered hazardous under the Resource Recovery and Conservation Act of 1987 (RCRA) [4]. The RCRA metals occur in chemical forms that are soluble or insoluble in groundwater. The soluble species are of concern from the dispersibility viewpoint. Hence, the test criterion to evaluate whether a given waste stream needs stabilization prior to disposal is based on how much a given hazardous metal dissolves in water in a standardized test. This EPA test, called the Toxicity Characteristic Leaching Procedure (TCLP) [5], is used not only to identify which waste streams need treatment, but also to assess whether the treated waste form is suitable for disposal. This test also sets limits on how little of a hazardous metal is permitted to leach out from a given waste to pass the waste for disposal. If the test determines that the waste is not suitable for safe

disposal and needs stabilization, then the same test is also used to decide whether the treatment has succeeded in stabilizing the metal.

In the TCLP, solid waste is crushed into powder, and the particles are passed through a screen of 0.95 cm mesh. The resulting surface area is $3.1 \text{ cm}^2/\text{g}$. Leaching is carried out with an extraction fluid prepared by adding an acid to deionized water and adjusting the pH of the solution to a desired value. Because CBPCs are either neutral or alkaline, the extraction fluid must have a pH of 2.8. This pH is obtained by adding hydrochloric acid and/or acetic acid. A volume of 20 times that of the weight of the powder is used, and extraction is done for 18 h by tumbling the mixture of powder and fluid in a vessel of glass or polyethylene. The fluid is then filtered and analyzed for the hazardous contaminants. The same procedure is also followed for stabilized and crushed waste forms.

Table 16.1 provides the maximum allowable limits to determine whether the waste needs prior treatment and if it is treated, whether the treatment is successful or not. The allowable limit is called the RCRA limit for the former and the Universal Treatment Standard (UTS) for the latter. Details of this test may be found in Ref. [5].

This test is the key to success of any stabilization method for treatment of hazardous waste. Because the waste is crushed and leached using acidic water, the actual leaching of the contaminants depends on their solubility. Thus, as in the case of CBPC formation discussed in Chapters 4–6, solution chemistry plays a major role in stabilization. For this reason, we review the solution chemistry of the hazardous contaminants before we proceed to the actual stabilization.

16.2.

CHEMICAL KINETICS OF STABILIZATION

Since water-soluble contaminants will easily leach into the groundwater and enter the food chain, reduction of their leaching is the most important issue during waste stabilization. It is essential that the contaminants be first converted into their most insoluble form by

Table 16.1.

Limits on Leaching (mg/l) as the Disposal Criteria in the TCLP Test.

Hazardous Metal	Oxidation State	RCRA Limit	UTS Limit
Ag	1	5	0.14
As	3, 5	5	–
Ba	2	100	–
Cd	2	1	0.11
Cr	2, 3, 6	5	0.6
Hg	1, 2	0.2	0.025
Ni	2, 3	7	11
Pb	2, 4	5	0.75
Zn	2	–	4.3

chemical treatment of the waste. The solubility of the converted contaminants must be very low in groundwater, whether it is slightly acidic (acid rain conditions), basic (limestone areas), or mostly neutral. The treated waste should also be insoluble in saline and carbonate water that represents some typical groundwater. These requirements imply that reduction of solubility of the contaminants is the most important stabilization factor. As we shall see, conversion of the contaminants into their phosphate forms renders them into insoluble and nonleachable forms. Therefore, CBPC technology offers one of the most effective ways of treating hazardous waste.

Oxides and hydroxides are the most common components of hazardous waste streams. This is partially because major industrial waste streams are utility and municipal solid waste (MSW) ash, mining waste, or some stream that has been exposed to air over a long time during storage, in which metal components are rusted and oxides are formed. Generally, inorganic contaminants occur in waste streams as metal salts or sparsely soluble oxides or hydroxides. When acidic or alkaline wastewater is treated for safe disposal, it is neutralized by a base or an acid. This step results in formation of salts, such as chlorides, sulfates, and nitrates of most metals, including hazardous ones. Several waste streams, such as ash from utility plants or ash produced by incineration of MSW, also contain carbonates that result from long exposure of the resulting ash to atmospheric carbon dioxide. Table 16.2 assesses the general solubility behavior of salts, oxides, and hydroxides of hazardous metals. With few exceptions, chlorides and nitrates are highly soluble. Carbonates often decompose during stabilization with acid phosphates. The resulting product is an oxide or a hydroxide with evolution of carbon dioxide. Sulfates are either soluble or sparsely soluble. Silicates are insoluble.

To evaluate the leaching performance of the waste streams, we assume that soluble and sparsely soluble compounds will leach out and fail the TCLP and, hence, should be target contaminants for stabilization. These soluble or sparsely soluble components may directly be treated with phosphates and converted to their insoluble, nonleachable forms. The literature is full of studies on stabilization of such divalent hazardous metal contaminants (Pb, Cd, and Zn, in particular), where treatment with various phosphates has been effective. These studies are summarized in Section 16.3.

Table 16.2.

Solubility of Compounds Formed with Hazardous Metals.

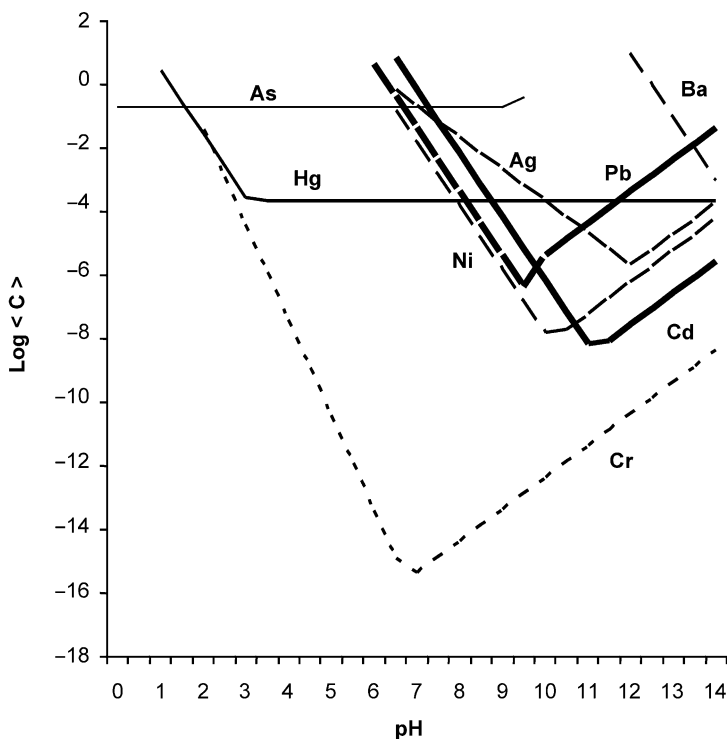
Compound	Solubility
Nitrates	All are soluble
Chlorides	All are soluble, except AgCl and Hg_2Cl_2 are insoluble
Hydroxides	All are sparsely soluble, except $\text{Ba}(\text{OH})_2$ and AgOH , which are moderately soluble
Sulfates	Sulfates of Cd, Ni, and Zn are soluble. Others are sparsely soluble. Hydrosulfates are more soluble than sulfates
Carbonates	Generally, carbonates decompose upon treatment with an acid phosphate
Silicates, phosphates	All are insoluble
Arsenates	Insoluble
Chromates	Soluble or sparsely soluble

The RCRA metals Pb, Ni, Cr, and As can also occur in higher oxidation states. Among these, Pb and Ni are found only in the divalent state in waste streams unless the stream is in a highly oxidizing environment, which is rare. For all practical purposes, one may assume that these two elements will remain in the divalent state in any waste stream. On the other hand, Cr and As are not only found as Cr and As oxides (Cr_2O_3 and As_2O_3), but as chromates and arsenates (Cr_3O_4^- and AsO_4^{3-}). As_2O_3 is sparsely soluble, but arsenates are insoluble, while Cr_2O_3 as well as chromates are sparsely soluble or fully soluble. Thus, the leaching behavior of each of these oxides needs to be considered individually in a given waste stream.

Soluble salts are stabilized mainly as silicates and phosphates. Conversion of contaminants into silicates requires a high-temperature treatment and is the basic approach behind vitrification [6] of difficult contaminants such as radioactive isotopes. This approach is not economical for stabilization of high-volume hazardous waste streams. Conventional cement converts the contaminants into hydroxides and reduces their solubility [3,7] and has shown good success in stabilizing several waste streams containing contaminants such as Pb and Cd. For large-scale stabilization, this process is economical and hence is used very widely. Nonetheless, since hydroxides are only sparsely soluble, cement stabilization is not a very rugged process, because hydroxides are only sparsely soluble and not insoluble like silicates and phosphates. The process is dependent on the pH of the waste because cement is very alkaline and does not set in an acidic environment. The waste loading possible with such a process is low. For these reasons, a better stabilization approach is needed. Phosphate treatment, because it can be carried out at room temperature in a simple washing process, is becoming more popular, as indicated by the large amount of literature that has sprung up in the last 10 years. This literature is reviewed in Section 16.3.

Because oxides and hydroxides of hazardous contaminants are the most common components of hazardous waste streams, we will focus on their behavior during stabilization. In this context, the role of the solution chemistry of oxides and acid phosphates in the formation of CBPCs, discussed in Chapters 4 and 5, is equally applicable to the stabilization of hazardous metals. When hazardous metal oxides or salts dissolve in a phosphate solution, as in the case of CBPC formation, insoluble phosphates of the hazardous contaminants are formed by acid–base reaction, and their leaching is arrested. Figure 16.1 shows the pH behavior related to the solubility of oxides of the RCRA metals. This figure has been drawn in accord with the approach described in Chapter 4. Most of these oxides exhibit amphoteric behavior, i.e., their solubility is high in both acidic and alkaline solution and has a minimum in between. Thus, with acid phosphate treatment, their solubility will increase, and they will readily react with the acid phosphate to form a neutral phosphate salt. The oxides or hydroxides are mostly alkaline, and the phosphate treatment initiates an acid–base reaction similar to the one discussed in the previous chapters. This reaction leads to formation of neutral phosphates that are insoluble in groundwater. Therefore, as in formation of the CBPC matrix, one takes advantage of the high solubility of the contaminants at lower pH to immobilize them into their insoluble phosphate form. A better insight into the aqueous leaching behavior of hazardous contaminants as well as into their stabilization kinetics may be gained from the following observations made from Fig. 16.1:

Fig. 16.1.



Dependence of solubility of hazardous metals on pH.

1. The solubility of each of the metal oxides/hydroxides, except those of Hg and As, has a minimum in the alkaline region and increases sharply when the pH is increased or lowered (note the logarithmic scale of the solubility). This implies that (a) these metals may leach in neutral or acidic groundwater, and (b) most of these metals are available in a soluble form for stabilization treatment in acid phosphates.
2. The minimum solubility of the major contaminants that are common in most waste streams decreases in the following order:

$$\text{Pb} > \text{Ag} > \text{Zn} > \text{Cd} > \text{Ni}$$

The metals Zn, Ag, Cd, and Ba have nearly the same minimum, though at different pH. In addition, Ag has a very high solubility and does not have a minimum within the pH range under consideration. Furthermore, the increase in the logarithm of the metal ion concentration in each case is linear on both sides of the minimum. Also, these lines are parallel for all these metals. As a result, the solubility of the various metal oxide/hydroxides at any pH will be in the same order as given above, and the same order will also follow in groundwater.

3. Both Pb and Zn will readily stabilize compared to the other three metals. Investigations by Bishop [7], in fact, conclude that Pb readily complexes with the cement matrix (alkaline environment) as compared to Cd. Later, we shall see that this is also true with phosphate treatment.
4. The solubility of Hg is not as low as that of the other common hazardous contaminants given above, but the minimum solubility curve remains high over a wide range of pH (3–14). Thus, Hg is readily available for stabilization by the CBPC treatment. In spite of this, as discussed later, because the regulatory limit for Hg leaching from the stabilized product is so low, even phosphate stabilization of Hg is not good enough. Additional sulfide stabilization is necessary prior to physical encapsulation of Hg by the phosphate matrix. To these observations, one may also add the following:
5. Chromate in a higher oxidation state, i.e., Cr^{6+} , is more soluble than its counterpart Cr_2O_3 in lower oxidation state Cr^{3+} . Again, this metal needs to be first reduced to its lower oxidation states and then stabilized using a phosphate treatment.
6. Arsenates have very low solubility, but As_2O_3 is sparsely soluble. Like HgO , its solubility in the entire acidic range is almost constant and relatively high. Because of its higher solubility, phosphate treatment should be able to stabilize this compound. However, because other arsenates are nearly insoluble, they can be encapsulated in the phosphate matrix and will not be available for leaching.

These observations imply that chemical immobilization of oxides of Pb, Cd, Zn, Ba, Ni, and As may be achieved by direct transformation into phosphates, while Cr and Hg will require some pretreatment with sulfides.

16.3.

GENERAL APPROACH TO PHOSPHATE STABILIZATION

The overall phosphate stabilization of hazardous waste streams may be put in two categories: simple phosphate washing to stabilize most of the contaminants and actual formation of a CBPC waste to treat more difficult contaminants. These two approaches are described below.

16.3.1. Stabilization by Phosphate Washing

Most hazardous waste streams contain contaminants (Pb, Cd, Ni, and Zn) that can be treated by contacting with a phosphate solution. This treatment entails simply washing the waste stream with a phosphate solution. The amount of phosphate stabilizer is small (5 wt%). At the end of the treatment, the waste stream retains its free-flowing characteristics and hence is easy to load on a truck, or to pump at a disposal site. Because the waste volume does not increase due to this treatment, disposal cost is low. Furthermore, the binder cost is also kept to a minimum.

Phosphate washing has been in use for many years. Over a decade ago, Wheelabrator Technologies [8,9] patented a process to treat waste incineration residue ashes from

municipal sewage with very dilute solution of phosphoric acid or acid phosphates. This process is employed to treat ash from waste-to-energy facilities in the US. The target hazardous metals (Pb and Cd) are converted to insoluble hydrophosphates or phosphates such that the treated ash passes the TCLP.

Over the last decade, extensive research has been conducted on conversion of hazardous metals from different waste streams using phosphate stabilizers. Eighmy and Eusden [10] searched the literature on phosphate amendment of various industrial waste streams. They found 39 patents in this area since 1994. An updated summary of the various waste streams, either treated or tested by phosphate amendment or solidification, is given in Table 16.3.

In addition to phosphoric acid, other acid phosphates have been used as a source of phosphate [8,9,21,22,30,31]. These include triple super phosphate [22,34], diammonium phosphate [22], and sodium dihydrogen phosphate [27]. These phosphates dissolve in water, release H_2PO_4^- ions, and drive the pH of the solution to the acidic side. The chemical compounds of Pb, Cd, and Zn dissolve in the acidic solution and react with H_2PO_4^- ions to form stable phosphates.

Many investigators have reported use of hydroxyapatite for stabilizing Pb [20,40, 46–54]. Among these extensive studies, the work of Zang *et al.* [47] reports on pH-dependent experiments to study the kinetics of stabilization. These investigators treated Pb carbonate (cerussite) with hydroxyapatite and found that both cerussite and hydroxyapatite dissolved in the solution at low pH, and a less-soluble chloropyromorphite [$\text{Pb}_5(\text{PO}_4)_3\text{Cl}$] precipitated, leading to pH stabilization. The following dissolution reactions were responsible for this precipitation:

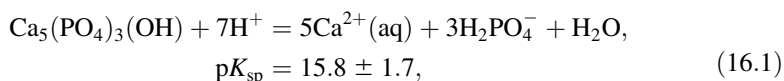
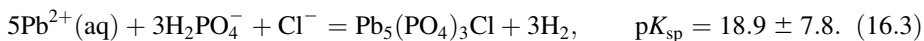


Table 16.3.

Literature on Phosphate Treated or Tested Hazardous Waste Streams.

Waste Stream	References
MSW and other ash	[8–14]
Contaminated soils	[15–35,53]
Contaminated sediments	[36,37]
Electric arc furnace dust	[38]
Smelter slags	[39,40]
Mine tailings	[41]
Heavy metal plating sludge	[39]
Industrial wastewater	[42,43]
Heavy metal contaminated sludge capping	[37,44]
U-contaminated groundwater and soil	[18,28,36,45]



These acid–base reactions raise the pH of the waste stream at which chloropyromorphite is formed. This compound precipitates out because it is extremely insoluble, $\text{p}K_{\text{sp}} = 84.4$ [10].

Chloropyromorphite is not the only stabilizing reaction product. Hydroxypyromorphite [$\text{Pb}_5(\text{PO}_4)_3\text{OH}$] has been suggested by Mavropoulos *et al.* [49] as a stabilized mineral for Pb, while the work of Basta *et al.* [25], Eighmy *et al.* [48], Hodson *et al.* [23], and Xu *et al.* [53] demonstrates that phosphates can stabilize Cd, Ni, and Zn. Eighmy and Eusden [10], in fact, have extended the concept of stabilizing hazardous metals to Cd and Zn into their corresponding apatite minerals, such as $\text{Cd}_5(\text{PO}_4)_3\text{Cl}$, $\text{Cd}_5(\text{PO}_4)_3\text{OH}$, $\text{Zn}_5(\text{PO}_4)_3\text{Cl}$, and $\text{Zn}_5(\text{PO}_4)_3\text{OH}$. In addition to the apatite forms such as pyromorphites, the authors have suggested stable forms of the tertiary metal phosphates $\text{Pb}_3(\text{PO}_4)_2$, $\text{Cd}_3(\text{PO}_4)_2$, and $\text{Zn}_3(\text{PO}_4)_2$, and even the quaternary metal phosphate $\text{Pb}_4\text{O}(\text{PO}_4)_2$. Furthermore, these authors have identified much more complex solid solution phases of these minerals with phosphates of Fe, Ca, and Al.

The studies by Eighmy and Eusden [10] are limited to stabilization of Pb, Cd, and Zn, which are sole contaminants of the MSW ash. By extension, it is believed that similar minerals are formed during phosphate treatment of other waste streams. For example, Singh *et al.* [50] have studied the interaction of Pb, Cd, and Zn with phosphatic clay and reported their investigations on the sorption and desorption of these metals. They report precipitation of Pb as fluoropyromorphite. In the case of Cd and Zn, their studies are not as conclusive, but Singh *et al.* suspect sorption and coprecipitation of phosphates are still the main mechanisms of stabilization.

16.3.2. Stabilization of More Difficult Waste Streams

As discussed in the previous section, stabilization of Cd, Ni, Pb, and Zn is possible with phosphate washing. Stabilizing As, Cr, and Hg is more formidable. Depending on their oxidation states, these metals need additional chemical treatment. Furthermore, if the waste stream contains radioactive elements, then the waste forms need to be solid for geologic burial. If the waste stream is ignitable, then the waste form should be converted into nonignitable form. Acidic or alkaline waste streams should be neutralized prior to disposal to reduce their reactivity. Full CBPC treatment can meet all these needs. Ceramic formation will provide integrity to the waste form, stabilize the contaminants chemically, and microencapsulate them and thus further reduce their leaching. Furthermore, it will convert ignitable waste stream into a nonignitable ceramic and will neutralize acidic or alkaline waste streams during the acid–base reaction. Finally, if the waste stream contains radioactive contaminants, the monolithic CBPC matrix will pass relevant leaching and strength tests designed for radioactive waste forms. Immobilization of radioactive contaminants by chemical stabilization and simultaneous microencapsulation will be discussed in the next chapter. We will limit this chapter to chemical stabilization of waste streams containing both radioactive and hazardous contaminants.

In the phosphate washing discussed above, only a small amount of acid phosphate is used to convert contaminants into their insoluble phosphate forms. To fabricate CBPC waste forms, however, a larger amount of binder is needed, so compared to the phosphate washing, the cost of the binder is high. This condition does not mean that the volume of the stabilized waste will increase. Typically, the washed waste is loosely packed, but the fully stabilized ceramic matrix is dense. As a result, the volume does not increase and, hence, the disposal cost will remain the same. Depending on the nature of the waste and amount of the phosphate binder used, the binder cost may be the only higher cost in the CBPC treatment compared to simple acid washing.

This incremental cost increase may be justified when stabilizing mixed waste streams or waste streams containing As, Cr, and Hg, because simple acid washing will not stabilize these waste streams. To stabilize Hg, in addition to the CBPC formation, a sulfide pretreatment is used [55]. The pretreatment converts the contaminants into their most insoluble sulfide forms, then the CBPC formation produces a waste form that is far superior to any other treatment. This dual treatment has the advantage of being performed at room temperature in a one-step mixing process.

To gain an insight into the sulfide stabilization, examine the solubility product constants for the sulfides and phosphates of hazardous metals listed in Table 16.4. In this table, except for barium sulfide, other sulfides as well as phosphates have very high pK_{sp} , indicating that their aqueous solubility is almost negligible. In particular, the pK_{sp} of HgS and Ag_2S is very high, and these two sulfides are insoluble in water. Therefore, when a waste stream contains one of these two, sulfide pretreatment followed by phosphate ceramic formation is an ideal way to treat the waste stream.

Most waste streams contain more than one contaminant. Some may have contaminants such as Hg, whose sulfide has a higher pK_{sp} than its phosphate, and Ba, whose sulfide is soluble, but phosphate is insoluble. Even in these cases, sulfide treatment followed by phosphate ceramic formation is very effective. The sulfide treatment will produce insoluble HgS that will be microencapsulated in the phosphate matrix, but Ba will be converted partially into soluble BaS, which subsequently will dissolve and will be converted to insoluble phosphate in the CBPC matrix. Thus, the dual treatment is very effective even when several contaminants with varying solubility of sulfides and phosphates are found in the same waste.

Wagh *et al.* [55] have demonstrated the effectiveness of Ceramicrete for the stabilization and microencapsulation of several waste streams, especially those containing Hg. Some of these are discussed below.

Table 16.4.

pK_{sp} of Sulfide and Phosphates of Hazardous Contaminants [56].

	Ag	Ba	Cd	Cr ³⁺	Hg	Ni	Pb
Sulfide	50	Soluble	26.1	20.4	52.4	25.7	27.9
Phosphate	16	22.6	32.6	22.6	12.4	30.3	42.1

16.3.2.1. STABILIZATION OF Hg

Table 16.5 lists the surrogate (simulated) waste streams that were part of this study. The ash stream represents radioactive waste from the inventory of US Department of Energy (DOE) facilities. The Delphi “DETOX” streams are secondary waste generated during destruction of organics from similar waste streams [57]. The soil represents the waste from Argonne National Laboratory’s inventory that was included in a site treatment plan for actual treatment.

To prepare the surrogate waste streams, waste components were mixed thoroughly for 24 h on a vibratory shaker. The resulting waste was then mixed with a binder containing 0.5 wt% sodium sulfide and a stoichiometric or slightly higher amount of water in a Hobart table-top mixer for 30 min. The resulting slurry was a slightly viscous liquid that could be poured easily. Once poured in a mold, it set in ≈ 2 h into a hard and dense ceramic waste form. In plastic containers, samples of ≈ 100 g were made.

The samples were stored for 3 weeks for curing. Each sample was then crushed and was subjected to the TCLP test. The TCLP test results on both the waste stream and the treated CBPC waste form are given in Table 16.6. The results on the untreated waste streams show that the leaching levels far exceed the regulatory limits. The results for the waste forms, on the other hand, are an order of magnitude below the EPA limit. These results indicate superior stabilization of Hg in the phosphate ceramic waste forms coupled with sulfide immobilization.

Wagh *et al.* [57] also studied the leaching performance of the ash waste form in acidic and alkaline environments to determine limits of stabilization. The leaching was conducted on monolithic ceramics for different time periods, as given in Table 16.7. The pH of the acidic solution was 3.5, which was obtained by adding acetic acid to the leachate water. The alkaline solution was NaOH with a pH of 11.

The data in Table 16.7 show that, as in the neutral aqueous environment, the leaching levels are undetectable in the alkaline environment (<0.025 $\mu\text{g/l}$). Even in the acidic environment, the levels are extremely small and close to the detection limit for the first

Table 16.5.

Surrogate Wastes and their Formulation.

Waste Identification	Composition (wt%)	Contaminants (wt%)
Delphi DETOX		
Oxide waste	Fe ₂ O ₃ , 93.6 FeCl ₂ , 4.9	In both waste streams, HgCl ₂ , Ce ₂ O ₃ , and Pb(NO ₃) ₂ were 0.5 each
Phosphate waste	FePO ₄ , 98.5	
DOE ash waste	Activated carbon, 5 Vermiculite, 20 Class F fly ash, 40 Coal bottom ash, 33	HgCl ₂ added such that Hg level was 0.5
Soil	Top soil from Argonne grounds	HgCl ₂ added such that Hg level was 0.1. Original waste had 2.7 ppm of Hg

Table 16.6.

TCLP Results for Hg (mg/l).

	Untreated Waste	Waste Form
Delphi DETOX		
Iron oxide	138	< 0.00002
Iron phosphate	189	0.01
DOE ash waste	40	0.00085
Soil	2.27	0.00015
EPA limits	0.2	0.025

72 h. After that, the leaching levels fall below the detection limit. These data suggest that the CBPC waste form is very stable and can sustain a range of chemical environments from acidic to alkaline.

The first deployment of CBPC for stabilization of Hg using Ceramcrete was reported by Singh *et al.* [58]. These authors used the CBPC process to stabilize crushed Hg light bulbs that were radioactively contaminated. Visual inspection of the waste revealed that 90 vol% of the waste was <60 mm in size. Typical size of the crushed glass ranged from 2 to 3 cm long by 1–2 cm wide down to fine particulates. Chemical analysis indicated an Hg concentration of 5 ppm. In addition, emissions from isotopes of ^{60}Co , ^{137}Cs , and ^{154}Eu were 1.1×10^{-5} , 4×10^{-4} , and 4×10^{-6} mCi/g, respectively.

Five-gallon size waste forms were fabricated. Typical waste loading was 35–40 wt%. A small amount of potassium sulfide was added to the Ceramcrete binder mixture for stabilization of Hg, and dense and hard ceramic waste forms were produced. Just before solidification, TCLP results were obtained on small aliquots of the mixing slurry that was separated and allowed to set. Mercury levels in the leachate were found to be 0.05 $\mu\text{g/l}$, well below the UTS limit of 0.025 mg/l. The entire waste was treated, removed from the inventory, and sent to the Radioactive Waste Management Complex at the Idaho National Engineering and Environmental Laboratory for disposal.

16.3.2.2. STABILIZATION OF Cr

Chromium occurs in three valence states 2 + , 3 + , and 6 + . The 2 + state is formed in extreme reducing environments, but the bulk waste streams such as utility fly ash and

Table 16.7.Leaching Levels ($\mu\text{g/l}$) of Hg from Ash Waste Forms in Acidic and Alkaline Water.

Time (h)	2	7	24	48	72	96–2136
Amount in acidic water	0.032	0.025	0.045	0.04	0.045	< 0.025
Amount in alkaline water	< 0.025 for all time intervals					

radioactive waste streams are either produced in oxidizing or in ambient conditions. When the waste is stored in ambient conditions, several metals including Cr may rust, thereby producing Cr_2O_3 and chromates that are in an anionic state.

As evident from Fig. 16.1, the dissolution behavior of Cr_2O_3 is similar to that of other divalent oxides. Its solubility is high in the acidic region, drops almost linearly as pH increases, has a minimum at almost pH = 7, and then increases with pH. Its overall behavior is that of a sparsely soluble oxide. As a result, Cr_2O_3 will react with acid phosphates and form insoluble hydrophosphates or phosphates.

Wagh *et al.* [45] demonstrated stabilization of Cr, along with Cd, Pb, and Hg from contaminated soil and wastewater in the Ceramicrete waste form. Table 16.8 shows the contaminant levels in the waste and the wastewater, and the corresponding TCLP result for the stabilized waste. The wastewater in the Ceramicrete slurry was equal in amount to the stoichiometric water needed for the stabilization process. Including this wastewater, the total waste loading was ≈ 77 wt%. The waste forms had open porosity of 2.7 vol% and a density of 2.17 g/cm^3 . Compression strength was 34 MPa (4910 psi).

The results show that the leaching levels for all contaminants, except Cd, are well below the regulatory requirements. Cd failed only marginally. It was found that Cd can be satisfactorily stabilized by extending the time of mixing, in which case one obtains leaching below 0.11 mg/l. The wastewater also contained uranium as a radioactive contaminant. Stabilization of this contaminant is discussed in Chapter 17.

In another similar case, Wagh *et al.* [59] simulated Pu-contaminated ash from Rocky Flats (one of the DOE sites) by incorporating various hazardous contaminants, including Cr as Cr_2O_3 , and stabilizing them in the CBPC matrix at a loading of 54 wt%. The TCLP results of their study are presented in Table 16.9.

As mentioned before, subsequent phosphate treatment does not affect the stable sulfide, and TCLP results show excellent stabilization of Cr in any oxidation state. Alternatively, a small amount of reductant in the waste will convert chromate into lower oxidation states. Such methods, however, are not preferred, because the reductant may also affect the solubility of other hazardous compounds. The exception is technetium-containing radioactive waste, in which chromate is also a contaminant. As we shall see in Chapter 17, a reductant is essential for stabilization of technetium, and that will also help in stabilization of chromium.

The stabilization of a range of contaminants, including Cr^{6+} , in Ceramicrete was demonstrated by Wagh *et al.* [60] with two liquid waste streams that simulated radioactive supernatant and sludge from Hanford tanks within the DOE complex. These waste streams

Table 16.8.

Levels of Contaminants in Soil and Wastewater and Results of the Leaching Tests.

	Cd	Cr	Pb	Hg
In soil (ppm)	1044	1310	2457	1002
TCLP result (mg/l)	0.18	0.13	<0.2	0.0015
UTS limit (mg/l)	0.11	0.86	0.37	0.025

Table 16.9.

TCLP Levels for Surrogate Waste Form (mg/l).

	Ba	Cr	Ni	Pb
Level in waste (ppm)	1077	5360	4890	8600
Leaching level (mg/l)	0.68	0.01	<0.05	<0.10
UTS limit (mg/l)	1.2	0.86	5.00	0.37

Table 16.10.

Contaminant Concentrations in Simulated Supernate Waste from Hanford Tank, their Waste Forms, and the TCLP Results.

	Cd	Cr	Ag	Pb	Zn
In waste (ppm)	2.3	937.6	11.5	37	7.04
In waste form (ppm)	0.91	373	4.6	14.8	2.8
TCLP result on waste form (mg/l)	<0.01	0.01	<0.05	<0.05	<0.05

Table 16.11.

Contaminant Concentrations in Simulated Sludge from Hanford Tanks, their Waste Forms, and the TCLP Results.

	Cd	Cr	Ni	Ag	Ba
In waste (ppm)	2568	126	1824	40	85
In the waste form (ppm)	852	42	605	13	28
TCLP result on waste form (mg/l)	0.0043	0.0013	0.21	0.027	0.032

are highly alkaline. They were stabilized at loadings of 40 and 32 wt%. Sodium sulfide was used to stabilize Ag and Cr⁶⁺. Tables 16.10 and 16.11 show the levels of the hazardous contaminants in the waste, the waste forms, and the TCLP leachates for simulated solid waste and sludge, respectively. The data indicate excellent stabilization of the contaminants, including Ag and Cr, which had undergone sulfidation followed by the phosphate treatment.

16.3.2.3. STABILIZATION OF ARSENIC

Arsenic has two oxidation states, 3+ and 5+. Figure 16.1 shows the dissolution characteristics of As for its 3+ state. Compared to other sparsely soluble oxides, this oxide is soluble, and up to pH 9 its solubility is constant and then increases with pH. Thus, As³⁺ will dissolve easily in the CBPC solution and can be converted to its phosphate form. Unlike the chromates, however, arsenates are insoluble in water but soluble or sparingly

soluble in acids. If the arsenates are insoluble, they should be encapsulated in the CBPC matrix, but in case they are soluble or sparingly soluble, the phosphate reaction should be able to stabilize them. Unfortunately, there is very little experimental evidence of stabilization of As in a CBPC matrix to verify these statements.

16.4.

CONCLUSIONS

The examples given above and the work done in the last 10 years on phosphate washing demonstrate that phosphates are very powerful stabilizers of inorganic hazardous contaminants. Phosphate washing is very economical, and once the treated waste is disposed, because phosphates are common fertilizer components, the soil becomes enriched with phosphates. Hence, the entire disposal process is ecologically sound.

Chapters 4 and 5 emphasized that solubility plays a key role in the kinetics of hazardous waste stabilization. As illustrated in the present chapter, solubility data allow one to predict the effect of the phosphate treatment on individual contaminants and also help in the evaluation of the waste form behavior in groundwater.

Because of the above advantages, it is not surprising that the literature on phosphate stabilization has undergone a sudden explosion. This interest is not limited to the stabilization of hazardous contaminants alone, but radioactive elements as well. The role of the phosphate treatment of radioactive wastes will be discussed in the next chapter.

REFERENCES

1. A.S. Wagh, "Waste generation," in *Encyclopedia of Environmental Analysis and Remediation*, ed. R.A. Meyers (Wiley, New York, 1998), pp. 5142–5147.
2. N. Beecher, K. Geiser, and K. Fischer, "Strategies in hazardous waste minimization used outside the US," *J. Hazard. Waste Mater.*, **5** [2] (1988) 177–184.
3. J.R. Conner, *Chemical Fixation and Solidification of Hazardous Wastes* (Van Nostrand Reinhold, New York, 1990), pp. 322–332.
4. US Environmental Protection Agency, Resource Conservation and Recovery Act, PL94-580 (1976); *Superfund Treatability Study Protocol: Identification/Stabilization of Soils Containing Metals, Phase II: Review Draft*, Office of Research and Development, Cincinnati, and Office of Emergency and Remedial Response, Washington, DC, 1990.
5. US Environmental Protection Agency, Toxicity Characteristic Leaching Procedure (TCLP), Method 1311, Rev. II, 1992.
6. I.W. Donald, B.L. Metcalfe, and R.N.J. Taylor, "Review of the immobilization of high level radioactive wastes using ceramics and glasses," *J. Mater. Sci.*, **32** (1997) 5851–5887.
7. P.L. Bishop, "Leaching of inorganic hazardous constituents from stabilized/solidified hazardous wastes," *Hazard. Waste Hazard. Mater.*, **5** [2] (1988) 129–143.
8. K.E. Forrester and N.H. Stratham, Immobilization of lead in bottom ash, assigned to Wheelabrator Environmental Systems, Inc., US Patent 5,245,114, 1993.
9. M. O'Hara and J.M. Surgi, Immobilization of lead and cadmium in solid residues from the combustion of refuse using lime and phosphate, assigned to Wheelabrator Environmental Systems, Inc., U.S. Patent 4,737,356, 1986.

10. T.T. Eighmy and J. Eusden, Phosphate stabilization of MSW combustion residues: geochemical principles, to appear in *Energy, Waste, and Environment—A Geochemical Perspective*, eds. R. Giere and P. Stille (Geological Society, London, to be published in 2004).
11. A. Nzihou and P. Sharrock, "Calcium phosphate stabilization of fly ash with chloride extraction," *Waste Mgmt*, **22** (2002) 235–239.
12. T. Eighmy, B. Crannell, J. Krzanowski, L. Butler, F. Cartledge, E. Emery, J. Eusden, E. Shaw, and C. Francis, "Characterization and phosphate stabilization of dusts from the vitrification of MSW combustion residues," *Waste Mgmt*, **18** (1998) 513–524.
13. B. Crannell, T. Eighmy, J. Krzanowski, J. Eusden, E. Shaw, and C. Francis, "Heavy metal stabilization in municipal solid waste combustion bottom ash using soluble phosphate," *Waste Mgmt*, **20** (2000) 135–148.
14. P. Piantone, F. Bodenau, R. Derie, and G. Depelsenaire, "Monitoring the stabilization of municipal solid waste incineration fly ash by phosphation: mineralogical and balance approach," *Waste Mgmt*, **23** (2003) 225–243.
15. T.H. Christensen and B.G. Nielsen, *Retardation of lead in soils*, Heavy Metals in the Environment (CEP Consultants, Edinburgh, 1987), pp. 319–321.
16. M.B. Rabinowitz, "Modifying soil and bioavailability by phosphate addition," *Bull. Environ. Contam. Toxicol.*, **51** (1993) 438–444.
17. M.V. Ruby, A. Davis, and A. Nicholson, "In situ formation of lead phosphates in soils as a method to immobilize lead," *Environ. Sci. Technol.*, **28** (1994) 646–654.
18. J. Wright, L. Peurrung, T. Moody, J. Conca, X. Chen, P. Didzerekis, and E. Wyse, In situ immobilization of heavy metals in apatite mineral formation, Tech. Report to the Strategic Environmental Research and Development Program, Department of Defense, Pacific Northwest Laboratory, Richland, WA, 1995.
19. J. Cotter-Howells and S. Caporn, "Remediation of contaminated land by formation of heavy metal phosphates," *Appl. Geochem.*, **11** (1996) 335–342.
20. V. Laperche, S. Traina, P. Gaddam, and T. Logan, "Chemical and mineralogical characterization of Pb in a contaminated soil: reactions with synthetic apatite," *Environ. Sci. Technol.*, **30** (1996) 3321–3326.
21. W. Berti and S. Cunningham, "In-place inactivation of Pb in Pb-contaminated soils," *Environ. Sci. Technol.*, **31** (1997) 1359–1364.
22. G. Hettiarachchi, G. Pierzynski, and M. Ransom, "In situ stabilization of soil lead using phosphorous and manganese oxide," *Environ. Sci. Technol.*, **34** (2000) 4614–4619.
23. M. Hodson, E. Valsami-Jones, and J. Cotter-Howells, "Bonemeal additions as a remediation treatment of metal contaminated soil," *Environ. Sci. Technol.*, **34** (2000) 3501–3507.
24. S. Raicevic, "Remediation of uranium contaminated water and soil using phosphate-induced metal stabilization (PIMS)," *Hemijska Industrija*, **55** (2001) 277–280.
25. N. Basta, R. Gradwohl, K. Snethen, and J. Schroder, "Chemical immobilization of lead, zinc and cadmium in smelter-contaminated soils using biosolids and rock phosphate," *J. Environ. Qual.*, **30** (2001) 1222–1230.
26. H. Gremen, J. Persolja, F. Lobnik, and D. Lestan, "Modifying lead, zinc, and cadmium bioavailability in soil by apatite and EDTA addition," *Fresenius Environ. Bull.*, **10** (2001) 727–730.
27. S.L. McGowen, N. Basta, and G. Brown, "Use of diammonium phosphate to reduce heavy metal solubility and transport in smelter-contaminated soil," *J. Environ. Qual.*, **30** (2001) 493–500.
28. L. Matheson, W. Goldberg, and W. Bostick, "Laboratory batch and column studies to evaluate apatite. II: Removal of soluble uranium from contaminated groundwater," *Am. Chem. Soc. Natl Meet., Div. Environ. Chem.*, **41** (2001) 109–113.
29. Y. Wang, T. Chen, K. Yeh, and M. Shue, "Stabilization of an elevated heavy metal contaminated site," *J. Hazard. Mater.*, **88** [1] (2001) 63–74.
30. J. Yang, D. Mosby, S. Casteel, and R. Blanchar, "Lead immobilization using phosphoric acid in a smelter-contaminated urban soil," *Environ. Sci. Technol.*, **35** (2001) 3553–3559.
31. J. Yang, D. Mosby, S. Casteel, and R. Blanchar, "In vitro lead bioaccessibility and phosphate leaching as affected by surface application of phosphoric acid in lead-contaminated soil," *Arch. Environ. Contam. Toxicol.*, **43** (2002) 399–405.
32. R. Stanforth and J. Qiu, "Effect of phosphate treatment on the solubility of lead in contaminated soil," *Environ. Geol.*, **41** (2001) 1–10.

33. X. Cao, L. Ma, M. Chen, S. Singh, and W. Harris, "Impacts of phosphate amendments on lead biogeochemistry at a contaminated site," *Environ. Sci. Technol.*, **36** (2002) 5296–5304.
34. P. Theodorates, N. Papassiopi, and A. Xenidis, "Evaluation of monobasic calcium phosphate for the immobilization of heavy metals in contaminated soils from Lavrion," *J. Hazard. Mater.*, **94** (2002) 135–146.
35. R. Hamon, M. McLaughlin, and G. Cozens, "Mechanisms of attenuation of metal availability in situ remediation treatments," *Environ. Sci. Technol.*, **36** (2002) 2991–3996.
36. J. Arey, J. Seaman, and P. Bertsch, "Immobilization of uranium in contaminated sediments by hydroxyapatite addition," *Environ. Sci. Technol.*, **33** (1999) 337–342.
37. B. Crannell, T. Eighmy, L. Butler, E. Emery, and F. Cartledge, "Use of phosphates to stabilize heavy metals in contaminated sediments," in *Dredged Material Management: Options and Environmental Concerns*, eds. J. Pederson and E. Adams (MIT Sea Grant Publications, Cambridge, MA, 2003), pp. 175–178.
38. B. Crannell, T. Eighmy, T. Krzanowski, and J. Eusden, "Phosphate stabilization mechanisms for heavy metals in electric arc furnace smelter dusts," in *Hazardous Wastes and Hazardous Materials*, eds. N. Nikolaidis, C. Erkey, and B. Smets (Technomic Publishing, Lancaster, PA, 1999), pp. 561–570.
39. L. Tickanan and P. Turpin, "Treatment of heavy metal-bearing wastes using a buffered phosphate stabilization system," in *Proceedings of the 51st Industrial Waste Conference*, eds. R. Wukasz and C. Dalton (CRC Press, Boca Raton, FL, 1997), pp. 627–635.
40. T. Ioannidis and A. Zouboulis, "Detoxification of a highly toxic lead-loaded industrial solid waste by stabilization using apatites," *J. Hazard. Mater.*, **97** (2003) 173–191.
41. J. Eusden, L. Gallagher, T. Eighmy, B. Crannell, J. Krzanowski, L. Butler, F. Cartledge, E. Emery, E. Shaw, and C. Francis, "Petrographic and spectroscopic characterization of phosphate-stabilized mine tailings from Leadville, CO," *Waste Mgmt*, **22** (2002) 117–135.
42. W. Admassu and T. Breese, "Feasibility of using natural fishbone apatite as a substitute for hydroxyapatite in remediating aqueous heavy metals," *J. Hazard. Mater.*, **69** [2] (1999) 187–196.
43. Y. Liu and M. Peng, "Applications of mineral apatites in the treatment of wastewater," *Anquan Yu Huanjing Xuebao*, **1** (2001) 9–12.
44. B. Crannell, T. Eighmy, L. Butler, F. Cartledge, E. Emery, C. Wilson, D. Reible, and M. Yin, "Reactive barriers for containment of metals, contaminated dredged materials: diffusion studies," in *Beneficial Use of Recycled Materials in Transportation Applications*, ed. T. Eighmy (Air and Waste Management Association, Sewickley, PA, 2003), pp. 377–388.
45. A. Wagh, S. Jeong, D. Singh, R. Strain, H. No, and J. Wescott, "Stabilization of contaminated soil and wastewater with chemically bonded phosphate ceramics," *Proceedings of the Waste Management Annual Meeting, WM '97*, eds. R. Post and M. Wacks, Tucson, AZ, 1997.
46. P. Zhang, J. Ryan, and L. Bryndzia, "Pyromorphite formation from goethite adsorbed lead," *Environ. Sci. Technol.*, **31** (1997) 2673–2678.
47. P. Zhang, J. Ryan, and J. Yang, "In vitro soil Pb solubility in the presence of hydroxyapatite," *J. Environ. Sci. Technol.*, **32** (1998) 2763–2768.
48. T. Eighmy, B. Crannell, L. Butler, F. Cartledge, E. Emery, J. Eusden, E. Shaw, and C. Francis, "Heavy metal stabilization in municipal solid waste combustion dry scrubber residue using soluble phosphate," *Environ. Sci. Technol.*, **37** (1997) 3330–3338.
49. E. Mavropoulos, A. Ross, A. Costa, C. Perez, J. Moreira, and M. Saldanha, "Studies on the mechanisms of lead immobilization by hydroxyapatite," *Environ. Sci. Technol.*, **36** (2002) 1625–1629.
50. S. Singh, L. Ma, and W. Harris, "Heavy metal interactions with phosphatic clay: sorption and desorption behavior," *J. Environ. Qual.*, **30** (2001) 1961–1968.
51. P. Zhang and J. Ryan, "Formation of pyromorphite in anglesite-hydroxyapatite suspensions under varying pH conditions," *Environ. Sci. Technol.*, **32** (1998) 3318–3324.
52. P. Viellard and Y. Tardy, "Thermochemical properties of phosphates," in *Phosphate Minerals*, eds. J. Nriagu and P. Moore (Springer, New York, 1984), Chapter 4.
53. Y. Xu, F. Schwartz, and S. Traina, "Sorption of Zn^{2+} and Cd^{2+} in hydroxyapatite surfaces," *Environ. Sci. Technol.*, **28** (1994) 1472–1480.
54. J. Ryan, P. Zhang, D. Hesterberg, J. Chou, and D. Sayers, "Formation of chloropyromorphite in a lead-contaminated soil amended with hydroxyapatite," *Environ. Sci. Technol.*, **35** (2001) 3798–3803.

55. A. Wagh, S. Jeong, and D. Singh, "Mercury stabilization in chemically bonded phosphate ceramics," *Ceram. Trans.*, **87** (1998) 63–73.
56. J. Dean and N. Lange, *Lange's Handbook of Chemistry* (McGraw Hill, New York, 1999).
57. A. Wagh, D. Singh, and S. Jeong, *Chemically bonded phosphate ceramics for stabilization and solidification of mixed waste*, in *Handbook of Mixed Waste Management Technology* (CRC Press, Boca Raton, FL, 2000), Chapter 6.3.
58. D. Singh, A. Wagh, M. Tlustochowicz, and S. Jeong, "Phosphate ceramic process for macroencapsulation and stabilization of low-level debris waste," *Waste Mgmt*, **18** (1998) 135–143.
59. A. Wagh, R. Strain, S. Jeong, D. Reed, T. Krause, and D. Singh, "Stabilization of Rocky Flats Pu-contaminated ash within chemically bonded phosphate ceramics," *J. Nucl. Mater.*, **265** (1999) 295–307.
60. A. Wagh, M. Maloney, G. Thomson, and A. Antink, Investigations in ceramic stabilization of Hanford tank wastes, *Proceedings of the Waste Management Conference 2003*, eds. R. Post and M. Wacks, Tucson, AZ, February 2003.

This page is intentionally left blank

Radioactive Wastes Stabilization

The nuclear age in the 20th century has left behind a legacy of radioactive waste streams that are in need of proper disposal or permanent storage. Solving this problem is a major technological and environmental challenge in the 21st century. Radioactive waste materials are stored in several countries that were active in the development and production of nuclear weapons; the United States, former Soviet Union countries, and Great Britain are prominent among these. In addition, other countries using nuclear energy for power production are accumulating their own inventories of radioactive waste.

The radioactive waste comes in all forms and shapes, and has various chemical and radiological characteristics. Solids, semi-solids, and liquids are stored at various US Department of Energy (DOE) sites and at former “closed cities” in Former Soviet Union countries, where nuclear weapons were produced. The level of radioactivity in these waste streams varies; in spent nuclear fuel rods it may be very high, whereas in personnel protective outfits used in laboratory research work, only suspect amounts of contamination may be present. The waste streams consist of uranium tailings, process liquids, dismantled components, incinerated residues, liquid salt wastes, and even cement debris of demolished buildings with fixed contamination. In addition, some waste streams may also contain chemical constituents that are chemically hazardous, corrosive, flammable, or volatile. These waste streams must be stabilized so they will not find their way into groundwater, air, or other pathways and affect human lives through air or the food chain. Because of the wide variation in the waste stream composition, physical form, and chemical and radioactive characteristics, no single economical method is available to treat these waste streams and isolate them from the environment for safe transport to and storage in waste repositories.

Over the years, several technologies, inspired by differing ideas, have been developed to treat radioactive waste streams. Some of them are based on efficient separation methods that remove radioactive contaminants from the waste streams to reduce radiological

risks [1], while some involve incineration of the streams to reduce their volume [2]. The most common approach is to vitrify the most difficult streams and encapsulate them in a nonleachable glass matrix [3]. Simpler ones are stabilized in cement that immobilizes contaminants in a rudimentary waste form [4].

Each method has its merits and drawbacks. For example, separation technologies remove some of the high-activity products from the streams and convert them into low-activity streams that are easier to stabilize, but generate separated components with high activity that also require stabilization. This two-phase approach adds to the total cost and may turn out to be very expensive.

Vitrification is a major stabilization process that has been in use to some extent. It is energy intensive and produces solidified waste forms with only a small loading of the waste in glass. The high temperature used during this process ($\approx 1500^{\circ}\text{C}$) may volatilize some of the hazardous and radioactive components of the waste streams. The airborne components must be collected and stabilized in this process; thus, a separate nonthermal stabilization technology is needed to immobilize the volatile streams. In addition, the process generates its own secondary waste streams such as contaminated furnaces, ducts, and ancillary equipment. Such thermal processes typically generate problems of feed stream and process controls, pretreatment requirements, off-gas treatment systems, management of secondary wastes from the separation, and air and water pollution control. The National Academy of Sciences (NAS) [5] recently issued a report that details waste stream problems with vitrification and called for development of alternative immobilization technologies, in particular, technologies based on polyphase ceramics. The NAS report cites not only the vitrification process, but also the separation processes as technological risks.

An alternative to high temperature processes, cement grout stabilization, is considered an inexpensive nonthermal technology that can be used to treat a range of waste streams, particularly those with very low activity. Cement has been a very familiar material because of its widespread use in the construction industry. It has also been successfully used to stabilize many chemical waste streams [6]. The problem with the conventional cement system is that, because it cannot accommodate a high loading of the waste, it generates a high volume of the waste form, and that leads to high transportation and disposal costs. In addition, because cement is an alkaline material, its chemistry is not always compatible with some of the waste streams, e.g., acids.

CBPCs hold promise as an alternative to vitrification and cement grouts. CBPC processes can treat a wide range of radioactive waste streams at room temperature. Case studies have demonstrated that Ceramicrete waste forms are comparable to vitrified waste forms in performance, and unlike other cement systems, they can incorporate high loading of a wide variety of waste streams. Ceramicrete produces ceramics at room temperature by chemically bonding the radioactive components and hence exhibits advantages of both glass and cement grout without the major drawbacks of either.

As in the case of hazardous contaminants discussed in Chapter 16, CBPC treatment converts radioactive constituents of waste streams into their nonleachable phosphate mineral forms. It follows the philosophy [7] that, if nature can store radioactive minerals as phosphates (apatite, monozites, etc.) without leaching them into the environment, researchers should be capable of doing the same by converting radioactive and hazardous

contaminants into their phosphates for safe storage or disposal. In the CBPC approach, the chemical contaminants are converted into these minerals by taking advantage of their solubility in the phosphate acid solution. For this reason, we will discuss the role of the solution chemistry of radioactive components in chemical immobilization and will also explore the mechanism of physical encapsulation that isolates the contaminants from the environment. We elaborate on how the chemical immobilization coupled with physical encapsulation helps in meeting requirements for storage (waste acceptance criteria) for a range of treated waste streams at different DOE sites in the United States. Among all forms of CBPCs, Ceramicrete has been tested the most in this application, and hence, data from several case studies are used to demonstrate the effectiveness of the CBPC treatment. In addition, macroencapsulation of contaminated large objects and use of Ceramicrete nuclear shields are briefly discussed.

17.1.

NATURE OF THE RADIOACTIVE CONTAMINANTS

Table 17.1 lists the most common radioactive contaminants categorized according to their solubility.

Of the contaminants listed in Table 17.1, the first three are radioactive. The last one is benign but still is an issue for waste stabilization because the salts are easily

Table 17.1.
Radioactive Contaminants and their Solubility.

Contaminants	Form in the Waste	Solubility
Actinides	Generally present in fully oxidized form, but salts such as nitrates, fluorides, and chlorides are common in solution	Fully oxidized forms are insoluble. Oxides of lower oxidation states may be slightly soluble. Actinide salts are soluble
Fission products	Cesium (Cs), strontium (Sr), barium (Ba), and technetium (Tc) are main isotopes present as salts (nitrates and chlorides). Tc may be present as oxides	All salts are soluble. Tc oxidizes as soluble pertechnetate, but in reduced state, it is less soluble
Radium (Ra), radon (Rn), and other isotopes	Ra disintegrates into Rn, which is a gas and hence is of main concern during stabilization	Ra is soluble. Solubility of other isotopes varies. Rn escapes into the atmosphere and contaminates air
Benign bulk salt components in radioactive streams	Sodium and potassium nitrate, nitrite, chloride, and sulfates	Highly soluble. Being in bulk quantity, their dissolution may affect integrity of the waste form

Table 17.2.

Typical Isotopes of Fission Products, their Half-Life, and Specific Activity [8].

Isotope	Half-Life	Specific Activity (Ci/g)
^{233}U	1.6×10^5 years	0.01
^{239}Pu	2.4×10^4 years	0.06
^{240}Pu	6.7×10^3 years	0.25
^{226}Ra	1.62×10^3 years	1.0
^{228}Ra	5.7 years	240
^{222}Rn	3.8 days	1.6×10^5
^{137}Cs	30 years	88
^{90}Sr	28 years	144
^{140}Ba	12.8 days	70,000
^{99}Tc	2.1×10^5 years	0.017

leachable and hence affect the overall integrity of the waste form. The salt waste components in these streams are produced when acid waste components, such as nitric acid, are neutralized by using sodium hydroxide to reduce their reactivity and corrosivity during storage. In addition, several waste streams contain both radioactive and hazardous contaminants that are difficult to separate. Such waste streams are called “mixed”.

Note that each of the radioactive contaminants has a certain half-life and specific activity. The half-life determines whether the particular isotope is long or short lived. Waste streams that contain long-lived isotopes must be stabilized in a matrix that is durable over a long period of time. The short-lived isotopes, on the other hand, may be stored for a shorter duration until their activity is almost exhausted. Table 17.2 lists various radioactive isotopes, their half-life, and their specific activity. Note from the table that the long-lived isotopes have a very low specific activity, while the short-lived ones exhibit very high activity. The high-activity isotopes can easily affect the stabilizing matrix due to internal radiation during storage. Thus, the requirements on the stabilizing matrix are twofold:

1. The matrix should be durable over time that is equal to or greater than the longest life of an isotope.
2. It should be stable in the presence of the intense radiation from the isotopes.

Based on the half-life and specific activity of commonly occurring isotopes in radioactive waste streams given in Table 17.2, each disposal site or repository of the treated waste has developed waste acceptance criteria (WAC). The WACs require that the treated waste pass certain test criteria, which vary from site to site depending on the nature of the waste stored. In a number of case studies discussed in this chapter, we will use these WACs to demonstrate compliance of the CBPC waste form.

17.2.

MECHANISMS OF RADIOACTIVE WASTE IMMOBILIZATION

The following three mechanisms play the major role in the immobilization of radioactive contaminants in a stabilized Ceramicrete waste form:

1. chemical stabilization,
2. physical microencapsulation, and
3. macroencapsulation.

As discussed in Chapter 16, chemical stabilization is a result of conversion of contaminants in a radioactive waste into their insoluble phosphate forms. This conversion is solely dependent on the dissolution kinetics of these components. In general, if these components are in a soluble or even in a sparsely soluble form, they will dissolve in the initially acidic CBPC slurry and react with the phosphate anions. The resultant product will be an insoluble phosphate that will not leach into the groundwater. On the other hand, if a certain radioactive component is not soluble in the acid slurry, it will not be soluble in more neutral groundwater, because the solubility of such components is lower in neutral than in acidic solutions. Such a component will be simply microencapsulated in the phosphate matrix of the CBPC. Thus, the solubility of hazardous and radioactive components is key to chemical immobilization.

Macroencapsulation is used for large objects such as concrete debris that is contaminated, or structural steel that has fixed contamination. The chemical stabilization and microencapsulation work together to immobilize chemical constituents, while the macroencapsulation is used to physically encapsulate large objects. For this reason, we will discuss chemical stabilization and microencapsulation together and address macroencapsulation in a separate section in this chapter.

17.3.

ROLE OF SOLUBILITY IN IMMOBILIZATION OF RADIOACTIVE ELEMENTS

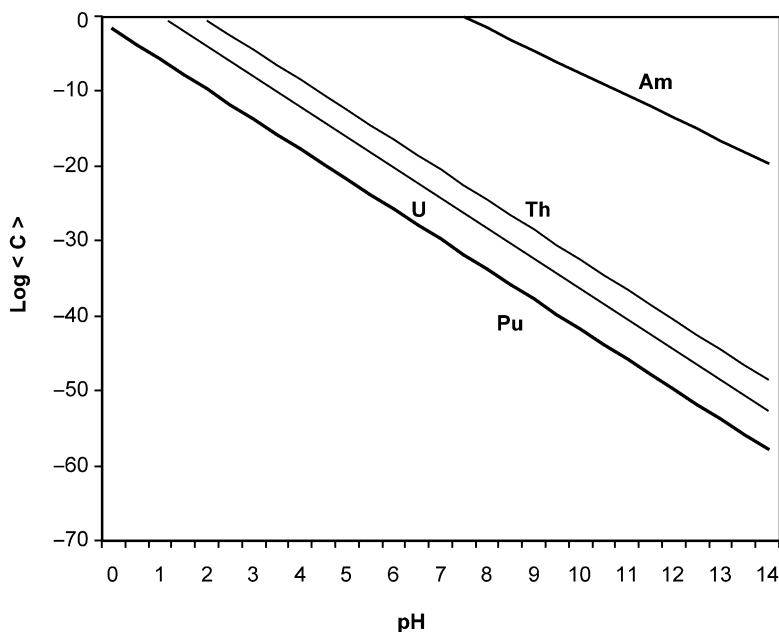
Again, as in the case of hazardous contaminants discussed in Chapter 16, the solubility of a radioactive contaminant plays a major role in its stabilization in a phosphate matrix. Therefore, one needs to understand the aqueous behavior of a radioactive contaminant prior to selecting the acid–base reaction that will form the CBPC used for fabricating the waste form matrix. In this respect, actinides, fission products, and salts have unique solubility behavior. This behavior is discussed below.

17.3.1. Solubility of Actinides and their Stabilization

The most common actinides found in radioactive waste streams are uranium (U), thorium (Th), plutonium (Pu), and americium (Am). Among these, only Th has one valence state (Th^{4+}), while the rest have four valence states (3–6); the most stable state is the 4+. Therefore, in most radioactive waste streams, these common actinides are found as ThO_2 , UO_2 , PuO_2 , and AmO_2 . Figure 17.1 shows the solubility of these common oxides as a function of pH. As evident from this figure, overall, solubility of these oxides is extremely low, and unless in highly acidic solution, they may be classified as insoluble oxides. They also exhibit amphoteric behavior, i.e., their solubility increases with increasing acidity and basicity and has a minimum close to neutral pH. In particular, the solubility is almost constant and the minimum is in the range of $4 < \text{pH} < 10$. Hence, if one selects an acid–base reaction to form a CBPC in this region, then these quadrivalent oxides will be stable as insoluble oxides (UO_2 , PuO_2 , etc.). (See the solubility product constants of these oxides in Appendix B) These oxides are mostly found in powder form, and hence their dispersibility is an issue. They can, however, be microencapsulated in a CBPC matrix in order to reduce their dispersibility.

Actinide oxides of higher oxidation states, such as UO_3 and PuO_3 , are rarely found in waste streams because they are formed only in a highly oxidizing environment [9]. If formed at all, they may result in oxides such as U_3O_8 , which is a solid solution of UO_2

Fig. 17.1.



Solubility variation of most common actinide oxides with pH.

and $2\text{U}_2\text{O}_3$. Such products, however, are very stable, as evidenced by their presence in naturally occurring minerals such as pitchblende, and can be easily microencapsulated in the ceramic matrix.

Often traces of actinide oxides in lower oxidation states are found along with the stable quadrivalent oxides. An example is Pu-contaminated combustion residue from Rocky Flats that contained traces of oxides of Pu in lower oxidation states along with more stable PuO_2 . Such oxides seem to oxidize fully into stable compounds, such as PuO_2 , in a phosphate matrix. Wagh *et al.* [10] used cerium in the reduced state as Ce_2O_3 and formed a CBPC by reacting with MgO and KH_2PO_4 (i.e., as Ceramicrete), and with the aid of X-ray diffraction analyses showed that Ce_2O_3 is converted to CeO_2 and microencapsulated in the matrix. It is likely that the oxides in reduced state will form their most stable forms in the $4+$ oxidation state. Therefore, oxides of actinides in their quadrivalent states will remain in their insoluble state within a phosphate matrix and will be simply microencapsulated. At the same time, those in the higher oxidation states will form stable solid solutions. These inferences are justified on the basis of the Pourbaix diagrams (E_h -pH diagrams), but much more experimental work is needed to confirm them.

Salts of actinides are very common in waste streams. In particular, nitrates, chlorides, and sulfates are found in tank waste streams that were formed by neutralization of highly acidic solutions at several DOE sites, such as Hanford and Savannah River. The aqueous solubility of these salts is very high, and hence, it is a challenge to stabilize them. As we shall see in case studies, the CBPC matrix has good promise in handling these waste streams.

Finally, some DOE sites also have stored hexavalent uranium fluoride (UF_6). The approach to stabilize this compound is to calcine it to form stable uranium oxide. There is no study reported in the literature on treatment of fluorides using a CBPC matrix, but considering that fluoroapatites are stable minerals, they should be applicable to stabilization of actinide compounds.

17.3.2. Stabilization of Fission Products

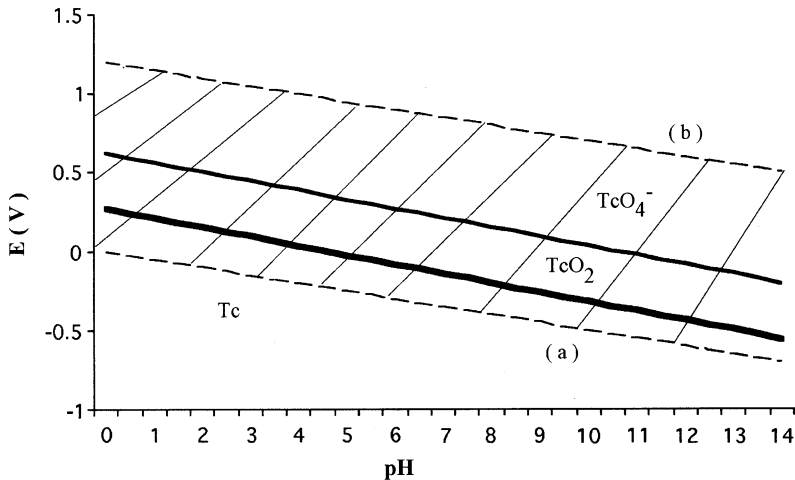
The fission products (Cs, Sr, Ba, and Tc) are found in waste streams with significantly high activity and comparatively short half-life (see Table 17.2). Their initial high activity requires that these elements must be stabilized in a waste form that is not affected by self-radiation.

Cs, Sr, and Ba are mostly found in salt waste streams as chlorides, nitrates, and sulfates and hence are soluble in water. Even Cs oxide is very soluble. Therefore, they readily react during phosphate stabilization and are chemically immobilized. We shall see in the case studies later in this chapter that such stabilization is very effective in a CBPC matrix.

Oxides of Ba and Sr are soluble in acidic and neutral aqueous solutions, and as seen from Fig. 17.1, like MgO, their solubility decreases as the pH increases on the alkaline side. Therefore, these two oxides may be easily stabilized in CBPC using the acid-base treatment.

Tc is a more complex isotope that is normally found in a quadrivalent state, but tends to oxidize to its heptavalent state as pertechnetate, which is easily leachable. As seen from Fig. 17.2, its oxidation potential in acidic and neutral environments is small; hence,

Fig. 17.2.



E_h -pH diagram of technetium. The shaded area shows stability region of water.

conversion from the penta- to heptavalent state is thermodynamically feasible. To retain the quadrivalent state in the CBPC waste form, the Ceramicrete process requires addition of a reductant [11] such as tin chloride ($SnCl_4$). Once this compound is reduced and microencapsulated in the phosphate matrix, it appears to be very stable and does not leach out even in accelerated long-term leaching tests. This leaching behavior will be discussed in detail in one of the case studies given later in this chapter.

17.3.3. Other Radioactive Isotopes

Many other isotopes are also found in radioactive wastes. The most important among them is radium (Ra). Because of its high aqueous solubility, Ra is also amenable to reaction with phosphates and forms less-soluble radium phosphate. The problem is that whether in soluble or insoluble form, Ra disintegrates into radioactive radon (Rn) gas that is released into the atmosphere. Fortunately, the half-life of Rn is very short (3.8 days); hence, it decays into daughter products that are solids. Thus, the stabilization matrix should microencapsulate Ra in such a manner that Rn, when emanated, cannot escape until its conversion to solid products. Entrapped in the phosphate matrix this way, Rn will disintegrate into its daughter product polonium (Po). As we shall see in the case study with stabilization of Fernald silo waste, the Ceramicrete matrix can convert Ra into its phosphates and then microencapsulate and reduce the Rn emanation significantly.

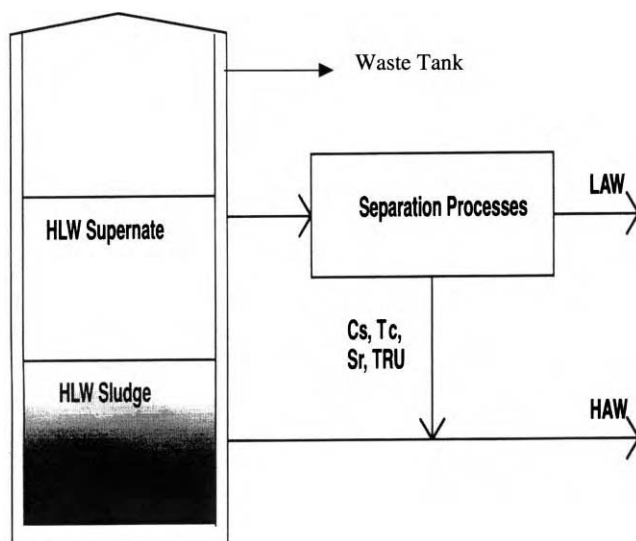
Other isotopes (I, Co, etc.) or their oxides and soluble salts can also be present. Stabilization of such contaminants is handled in a manner similar to the stabilization of hazardous metals, as discussed in Chapter 16, because most of them are sparsely soluble compounds.

17.3.4. Salt Waste Streams

Salts are components of several liquid and sludge waste streams that are a result of a plutonium separation process called PUREX (plutonium and uranium extraction process [12]), which produces highly acidic residues that are neutralized by alkaline sodium hydroxide for safe storage. The product is a liquid waste solution of sodium nitrate that contains mainly fission products and salts of Na, such as chlorides and sulfates. These are stored in buried tanks at various DOE sites such as Hanford and Savannah River. In places such as Idaho National Engineering and Environmental Laboratory in the US and P.R. Mayak in the Russian Federation, such a neutralization has not been undertaken, and hence the liquid waste is still highly acidic and rich in nitric acid. Over the years, the liquids in these tanks have settled, and it is now possible to separate sludge from the top supernatant. Both the supernatant and the sludge contain nitrates and radioactive and hazardous contaminants. Several separation processes have been developed to remove high-activity components [1], such as Tc and Cs, from the supernatant and to convert the bulk waste into a low-activity waste stream. The separated components may be added to the remaining sludge to produce a high-activity waste stream (see Fig. 17.3). Thus, the resultant waste stream is either smaller volume but high-activity waste (HAW) or large-volume, low-activity waste (LAW).

Many of the waste streams contain characteristically high concentrations of nonradioactive chlorides, sulfates, and nitrates of K, Na, and Ca, together with radioactive components. Stabilizing these waste streams poses two problems. The first is the large

Fig. 17.3.



Separation process of liquid tank waste and production of supernatant and sludge streams.

amount of water that needs to be removed prior to stabilization. The second is the salt content that is highly soluble in water, and waste forms made of these salts may easily leach into groundwater. These two problems complicate achieving economic stabilization and disposal of these waste streams. The case study discussed in this chapter shows that CBPC technology may provide a solution to stabilization of both the LAW and HAW streams with very high waste loading.

17.4.

WASTE ACCEPTANCE CRITERIA

Treated waste streams are stored at sites designated for low- or high-level waste forms. In the US, several WAC are in effect at each site, depending on the US Environmental Protection Agency's (EPA's) requirements on hazardous constituents of the waste (as discussed in Chapter 16), the Nuclear Regulatory Commission's (NRC's) and DOE's requirements on radioactive waste, and the requirements imposed by individual states where the waste is destined to be stored. In addition, the waste forms must satisfy several requirements to qualify them as suitable for transportation and interim storage. The overall requirements include passing various tests to demonstrate minimal leaching of radioactive and hazardous contaminants and salts, the absence of radiolytically generated hydrogen in the storage container, nonignitability of the waste form in the event of an accident, and waste form physical stability. These requirements translate into passing many standardized tests. The most common tests are briefly described below.

17.4.1. Leaching Tests

In addition to the TCLP test discussed in Chapter 16 for hazardous metals, three prominent leaching tests are used to evaluate the performance of waste forms for their safe transportation, disposal, or storage. Each test has particular significance in demonstrating the compliance of the waste form to the respective WACs. Therefore, depending on the conditions in which the waste forms are transported or stored, each site uses a different set of tests. Table 17.3 lists these tests, the recommending agency [13–16], and their significance, while Table 17.4 provides process parameters used in each test.

It is possible that the underground repository temperature will be somewhat high because of the storage of active isotopes that will radiate and heat up the atmosphere. This condition dictates that the tests be conducted at elevated temperature. In addition, because in the worst-case scenario, the waste form could be fractured in the repository in the event of a catastrophe such as an earthquake, the tests should also include leaching from a crushed waste form. For these reasons, as seen in Table 17.4, the PCT [14] requires that the waste form be crushed and leaching be conducted at an elevated temperature, typically 90°C. After testing for 90 days, the leachate is analyzed for components of the solid matrix to determine their rate of dissolution and thereby evaluate the durability of the matrix. Because this test was designed for glass, one looks for leaching of components such as Si,

Table 17.3.

Leaching Tests, Recommending Agency, Test Function, and Significance.

Test	Agency	Test Function and Significance
Toxicity characteristic leaching procedure (TCLP)	US EPA [13]	Measures the solubility of hazardous constituents. Used to determine if a waste is hazardous and to pass/fail the waste form for disposal
Product consistency test (PCT)	DOE [14]	Measures dissolution of structural elements of the waste form. Determines durability of radioactive waste forms in hot aqueous environment during storage
ANS 16.1	American Nuclear Society [15]	Measures bulk diffusivity of waste constituents. Evaluates long-term leaching of radioactive contaminants from low-level waste forms
MCC-1	American Society for Testing and Materials [16]	Evaluates long-term leaching rate of radioactive contaminants from high- and low-level radioactive waste forms

Na, and B from a glass waste form. If, on the other hand, this test is to be adopted for a CBPC waste form, such as Ceramicrete, one may look for Mg, K, and P as the matrix components. Thus, the PCT evaluates the durability of the matrix material, which is a result of the integrity of the individual elements within the matrix.

The PCT was designed for glass, and the test is tailored to producing crushed particles of a definite surface area, $0.02 \text{ m}^2/\text{g}$. This surface area poses problems for using PCT with any other waste forms. Other waste forms, particularly cement and CBPC, will crush into a different particle size distribution. Moreover, the repeated washing recommended in the test may wash out the matrix components. For these reasons, it is questionable whether this test is applicable to cement and CBPC waste forms. The test could be modified to avoid the repeated washing, but the definite surface area is essential because it is used in the calculation of the normalized leaching rate, which is a measure of the dissolution of the matrix elements. The problems arising out of the difficulty with the PCT in the CBPC waste forms are discussed in detail in the case studies given in Section 17.5.

Table 17.4.

Process Parameters Used in Leaching Tests.

Test	Sample Form	Leaching Temperature (°C)	Duration of Leaching	Leachate Medium
TCLP	Crushed	20	28 h	Aqueous acidic of pH = 5
ANS 16.1	Monolith	20	90 days	Deionized water
PCT	Crushed and washed to obtain a surface area of $0.02 \text{ m}^2/\text{g}$ in glass	90	90 days	Deionized water
MCC-1	Monolith	90	90 days	Deionized water

The ANS 16.1 [15] and MCC-1 [16] tests measure the mobility of radioactive contaminants that result from their diffusion within the waste forms. This diffusion transport may move the contaminants to the surface of the waste form and facilitate their leaching over a long time period. Thus, these tests essentially measure the extent of the long-term leaching of the contaminants. The diffusion transport is controlled by how well a contaminant atom is bound chemically to the reaction product. It will also depend on how big and heavy the molecule of the contaminant reaction product is: the bigger, the less mobile. In ANS 16.1, the diffusion constant of the individual contaminant is measured and expressed as the leaching index (LI, which is the negative logarithm of the diffusion constant). In MCC-1, the leaching rate, which is a result of the diffusion mechanism, is measured.

17.4.2. Physical Properties of Waste Forms

In addition to the superior leaching performance, the waste forms should pass certain tests to demonstrate the physical integrity during transportation and storage. Compressive strength and porosity of the waste forms are the most relevant properties that affect the performance of the waste forms during transportation and storage. A minimum compressive strength of 500 psi (3.5 MPa) is required to assure that the waste forms are not crushed under an overburden [17]. Open porosity should be minimal, because high porosity allows intrusion of groundwater, exposes a larger surface area within the waste form to groundwater, and facilitates leaching of the contaminants and matrix components.

17.4.3. Ignitability

For transport and interim storage of the waste forms, it is essential that the packaged waste be nonflammable. To test ignitability of waste packages, the EPA has recommended a test [18]. During this test, a mixture is made of equal weights of the waste form powder and softwood dust. This mixture is poured on a loop of Kanthal wire of prescribed radius and is ignited by passing an electrical pulse through the wire. As per the test guidelines, the time taken by the flame to consume the entire mixture is recorded and compared with the time taken when standard materials, such as potassium bromate and ammonium persulfate, are subjected to the same test.

17.4.4. Radiolysis

The radioactive isotopes such as the fission products irradiate β - and γ -rays within the waste form, while actinides will also emit α -rays. The resulting self-radiation of the matrix may decompose this water or organic compounds that are present in the waste form, and this reaction may lead to production of gases, such as hydrogen. These gases may pressurize the containers during storage of the waste forms. In particular, since a CBPC matrix contains bound water, it is vulnerable to such radiolysis effects. For this reason, a gas generation test on CBPC waste forms that contain transuranics and fission products is

needed. This test should demonstrate that gas generation is minimal and radiolysis is not a major concern in the CBPC radioactive waste forms. More details of this test may be found in Ref. [10]. Here, we provide a brief summary of the test.

In this test, preweighed samples (6.0–19.1 g) of the crushed waste form are loaded into 100-ml Pyrex beakers. These beakers are then placed in 300-cm³ stainless steel high-pressure vessels. The vessels are sealed and leak tested by evacuating each vessel and monitoring the pressure for ≈ 2 –3 h. The vessels are pressurized to approximately 1000 Torr with nitrogen, evacuated, and repressurized to the same pressure. The dead volume, i.e., the gas phase in each vessel, is determined from the volume of the vessel, the beaker, and the sample. The vessels are maintained in a once-through nitrogen atmosphere glovebox. Glovebox temperature is controlled at $25 \pm 3^\circ\text{C}$.

The vessels are sampled periodically by expanding the dead volume of each vessel into an evacuated manifold. The pressure of the vessels after expansion is recorded with a traceable pressure gauge. The vessels are isolated from the manifold, and the content of the manifold is expanded into an evacuated gas-sampling vessel. The content of the gas-sampling vessel is analyzed by gas chromatography for hydrogen, oxygen, nitrogen, and hydrocarbons depending on the content of the waste forms. The results are expressed as a *G* value, defined as the ratio of the radiation chemical yield to the energy absorbed, and expressed in terms of the number of molecules generated per 100 eV.

17.4.5. Pyrophoricity

Pyrophoricity is a property of metals and oxides of lower oxidation states, including radioactive ones, in which they spontaneously ignite during or after stabilization. If the waste also contains other combustible matter, it will burn. For a waste form to be safe from spontaneously igniting, the metals and oxides of lower oxidation states must be fully oxidized. To determine whether a particular waste is pyrophoric or not, one must identify the pyrophoric components within the waste. Such identification is done by analytical methods such as X-ray diffraction.

The acid–base reaction that forms the Ceramicrete waste forms also creates an oxidizing environment in which species of lower oxidation states are automatically converted to their fully oxidized states. Hence, pyrophoric components (such as Pu₂O₃) should be converted to their most stable and fully oxidized forms (such as PuO₂) that are no longer pyrophoric. Wagh *et al.* [10] have demonstrated such transformations in the Ceramicrete process by using surrogates of Pu (see the case study in Section 17.5.4).

17.5.

CASE STUDIES IN STABILIZATION OF RADIOACTIVE WASTE STREAMS

Unlike the case for hazardous waste streams using phosphates, the literature on stabilization of radioactive waste streams using CBPC processes is mainly limited to work

Table 17.5.

Acceptance Criteria and Examples of Ceramicrete Waste Forms that Meet the Criteria.

Criterion	Example Selected in this Article
Leaching of contaminants	Fission products: Tc, partitioned from high-level waste tanks, debris from contaminated pipes from K-25 plant at Oak Ridge; Cs, from salt supernatant and sludge, silico-titanates, and wastewater Radioactive components: Ra, Fernald silo waste, transuranics, simulated and actual Rocky Flats ash waste, wastewater
Leaching of salts	Simulated salt waste streams (both supernatant and sludge)
Leaching of matrix components	Simulated salt waste streams (both supernatant and sludge) from Hanford tanks
Physical properties	All of the above
Ignitability	Simulated salt waste
Radiolysis	U–Pu alloy, Pu-contaminated ash
Pyrophoricity	Oxidation of Ce_2O_3 to CeO_2

conducted at Argonne National Laboratory. Two other attempts have been made to immobilize uranium from contaminated sediments and groundwater using hydroxyapatite. Arey *et al.* [19] conducted batch equilibration experiments to evaluate the ability of hydroxyapatite to remove uranium from contaminated sediments at the Savannah River site of DOE. Their results showed that removal of U was due to secondary phosphate minerals that had solubility even lower than autunite ($Ca(UO_2)_2(PO_4)_2 \cdot 10H_2O$). The authors suggest formation of Al/Fe secondary phosphate. A similar approach was taken by Fuller *et al.* [20], who conducted a feasibility study of using apatite as an in situ permeable reactive barrier to uranyl ions. In batch experiments with different concentrations of hexavalent uranium, they found that >99.5% removal was possible by using synthetic hydroxyapatite. For a concentration <4700 ppm, surface adsorption of uranium on apatite was the main mechanism. For concentration >7000 ppm, a crystalline uranium phase was observed, and was identified as chernikovite [20]. Autunite also appeared at a molar ratio U : P \geq 0.2. These studies suggest that hexavalent uranium is amenable to stabilization by apatites.

In contrast to the two studies mentioned above, the work at ANL has been mainly in demonstrating treatment of a range of radioactive waste streams (both simulated and actual) from the US DOE complex in the Ceramicrete matrix. The reader is referred to Ref. [21] and additional references therein. In this section, we provide an overview in the form of case studies. Table 17.5 lists acceptance criteria and the corresponding case studies selected to demonstrate compliance by the Ceramicrete waste forms with those criteria.

17.5.1. Stabilization of Technetium

As discussed in Section 17.3.2, Tc is highly mobile in its soluble Tc^{7+} oxidation state. Also, because Tc^{7+} is volatile at high temperatures, waste streams that contain Tc must be stabilized at ambient temperatures.

Table 17.6.PCT and ANS 16.1 Results of Ceramicrete Specimens with Precipitated ^{99}Tc .

Concentration of ^{99}Tc (ppm) in waste form (waste loading)	41	164	903
Normalized leach rate (g/m^2 day) in PCT	0.07	0.1	0.036
Leachability index in ANS 16.1 test	14.6	13.3	14.6

Ceramicrete stabilization of ^{99}Tc , partitioned from high-level tank wastes, was demonstrated by Singh *et al.* [11]. The waste stream was a product of a complexation-elution process that separates ^{99}Tc from HLW, such as supernatant from salt waste tanks at Hanford and Savannah River. A typical waste solution generated during the complexation-elution process contains 1 M NaOH, 1 M ethylenediamine, and 0.005 M Sn^{2+} .

Waste forms were fabricated by solidifying partitioned Tc oxide in Ceramicrete. A small amount of SnCl_2 (0.5 wt%) was used to reduce Tc from its 7+ to its 4+ state; it was added in the binder mixture, which was blended with the waste and water to form the slurry. After mixing for 20 min, the slurry was allowed to set into a hard ceramic waste form. The hardened form was cured for 3 weeks and then subjected to leaching tests. Table 17.6 presents the PCT and ANS 16.1 tests on the waste forms. The normalized leach rate for ^{99}Tc , according to the PCT [14], was low even at 90°C. This rate is close to the value reported by Ebert *et al.* [22] for Tc leached from Defense Waste Processing Facility glasses. For all Tc loadings, the LI has been consistently high, between 13.3 and 14.6, higher than that of Cs and Sr in glass. The compressive strength of the waste forms was ≈ 30 MPa, and the waste forms were durable in an aqueous environment. These results demonstrate the effectiveness of a reducing environment in the Ceramicrete matrix.

In another study, researchers stabilized debris waste produced from scraping the internal surface of pipes from the Oak Ridge K-25 plant that was destined for demolition at one of the DOE sites [23]. The actual work was conducted at ANL.

Two waste streams were used in this study. Both were flaky materials, brown in color. The analysis of the first, provided by the sponsor, Bechtel Jacobs, showed a Tc level of 33,886 pCi/g (2020 ppm) and a U level of 107.05 pCi/g (40.1 ppm), with $^{233/234}\text{U}$ and ^{238}U as the major contaminants. It contained plastic washers and elongated pieces of materials and could not be crushed easily, so pieces were cut into smaller ones before stabilization. The second debris waste had some metal wire pieces, which were cut into smaller pieces. The analysis provided by the sponsor showed a Tc level of 1750 pCi/g (104 ppm) and U level of 107.05 pCi/g (96,000 ppm) with $^{233/234}\text{U}$ and ^{238}U as the major phases.

The composition of the produced waste forms is shown in Table 17.7. The powders and the waste were added to the water. Again, SnCl_2 was used as the reductant to suitably stabilize Tc. Because the amount of waste was small, the mixing was accomplished with a spatula by hand. The powder and water were mixed for 25 min so that it formed a pourable slurry. This slurry was then poured into plastic molds and was allowed to set; it set hard within hours, but was cured in air for 3 weeks so the samples gained nearly full strength and integrity.

Table 17.7.

Composition Used in Microencapsulation of K-25 Debris Waste Streams.

Components	Composition (wt%)
Ceramicrete binder	40
Class F fly ash	19.8
Waste	40
Tin chloride	0.2
Water	21% of total powders

The LIs in the ANS 16.1 study were found to be 12 and 17.7, respectively, which are high and consistent with values obtained for the other waste streams described above. Thus, this second example again proves the effectiveness of Ceramicrete with a reductant for stabilization of Tc.

17.5.2. Stabilization of Cesium

Several studies [24–26] have been reported on the stabilization of Cs with Ceramicrete, and various tests have been employed to estimate the leaching of Cs. These tests are listed in Table 17.8. (Detailed compositions of the first two waste streams may be found in Table 17.11.)

As may be seen from Table 17.8, Cs was added either as CsNO_3 or CsCl in the first three waste streams, whereas the form of Cs was not known in the last case, but certainly it was soluble because it was detected in wastewater. The TCLP results indicate that Cs, although added as nitrate or some other soluble form, is well immobilized. The LI is not as high as 18 that was reported by Bamba *et al.* [27] for a glass waste form, but it is certainly higher than the minimum of 6 expected from cement waste forms [28].

Table 17.8.

Studies on Cs Leaching and Results of Tests.

Waste	Form of Cs	Cs in Waste Form (ppm)	Test	Results	Reference
Salt supernatant	CsNO_3	14.9	TCLP	0.16 mg/l	[24]
Salt sludge	CsNO_3	4.3	ANS 16.1	LI of 8.72	[24]
Silicotitanate	CsCl	2790–3670	PCT	1.66–2.42 mg/l total leaching	[25]
			MCC-1	1.78–3.18 mg/l total leaching	[25]
Wastewater	Unknown ^{137}Cs	47.3 pCi/ml	TCLP	<0.2 pCi/ml	[26]

Langton *et al.* [25], who encapsulated silicotitanate waste in a Ceramicrete matrix, report that, in spite of good immobilization of Cs in the matrix, the leaching levels in the PCT and MCC-1 tests are significantly higher than in corresponding glass forms. They report that, in glass waste forms, the best leaching results are 0.011 mg/l in PCT and 0.8 mg/l in MCC-1 tests. Thus, the waste forms of silicotitanates produced by Langton *et al.* [25] did not perform well when compared with glass.

There are two reasons why Ceramicrete waste forms of silicotitanates did not perform as well as glass. PCT and MCC-1 tests are designed to test glass, not a ceramic. As discussed in Section 17.4, repeated washing of the crushed waste form with an ultrasonic bath is a requirement in these tests. This step results in particles with a surface area of $0.02 \text{ m}^2/\text{g}$ for glass, and this value is used in the calculation of the leaching levels. In practice, however, Wagh *et al.* [24] performed (see Section 17.5.7) detailed particle size measurements on supernatant waste forms and found that the same procedure, when used for Ceramicrete waste forms, produces much finer particles. The surface area of these particles is $6.67 \text{ m}^2/\text{g}$, which is 333.5 times greater than that for glass particles. This finding implies that, while conducting the PCT for Ceramicrete waste forms (and probably for cement waste forms), the actual surface area of the crushed waste forms should be measured and used in the calculations of the leaching levels.

The second problem concerns the composition of the matrix used in the silicotitanate waste forms. Basic Ceramicrete binder containing MgO and KH_2PO_4 was used to form the matrix without any modification. This binder composition gave a highly porous (23 vol%) matrix. Wagh *et al.* [28] reported that the Ceramicrete matrix incorporating any form of ash, particularly fly ash, performs better. Fly ash doubles the compressive strength of the waste forms and reduces the porosity significantly. There is some evidence that amorphous silica in fly ash forms silicophosphate phases, which provide much better strength and lower porosity in the matrix. Thus, Langton *et al.* [25] would probably have seen better performance of the waste form, both in the PCT and MCC-1 test, if they had used ash in their composition.

17.5.3. Stabilization of Radioactive Elements

As mentioned in Section 17.3.1, retention of quadrivalent actinide oxides within the phosphate matrix is not a major issue because these oxides are insoluble in water, and all that is needed is their microencapsulation by the phosphate components of the matrix. This was demonstrated in a number of studies on UO_2 and PuO_2 and their surrogate CeO_2 . If the actinides are found in a trace amount in the waste, their chemical form is not so important because the phosphate matrix immobilizes them very effectively. For example, the wastewater in the case study given in Section 16.3.2.2 contained 32 pCi/ml of ^{238}U and 0.6 pCi/ml of ^{235}U . The ANS 16.1 tests conducted on the waste forms with 18.6 pCi/g loading of combined U in the waste form showed that the leaching index was 14.52. TCLP tests also showed that levels in the leachate were below the detection limit of 0.2 pCi/ml. This implies that microencapsulation of trace-level U is very effective in the Ceramicrete matrix.

As was mentioned before, Arey *et al.* [19] conducted batch equilibration experiments to evaluate the ability of hydroxyapatite to remove uranium from contaminated sediments at the Savannah River Site of DOE and showed that removal of U was due to secondary phosphate minerals that had solubility even lower than autunite ($\text{Ca}(\text{UO}_2)_2(\text{PO}_4)_2 \cdot 10\text{H}_2\text{O}$). The authors suggest formation of Al/Fe secondary phosphate. A similar conclusion was reached by Fuller *et al.* [20], who showed that uranyl ions can be removed by using hydroxyapatite.

17.5.4. Stabilization and Pyrophoricity of Actinides in High Concentrations

To demonstrate that actinide oxides, even at high concentrations, are encapsulated very effectively in the Ceramicrete matrix, Wagh *et al.* [10] conducted tests on surrogate waste streams. They simulated Pu-containing combustion residue from Rocky Flats by introducing CeO_2 as a surrogate of the actinide oxides. The level of CeO_2 in the waste was 11.3 wt%. The major components were silica, 41.3 wt%; alumina, 3.3 wt%; CaO , 4.01 wt%; Fe_2O_3 , 5.48 wt%; MgO , 4.41 wt%; and C, 18.5 wt%. Wagh *et al.* conducted TCLP for Ce (though this is not a regulatory requirement) and ANS 16.1 leaching tests on the waste forms and found that the TCLP leachate level was below the detection limit of 0.05 mg/l, and the LI was 19.7. These numbers clearly indicate that Ceramicrete is a superior microencapsulating matrix for the immobilization of actinide oxides.

Often, actinide oxides are found in a lower oxidation state, such as oxides in the trivalent state (for example, U_2O_3 or Pu_2O_3). The solubility of such oxides is higher than that of their counterparts in the fully oxidized state. Once dissolved, they are likely to be oxidized in the aqueous phosphate slurry during formation of the stabilized matrix into insoluble fully oxidized compounds; this likelihood may be confirmed with reduction–oxidation diagrams of actinide–water systems (see, for example, Ref. [9], pp. 208–210). Wagh *et al.* [10] tested the likelihood by introducing Ce, the surrogate of U and Pu, as Ce_2O_3 . The X-ray diffraction patterns from the waste form did not show any evidence of the presence of Ce_2O_3 , but contained only CeO_2 .

This conversion of actinide oxides of lower oxidation states into fully oxidized forms has a great advantage. The actinides of lower oxidation states are pyrophoric. Once converted into their fully oxidized form and encapsulated in the phosphate matrix, they are not spontaneously combustible and, hence, are safe for transportation and storage. Thus, because of this oxidation, the phosphate matrix removes the pyrophoricity during the stabilization process.

17.5.5. Stabilization of Radium

Wagh *et al.* [29] demonstrated that radium-rich wastes from Fernald silos can be stabilized in the Ceramicrete matrix. The total specific activity of all the isotopes in the waste was $3.85 \mu\text{Ci/g}$, of which radium (^{226}Ra) alone accounted for $0.477 \mu\text{Ci/g}$. This finding

Table 17.9.

Specific Activities in Ra-Containing Waste (as-received), Waste Form (calculated), and TCLP Leachate.

Activities	Alpha	Beta	Total
In the waste as-received ($\mu\text{Ci/g}$)			
Total	—	—	3.85
^{226}Ra	—	—	0.477
Calculated in the waste form ($\mu\text{Ci/g}$)			
Total	—	—	2.06
^{226}Ra	—	—	0.255
Specific activities in TCLP leachate (pCi/ml)	25 ± 2	98 ± 10	221 ± 22^a

^a As an approximation, we have assumed gamma and beta activities to be equal.

indicated that Rn gas, which acts as a daughter product of radium in the waste, could pose a serious handling problem during this study. To avoid Rn contamination in the laboratory, the waste form samples were made in a glovebox, with an actual waste loading of 66.05 wt%. The samples were subjected to the TCLP test, and the leachate was analyzed for its specific activity. The data obtained were used to estimate the level of encapsulation of Ra in the matrix.

As shown in Table 17.9, the alpha activity in the leachate was 25 ± 2 pCi/ml, and the beta activity was 98 ± 10 pCi/ml. These activities are small when compared with the activities of their counterparts in the waste, which were in $\mu\text{Ci/g}$. The very low activity in the leachate was attributed to the efficient stabilization of Ra as insoluble radium phosphate in the waste form. In particular, because Ra is water soluble, the leachate would provide a pathway for it, but the levels in the leachate are only in pCi/ml and, hence, much lower than the levels in the waste. This finding implies that radium and most other isotopes are stabilized in the waste forms. Thus, the Ceramicrete process is a good method to arrest leaching of even the most soluble Ra.

17.5.6. Evaluation of Radiolysis and Gas Generation

The Ceramicrete matrix material, $\text{MgKPO}_4 \cdot 6\text{H}_2\text{O}$, contains 6 mol of water for every mole of the magnesium potassium phosphate. Radiolytic decomposition of the water and any organic compounds present in the waste may pressurize sealed containers during storage of the waste forms. For this reason, Pu-containing waste forms were subjected to gas generation tests as per the procedure summarized in Section 17.4.4. The results are given in Table 17.10 in terms of G values, i.e., the ratio of the radiation chemical yield to the energy absorbed, expressed in terms of the number of molecules generated per 100 eV.

Results on the first four examples given in Table 17.10 are from the literature [10, 30–32]. The last two provide the results on Ceramicrete waste forms. The transuranic (TRU) combustion residue was obtained originally from Rocky Flats. It was fully calcined for safe transport to ANL. Therefore, all organics and combustibles were completely incinerated, and that step enhanced the Pu concentration. The U–Pu oxide mixture was a

Table 17.10.

Radiolysis Yield in Various Conditions and in Ceramicrete.

Material Tested	G(H ₂), mol H ₂ /100 eV
²³⁹ Pu in water	1.6
Tritiated water in concrete	0.6
FUETAP concrete	0.095
Hanford acid waste in FUETAP cement	0.43
Transuranic ash in Ceramicrete with 7.87 wt% Pu in ash	0.1
U–Pu alloy in Ceramicrete with 5.2 wt% Pu	0.13

result of corrosion of a U–Pu alloy [10]. Both the TRU ash and U–Pu alloy were stabilized in the Ceramicrete waste forms.

As Table 17.10 indicates, the *G* values in Ceramicrete waste forms are lower than in most other grout systems and comparable to that in FUETAP (Formed Under Elevated Temperature and Pressure) concrete. These results indicate that the gas yield is minimal in the Ceramicrete waste forms.

17.5.7. Salt Stabilization

Unlike Portland cement, the Ceramicrete slurry sets into a hard ceramic even in the presence of salts such as nitrates and chlorides; hence, the Ceramicrete process has a great advantage over conventional cement technology with respect to the stabilization of some difficult waste streams, such as those from Hanford and Savannah River tanks. Wagh *et al.* demonstrated this advantage in several studies, wherein they produced monolithic Ceramicrete solids by using concentrated sodium nitrate and sodium chloride solutions in place of water to stabilize the waste streams. Details of some of these studies may be found in Ref. [21].

In a detailed study, Wagh *et al.* [24] stabilized simulated tank waste streams, i.e., the supernatant and sludge discussed in Section 17.3.4 (see also Fig. 17.3). The solids content in the supernatant was higher because it contained more dissolved solids. Both streams were highly alkaline and contained a significant amount of NaNO₃. The waste form compositions and properties are listed in Table 17.11. Details may be found in Ref. [24]. Compared to earlier studies, the waste loading was conservative in this study. The waste forms were dense ceramics with smooth surfaces, indicating some formation of glassy phase. These waste forms were subjected to various leaching tests (TCLP, PCT, and ANS 16.1).

The densities of the final waste forms were 1.70 and 1.9 g/cm³, and the compression strengths ranged from 1400 to 1900 psi (9.8–11.9 MPa) for both the chloride and nitrate waste forms. These values are significantly higher than the NRC land disposal requirement of 500 psi (3.5 MPa) for cement-based waste forms [17]. Thus, salt waste forms of the CBPC at high loadings are relatively dense hard materials that are suitable for salt waste

Table 17.11.

Details of Salt Waste Streams and their Waste Forms.

Waste Streams and Waste Forms	Supernatant	Sludge
Waste stream details		
Form	Liquid	Sludge
Solids content (wt%)	53.4	25.2
Density (g/cm ³)	1.4	1.3
pH	13.7	12.8
Na content (wt%)	17	3.3
NO ₃ content (wt%)	11.5	7.7
Waste form properties		
Loading (wt%)	39.8	32
Density (g/cm ³)	1.9	1.7
Open porosity (vol%)	7.9	4.5

stabilization. The TCLP performance was also excellent. The results showed that the leaching levels were well below the EPA's UTS limits for all of the contaminants.

Singh *et al.* [33] patented a macroencapsulation technique in which waste forms are coated with a polymer for successful retention of Cl and NO₃. This macroencapsulation of the waste forms reduced the nitrate leaching further in the ANS 16.1 test. Details may be found in Ref. [5].

Recently, Wagh *et al.* [25] conducted a comprehensive study on simulated supernatant and sludge streams that mimicked many of the salt waste streams at the DOE site. Table 17.11 provides details about the waste streams that were used, and the waste forms that were produced from these waste streams. The solids content was higher in the supernatant than in the sludge because the sludge had more dissolved solids. Both streams were highly alkaline and contained a significant amount of NaNO₃. When compared with earlier studies, the waste loading in this study was conservative. The waste forms were dense ceramics with smooth surfaces, indicating some formation of glassy phase.

As in all the waste forms discussed above, the TCLP results showed excellent retention of the hazardous contaminants in the matrix (Cd, Cr, Ag, Pb, and Zn) for both waste forms. The leaching levels for these contaminants were either below the detection limit or well below the UTS limits. While conducting this test for the sludge waste form, the investigators also tested leaching of Na, which is a bulk component, and Cs and Re, which are used as surrogates of radioactive Cs and Tc.

The Na level in the original waste was 3.26 wt%, and its level in the waste form was 1.08 wt%. In the TCLP leachate, it was only 634 mg/l. This partial Na immobilization may be due to the formation of less soluble compounds, such as MgNaPO₄·*n*H₂O, and their subsequent microencapsulation within the matrix. It is very difficult to identify such compounds by X-ray diffraction studies, because they are invariably glassy phases and are only represented by broad humps in the X-ray diffraction pattern.

The PCT was conducted on crushed waste form samples from supernatant and sludge. The fineness of the particles, compared with what is prescribed in the test procedure (see Section 17.4.1), was recognized from the beginning, and hence the actual measured

Table 17.12.Normalized Leaching Rates ($\text{g}/\text{cm}^2 \text{ day}$) for the Matrix Components in the Supernatant and Sludge Waste Forms.

Waste Form	Matrix Components				
	Mg	K	P	Na	NO_3
Supernatant	1.4×10^{-6}	0.009	0.006	0.008	0.077
Sludge	0.000111	0.00855	Not done	0.02	0.024

surface area was used in the calculation of leaching rates. The results are presented in Table 17.12. These normalized leaching rates are low and well below the $0.16\text{--}0.4 \text{ g}/\text{cm}^2 \text{ day}$ suggested as the WAC for borosilicate glass waste forms for storage at Yucca Mountain or the WAC of $0.28 \text{ g}/\text{cm}^2 \text{ day}$ for the Hanford disposal facility for LAW [34]. Thus, the overall performance of the waste form in the PCT is very good.

Leaching of Mg is much lower than leaching of other components. This might be because, overall, Mg is not as mobile as K, Na, or NO_3 . Moreover, some of the MgO remains unreacted in the waste form, and its solubility in alkaline water is extremely low. Both the supernatant and sludge waste streams were highly alkaline, and hence, the waste forms must have increased the alkalinity of the leachate water. This alkalinity will reduce the leaching level of Mg.

The leaching rates of Na and NO_3^- must be coupled. If Na forms less soluble compounds such as $\text{MgNaPO}_4 \cdot n \text{H}_2\text{O}$, NO_3^- must be released into the solution and should form its own compounds. The X-ray diffraction studies conducted on nitrate waste streams have indicated the presence of KNO_3 , implying at least a partial conversion of NaNO_3 to KNO_3 [24]. The solubility of KNO_3 is $27.7 \text{ g}/\text{l}$, whereas that of NaNO_3 is $47.7 \text{ g}/\text{l}$. This may partially explain the lower solubility of NO_3 , but may not be the only mechanism. Detailed investigations are needed to find additional stabilization mechanisms.

In addition to the TCLP and PCT tests, the ANS 16.1 test was conducted on the waste forms for Pb, Cr, and Cs, and also for Na, NO_3^- , and NO_2^- to gain insight into leaching of Na and the anions. The test was conducted for 120 h. The results are presented in Table 17.13.

Table 17.13.

Waste Content and LI for Contaminants and Bulk Components of Supernatant Waste Form.

	Contaminants in ppm			Bulk Components in wt%		
	Pb	Cr	Cs	Na	NO_2^-	NO_3^-
Waste content	37	937.6	11.37	17.2	7.73	11.49
Leaching index	10.1	12	8.72	7.07	7.17	6.98

We may compare the LI values in Table 17.13 with similar earlier tests reported in the literature. Gilliam *et al.* [35] stabilized gaseous diffusion plant waste that contained 14 ppm of technetium (^{99}Tc) in cement grout. Long-term leaching studies showed an LI of 6; compared with that, the LI values in all the cases presented here are higher. The highest among them are for the hazardous metals Pb and Cr. Given that an increase in the LI by one number is essentially a reduction in the diffusion constant by a factor of 10, Ceramicrete would appear to be very effective for stabilizing salt waste streams.

Though the leaching index, which is the negative logarithm of the diffusion constant, is a material property, the actual leaching levels will increase with the surface area exposed to the leaching environment. Small samples with a larger ratio of surface area to volume will leach a higher fraction of the contaminants. Wagh *et al.* [24] estimated that the fraction that will leach from a laboratory-size sample will be five times that from a 55-gal drum. This finding implies that the actual fraction that will leach from a 55-gal waste form is reduced by a factor of five because of the surface-to-volume ratio. This observation is very important when estimating leaching levels of Na, NO_3^- , and NO_2^- .

17.5.8. Ignitability of Salt Waste Forms

In the case of salt waste forms, ignitability is a major concern because salt waste streams containing NaNO_3 are ignitable. The ignitability test was conducted on the nitrate waste forms, according to the EPA oxidation test procedure [18] described in Section 17.4.3. A mixture of crushed nitrate waste form that contained 40 wt% NaNO_3 was prepared with the waste form powder and soft wood dust, each in the weight ratio of 1 : 1. The mixture was ignited by passing an electrical pulse through a Kanthal loop. The time taken by the flame to consume the entire mixture was recorded.

The results of the test are presented in Table 17.14. The data indicate extremely rapid burning of mixtures of sawdust and known flammable salts, such as potassium bromate and ammonium persulfate. The mixture of surrogate waste and saw dust also burns rapidly, although not as fast as the mixtures of the standard materials. The time for burning of a waste form and the sawdust mixture, however, is > 8 min, much longer than the time for a standard mixture of ammonium persulfate and sawdust (49 s) or for the waste (87 s). This finding implies that salt wastes solidified in phosphate ceramic are not ignitable and, hence, would not require any special packaging. Because phosphate ceramics are

Table 17.14.

Combustion Time for Various Mixtures Subjected to Ignitability Test.

Mixture	Combustion Time (s)
Potassium bromate and sawdust	19
Ammonium persulfate and sawdust	49
Surrogate waste and sawdust	87
Waste form and sawdust	> 480

inorganic and nonignitable, they inhibit the spread of flames and are excellent solidification media for flammable salt wastes.

17.6.

MACROENCAPSULATION OF LARGE OBJECTS

The demolition of buildings and other structures used in weapons production, along with disposal of the resultant radioactively contaminated debris, is a major task for DOE contractors. For example, at Oak Ridge in Tennessee, at the K-25 and K-27 plants alone, the footprints of the buildings being demolished are 1,630,000 and 383,000 ft², and these plants contain loose and fixed contamination. This activity has created a pressing need for the permanent, but safe and environmentally sound disposal of thousands of large converters, compressors, coolers, pumps, valves, motors, tubing, and piping sections that are radiologically contaminated with low to highly enriched uranium. One way to safely dispose of these components is to macroencapsulate them in a dense nonleachable matrix and send them to geologic repositories for burial. The Ceramicrete matrix provides an excellent encapsulating matrix for this purpose.

To demonstrate this capability, Wagh *et al.* group worked with Bechtel Jacobs Co., the contractor at Oak Ridge, and conducted a feasibility study. The study comprised macroencapsulation of internally contaminated pipe sections [23].

Two cast iron pipe sections (Schedule 40, carbon steel), 4.5 in. (11 cm) diameter and 7 in. (18 cm) long, were used. Both ends of the pipes were sealed by welding cast iron round plates on them. They were contaminated internally with one of the debris wastes described in Section 17.5.1.

The Ceramicrete matrix formulation used in the macroencapsulation test contained 5 wt% glass fiber (1/2-in. long), which arrested any crack propagation within the material that might be a result of any mismatch between Ceramicrete and the pipe section. The high percentage of glass fiber could be added only because, unlike cement waste forms, the Ceramicrete slurry becomes very thin during mixing. KH₂PO₄, one of the ingredients used in Ceramicrete, helps achieve good dispersion of the fiber strands. Addition of fibers did not alter the already high compressive strength of 13,000 psi (90 MPa). The flexural strength and fracture toughness of the resultant product are 1500 psi (10.5 MPa) and 0.65 MPa·m^{1/2}, respectively. These values are at least two times that of conventional cements. The density of Ceramicrete is 1.8 g/cc, which indicates that Ceramicrete is 30 wt% lighter than conventional Portland cement. Due to a slight expansion of Ceramicrete during setting, no shrinkage cracks were generated during macroencapsulation. Rusting of the iron pipe sections was arrested successfully by macroencapsulating them in a dense Ceramicrete matrix. No leaching of Fe due to rusting of pipes was detected in the 90-day immersion tests (ANS 16.1) on macroencapsulated specimens, but unprotected pipes rusted profusely in such leaching tests at a rate of 4.33 g/cm² day. The neutral matrix of Ceramicrete is also likely to protect the pipes from corrosion in near neutral groundwater, as compared to conventional cement, which is more alkaline. In the

same test, leaching levels of U and Tc were also below detection limits for most of the leaching periods, and hence, the LI could not be calculated. This result implies that practically no leaching of any contaminants occurred. Thus, the Ceramicrete matrix, because of its neutral behavior, does not rust encapsulated iron and may thus be an ideal matrix material for macroencapsulation of iron debris. Being highly alkaline, cement will corrode iron eventually and is not a suitable material for such applications.

17.7.

OTHER NUCLEAR APPLICATIONS

Because Ceramicrete, is a superior grouting material, it is being considered for many other applications in nuclear industries. One such application is as a nuclear shield; this application is being promoted in a program among ANL, Eagle Picher Industries, and two Russian institutions (Spektr Conversion at Snezhinsk and Russian Federal Nuclear Center at Sarov). In the first major evaluation of Ceramicrete as a nuclear shield, tests have been conducted on boron- and iron-doped material [36]. Results have been very favorable, and now, nuclear shield applications are being demonstrated in full scale.

17.8.

CONCLUSIONS

The various case studies discussed in this paper demonstrate that CBPCs are a very versatile material for the stabilization of hazardous and radioactive waste streams. CBPCs chemically immobilize and microencapsulate the contaminants, and reduce leaching to levels that meet WAC at DOE sites. They are also suitable for the macroencapsulation of various contaminated objects.

Several additional favorable properties of CBPCs make them an even better candidate for stabilization. The waste form is a dense matrix, generally with very good mechanical properties. Also it is nonleachable, does not degrade over time, is neutral in pH, converts even flammable waste into nonflammable waste forms, performs well within acceptable levels in radiolysis tests, and can incorporate a range of inorganic waste streams (solids, sludge, liquids, and salts).

The CBPC technologies are not targeted for stabilizing organics, although several tests with Ceramicrete have shown that it performs better than other methods. Organics are generally destroyed by combustion or other chemical means, and their volume is reduced. The resultant ash or waste can then be immobilized in Ceramicrete.

Unfortunately, for two reasons the full potential of CBPCs has not yet been exploited in the DOE complex. In spite of its high technical success, this technology is only one decade old and is experiencing growing pains. Considerable familiarity is needed before a DOE contractor will accept the technology as a low risk venture. Also the technology has been

developed at ANL, which does not have the weapons waste with which the technology could be realistically demonstrated on site. Only good cooperation between ANL and other DOE sites will advance this technology.

REFERENCES

1. N. Schroeder, S. Radinski, J. Ball, K. Ashley, S. Cobb, B. Cutrell, J. Adams, C. Johnson, and G. Whitner, Technetium partitioning for the Hanford tank waste remediation system: anion exchange studies for partitioning technetium from synthetic DSSF and DSS simulants and actual Hanford wastes (101-SY and 103-SY) using Reillex™-HPQ resin, Annual Report, LA-UR-95-4440 (Los Alamos National Laboratory, 1995).
2. *Incineration of Radioactive Waste*, ed. A.J. van Loon (Kluwer Academic Publishers, London, 2004).
3. National Academy of Science *Glass as a Waste Form and Vitrification Technology: Summary of an International Workshop* (The National Academies Press, Washington, DC, 1997).
4. G. Dole, G. Rogers, M. Morgan, D. Stinton, J. Kessler, S. Robinson, and J. Moore, Cement-based radioactive waste hosts formed under elevated temperatures and pressures (FUETAP concrete) for Savannah River Plant high-level waste, Report No. ORNL/TM-8579 (Oak Ridge National Laboratory, 1983).
5. National Academy of Sciences *Research Needs for High-Level Waste Stored in Tanks and Bins at US Dept. of Energy Sites* (National Research Council, Washington, DC, 2001).
6. J.R. Connor, *Chemical Fixation and Solidification of Hazardous Wastes* (Van Nostrand Reinhold, New York, 1990).
7. G. McCarthy, W. White, D. Smith, A. Lasaga, R. Ewing, A. Nicol, and R. Roy, ed. R. Roy, Mineral Models for Crystalline Hosts for Radionuclides in Radioactive Waste Disposal, The Waste Package, vol. 1. (Pergamon Press, New York, 1982), pp. 184–232.
8. *Handbook of Radioactive Nuclides*, ed. Y. Wang (Chemical Rubber Company, Cleveland, 1969), pp. 34–59.
9. M. Pourbaix, *Atlas of Electrochemical Equilibria in Aqueous Solutions* (NACE/Cebelcor, Houston/Brussels, 1974).
10. A.S. Wagh, R. Strain, S.Y. Jeong, D. Reed, T. Krause, and D. Singh, “Stabilization of Rocky Flats Pu-contaminated ash within chemically bonded phosphate ceramics,” *J. Nucl. Mater.*, **265** (1999) 295–307.
11. D. Singh, A.S. Wagh, and S. Jeong, Method for producing chemically bonded phosphate ceramics and for stabilizing contaminants encapsulating therein utilizing reducing agents, US Patent 6,133,498, 2000.
12. M. Benedict, T. Pigford, and H. Levi, *Nuclear Chemical Engineering*, 2nd ed. (McGraw Hill, New York, 1981), p. 467.
13. US Environmental Protection Agency, Treatment standards for hazardous debris, 40CFR Part 268.45, 1994.
14. American Society for Testing of Materials, Standard test methods for determining chemical durability of nuclear, hazardous, and mixed waste glasses: the product consistency test, ASTM C 1285-97, 1997.
15. American Nuclear Society, American National Standard Measurement of the leachability in solidified low-level radioactive wastes by a short term test procedure, Method ANSI/ANS 16.1-1986, 1986.
16. American Society for Testing of Materials, Standard test method for static leaching of monolithic waste forms for disposal of radioactive waste, ASTM C 1220-98, 1998.
17. J. Mayberry, L. Harry, and L. Dewit, *Technical Area Status Report for Low-Level Mixed Waste Final Forms*, DOE/MWIP-3, Vol. 1. (US Department of Energy, 1992).
18. Guidelines for Classification and Packing Group Assignment of Division 5.1 Materials, CFR CH1 (10-1-95 Ed.), Appendix F to Part 173, 1995.
19. J. Arey, J. Seaman, and P. Bertsch, “Immobilization of uranium in contaminated sediments by hydroxyapatite addition,” *Environ. Sci. Technol.*, **33** (1999) 37–342.
20. C. Fuller, J. Bargar, J. Davis, and M. Piana, “Mechanisms of uranium interactions with hydroxyapatite: implications for groundwater remediation,” *Environ. Sci. Technol.*, **36** (2002) 158–165.
21. A.S. Wagh, D. Singh, and S.Y. Jeong, “Chemically bonded phosphate ceramics,” in *Handbook of Mixed Waste Management Technology*, ed. C. Oh (CRC Press, Boca Raton, LA, 2001), pp. 6.3-1–6.3-18.

22. W.L. Ebert, S.F. Wolf, and J.K. Bates, "The release of technetium from defense waste processing facility glasses," *Mater. Res. Soc. Symp. Proc.*, **412** (1996) 221–227.
23. J. Lichtenwalter and R.S. Seigler, Macroencapsulation of gaseous diffusion plant equipment for burial, *Proc. Spectrum Conf., Amer. Nucl. Soc.*, 2002.
24. A.S. Wagh, M.D. Maloney, G.H. Thomson, and A. Antink, Investigations in Ceramicrete stabilization of Hanford tank wastes, *Proc. Waste Management '03, Tucson, AZ*, 2003.
25. C. Langton, D. Singh, A. Wagh, M. Tlustochowicz, and K. Dwyer, Phosphate ceramic solidification and stabilization of cesium-containing crystalline silicotitanate resins, *Proc. 101st Annual Meeting of the Amer. Ceram. Soc., Indianapolis*, 1999.
26. A.S. Wagh, S.Y. Jeong, D. Singh, R. Strain, H. No, and J. Wescott, Stabilization of contaminated soil and wastewater with chemically bonded phosphate ceramics, *Proc. Waste Management 97, Tucson*, 1997.
27. T. Bamba, H. Kamizono, S. Nakayama, H. Nakamura, and S. Tashiro, Studies of glass waste form performance at the Japan Atomic Energy Institute, in *Performance of High Level Waste Forms and Engineered Barriers Under Repository Conditions*, International Atomic Energy Agency Report IAEA-TECDOL-582, 1991, pp. 165–190.
28. A.S. Wagh, S.Y. Jeong, and D. Singh, High strength phosphate cement using industrial byproduct ashes, *Proc. First Intl. Conf. on High Strength Concrete, Kona, HI*, eds. A. Aziznamini, D. Darwin, C. French, 1997, pp. 542–553.
29. A.S. Wagh, D. Singh, S.Y. Jeong, D. Graczyk, and L.B. TenKate, Demonstration of packaging of Fernald silo I waste in chemically bonded phosphate ceramic, *Proc. Waste Management 99, Conditioning of Operational and Decommissioning Waste, Tucson*, February 28–March 4, 1999.
30. N.E. Bibler and E.G. Orebaugh, Radiolytic gas production from tritiated waste forms—gamma and alpha radiolysis studies, Report No. DP-1459 (Savannah River Laboratory, 1977).
31. L.R. Dole and H.A. Friedman, Radiolytic gas generation from cement-based waste hosts for DOE low-level radioactive wastes, Report No. CONF-860605-14 (Oak Ridge National Laboratory, 1986).
32. B. Siskind, Gas generation from low-level waste: concerns for disposal, Report No. BNL-NUREG-47144 (Brookhaven National Laboratory, 1992).
33. D. Singh, A. Wagh, and K. Patel, Polymer coating for immobilizing soluble ions in a phosphate ceramic product, US Patent 6,153,809, 2000.
34. G. Smith, D. Bates, R. Goles, I. Greenwood, R. Lettan, G. Piepel, M. Schweiger, H. Smith, M. Urie, and J. Wagner, Vitrification and product testing of C-104 and AZ-102 pretreated sludge mixed with flowsheet quantities of secondary waste, Report No. PNNL-13452 (Pacific Northwest National Laboratory, 2001), 92 pp.
35. T.M. Gilliam, R.D. Spence, W.D. Bostick, and J.L. Shoemaker, Solidification/stabilization of technetium in cement-based grouts, *Proc. 2nd Annual Gulf Coast Haz. Substance Research Center Symp., Solidification/Stabilization Mechanisms and Applications, Beaumont, TX* February 15–16, 1990.
36. M. Gorbotenko and V. Yuferev, Ceramicrete as a means for radioactive waste containment and nuclear shielding, Reports by All-Russian Research Institute of Experimental Physics, Sarov, Russian Federation, Reports to Argonne National Laboratory (unpublished), 2002.

This page is intentionally left blank

Dental Cements and Bioceramics

We summarized the early development of zinc-based CBPC dental cement in Chapter 2. The early development of zinc phosphate cement was, in fact, motivated by the need for good dental cements. The reader is referred to the book by Wilson and Nicholson [1] for a detailed account. In recent years, the use of CBPCs has been extended to bone substitutes. In situ setting bone cements are needed to fill large gaps within a skeletal system, those caused by trauma or tumors. Bone from another part of the body (autografting) or bone from a cadaver (allografting) are alternatives, but have their own disadvantages. The former requires harvesting bone from another part within the body and then using that material to fill the gap. This often leads to complications in wound healing and an inadequate supply of bone to fill the gap. Allografting may lead to rejection of the substitute by the host body, and runs the risk of causing AIDS or other infectious diseases. Artificial ceramics, if developed, may provide excellent alternative [2].

Considerable development has occurred on sintered ceramics as bone substitutes. Sintered ceramics, such as alumina-based ones, are unreactive materials as compared to CBPCs. CBPCs, because they are chemically synthesized, should perform much better as biomaterials. Sintered ceramics are fabricated by heat treatment, which makes it difficult to manipulate their microstructure, size, and shape as compared to CBPCs. Sintered ceramics may be implanted in place but cannot be used as an adhesive that will set in situ and form a joint, or as a material to fill cavities of complicated shapes. CBPCs, on the other hand, are formed out of a paste by chemical reaction and thus have distinct advantages, such as easy delivery of the CBPC paste that fills cavities. Because CBPCs expand during hardening, albeit slightly, they take the shape of those cavities. Furthermore, some CBPCs may be resorbed by the body, due to their high solubility in the biological environment, which can be useful in some applications. CBPCs are more easily manufactured and have a relatively low cost compared to sintered ceramics such as alumina and zirconia. Of the dental cements reviewed in Chapter 2 and Ref. [1], plaster of paris and zinc phosphate

cements are the only chemically bonded materials. The rest are sintered ceramics and glasses.

The biocompatible CBPC development has occurred only in the last few years, and the recent trend has been to evaluate them as biocompatible ceramics. After all, biological systems form bone and dentine at room temperature, and it is natural to expect that biocompatible ceramics should also be formed at ambient temperature, preferably in a biological environment when placed in a body as a paste. CBPCs allow such placement. We have discussed such calcium phosphate-based cements in Chapter 13. Calcium-based CBPCs, especially those constituting hydroxyapatite (HAP), are a natural choice. HAP is a primary mineral in bone [3], and hence calcium phosphate cements can mimic natural bone. Some of these ceramics with tailored composition and microstructure are already in use, yet there is ample room for improvement. This Chapter focuses on the most recent biocompatible CBPCs and their testing in a biological environment. To understand biocompatible material and its biological environment, it is first necessary to understand the structure of bone and how it is formed.

18.1.

BONE AS A COMPOSITE MATERIAL

Bone is composed of living cells in a ceramic matrix. The matrix itself consists of inorganic (ceramic) and organic matter, along with water. The composition and structure of bones are very complex, and simulating a material similar to bone by artificial means is very difficult. CBPCs, however, hold promise toward producing materials similar to bone in composition, if not in exact structure.

Typically, bone has a solid outer portion called “cortical bone” and a porous inner part called “cancellous bone.” The amounts of each vary with location in the body. The cortical bone is a ceramic containing calcium compounds and viscous liquids, a protein called “collagen”, and an organic polymer. In addition to HAP, bone consists of calcium carbonate and calcium phosphate. HAP is 69 wt.% of total calcium phosphate compounds [4]. Part of the Ca in these compounds is substituted by Na, K, Mg, and Sr. Hydroxyl ions in the HAP are also substituted by F, CO₃, or Cl, which makes the apatite a fluoroapatite, dahllite or chloroapatite, respectively. These substitutions are considered to play significant roles in the structure and mechanical properties of bones.

Collagen is the major protein in the body, 13 types of which have been identified, based on their peptide chains. Collagen fibers form the connective tissues, or cartilage, and are present in bone. The high tensile strength of collagen fibrils strengthen the skeletal system and its connections.

New bone material is formed chemically by cells called “osteoblasts”. These cells contain water in place of minerals. Gradually, calcification of the organic matrix (osteoid) occurs due to catalysis of the elements of the collagen structure, and this matrix grows to form the ceramic portion of the bone. The initial mineralization in humans is fast, 70% within the first four days. It takes months to reach normal mineral capacity thereafter.

Bone is an anisotropic and viscoelastic ceramic matrix composite and is distinct from conventional ceramics. Its mechanical properties depend on its porosity, degree of mineralization, collagen fiber orientation, and other structural details. The data in Table 18.1 may be used to compare the physical and mechanical properties of bone, hydroxyapatite (the major mineral in bone, and hence, the most relevant material as a bioceramic), and CBPCs.

As shown in Table 18.1, bone is a lightweight (low density) material. Most of the orthopedic substitutions currently used, such as steel, titanium, and alumina, are much denser than bone. Comparatively, CBPC materials come close to the density of compact bone.

Cancellous bone is a very porous material, with an average density of 1.3 g cm^{-3} , implying a porosity of nearly 35%. In practice, the density lies between 5 and 95% varying gradually between cortical and cancellous regions. The pore size distribution is bimodal. The pores are elongated and filled with soft tissues that include bone marrow, blood vessels, and various bone-related cells. It is the overall porosity and the pore size distribution that mostly control the mechanical properties of bone.

Most of the cortical bone has a lamellar structure, with each lamella being about $5 \mu\text{m}$ thick. Embedded in between are small chambers of size $5\text{--}10 \mu\text{m}$ called “lacunae” that are connected to each other by microchannels called “canaliculi” or “little channels”. These little channels are typically $0.2 \mu\text{m}$. Lacunae and canaliculi comprise the porosity within bones.

Osteoblasts become trapped in lacunae, in the process of forming the bone and are then termed “osteocytes”. Osteocytes are considered to be important in the mineralization process. Thus, if an artificial bone is to be fabricated that should eventually be mineralized to a natural bone, then the artificial bone should have a porous structure with canaliculi and lacunae. The porous structure will enable new osteocytes to enter the artificial bone and cause mineralization.

As we move from the periphery of the bone to the center, the structure becomes anisotropic and tubular. This structure, called “osteons”, consists of tubes of approximately $200\text{--}\mu\text{m}$ diameter with a central canal called the “Haversian canal” to house blood vessels. Lamellae are arranged concentric to this canal and parallel to the

Table 18.1.

Summary of Mechanical Properties of Bone, Dentine [3], Hydroxyapatite [3], and CBPCs.

Property	Natural Biomaterials			
	Cortical bone	Dentine	Sintered hydroxyapatite	Dense CBPCs
Specific gravity (g cm^{-3})	1.7–2.1	1.3	3.1	1.7–2.0
Tensile strength (MPa)	60–160	50–60	40–300	2.1–14
Compression strength (MPa)	130–180	300–380	300–900	20–910
Young’s modulus (GPa)	3–30	15–20	80–120	35–105
Fracture energy (J m^{-2})	390–560	–	2.3–20	
Fracture toughness ($\text{MPa m}^{1/2}$)	2–12	–	0.6–1.0	0.3–0.8
Composition	Inorganic + organic	Inorganic	Inorganic	Inorganic

shaft of the bone. The entire structure is in the bone matrix. The canals are dug by osteoclasts, which are bone-destroying cells. At the same time, osteoblasts fill the canals in a remodeling phenomenon.

In the early stages of bone formation, the osteons dominate the bone structure to make an overall structure of fiber–matrix composite. While the primary bone has a dense structure, the secondary bone structure is this composite. As a result, the cortical bone structure becomes very complex. It is microscopically porous, has a lamellar structure, and is also a fiber–matrix composite. Size and packing of osteons and canals, and their orientation, determine the mechanical properties of these bones.

This brief description of processes in bone indicates that it is chemically very active. For this reason, the objective of research in bioceramic is to mimic the internal processes and the structure of bone with man-made materials. Once placed, there should be little distinction between the natural bone and man-made ceramic implant or an artificial graft.

18.2.

CHEMICALLY BONDED PHOSPHATE-BASED BIO CERAMICS

CBPCs are excellent candidates for bioceramics for the following reasons:

1. Since bone contains mainly calcium phosphate compounds, and in particular HAP as the major mineral, calcium-based CBPC materials can provide the necessary bone composition.
2. CBPCs may be placed as a paste or can be injected at the right place in a human body. It will harden rapidly after its delivery. It will attach itself to the adjacent surfaces and form a firm bond. The process is less intrusive as compared to hardened ceramics that need to be implanted surgically.
3. Chemically bonded ceramics are more resorbable and surface reactive as compared to sintered counterparts. This is because they are more soluble within the body fluids as compared to the sintered ceramics. By controlling the composition, their solubility can be tailored to the desired value.
4. Because of the ease of formation and placement of CBPCs, they can be tailored to mimic the composition and microstructure of bones. In the case of sintered ceramics, it is difficult to control the microstructure during the sintering process. Application of CBPCs as a paste, on the other hand, can be controlled by suitable computer programs with desired compositions as input. This process, known as “rapid prototyping”, allows one to form these ceramics in desired microstructure locally to change the microstructure spatially. Such ceramics in which microstructure varies gradually with distance are called “functionally gradient”. These advantages of CBPCs are not available in sintered ceramics.

The first feature discussed above has been well recognized, and much modern research has been focussed on developing biocompatible calcium-based ceramics. Manipulation of the microstructure, however, has not been attempted sufficiently, and much of the rapid prototyping has been to develop suitable macroscopic forms for sintered ceramics.

Tailoring of microstructure and localized composition is open for research. Thus, this chapter concentrates on the development of suitable bioceramic mineralogy, rather than the microstructure.

18.3.

RECENT ADVANCES IN CBPC-BASED BIOMATERIALS

There have been significant advances in CBPC-based biomaterials in the last few years, particularly Ceramicrocrete-based dental cement and dahllite-based bioceramics.

A US patent was granted to Bindan Corp. on a Ceramicrocrete-based composition [5]. This patent emphasizes the importance of recent Mg-based CBPC formulations for dental cements and bioceramics.

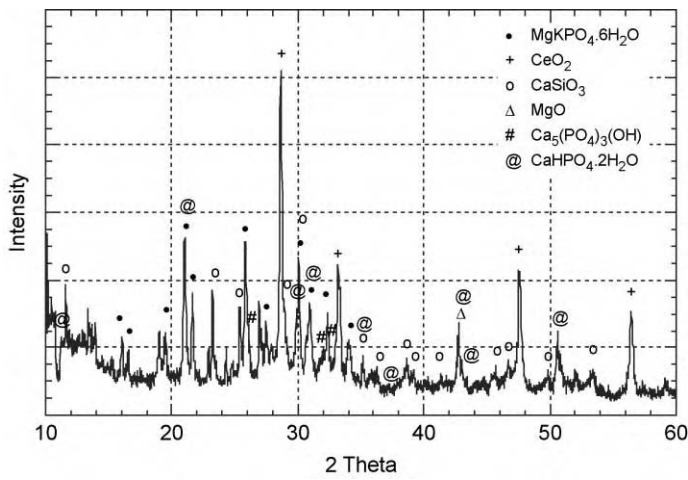
Wagh and Primus worked in collaboration with Dentsply, Inc., and developed Ceramicrocrete-based dental cement for root canal applications [6]. The main advantage of this material over acrylic and other polymer cements is that it is insensitive to moisture. Adding phosphoric acid or a highly acidic phosphate, Wagh and Primus increased the acidity of Ceramicrocrete paste and produced a very rapid-setting cement. The paste was formed by mixing the acid, water, and the powders for 1 min. Their method allowed 5 min for application either with a spatula or a syringe.

Wollastonite was added to improve the flexural strength, bismuth oxide and cerium oxide to improve radiopacity, and hydroxyapatite to improve biocompatibility. Ultrafine and chemical grade powders were used in this study. The acicular microstructure of wollastonite improved the mechanical properties of the cement. Because of the rapid-setting nature of the cement paste, it heated by a few degrees during hardening. The heating caused some dissolution of wollastonite, which has its highest solubility at 63°C [calculated by using Eq. (6.37)] and that helped in the rapid development of the strength. The one-day compressive strength varied between 10,000 and 13,100 psi (70 and 91 MPa). The flexural strength and fracture toughness also must have been high, because as described in Chapter 13 (see Table 13.5), the flexural strength of wollastonite-containing Ceramicrocrete is in the range of 8.5–10 MPa (1236–1474 psi), and the fracture toughness is ≈ 0.63 for 50 and 60 wt% loading. These mechanical properties are superior to those of conventional cement.

The X-ray diffraction pattern for the maximum strength CBPC is given in Fig. 18.1. The pattern contains very sharp peaks of the binder phase $\text{MgKPO}_4 \cdot 6\text{H}_2\text{O}$, unreacted MgO , CeO_2 , CaSiO_3 , and hydroxyapatite ($\text{Ca}_5(\text{PO}_4)_3(\text{OH})$). The retention of $\text{Ca}_5(\text{PO}_4)_3(\text{OH})$ and the formation of $\text{CaHPO}_4 \cdot 2\text{H}_2\text{O}$ during the setting reaction make this material biocompatible.

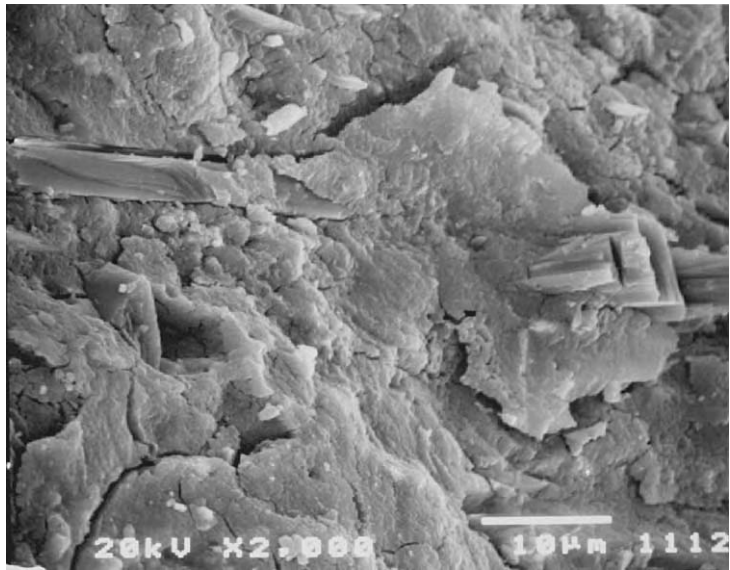
Figure 18.2 shows the scanning electron microphotograph of the fractured surface of the sample. Considerable featureless material, possibly amorphous or microcrystalline, is visible. Due to the very fine starter powders used in this material, it is likely that the resulting crystals of magnesium potassium phosphate are also very fine and, hence, are not easily visible in the micrograph. The elongated crystals of calcium silicates are embedded in this amorphous mass. Also notice the crack due to fracture of the material, which is diverted by

Fig. 18.1.



X-ray diffraction pattern of the sample with maximum compressive strength.

Fig. 18.2.



Scanning electron micrograph of the fractured surface of the sample with maximum compressive strength.

an elongated crystal. This crack deflection is responsible for higher fracture toughness. Furthermore, the elongated crystals themselves provide better flexural strength.

The micrograph does not exhibit any pores within the material. This visual evidence indicates that the porosity is near zero.

Wollastonite-containing Ceramicrete is being subjected to histological tests at this time. The material itself is being targeted for dental cement applications, such as root canal sealing, root canal obturation and repair, pulp capping, prosthodontic crowning, implant insertion, dental ridge augmentation and periodontal defect filling. It is also a good temporary cement and restorative material, as well as a cement for artificial joints and for bone stabilization.

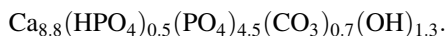
18.4.

CALCIUM-BASED CBPC BIOMATERIALS

The Ceramicrete composition described above was developed mainly for dental applications. It is Mg-based, and calcium is introduced via calcium silicate and HAP. Because of the compatibility of calcium phosphate cements with natural bone, bone cements are mainly calcium-based. In particular, formulations that produce HAP have been the major candidates for this application. As described in Chapter 13, formation of HAP in CBPCs is facilitated by the reaction of either anhydrous dicalcium phosphate, DCPA (CaHPO_4) or dicalcium hydrophosphate dihydrate ($\text{CaHPO}_4 \cdot 2\text{H}_2\text{O}$), and tetracalcium phosphate [$\text{Ca}_4(\text{PO}_4)_2 \cdot \text{O}$]. The reaction is facilitated by phosphoric acid solution. For example, Brown and Chow [7] used 20 mM of H_3PO_4 solution, instead of water (see Eq. 13.13) and produced a ceramic that had a compressive strength of ≈ 5000 psi (3.5 MPa) which is higher than that of portland cement. Most of this strength is gained within a day [8]. In spite of such advancements, several problems still persist in producing a biocompatible CBPC. These may be classified into two categories.

1. *Mineralization in body fluids.* In vitro (outside the body) CBPC formation may not be the same as in vivo (inside the body). The body fluids will affect the mineralization process. Blood may wash away or dissolve the CBPC minerals prior to their setting. The components of blood may also become incorporated within the CBPC, modify its composition, and change the physical properties.
2. *Lack of carbonated or fluorinated hydroxyapatite.* The HAP formation by the reaction in Eq. 13.13 still does not produce a composition exactly the same as that of the bone. Bone contains carbonated and fluorinated apatite, or dahllite, and it is difficult to mimic such a composition by chemical reactions.

Constantz *et al.* [9,10], however, have succeeded in producing dahllite-based bioceramic with the stoichiometric formula



They reacted a mixture of monocalcium phosphate monohydrate ($\text{Ca}(\text{H}_2\text{PO}_4)_2 \cdot \text{H}_2\text{O}$), α -tricalcium phosphate ($\text{Ca}_3(\text{PO}_4)_2$), and calcium carbonate (CaCO_3) with a solution of trisodium phosphate (Na_3PO_4) to produce this rapid-setting cement. They have been able to apply this cement as a paste that sets within minutes under physiological conditions. The mixing time is ≈ 5 min, and the paste sets by crystallizing into dahllite in another 10 min.

The initial compressive strength is ≈ 10 MPa (1428.5 psi) and increases to ≈ 55 MPa (7850 psi) within 24 h. The ultimate tensile strength is ≈ 2.1 MPa (300 psi). The compressive strength is approximately the same as that of cancellous bone, while the tensile strength appears to be lower than that of bone.

In clinical tests the dahllite-based material was injected as an implant for internal stabilization of a wrist fracture. The ingredients were mixed to form a slurry that was injected in the patient's body. The paste set within minutes under physiological conditions. The material was allowed to harden in situ before a cast was applied. The healing process was more rapid compared to conventional techniques. The new biomaterial resisted compressive forces from the musculature and the wrist healed faster than indicated by historical controls.

The high brilliance X-ray diffraction pattern of the new biomaterial was compared with that of the cortical bone of a rabbit and also sintered HAP. The dahllite-based biomaterial had a diffraction pattern very similar to that of the bone, while sintered HAP was highly crystalline. The crystallite sizes of bone as well as their biomaterial were very similar, equal to an average size of 5 nm. Unlike bone, however, the crystallites in the biomaterial oriented unidirectionally because they were rapidly formed in the absence of an organic matrix. The density of the new biomaterial was found to be 1.3 g cm^{-3} , and the average pore diameter was 30 nm. These measurements indicate that both crystallite size and the porosity are at the nanoscale and result in broad peaks in the X-ray diffraction pattern. Bigger crystallites would have yielded sharper peaks in the sintered HAP.

18.5.

CONCLUSIONS

The advancements in dental and biomaterials presented here demonstrate that CBPCs have distinct advantages over sintered ceramics. By means of room temperature processing, it has been possible to develop CBPCs that set under biological conditions, mimic bones with carbonate apatite, and are compatible with actual bones. Thus, chemical bonding to produce biomaterials may be a natural way to go.

CBPCs may have an important role even in the production of artificial implants. Typically, one may exploit rapid-prototyping to produce exact shapes of the implants. From a practical standpoint, formation of a ceramic out of a paste would appear to be most suitable for rapid-prototyping processes [11]. Thus, coupling CBPC with rapid-prototyping should lead to artificial body parts that not only match the natural bones in their composition, but in structure as well. The science of CBPCs paves the way for their use not only as dental cements and bioceramics for the 21st century, but as discussed in earlier chapters, many other applications as well.

REFERENCES

1. A.D. Wilson and J.W. Nicholson, *Acid-Base Cements* (Cambridge University Press, Cambridge, UK, 1993).
2. C. Lavernia and J. Schoenung, "Calcium phosphate ceramics as bone substitutes," (*Ceram. Bull.*, **70** 1) (1991) 95–100.
3. A. Ravaglioli and A. Krajewski, *Bioceramics* (Chapman & Hall, New York, 1992), p. 44.
4. R.B. Martin, "Bone as a Ceramic Composite Material," in *Bioceramics*, ed. J.F. Shackelford (Trans Tech Publications, Brandrain, 1999), p. 9.
5. T. Lally, Bio-adhesive composition, method for adhering objects to bone, US Patent 6,533,821 B1, 2003.
6. A.S. Wagh and C. Primus, Method and product for phospho-silicate slurry for use in dentistry and related bone cements, US Patent Application, no. 60/493,958, 2003.
7. W.E. Brown and L.C. Chow, *A New Calcium Phosphate, Water-Setting Cement, Cement Research Progress*, ed. P.W. Brown (American Ceramic Society, Westerville, OH, 1986), pp. 352–379.
8. Y. Fukase, E.D. Eanes, S. Takagi, L.C. Chow, and W.E. Brown, "Setting reactions and compressive strengths of calcium phosphate cements," *J. Dent. Res.*, **December** (1990) 1852–1856.
9. B.R. Constantz, M.T. Fulmer, and B.M. Barr, In situ prepared calcium phosphate composition and method, US Patent 5,336,264, issued to Norian Corp, Mountain View, CA, 1994.
10. B.R. Constantz, I. Ison, M. Fulmer, R. Poser, S. Smith, M. VanWagoner, J. Ross, S. Goldstein, J. Jupiter, and D. Rosenthal, "Skeletal repair by in situ formation of the mineral phase of bone," *Science*, **67** (1995) 1796–1799.
11. W. Lemont, *Rapid Prototyping: An Introduction* (Industrial Press, New York, 1993).

This page is intentionally left blank

Appendices

The appendices contain the thermodynamic data, the solubility product constants that are relevant to CBPC formation or their durability, and formulae of minerals that were discussed in the text. The thermodynamic data of phosphates is difficult to find in the common literature. Some excellent sources such as *Phosphate Minerals* by Nriagu and Moore and *Inorganic Phosphate Materials* by Kanazawa are out of print. The most commonly used data books such as *CRC Handbook of Physics and Chemistry* do not contain data on most phosphate compounds. For this reason, these appendices are provided to facilitate the discussion in the text and also for the benefit of those who wish to pursue further research in CBPCs.

The data from different sources does not often match exactly, while it has been necessary to use the data on oxides from one source and phosphates of the same elements from another. To avoid any confusion resulting from this, we have used a certain order in using these sources. Pourbaix's *Atlas of Electrochemical Equilibria* [1] is the first source that we have used for the Gibb's free energy of oxides and ions, and for the solubility product constants. This is prompted by the fact that much of the formulation discussed in this book is hinged to Pourbaix's treatment, and to be consistent, Pourbaix's data is preferred over others. *The CRC Handbook of Chemistry and Physics* [2] is the next source from which much of the enthalpy and specific heat of oxides and ions are taken. The data on phosphates comes from *The Phosphate Minerals* [3], while the mineral formulae are from *Dana's Mineralogy Handbook* [4] and also from *The Phosphate Minerals* [3]. These detailed references and additional ones [5,6] useful for further development of CBPC materials are given below.

REFERENCES

1. M. Pourbaix, *Atlas of Electrochemical Equilibria in Aqueous Solutions* (NACE, Houston, and Cebelcor, Brussels, 1974).
2. *Handbook of Chemistry and Physics*, ed. D.R. Lide, 77th ed. (CRC Press, Boca Raton, FL, 1996).
3. J.O. Nriagu and P.B. Moore, *Phosphate Minerals* (Springer, New York, 1984).
4. C. Klein and C. Hurlbut, Jr., *Manual of Mineralogy*, 20th ed. (John Wiley and Sons, New York, 1985), p. 596.
5. *Thermochemical Properties of Inorganic Substances*, eds. O. Knacke, O. Kubaschewski, and K. Hesselmann (Springer, Berlin, 1991).
6. J. Dean and N. Lange, *Lange's Handbook of Chemistry*, 15th ed. (McGraw Hill, New York, 1999).

APPENDIX A.

THERMODYNAMIC PROPERTIES OF SELECTED MATERIALS

a. Oxides, Hydroxides, Phosphates

Table A1.

Material	ΔH (kJ/mol)	ΔG (kJ/mol)	C_p (J/mol/K)
H (atomic)	218.0	203.2	20.8
H ₂ (natural)	0.0	0.0	28.8
O ₂	0.0	0.0	
H ₂ O (liquid)	-285.8	-236.7	75.3
H ₂ O (gas)	-241.8	-228.6	33.6
Na ₂ O	-414.2	-376.6	38.6
NaOH	-425.6	-377.0	59.5
NaH ₂ PO ₄	-1543.9		135.0
Na ₃ PO ₄	-1913.6		
K ₂ O	-361.5	-318.8	84.5
KOH (crystalline)	-424.6	-374.5	64.9
KH ₂ PO ₄	-1570.7	-1418.3	116.6
KUO ₂ PO ₄		-2386.6	
Cs ₂ O	-345.4	-274.5	76.0
CsOH	-417.2	-355.2	67.8
MgO	-601.6	-569.6	37.2
Mg(OH) ₂	-924.5	-596.6	77.0
Mg(H ₂ PO ₄) ₂ ·2H ₂ O		-3200.3	
MgHPO ₄ ·3H ₂ O	-2603.8	-2288.9	
MgNH ₄ PO ₄		-1624.9	
MgNH ₄ PO ₄ ·6H ₂ O	-3681.9		
Mg ₅ F(PO ₄) ₃		-5854.2	
Mg ₅ OH(PO ₄) ₃		-5758.0	
Mg ₅ Cl(PO ₄) ₃		-3791.5	
Mg ₄ O(PO ₄) ₂		-4172.7	
Mg ₂ FPO ₄		-2305.4	

Table A1—continued

Material	ΔH (kJ/mol)	ΔG (kJ/mol)	C_p (J/mol/K)
Mg ₅ (PO ₄) ₂ ·8H ₂ O	− 3780.7	− 3538.8	
Mg ₅ (PO ₄) ₂		− 5450.5	
Mg ₅ (PO ₄) ₂ ·22H ₂ O		− 8751.8	
MgKPO ₄ ·6H ₂ O	− 3724.3	− 3241.0	
CaO	− 634.9	− 604.2	42.0
Ca(OH) ₂	− 985.2	− 659.6	87.5
CaSiO ₃	− 1634.9	− 1549.7	85.2
2CaO·SiO ₂ (β)	− 2315.7	− 2190.7	128.7
3CaO·SiO ₂	− 2926.4	− 2781.4	171.7
3CaO·2SiO ₂	− 3957.2	− 3757.8	214.2
CaO·Al ₂ O ₃	− 2324.1	− 2206.6	120.7
CaO·2Al ₂ O ₃	− 3973.9	− 3767.0	200.6
3CaO·Al ₂ O ₃	− 3584.3	− 3408.4	209.7
CaO·Al ₂ O ₃ ·SiO ₂	− 3293.2	− 3650.6	156.6
3CaO·Al ₂ O ₃ ·2SiO ₂	− 3981.9	− 3780.0	205.2
3CaO·Al ₂ O ₃ ·3SiO ₂	− 6646.2	− 6718.1	323.1
CaO·MgO·SiO ₂	− 2262.7	− 2296.0	123.2
CaO·MgO·2SiO ₂	− 3203.2	− 3245.9	156.1
CaHPO ₄	− 1814.4	− 1681.3	111.4
Ca(H ₂ PO ₄) ₂ ·H ₂ O	− 3409.7	− 3058.4	258.8
Ca ₈ H ₂ (PO ₄) ₆ ·5H ₂ O		− 12,263.3	
CaU(PO ₄) ₂ ·2H ₂ O	− 4304.6		
Ca(UO ₂) ₂ (PO ₄) ₂ ·10H ₂ O		− 7147.0	
CaNaPO ₄	− 2004.1		
Ca ₁₀ O(PO ₄) ₆		− 12,307.8	
Ca ₅ F(PO ₄) ₃	− 6872.0	− 6491.5	376.0
Ca ₅ OH(PO ₄) ₃	− 6738.5	− 6338.5	385.0
Ca ₅ Cl(PO ₄) ₃	− 6636.0	− 6257.0	378.9
Ca ₅ Br(PO ₄) ₃		− 6191.3	
Ca ₄ O(PO ₄) ₂		− 4588.0	
Ca ₂ FPO ₄		− 2522.1	
Ca ₂ ClPO ₄		− 2371.7	
NH ₄ H ₂ PO ₄	− 1445.1	− 1210.6	142.2
NH ₄ UO ₂ PO ₄		− 2201.6	
SrO	− 592.0	− 559.8	45.0
Sr(OH) ₂	− 959.0	− 632.2	
BaO	− 548.0	− 528.4	47.3
Ba(OH) ₂	− 944.7	− 655.2	101.6
RaO		− 491.0	
Al ₂ O ₃ ·3H ₂ O (hydrargillite, gibbsite)	− 2586.6	− 1608.9	183.4
	− 2576.4	− 1600.0	
Al ₂ O ₃ ·3H ₂ O (bayerite)	− 1980.8	− 1582.8	131.2
Al ₂ O ₃ ·H ₂ O (boehmite)			
Al ₂ O ₃ ·H ₂ O (diaspore)	− 1999.6	− 1576.4	106.6
Al ₂ O ₃ (corundum)	− 1675.7	− 1536.9	79.0
Al(OH) ₃ (amorphous)	− 1274.8	− 1136.6	93.1

Table A1—*continued*

Material	ΔH (kJ/mol)	ΔG (kJ/mol)	C_p (J/mol/K)
AlPO ₄		– 4237.1	
Al ₂ K(PO ₄) ₂ (OH)·2H ₂ O		– 4044.7	
Al ₂ NH ₄ (PO ₄) ₂ (OH)·2H ₂ O	– 6567.7	– 6077.5	
Al ₄ (PO ₄) ₃ (OH) ₃		– 2809.6	
Al ₂ PO ₄ (OH) ₃			
Y ₂ O ₃	– 1905.3	– 1682.0	102.5
Y(OH) ₃		– 1858.0	
Ce ₂ O ₃	– 1796.2	– 1706.2	114.6
Ce(OH) ₃		– 1896.6	
CeO ₂	– 1088.7	– 916.3	61.6
Nd(OH) ₃		– 1876.6	
Nd ₂ O ₃	– 1807.9	– 1759.8	111.3
TiO	– 519.7	– 489.2	40.0
Ti ₂ O ₃	– 1520.9	– 1432.2	97.4
Ti(OH) ₃		– 1388.0	
Ti ₃ O ₅	– 2459.4	– 2314.3	154.8
TiO ₂	– 944.0	– 888.4	55.0
TiO ₂ ·H ₂ O		– 821.3	
ZrO ₂	– 1100.6	– 1036.4	56.2
Zr(OH) ₄	– 1661.9	– 1073.7	
Cr(OH) ₂		– 350.7	
Cr(OH) ₃ (hexagonal)		– 1090.1	
Cr ₂ O ₃	– 1139.7	– 1058.1	
Cr(OH) ₃ (orthorhombic)		– 1046.8	
Cr(OH) ₃ <i>n</i> H ₂ O		– 1008.1	
Cr(OH) ₄		– 539.7	118.7
Cr ₂ O ₃	– 1139.7	– 1081.1	
CrPO ₄	– 587.0	– 1363.4	
H ₂ CrO ₄ (dissolved)		– 777.9	
MnO	– 385.2	– 362.9	45.4
Mn(OH) ₂ (rhombic)		– 377.4	
Mn(OH) ₂ (cubic)		– 363.2	
Mn ₃ O ₄	– 1387.8	– 1280.3	
Mn ₂ O ₃	– 959.0	– 888.3	
Mn(OH) ₃		– 803.1	
MnO ₂	– 520.0	– 464.8	54.1
TcO ₂		– 369.4	
TcO ₃		– 460.5	
Tc ₂ O ₇		– 931.1	
Tc ₂ O ₇ ·H ₂ O (or HTcO ₄)		– 1182.2	
Re(OH) ₃		– 579.9	
ReO ₂		– 372.4	
ReO ₃		– 532.6	
Re ₂ O ₇		– 1057.3	

Table A1—continued

Material	ΔH (kJ/mol)	ΔG (kJ/mol)	C_p (J/mol/K)
FeO	− 265.9	− 283.7	48.0
Fe(OH) ₂	− 1118.4	− 246.4	143.4
Fe ₃ O ₄	− 824.2	− 1014.2	103.9
Fe ₂ O ₃		− 741.0	
Fe(OH) ₃		− 677.52	
CoO	− 237.9	− 214.2	55.2
Co(OH) ₂ (rhombic)	− 539.7	− 218.9	
Co(OH) ₂ (cubic)	− 541.4	− 205.2	
Co ₃ O ₄	− 891.0	− 702.2	123.4
Co(OH) ₃		− 481.7	
CoO ₂		− 216.9	
Ni(OH) ₂ (rhombic)	− 529.7	− 215.9	
Ni(OH) ₂ (cubic)		− 214.7	
Ni ₃ O ₄ ·2H ₂ O		− 711.9	
Ni ₂ O ₃ ·H ₂ O		− 469.7	
Ni ₃ (PO ₄) ₂		− 2347.3	
Cu ₂ O	− 168.6	− 146.4	63.6
CuO	− 157.3	− 127.2	42.3
Cu(OH) ₂	− 449.8	− 117.8	
Ag ₂ O	− 31.1	− 10.8	65.9
Ag(OH) ₂		53.2	
AgO		10.9	
Ag ₂ O ₃	33.9	87.0	
Ag ₃ PO ₄		− 887.6	
ε-Zn(OH) ₂		− 321.9	
Zn(OH) ₂ (inactive)		− 320.6	
γ-Zn(OH) ₂		− 320.6	
β-Zn(OH) ₂		− 319.8	
Zn(OH) ₂ (active)	− 641.9	− 316.7	
α-Zn(OH) ₂		− 314.8	
Zn(OH) ₂ (amorphous)		− 314.5	
ZnO	− 350.5	− 321.3	
ZnHPO ₄		1255.1	
Zn ₃ (PO ₄) ₂ ·H ₂ O	− 4077.7	− 3606.3	
CdO	− 258.4	− 224.8	43.4
Cd(OH) ₂	− 560.7	− 473.6	
Cd(OH) ₂ (brown)		− 232.8	
CdO		− 225.1	
HgO (red)	− 90.8	− 58.5	44.1
HgO (yellow)		− 58.4	
Hg(OH) ₂		− 274.9	
Hg ₂ HPO ₄		− 1006.5	
SiO ₂ (quartz)	− 910.7	− 805.0	44.4
SiO ₂ (cristobalite)		− 803.7	

Table A1—*continued*

Material	ΔH (kJ/mol)	ΔG (kJ/mol)	C_p (J/mol/K)
SiO ₂ (tridymite)		– 802.9	
SiO ₂ (vitreous)	– 902.1	– 798.8	
H ₂ SiO ₃ (amorphous)		– 785.8	
H ₂ SiO ₃ (colorless)	– 1188.7	– 1012.5	
H ₄ SiO ₄	– 1481.1	– 1332.9	
PbO	– 219.0	– 189.3	45.8
Pb(OH) ₂		– 183.7	
Pb ₃ O ₄	– 718.4	– 617.6	146.9
Pb ₂ O ₃		– 411.8	
PbO ₂	– 277.4	– 219.0	64.6
Pb ₃ (PO ₄) ₂		– 2364.0	
PbHPO ₄		– 1178.9	
Pb ₄ O(PO ₄) ₂		– 2582.8	
H ₃ PO ₄	– 1271.7	– 1123.6	145.0
As ₂ O ₃	– 924.9	– 576.0	116.5
As ₂ O ₅		– 772.4	
H ₃ AsO ₃		– 639.9	
HAsO ₂		– 402.7	
ThO ₂	– 1226.4	– 1164.1	61.8
Th(OH) ₄		– 1111.3	
UO		– 514.6	
U(OH) ₃		– 1490.9	
UO ₂	– 1085.0	– 1031.8	63.6
U(OH) ₄		– 996.7	
U ₃ O ₈	– 3574.8	– 3363.9	
UO ₃ H ₂ O		– 1197.9	
UO ₃ ·2H ₂ O		– 1194.4	
UO ₃	– 1223.8	– 1142.2	81.7
U ₃ O ₇	– 3427.1	– 3242.9	215.5
U ₄ O ₉	– 4510.4	– 4275.1	293.3
Pu(OH) ₃		– 1633.1	
PuO ₂		– 979.1	
Pu(OH) ₄		– 948.2	
PuO ₂ OH		– 1827.2	
PuO ₂ (OH) ₂		– 929.7	
Am(OH) ₃		– 1798.8	
Am ₂ O ₃		– 1682.0	
Am(OH) ₄		– 977.5	
AmO ₂		– 966.5	
AmO ₂ OH		– 1896.6	
AmO ₂ (OH) ₂		– 880.8	

b. Cations and Anions in Aqueous State

The ions listed in Table A2 are all dissolved species, and for the sake of convenience of notation, the notation (aq) has not been used.

Table A2.

Ions	ΔH (kJ/mol)	ΔG (kJ/mol)	C_p (J/mol/dK)
H^+	0.0	0.0	0.0
OH^-	-230.0	-157.3	-148.5
e^-	0.0	0.0	
Na^+	-240.3	-261.9	46.4
K^+	-252.4	-282.2	21.8
Cs^+	-258.3	-282.0	-10.5
Mg^{2+}	-466.9	-456.0	38.5
$MgOH^+$		-626.7	
Ca^{2+}	-542.8	-553.0	0.8
$CaOH^+$		-718.4	
Sr^{2+}	-545.8	-557.3	
$SrOH^+$		-721.3	
Ba^{2+}	-537.6	-560.7	
Ra^{2+}	-527.6	-562.7	
Al^{3+}	-531.0	-481.2	38.1
$AlOH^{2+}$		-694.1	
AlO_2^-	-930.9	-839.8	
$Al(OH)_4^-$	-1502.5	-1305.3	
Y^{3+}	-723.4	-686.6	-26.8
$Y(OH)^{++}$		-879.1	
Ce^{3+}	-696.2	-671.9	
Ce^{4+}	-537.2	-503.8	
$Ce(OH)^{3+}$		-790.4	
$Ce(OH)_2^{2+}$		-1025.9	
Nd^{3+}	-696.2	-703.7	-21.0
Ti^{2+}		-314.2	
Ti^{3+}		-349.8	
TiO^{2+}		-577.4	
$HTiO_3^-$		-955.9	
TiO_2		-467.2	
Zr^{4+}	-554.5	-519.7	
ZrO^{2+}		-843.1	
$HZrO_3^-$		-1207.1	

Table A2—continued

Ions	ΔH (kJ/mol)	ΔG (kJ/mol)	C_p (J/mol/dK)
Cr ²⁺	− 143.5	− 176.1	
Cr ³⁺	− 256.1	− 215.5	
CrOH ²⁺		− 430.9	
Cr(OH) ₂ ⁺		− 432.7	
CrO ₂ [−]		− 535.9	
CrO ₃ ^{3−}		− 603.4	
HCrO ₄		− 773.6	
CrO ₄ ^{2−}	− 881.2	− 736.8	
Cr ₂ O ₇ ^{2−}	− 1490.3	− 1319.6	
Mn ²⁺	− 220.8	− 227.6	50.0
MnOH ²⁺	− 450.6	− 405.0	
HMnO ₂ [−]		− 505.8	
Mn ³⁺		− 82.0	
MnO ₄ ^{2−}	− 997.9	− 503.7	
MnO ₄ [−]	− 541.4	− 449.4	
Tc ²⁺		77.2	
TcO ₄ [−]		− 630.6	
HTcO ₄ (dissolved)		− 629.5	
Re ⁺		− 33.0	
Re [−]	46.0	38.5	
Re ³⁺		86.8	
ReO ₄ ^{2−}		− 631.6	
ReO ₄ [−]		− 699.1	
Fe ²⁺	− 89.1	− 84.9	
HFeO ₂ [−]		− 379.2	
Fe ³⁺	− 48.5	− 10.6	24.7
FeOH ⁺	− 324.7	− 277.4	
FeOH ²⁺	− 290.8	− 233.9	
Fe(OH) ²⁺		− 444.3	
FeO ₄ ^{2−}		− 467.3	
Co ²⁺	− 58.2	− 53.6	
HCoO ₂ [−]		− 347.1	
Co ³⁺	92.0	120.9	
Ni ²⁺	− 54.0	− 48.2	
NiOH ²⁺	− 287.9	− 227.6	
HNiO ₂ [−]		− 349.2	
Cu ⁺	71.7	50.2	
Cu ²⁺	64.8	65.0	
HCuO ₂ [−]		− 257.0	
CuO ₂ ^{2−}		− 182.0	
Ag ⁺	105.6	77.1	21.8
AgO [−]		− 23.0	
Ag ²⁺		268.2	
AgO ⁺		225.5	

Table A2—continued

Ions	ΔH (kJ/mol)	ΔG (kJ/mol)	C_p (J/mol/dK)
Zn^{2+}	– 153.9	– 147.2	46.0
ZnOH^+		– 329.3	
HZnO_2^-		– 464.0	
ZnO_2^{2-}		– 389.2	
Cd^{2+}	– 75.9	– 77.7	– 73.2
CdOH^+		– 261.1	
HCdO_2		– 361.9	
CdH		– 233.2	
Hg_2^{2+}	172.4	152.1	
Hg^{2+}	171.1	164.8	
Hg(OH)_2		– 274.9	
Hg(OH)^+	– 84.5	– 52.3	
HHgO_2^-		– 190.0	
HSiO_3^-		– 955.5	
SiO_3^{2-}		– 887.0	
Pb^{2+}	– 1.7	– 24.3	– 52.7
PbOH^+		– 226.3	
HPbO_2^-		– 338.9	
Pb^{4+}		– 302.5	
PbO_3^{2-}		– 277.6	
PbO_4^{4-}		– 282.1	
NH_4^+	– 132.5	– 79.5	79.9
H_2PO_4^-	– 1292.1	– 1135.1	– 43.9
HPO_4^{2-}	– 1299.0	– 1094.1	– 265.7
PO_4^{3-}	– 1277.4	– 1025.5	– 334.7
AsO^+		– 163.6	
AsO_2^-	– 429.0	– 350.2	
H_3AsO_3		– 639.9	
H_2AsO_3^-	– 714.8	– 587.4	
H_3AsO_4		– 769.0	
H_2AsO_4^-	– 909.6	– 748.5	
HAsO_4^{2-}		– 707.1	
AsO_4^{3-}	– 888.1	– 636.0	
Th^{4+}	– 769.0	– 733.0	
Th(OH)^{3+}	– 1030.1		
Th(OH)_2^{2+}	– 1282.4		
U^{3+}	– 489.1	– 520.5	
U^{4+}	– 591.2	– 529.1	
UOH^{3+}		– 809.6	
UO^{2+}		– 994.1	
UO_2^{2+}	– 1019.0	– 989.1	

Table A2—continued

Ions	ΔH (kJ/mol)	ΔG (kJ/mol)	C_p (J/mol/dK)
Pu ³⁺		− 587.8	
Pu ⁴⁺	− 536.4	− 494.5	
PuO ₂ ⁺		− 857.3	
PuO ₂ ²⁺		− 767.8	
Am ³⁺	− 616.7	− 599.1	
Am ⁵⁺		− 461.1	
AmO ₂ ⁺		− 813.8	
AmO ₂ ²⁺		− 655.7	

APPENDIX B.

SOLUBILITY PRODUCT CONSTANTS

Table B1.

Oxide	Reaction	pK _{sp}
BaO	$\text{BaO} + 2\text{H}^+ = \text{Ba}^{2+}(\text{aq}) + \text{H}_2\text{O}$	47.24
BaHPO ₄	$\text{BaHPO}_4 + \text{H}^+ = \text{Ba}^{2+}(\text{aq}) + \text{H}_2\text{PO}_4^-$	− 0.20
MgO	$\text{MgO} + 2\text{H}^+ = \text{Mg}^{2+}(\text{aq}) + \text{H}_2\text{O}$	21.68
MgO	$\text{MgO} + \text{H}_2\text{O} = \text{Mg}_2^{2+}(\text{aq}) + 2(\text{OH}^-)$	6.32
MgHPO ₄ ·3H ₂ O	$\text{MgHPO}_4 \cdot 3\text{H}_2\text{O} + \text{H}^+ = \text{Mg}^{2+}(\text{aq}) + \text{H}_2\text{PO}_4^- + 3\text{H}_2\text{O}$	1.38
Mg(NH ₄)PO ₄ ·6H ₂ O	$\text{Mg}(\text{NH}_4)\text{PO}_4 \cdot 6\text{H}_2\text{O} + 2\text{H}^+ = \text{Mg}^{2+}(\text{aq}) + \text{NH}_4^+ + \text{H}_2\text{PO}_4^- + 6\text{H}_2\text{O}$	− 6.85
Mg ₃ (PO ₄) ₂	$\text{Mg}_3(\text{PO}_4)_2 + 4\text{H}^+ = 3\text{Mg}^{2+}(\text{aq}) + 2\text{H}_2\text{PO}_4^-$	15.82
Mg ₃ (PO ₄) ₂ ·8H ₂ O	$\text{Mg}_3(\text{PO}_4)_2 \cdot 8\text{H}_2\text{O} + 4\text{H}^+ = 3\text{Mg}^{2+}(\text{aq}) + 2\text{H}_2\text{PO}_4^- + 8\text{H}_2\text{O}$	13.9
Mg ₃ (PO ₄) ₂ ·22H ₂ O	$\text{Mg}_3(\text{PO}_4)_2 \cdot 22\text{H}_2\text{O} + 4\text{H}^+ = 3\text{Mg}^{2+}(\text{aq}) + 2\text{H}_2\text{PO}_4^- + 22\text{H}_2\text{O}$	16.0
MgKPO ₄ ·6H ₂ O	$\text{MgKPO}_4 \cdot 6\text{H}_2\text{O} + 2\text{H}^+ = \text{K}^+(\text{aq}) + \text{Mg}^{2+}(\text{aq}) + \text{H}_2\text{PO}_4^- + 6\text{H}_2\text{O}$	− 3.55
Al ₂ O ₃	$\text{AlO}_{3/2} + \frac{3}{2}\text{H}_2\text{O} = \text{Al}^{3+}(\text{aq}) + 3(\text{OH}^-)$	− 33.5
Al ₂ O ₃ ·3H ₂ O	$\text{AlO}_{3/2} \cdot \frac{3}{2}\text{H}_2\text{O} = \text{Al}^{3+}(\text{aq}) + 3(\text{OH}^-)$	− 36.3
Al ₂ O ₃ ·H ₂ O	$\text{AlO}_{3/2} \cdot \text{H}_2\text{O} + \frac{1}{2}\text{H}_2\text{O} = \text{Al}^{3+}(\text{aq}) + 3(\text{OH}^-)$	− 34.02
Al(OH) ₃	$\text{Al}(\text{OH})_3 = \text{Al}^{3+}(\text{aq}) + 3(\text{OH}^-)$	− 32.34
AlPO ₄ ·2H ₂ O	$\text{AlPO}_4 \cdot 2\text{H}_2\text{O} + 2\text{H}^+ = \text{Al}^{3+}(\text{aq}) + \text{H}_2\text{PO}_4^- + 2\text{H}_2\text{O}$	− 2.52
CaO	$\text{CaO} + 2\text{H}^+ = \text{Ca}^{2+}(\text{aq}) + \text{H}_2\text{O}$	32.63
CaO	$\text{CaO} + \text{H}_2\text{O} = \text{Ca}^{2+}(\text{aq}) + 2(\text{OH}^-)$	− 4.63
Ca ₃ (PO ₄) ₂	$\text{Ca}_3(\text{PO}_4)_2 + 4\text{H}^+ = 3\text{Ca}^{2+}(\text{aq}) + 2\text{H}_2\text{PO}_4^-$	10.18
CaHPO ₄	$\text{CaHPO}_4 + \text{H}^+ = \text{Ca}^{2+}(\text{aq}) + \text{H}_2\text{PO}_4^-$	0.55
CaHPO ₄ ·2H ₂ O	$\text{CaHPO}_4 \cdot 2\text{H}_2\text{O} + \text{H}^+ = \text{Ca}^{2+}(\text{aq}) + \text{H}_2\text{PO}_4^- + 2\text{H}_2\text{O}$	0.65
Ca ₈ H ₂ (PO ₄) ₆ ·5H ₂ O	$\text{Ca}_8\text{H}_2(\text{PO}_4)_6 \cdot 5\text{H}_2\text{O} + 10\text{H}^+ = 8\text{Ca}^{2+}(\text{aq}) + 6\text{H}_2\text{PO}_4^- + 5\text{H}_2\text{O}$	23.48
Ca ₅ (PO ₄) ₃ OH	$\text{Ca}_5(\text{PO}_4)_3\text{OH} + 6\text{H}^+ = 5\text{Ca}^{2+}(\text{aq}) + 3\text{H}_2\text{PO}_4^- + \text{OH}^-$	8.49
Ca ₅ (PO ₄) ₃ F	$\text{Ca}_5(\text{PO}_4)_3\text{F} + 6\text{H}^+ = 5\text{Ca}^{2+}(\text{aq}) + 3\text{H}_2\text{PO}_4^- + \text{F}^-$	− 3.57

Table B1—continued

Oxide	Reaction	pK_{sp}
$\text{Ca}_5(\text{PO}_4)_3\text{Cl}$	$\text{Ca}_5(\text{PO}_4)_3\text{Cl} + 6\text{H}^+ = 5\text{Ca}^{2+}(\text{aq}) + 3\text{H}_2\text{PO}_4^- + \text{Cl}^-$	11.14
$\text{Ca}_{9.54}\text{Na}_{0.33}\text{Mg}_{0.13}(\text{PO}_4)_{4.8}(\text{CO}_3)_{1.2}\text{F}_{2.48}$	$\text{Ca}_{9.54}\text{Na}_{0.33}\text{Mg}_{0.13}(\text{PO}_4)_{4.8}(\text{CO}_3)_{1.2}\text{F}_{2.48} + 9.6\text{H}^+ = 9.54\text{Ca}^{2+}(\text{aq}) + 0.33\text{Na}^+(\text{aq}) + 0.33\text{Mg}^{2+} + 1.2\text{CO}_3^{2-} + 4.8\text{H}_2\text{PO}_4^- + 2.48\text{F}^-$	-20.56
$\text{CaU}(\text{PO}_4)_2 \cdot 2\text{H}_2\text{O}$	$\text{CaU}(\text{PO}_4)_2 \cdot 2\text{H}_2\text{O} + 4\text{H}^+ = \text{Ca}^{2+}(\text{aq}) + \text{U}^{4+}(\text{aq}) + 2\text{H}_2\text{PO}_4^- + 2\text{H}_2\text{O}$	-16.83
$\text{Ca}(\text{UO}_2)_2(\text{PO}_4)_2 \cdot 10\text{H}_2\text{O}$	$\text{Ca}(\text{UO}_2)_2(\text{PO}_4)_2 \cdot 10\text{H}_2\text{O} + 4\text{H}^+ = \text{Ca}^{2+}(\text{aq}) + 2\text{UO}_2^{2+}(\text{aq}) + 2\text{H}_2\text{PO}_4^- + 10\text{H}_2\text{O}$	-9.72
Ce_2O_3	$\text{Ce}_2\text{O}_3 + 6\text{H}^+ = 2\text{Ce}^{3+}(\text{aq}) + 3\text{H}_2\text{O}$	-19.85
CePO_4	$\text{CePO}_4 + 2\text{H}^+ = \text{Ce}^{2+}(\text{aq}) + \text{H}_2\text{PO}_4^-$	-2.69
ThO_2	$\text{ThO}_2 + 4\text{H}^+ = \text{Th}^{4+}(\text{aq}) + 2\text{H}_2\text{O}$	7.47
ThO_2	$\text{ThO}_2 + 2\text{H}_2\text{O} = \text{Th}^{4+}(\text{aq}) + 4\text{OH}^-$	48.53
$\text{Th}(\text{HPO}_4)_2$	$\text{Th}(\text{HPO}_4)_2 + 2\text{H}^+ = \text{Th}^{4+}(\text{aq}) + 2\text{H}_2\text{PO}_4^-$	-6.63
$\text{Th}_3(\text{PO}_4)_4$	$\text{Th}_3(\text{PO}_4)_4 + 8\text{H}^+ = 3\text{Th}^{4+}(\text{aq}) + 4\text{H}_2\text{PO}_4^-$	-0.40
UO_2	$\text{UO}_2 + 4\text{H}^+ = \text{U}^{4+}(\text{aq}) + 2\text{H}_2\text{O}$	3.8
UO_2	$\text{UO}_2 + 2\text{H}_2\text{O} = \text{U}^{4+}(\text{aq}) + 4\text{OH}^-$	52.2
UO_2	$\text{UO}_2 + 3\text{H}^+ = \text{U}(\text{OH})^{3+}(\text{aq}) + \text{H}_2\text{O}$	2.63
UO_3	$\text{UO}_3 + 2\text{H}^+ = \text{UO}_2^{2+}(\text{aq}) + \text{H}_2\text{O}$	4.97
UO_2HPO_4	$\text{UO}_2\text{HPO}_4 + \text{H}^+ = \text{UO}_2^{2+}(\text{aq}) + \text{H}_2\text{PO}_4^-$	-3.48
$\text{UO}_2\text{HPO}_4 \cdot 4\text{H}_2\text{O}$	$\text{UO}_2\text{HPO}_4 \cdot 4\text{H}_2\text{O} + \text{H}^+ = \text{UO}_2^{2+}(\text{aq}) + \text{H}_2\text{PO}_4^- + 4\text{H}_2\text{O}$	-3.42
$(\text{UO}_2)_3(\text{PO}_4)_2$	$(\text{UO}_2)_3(\text{PO}_4)_2 + 4\text{H}^+ = 3\text{UO}_2^{2+}(\text{aq}) + 2\text{H}_2\text{PO}_4^-$	-7.2
$\text{H}_2(\text{UO}_2)_3(\text{PO}_4)_2 \cdot 10\text{H}_2\text{O}$	$\text{H}_2(\text{UO}_2)_3(\text{PO}_4)_2 \cdot 10\text{H}_2\text{O} + 2\text{H}^+ = 2\text{UO}_2^{2+}(\text{aq}) + 2\text{H}_2\text{PO}_4^- + 10\text{H}_2\text{O}$	-11.85
$\text{U}(\text{HPO}_4)_2$	$\text{U}(\text{HPO}_4)_2 + 2\text{H}^+ = \text{U}^{4+}(\text{aq}) + 2\text{H}_2\text{PO}_4^-$	-13.09
$\text{UO}_2(\text{NH}_4)\text{PO}_4$	$\text{UO}_2(\text{NH}_4)\text{PO}_4 + 2\text{H}^+ = \text{UO}_2^{2+}(\text{aq}) + \text{NH}_4^+ + \text{H}_2\text{PO}_4^-$	-6.85
$\text{UO}_2\text{NH}_4\text{PO}_4 \cdot 4\text{H}_2\text{O}$	$\text{UO}_2\text{NH}_4\text{PO}_4 \cdot 4\text{H}_2\text{O} + 2\text{H}^+ = \text{UO}_2^{2+}(\text{aq}) + \text{NH}_4^+ + \text{H}_2\text{PO}_4^- + 4\text{H}_2\text{O}$	-5.89
Pu_2O_3	$\text{Pu}_2\text{O}_3 + 6\text{H}^+ = \text{Pu}^{3+}(\text{aq}) + 3\text{H}_2\text{O}$	22.28
PuO_2	$\text{PuO}_2 + 2\text{H}_2\text{O} = \text{Pu}^{4+}(\text{aq}) + 4\text{OH}^-$	33.72
PuO_2	$\text{PuO}_2 + 4\text{H}^+ = \text{Pu}^{4+}(\text{aq}) + 2\text{H}_2\text{O}$	-1.78
PuO_3	$\text{PuO}_3 + 2\text{H}^+ = \text{PuO}_2^{2+}(\text{aq}) + \text{H}_2\text{O}$	13.19
$\text{Pu}(\text{HPO}_4)_2$	$\text{Pu}(\text{HPO}_4)_2 + 2\text{H}^+ = \text{Pu}^{4+}(\text{aq}) + 2\text{H}_2\text{PO}_4^-$	-13.29
Am_2O_5	$\text{Am}_2\text{O}_5 + 2\text{H}^+ = 2\text{AmO}_2^+(\text{aq}) + \text{H}_2\text{O}$	-2.8
AmO_3	$\text{AmO}_3 + 2\text{H}^+ = \text{AmO}_2^{2+}(\text{aq}) + \text{H}_2\text{O}$	2.26
Am_2O_3	$\text{Am}_2\text{O}_3 + 6\text{H}^+ = 2\text{Am}^{3+}(\text{aq}) + 3\text{H}_2\text{O}$	22.43
Am_2O_3	$\text{Am}_2\text{O}_3 + 3\text{H}_2\text{O} = 2\text{Am}^{3+}(\text{aq}) + 6(\text{OH})^-$	19.57
ZrO_2	$\text{ZrO}_2 + 4\text{H}^+ = \text{Zr}^{4+}(\text{aq}) + 2\text{H}_2\text{O}$	5.64
ZrO_2	$\text{ZrO}_2 + 4\text{H}^+ = \text{Zr}^{4+}(\text{aq}) + 2\text{H}_2\text{O}$	50.36
ZrO_2	$\text{ZrO}_2 + 2\text{H}^+ = \text{ZrO}^{2+}(\text{aq}) + \text{H}_2\text{O}$	7.7
CrO	$\text{CrO} + 2\text{H}^+ = \text{Cr}^{2+}(\text{aq}) + \text{H}_2\text{O}$	10.99
CrO	$\text{CrO} + \text{H}_2\text{O} = \text{Cr}^{2+}(\text{aq}) + 2\text{OH}^-$	17.01
Cr_2O_3	$\text{Cr}_2\text{O}_3 + 6\text{H}^+ = 2\text{Cr}^{3+}(\text{aq}) + 3\text{H}_2\text{O}$	8.39
Cr_2O_3	$\text{Cr}_2\text{O}_3 + 4\text{H}^+ = 2\text{CrOH}^{2+}(\text{aq}) + \text{H}_2\text{O}$	4.58
Cr_2O_3	$\text{Cr}_2\text{O}_3 + 2\text{H}^+ + \text{H}_2\text{O} = 2\text{Cr}(\text{OH})_2^-(\text{aq})$	-1.64
CrPO_4	$\text{CrPO}_4 + 2\text{H}^+ = \text{Cr}^{2+}(\text{aq}) + \text{H}_2\text{PO}_4^-$	-3.07

Table B1—continued

Oxide	Reaction	pK_{sp}
MnO	$MnO + 2H^+ = Mn^{2+}(aq) + H_2O$	17.82
MnO	$MnO + H_2O = Mn^{2+}(aq) + 2OH^-$	10.18
FeO	$FeO + 2H^+ = Fe^{2+}(aq) + H_2O$	13.29
FeO	$FeO + H_2O = Fe^{2+}(aq) + 2OH^-$	14.71
Fe ₂ O ₃	$Fe_2O_3 + 6H^+ = 2Fe^{3+}(aq) + 3H_2O$	-0.72
Fe ₂ O ₃	$Fe_2O_3 + 4H^+ = 2FeOH^{2+}(aq) + H_2O$	-3.15
Fe ₂ O ₃	$Fe_2O_3 + 2H^+ + H_2O = 2Fe(OH)_2^+(aq)$	-7.84
Fe ₂ O ₃	$Fe_2O_3 + 3H_2O = 2Fe^{3+}(aq) + 6OH^-$	42.72
FePO ₄	$FePO_4 + 2H^+ = Fe^{2+}(aq) + H_2PO_4^-$	-2.34
CoO	$CoO + 2H^+ = Co^{2+}(aq) + H_2O$	15.03
CoO	$CoO + H_2O = Co^{2+}(aq) + 2OH^-$	12.97
Co ₂ O ₃	$Co_2O_3 + 6H^+ = 2Co^{3+}(aq) + 3H_2O$	-1.05
Co ₂ O ₃	$Co_2O_3 + 3H_2O = 2Co^{3+}(aq) + 6OH^-$	43.05
CoHPO ₄	$CoHPO_4 + H^+ = Co^{2+}(aq) + H_2PO_4^-$	0.49
Co ₃ (PO ₄) ₂	$Co_3(PO_4)_2 + 4H^+ = 3Co^{2+}(aq) + 2H_2PO_4^-$	4.36
Co(UO ₂) ₂ (PO ₄) ₂ ·7H ₂ O	$Co(UO_2)_2(PO_4)_2 \cdot 7H_2O + 4H^+ = Co^{2+}(aq) + 2UO_2^{2+}(aq) + 2H_2PO_4^- + 7H_2O$	-9.90
NiO	$NiO + 2H^+ = Ni^{2+}(aq) + H_2O$	12.41
NiO	$NiO + H_2O = Ni^{2+}(aq) + 2OH^-$	15.59
Ni ₃ (PO ₄) ₂	$Ni_3(PO_4)_2 + 4H^+ = 3Ni^{2+}(aq) + 2H_2PO_4^-$	8.82
Ni(UO ₂) ₂ (PO ₄) ₂ ·7H ₂ O	$Ni(UO_2)_2(PO_4)_2 \cdot 7H_2O + 4H^+ = Ni^{2+}(aq) + 2UO_2^{2+}(aq) + 2H_2PO_4^- + 7H_2O$	-9.50
Cu ₂ O	$Cu_2O + 2H^+ = 2Cu^{2+}(aq) + H_2O$	-0.84
CuO	$CuO + 2H^+ = Cu^{2+}(aq) + H_2O$	7.89
CuO	$CuO + H_2O = Cu^{2+}(aq) + 2OH^-$	20.11
Cu ₃ (PO ₄) ₂	$Cu_3(PO_4)_2 + 4H^+ = 3Cu^{2+}(aq) + 2H_2PO_4^-$	2.21
Cu ₃ (PO ₄) ₂ ·3H ₂ O	$Cu_3(PO_4)_2 \cdot 3H_2O + 4H^+ = 3Cu^{2+}(aq) + 2H_2PO_4^- + 3H_2O$	3.98
Cu(UO ₂) ₂ (PO ₄) ₂ ·7H ₂ O	$Cu(UO_2)_2(PO_4)_2 \cdot 7H_2O + 4H^+ = Cu^{2+}(aq) + 2UO_2^{2+}(aq) + 2H_2PO_4^- + 7H_2O$	-12.80
SrO	$SrO + 2H^+ = Sr^{2+}(aq) + H_2O$	41.15
SrHPO ₄	$SrHPO_4 + H^+ = Sr^{2+}(aq) + H_2PO_4^-$	0.29
Ag ₂ O	$Ag_2O + 2H^+ = 2Ag^{2+}(aq) + H_2O$	6.33
AgO	$AgO + 2H^+ = Ag^{2+}(aq) + H_2O$	-3.53
AgO	$AgO + H_2O = Ag^{2+}(aq) + 2OH^-$	31.53
Ag ₂ O ₃	$Ag_2O_3 + 2H^+ = 2AgO^+(aq) + H_2O$	-11.10
Ag ₃ PO ₄	$Ag_3PO_4 + 2H^+ = 3AgO^+(aq) + H_2PO_4^-$	2.0
Zn(OH) ₂	$Zn(OH)_2 + 2H^+ = Zn^{2+}(aq) + 2H_2O$	12.26
ε-Zn(OH) ₂	$\epsilon\text{-Zn(OH)}_2 + 2H^+ = Zn^{2+}(aq) + 2H_2O$	10.96
Zn(OH) ₂	$Zn(OH)_2 = Zn^{2+}(aq) + 2OH^-$	15.74
ε-Zn(OH) ₂	$\epsilon\text{-Zn(OH)}_2 = Zn^{2+}(aq) + 2OH^-$	17.04
Zn ₃ PO ₄	$Zn_3PO_4 + 4H^+ = 3Zn^{2+}(aq) + 2H_2PO_4^-$	7.6
α-Zn ₃ PO ₄ ·4H ₂ O	$\alpha\text{-Zn}_3PO_4 \cdot 4H_2O + 4H^+ = 3Zn^{2+}(aq) + 2H_2PO_4^- + 4H_2O$	3.84
Zn ₅ (PO ₄) ₃ OH	$Zn_5(PO_4)_3OH + H^+ = 5Zn^{2+}(aq) + 3PO_4^{3-} + H_2O$	9.1
CdO	$CdO + 2H^+ = Cd^{2+}(aq) + H_2O$	15.76
CdO	$CdO + H_2O = Cd^{2+}(aq) + 2OH^-$	12.24

Table B1—continued

Oxide	Reaction	pK_{sp}
HgO	$\text{HgO} + 2\text{H}^+ = \text{Hg}^{2+}(\text{aq}) + \text{H}_2\text{O}$	2.44
HgO	$\text{HgO} + \text{H}_2\text{O} = \text{Hg}^{2+}(\text{aq}) + 2\text{OH}^-$	25.56
Hg ₂ HPO ₄	$\text{Hg}_2\text{HPO}_4 + \text{H}^+ = \text{Hg}^{2+}(\text{aq}) + \text{H}_2\text{PO}_4^-$	-5.2
PbO	$\text{PbO} + 2\text{H}^+ = \text{Pb}^{2+}(\text{aq}) + \text{H}_2\text{O}$	12.65
PbO	$\text{PbO} + \text{H}_2\text{O} = \text{Pb}^{2+}(\text{aq}) + 2\text{OH}^-$	15.35
PbO ₂	$\text{PbO}_2 + 4\text{H}^+ = \text{Pb}^{4+}(\text{aq}) + 2\text{H}_2\text{O}$	-8.26
Pb ₃ (PO ₄) ₂	$\text{Pb}_3(\text{PO}_4)_2 + 4\text{H}^+ = 3\text{Pb}^{2+}(\text{aq}) + 2\text{H}_2\text{PO}_4^-$	-4.43
PbHPO ₄	$\text{PbHPO}_4 + \text{H}^+ = \text{Pb}^{2+}(\text{aq}) + \text{H}_2\text{PO}_4^-$	-2.65
Pb ₅ (PO ₄) ₃ OH	$\text{Pb}_5(\text{PO}_4)_3\text{OH} + 6\text{H}^+ = 5\text{Pb}^{2+}(\text{aq}) + 3\text{H}_2\text{PO}_4^- + \text{OH}^-$	-18.15
Pb ₅ (PO ₄) ₃ F	$\text{Pb}_5(\text{PO}_4)_3\text{F} + 6\text{H}^+ = 5\text{Pb}^{2+}(\text{aq}) + 3\text{H}_2\text{PO}_4^- + \text{F}^-$	-20.47
As ₂ O ₃	$\text{As}_2\text{O}_3 + 2\text{H}^+ = 2\text{AsO}^+(\text{aq}) + \text{H}_2\text{O}$	-1.02
As ₂ O ₃	$\text{As}_2\text{O}_3 + \text{H}_2\text{O} = 2\text{HAsO}_2$	-0.68
As ₂ O ₅	$\text{As}_2\text{O}_5 + 3\text{H}_2\text{O} = 2\text{H}_3\text{AsO}_4$	4.74
RaO	$\text{RaO} + 2\text{H}^+ = \text{Ra}^{2+}(\text{aq}) + \text{H}_2\text{O}$	54.0

APPENDIX C.

LIST OF MINERALS AND THEIR FORMULAE

Table C1.

Mineral Name	Formula
Analcime	$\text{NaAlSi}_2\text{O}_6 \cdot \text{H}_2\text{O}$
Anglesite	PbSO_4
Autunite	$\text{Ca}(\text{UO}_2)_2(\text{PO}_4)_2 \cdot 10\text{H}_2\text{O}$
Bayerite	$\text{Al}_2\text{O}_3 \cdot 3\text{H}_2\text{O}$
Berlinite	AlPO_4
Bobierite	$\text{Mg}_3(\text{PO}_4)_2 \cdot 8\text{H}_2\text{O}$
Böhmite	$\gamma\text{-AlO} \cdot \text{OH}$
Brushite	$\text{CaHPO}_4 \cdot 2\text{H}_2\text{O}$
Brucite	$\text{Mg}(\text{OH})_2$
Calamine	ZnCO_3
Cancrinite	$\text{Na}_6\text{CaCO}_3\text{AlSiO}_4 \cdot \text{H}_2\text{O}$
Cerrusite	PbCO_3
Cherincovite	$(\text{H}_3\text{O})(\text{UO}_2)_2(\text{PO}_4)_2 \cdot 6\text{H}_2\text{O}$
Chlorite	$(\text{Mg,Fe})_3(\text{Si,Al})_4\text{O}_{10}(\text{OH})_2(\text{Mg,Fe})_3(\text{OH})_6$
Chloroapatite	$\text{Ca}_5(\text{PO}_4)_3\text{Cl}$
Chloropyromorphite	$\text{Pb}_5(\text{PO}_4)_3\text{Cl}$
Corundum	Al_2O_3
Crandellite	$\text{CaAl}_3(\text{PO}_4\text{CO}_3)(\text{OH,F})$
Dahllite	$\text{Ca}_5(\text{PO}_4)_3\text{CO}_3$
Dittmerite	$\text{MgNH}_4\text{PO}_4 \cdot \text{H}_2\text{O}$

Table C1—*continued*

Mineral Name	Formula
Dolomite	$\text{CaMg}(\text{CO}_3)_2$
Farringtonite	$\text{Mg}_3(\text{PO}_4)_2$
Fluoroapatite	$\text{Ca}_5(\text{PO}_4)_3\text{F}$
Fluoropyromorphite	$\text{Pb}_5(\text{PO}_4)_3\text{F}$
Gehlenite	$\text{Ca}_2\text{Al}_2\text{SiO}_7$
Gibbsite	$\text{Al}(\text{OH})_3$
Goethite	$\alpha\text{-FeOOH}$
Haysite	$\text{MgHPO}_4 \cdot \text{H}_2\text{O}$, $\text{MgHPO}_4 \cdot 2\text{H}_2\text{O}$
Hematite	Fe_2O_3
Heterosite	FePO_4
Hilgenstockite	$\text{Ca}_4\text{O}(\text{PO}_4)_2$
Hopeite	$\text{Zn}_3(\text{PO}_4)_2 \cdot 4\text{H}_2\text{O}$
Hydrargillite	$\text{Al}_2\text{O}_3 \cdot 3\text{H}_2\text{O}$
Hydrogen autunite	$\text{H}_2(\text{UO}_2)_2(\text{PO}_4)_2 \cdot 10\text{H}_2\text{O}$
Hydroxyapatite	$\text{Ca}_5(\text{PO}_4)_3\text{OH}$
Hydroxy-pyromorphite	$\text{Pb}_5(\text{PO}_4)_3\text{OH}$
Lünebergite	$\text{Mg}_3\text{B}_2(\text{PO}_4)_2(\text{OH})_6 \cdot 6\text{H}_2\text{O}$
Magnesite	MgCO_3
Magnetite	Fe_3O_4
Minyunit	$\text{KAl}_2(\text{PO}_4)_2(\text{OH}) \cdot 2\text{H}_2\text{O}$
Monazite	$(\text{Ce}, \text{La}, \text{Y}, \text{Th})\text{PO}_4$
Montmorillonite	$(\text{Al}, \text{Mg})_8(\text{Si}_4\text{O}_{10})_3(\text{OH})_{10} \cdot 12\text{H}_2\text{O}$
Newberyite	$\text{MgHPO}_4 \cdot 3\text{H}_2\text{O}$
Ningyoite	$\text{CaU}(\text{PO}_4)_2 \cdot 2\text{H}_2\text{O}$
Pitchblende	Impure form of UO_2
Schertelite	$\text{Mg}(\text{NH}_4, \text{HPO}_4)_4\text{H}_2\text{O}$
Serpentine	$\text{Mg}_3\text{Si}_2\text{O}_5(\text{OH})_4$
Silicic acid	H_4SiO_4
Stercorite	$\text{MgNH}_4\text{PO}_4 \cdot 4\text{H}_2\text{O}$
Strengite	$\text{FePO}_4 \cdot 2\text{H}_2\text{O}$
Struvite	$\text{MgNH}_4\text{PO}_4 \cdot 4\text{H}_2\text{O}$
Quartz	SiO_2
Smithsonite	ZnCO_3
Spodiosite	Ca_2FO_4
Trolleite	$\text{Al}_4\text{PO}_4(\text{OH})_3$
Variscite	$\text{AlPO}_4 \cdot 2\text{H}_2\text{O}$
Wagnerite	$\text{Mg}_2\text{F}(\text{PO}_4)$
Wavellite	$\text{Al}_3(\text{PO}_4)_2(\text{OH})_3$
Whitlockite	$\text{Ca}_3(\text{PO}_4)_2$
Wollastonite	CaSiO_3
Wüstite	FeO
Zinc blende	ZnS

INDEX

A

- α -rays, 228
- AASHTO, 173
- accretion process, 10
- acicular, 30
- acicular microstructure, 249
- acid rain, 160
- acid rain conditions, 201
- acid waste components, 220
- acid–base cements, 3, 4, 11, 12
- acrylic, 249
- activated carbon, 208
- active isotopes, 226
- adobe style houses, 5
- AIDS, 245
- air and water pollution control, 218
- Alaska, 172, 178
- Albeian condensed Glauconitic Limestone, 143
- Alcoa (Point Comfort) Red Mud, 167
- alkali carbonation, 190
- allografting, 245
- alpha activity, 235
- alumina, 247
- alumina gels, 122
- alumina sols, 122
- aluminum hydrophosphate $[\text{AlH}_3(\text{PO}_4)]$ gel, 187
- aluminum phosphates, 30
- American Association of State Highway Transportation Officials, 173
- American Nuclear Society [15], 227
- American Petroleum Institute, 179
- American Society for Testing and Materials [16], 227
- ammonium polyphosphate fertilizer, 148
- amorphous, 17
- amorphous gel, 121
- amorphous silica, 233
- amphoteric, 41, 59, 60, 115, 123
- amphoteric behavior, 125, 202, 222
- analcime, 190
- Angkor Thom, 6, 12
- Angkor Wat, 5
- ANL, 173, 174, 178, 186, 187, 190, 196, 230, 231, 235, 241, 242
- ANL and BNL, 186
- annular space, 185
- annulus, 178, 182
- ANS 16.1, 227, 228, 231, 232, 234
- apatite, 90, 91, 218, 230, 246
- apatite forms, 206
- apatite minerals, 206
- apatite structure, 91
- API, 180, 196
- API recommended practice, 179
- API Spec. 10, 180, 183
- API Spec., 181, 184
- API specifications, 179
- API-recommended permeameter, 184
- aqueous solubility, 41, 63
- aquosol, 53, 55, 57, 122, 137
- Archeological findings, 157
- Architectural moldings, oil well cements, 160
- architectural products, 157, 158
- Arctic, 178
- Arctic climates, 192
- Arctic oil fields, 172
- Arctic region, 172
- Argonne, 5
- Argonne National Laboratory, 5, 15, 172, 178, 208, 230
- Arrhenius, 66
- artificial fibers, 169
- artificial graft, 152
- artificial implants, 252
- artificial joints, 251
- ash, 105, 161–163, 165, 169, 171, 174, 198, 201, 205, 236, 241

ash cenospheres, 161
 ash stream, 208
 ash waste form, 208, 209
 ash-based phosphate-cement products, 162
 ash, mining waste, 201
 ash, sawdust, 158
 ASTM, 173
 ASTM freeze-thaw, 173
 ASTM standard, 192
 ASTM standard specimens, 185
 atmosphere, 24, 184
 autografting, 245
 automobile industry, 158, 166
 autunite, 94, 230, 234
 axle of the paddle, 183

B

β - and γ -rays, 228
 bauxite, 5, 10, 123, 167
 bauxite minerals, 123
 bauxitic soils, 135
 Bayer process, 10, 123, 135, 167
 Bayer process residue, 158
 bayerite, 61
 Bechtel Jacobs, 231, 240
 benign waste, 23, 24
 benign waste streams, 158
 berlinite, 121–123, 127–132, 190
 beta activity, 235
 bimodal, 132
 Bindan Corp., 173
 Bindan Monopatch, 173
 bioceramic mineralogy, 249
 bioceramics, 4, 92, 245, 248, 252
 biocompatible, 4
 biocompatible ceramics, 246
 biocompatible material, 246
 biological environment, 245, 246
 biological systems, 246
 biomaterial, 4, 24, 30, 41, 157, 245, 247, 249, 251, 252
 biomaterial applications, 154
 biomedical applications, 152, 154
 bird houses, 5, 7, 12
 blood vessels, 247
 BNL, 178, 186, 187, 190, 196
 boehmite, 61
 bohmite, 123, 124, 127
 bohmitic, 123
 bond strength, 185, 192, 193
 bonding force, 185
 bonding mechanism, 86
 bone, 24, 91, 152
 bone cements, 4, 245, 251

bone marrow, 247
 bone material, 246
 bone minerals, 154
 bone stabilization, 251
 bone substitutes, 245
 borates, 101
 borehole, 172, 178, 182, 184, 185, 196
 borehole sealants, 177, 178
 boric acid, boron carbide, 20, 98, 101–103, 160, 186
 Born equation, 55–57
 borosilicate glass waste forms, 238
 BP-Amoco, 178
 branch chain polymers, 43
 brick, 1, 2, 11, 168
 brick mold, 168
 bridges, 172
 Brookhaven National Laboratory, 15, 178
 brucite, 103
 BTU, 175

C

C ash, 163, 195
 C fly ash, 163
 cadaver, 245
 calcination, 17, 61, 98–100
 calcining of zinc oxide, 113
 calcium, 30
 calcium aluminate cement, 1, 123
 calcium fluorophosphate, 30
 calorimeter, 184
 Cambodia, 5, 6, 12
 canal structures in Venice, 7
 canaliculi, 247
 cancellous bone, 246, 247, 252
 cancellous regions, 247
 cancrinite, 190
 carbon steel, 240
 carbonate apatite, 91, 252
 carbonate rocks, 5, 9
 carbonate water, 201
 carbonated, 251
 carbonated hydroxyapatite, 152
 carbonation, 190
 caries-producing debris, 114
 cartilage, 246
 Casa Grande, 174
 casing, 178, 182, 185
 casing steel, 192, 193
 cast iron, 240
 castables, 101
 caustic soda, 10, 123, 168
 CBPC matrix, 210

- CBPC matrix composite, 157, 158, 161, 162, 165, 169, 171, 172
CBPC processes, 229
CBPC radioactive waste forms, 229
CBPC treatment, 219
CBPC waste form, 207, 208, 209, 220, 227, 228
CBS, 178, 179, 181, 184, 190–196
CBS formulation, 180, 183, 184
CBS slurry, 178, 181, 185
cement grout stabilization, 218
cement matrix, 204
cement waste forms, 232, 240
cement-based waste forms, 236
cements, 2, 9, 11, 12, 49
cenospheres, 161, 165, 171, 191, 192
centipoise viscosity, 184
Central America, 5
ceramic matrix composites, 157, 166
ceramic waste form, 208, 209
Ceramicrete, 107–109, 149, 158, 162–166, 168–172, 174, 186, 192, 195, 207, 210, 218, 219, 223, 227, 231–236, 239–241
Ceramicrete binder, 187, 209, 232, 233
Ceramicrete matrix, 168, 169, 230, 231, 233–235, 240, 241
Ceramicrete matrix composite, 158, 160, 161, 163, 173
Ceramicrete nuclear shields, 219
Ceramicrete process, 229, 236
Ceramicrete slurry, 193, 194, 210, 236, 240
Ceramicrete solids, 236
Ceramicrete stabilization, 231
Ceramicrete waste form, 210, 218, 221, 229, 230, 233, 235, 236
Ceramicrete-based permafrost, 191
Ceramicrete-based permafrost cement, 188, 192
Ceramicrete-based permafrost sealant, 192
cerussite, 205
chain, 43
chain phosphates, 49
chain polymers, 43
chart recorder, 183
chemical contaminants, 219
chemical destruction method, 198
chemical equilibrium constants, 49
chemical immobilization, 198, 219, 221
chemical immobilization of oxides, 204
chemical potential, 64, 78, 79
chemical stabilization, 206, 221
chemical waste streams, 218
chemical, medical, 197
chernikovite, 230
Chevron, 178
chiller, 183
chlorite, 10
chloro-, 92
chloroapatite, 91, 92, 246
chloropyromorphite, 205, 206
circulating temperature, 179, 180
civil engineering applications, 161
class C, 159, 162, 163
class C and F, 163
class C and F ashes, 186
class C fly ash, 162–164, 186, 187
class F, 162, 163
class F ash, 105, 161–163
class F fly ash, 162–165, 173, 190, 191, 208, 232
class F loading, 163
clay minerals, 10, 11
Clean Air Act requirements, 161
CO atmospheres, 121
CO₂ environment, 190, 192
coal ashes, 23
coal bottom ash, 208
cohesive forces, 178
cold climate, 158, 172
collagen, 246
collagen fiber, 246, 247
collagen fibrils, 246
combustion, 241
combustion products, 159, 161
combustion residue, 223, 235
complexation-elution process, 231
compressibility, 65
compression strength, 1, 163, 210, 236, 247
compressive, 17, 117, 121, 149
compressive strength, 3, 18, 105, 108, 114, 139, 147, 148, 149, 151, 153, 154, 160, 162, 164, 166, 173, 185, 190, 191, 228, 231, 233, 240, 249–252
compressors, 240
computer, 183
conches, 5, 9
concrete, 29, 107
concrete structures, 151
condensation polymerization, 48
condensed phosphates, 48
consistency, 183, 186, 188, 189
consistometer, 182–186
consistometer assembly, 182
consistometer cell, 193
construction industry, 24, 161, 172, 218
construction material, 158
construction products, 23, 29, 168
container drum, 52
contaminant, 30, 197–202, 204, 206–208, 210–212, 219, 224, 228, 231, 237, 241

contaminant atom, 228
 contaminant concentrations, 211
 contaminant levels, 210
 contaminant reaction product, 228
 contaminated sediments, 205, 230
 contaminated soil, 205, 210
 contamination, 198, 217
 conventional portland cement, 149, 150
 converters, 240
 coolers, pumps, 240
 coordination number, 87–89
 Coordination Principle, 87
 coral reefs, 7
 corals, 10
 corrosion, 121, 169, 240
 corrosion resistance, 1, 9
 corrosion resistant, 2, 3
 corrosive environments, 158
 cortical, 247
 cortical bone, 246–248, 252
 corundum, 3, 61, 123, 124, 127, 128, 132, 147
 cotton, 169
 Coulomb, 86
 Coulomb's law, 55
 counterions, 3
 covalent, 2, 86, 87, 93
 covalent bonds, 2, 86, 87
 covalent network, 122
 covalent phosphate structure, 92, 93
 covalent structure, 92
 crushed glass, 209
 crushed Hg light bulbs, 209
 crushed waste forms, 233
 cryogenic fluids, 174, 192
 curing chamber, 183, 185, 186
 cyclic, 43

D

90-day immersion tests, 240
 dahllite, 91, 152, 154, 246, 251
 dahllite-based bioceramic, 249, 251
 dahllite-based biomaterial, 252
 dahllite-based material, 252
 darcies, 184
 debris waste, 231
 Debye's theory, 70
 decontamination, 197
 decontamination and decommissioning work, 151
 decontamination technologies, 198
 deep and geothermal, 187
 deep well, 163, 180, 193
 deep well cement, 189

deep well compositions, 193
 Defense Waste Processing Facility glasses, 231
 deionized water, 200
 Delphi DETOX, 208, 209
 dental, 4, 154
 dental applications, 4
 dental cements, 3, 4, 15–18, 23, 24, 30, 41, 113, 115,
 121, 160, 165, 245, 249, 251, 252
 dental material, 23, 121
 dental phosphate cements, 16
 dental products, 143
 dental ridge augmentation, 251
 dentine, 246, 247
 dentist, 17, 113, 116
 dentistry, 19, 114
 Dentsply, Inc., 249
 Department of Transportation, 198
 desert, 5
 desert grass, 5, 7
 desert soils, 5
 desiccator, 153
 detection limit, 208, 234, 237, 241
 detergent, 166
 dewar, 192, 174
 dielectric constant, 55, 56
 dielectrics, 55
 differential scanning calorimetry (DSC), 148, 186
 differential thermal, 186
 differential thermal analysis, 102, 108, 122, 163
 differential thermal output, 165
 diffusion constant, 228, 239
 diffusion mechanism, 228
 diffusion transport, 228
 diffusivity, 227
 dipole attraction, 86
 dipole forces, 87
 dismantled components, 217
 dispersibility, 222
 'dissociation (ionization) constant', 49
 dissociation constants, 49, 50, 153
 dissolution model, 23, 24
 dissolution–precipitation process, 10
 dittrmarite, 20, 105, 106
 DOE, 219, 226, 227, 230, 234
 DOE ash waste, 208, 209
 DOE complex, 210, 241
 DOE contractor, 240, 241
 DOE site, 152, 210, 223, 225, 231, 237, 241, 242
 dolomite, 185, 193
 downhole cement, 179, 185, 192
 downhole cements in geothermal wells, 148
 downhole conditions, 181
 downhole environment, 192

downhole gas environment, 181
 downhole pressure, 181
 downhole rocks, 185, 192, 193
 downhole static temperature, 185
 downhole temperature, 180, 181, 184, 186, 187, 193
 downhole temperature and pressure, 181, 183
 drill cuttings, 166
 drilling and completion industry, 172, 177
 drilling cements, 24, 70, 161, 163
 drum, 52
 DSC, 148, 149
 DTA, 109, 128, 163
 dye casting, 104, 105, 168
 dynamic temperature, 186, 187

E

Eagle Picher Industries, 241
 earth materials, 24
 earthquake, 226
 Earth's Crust, 41
 EDX, 130
 efficient separation methods, 217
 Egyptians, 12
 E_h -pH diagram, 81, 137, 138, 141, 224
 electric arc furnace dust, 205
 electric current, 7
 electric fields, 55
 electrical, 70, 121
 electrical insulating components, 121
 electrical pulse, 228, 239
 electricity, 86
 electrochemical equilibrium, 76
 electrochemical potential, 79, 84
 electrochemical reaction, 76–79
 electrochemistry, 76, 81
 electrode, 9, 78
 electrode potential, 79, 80, 84
 electromotive force, 78
 electromotive potential, 78
 electromotive potential difference, 78
 electronics, 197
 electrostatic precipitators, 161
 endotherm, 102, 128
 endothermic dissolution reaction, 70
 endothermic reaction, 67
 energy dispersive X-ray analysis, 107, 130
 enthalpies of formation, 116
 enthalpy, 63–65, 67, 70, 73, 181, 184
 entropy, 63, 64, 71, 181
 entropy change, 70
 EPA, 228, 237

EPA limit, 208, 209
 EPA oxidation test, 239
 equilibrium electrode potential difference, 79
 erosion, 9
 Europe, 151
 exothermic, 29, 67, 70
 exothermic acid–base reaction, 69
 exothermic dissolution reaction, 69, 70
 exothermic heat evolution, 149
 exothermic quantity, 68
 exothermic reaction, 67, 68
 extenders, 158, 186, 192
 extensospheres, 161
 Exxon–Mobil, 178

F

F ash, 163, 195
 F fly ash, 159
 Fahrenheit, 179
 Faraday constant, 79
 Fernald silo waste, 224, 230
 Fernald silos, 234
 fertilizer, 90, 105, 148
 fertilizer chemicals, 30
 fertilizer components, 212
 fiber reinforcement, 169
 fiber-reinforced ash containing Ceramicrete, 172
 fiber-reinforced composites, 169
 filters, 1, 198
 first coordination shell, 88
 Fisher Scientific, 128
 fission products, 23, 75, 92, 219–221, 223, 225, 228, 230
 fixed contamination, 217, 221
 flammable polymers, 24
 flammable salt wastes, 240
 flammable salts, 239
 flammable waste, 241
 flash set, 183, 191
 flash-setting cements, 183
 flexural strength, 18, 30, 149, 150, 160, 169, 170, 240, 249, 250
 flocculants, 16
 Florida, 30
 fluoride fluxes, 17
 fluorides, 17, 114
 fluorinated apatite, 252
 fluorinated hydroxyapatite, 251
 fluoroapatite, 91, 92, 151, 223, 246
 fluoropyromorphite, 206
 fly ash, 24, 30, 108, 158, 160, 161, 163, 187, 233
 fly ash, mineral waste, 158

fly ash, wollastonite, 160
 food chain, 197, 200, 217
 food cycle, 198
 force, 86
 forest product waste, 158
 formation, 182, 184, 185
 formed under elevated temperature and pressure, 236
 former 'closed cities', 217
 former Soviet Union countries, 217
 fossil fuels, 161
 foundations for buildings, 172
 fracture energy, 150, 169, 247
 fracture toughness, 21, 149, 150, 160, 169, 171, 240, 247, 249, 250
 fractured surface, 150, 172
 free water, 181, 184
 freeze-thaw, 148
 freeze-thaw cycles, 147, 173, 191, 192
 freeze-thaw durability, 173
 freeze-thaw durability factor, 160
 freezing point, 186
 frost, 192
 FUETAP, 236
 FUETAP cement, 3, 236
 FUETAP concrete, 236
 functionally gradient, 248
 furnaces, 198

G

55-gal waste form, 239
 γ -ray absorption, 160
 γ -ray shield, 171
 G-class portland cement, 190
 galvanic cell, 77, 79
 gamma, 235
 gas, 186
 gas chromatography, 229
 gas constant, 66
 gas hydrate region, 191, 192
 gas migration, 177, 185, 192
 gas permeability, 181, 184, 191
 gaseous diffusion plant waste, 239
 gehlenite, 147
 gel, 12, 122, 129, 190
 gelatinous coating, 113, 121
 gelatinous substance, 113, 121
 gelation, 11, 12, 18
 geochemists, 6
 geologic repositories, 240
 geological time scale, 11
 geopolymer, 3, 9
 geotechnical structures, 151

geothermal, 187
 geothermal wells, 49, 70, 177, 178, 180, 186, 187, 190
 Gibbs free energy, 63–67, 70, 72, 78, 125, 136, 145, 180
 Gibbs–Duhem relations, 65
 Gibbs–Helmholtz equations, 70, 126
 gibbsite, 123, 124, 126, 127
 gibbsitic, 123
 glass fiber, 160, 169, 171, 240
 glass forms, 233
 glass waste form, 227, 232, 233
 glass-ceramics, 1
 glass-ionomer cement, 3
 glassy phases, 237
 global coral reef alliance, 7
 Global Petroleum Research Institute, 178
 glovebox, 229, 235
 grain growth, 116
 Grancrete, 174
 Great Britain, 217
 groundwater, 30, 197–203, 212, 221, 226, 228, 240

H

half-life, 220, 223, 224
 Halliburton Energy Services, 178, 190, 191
 Hanford, 225, 231
 Hanford acid waste, 236
 Hanford and Savannah River, 223
 Hanford and Savannah River tanks, 236
 Hanford disposal facility, 238
 Hanford tank, 210, 211, 230
 HAP, 153, 246, 248, 251, 252
 hardened CBS, 184
 Haversian canal, 247
 HAW, 226
 Haysite, 20
 hazard potential, 198
 hazardous, 23, 24, 30, 197, 199
 hazardous and radioactive components, 218, 221
 hazardous and radioactive waste streams, 241
 hazardous constituents, 226, 227
 hazardous contaminants, 23, 95, 200, 202, 204, 206, 207, 210, 211, 218, 221, 225, 237
 hazardous metal contaminants, 201
 hazardous metal oxides, 202
 hazardous metals, 75, 199, 200, 201, 205–207, 226
 hazardous or radioactive, 197
 hazardous waste, 19, 23, 200, 201
 hazardous waste stabilization, 197

hazardous waste streams, 97, 107, 197, 201, 202, 204, 205, 229
heat exchange, 64
heat of formation, 184, 185, 192
heat of fusion, 191
heat of hydration, 181, 184
heavy metal contaminated sludge capping, 205
heavy metal plating sludge, 205
hematite, 5, 10, 23, 61, 75, 77, 78, 135–137, 139, 166, 192
high brilliance X-ray diffraction, 252
high carbon ash, 161
high temperature processes, 218
high temperature superconductors, 1
high-activity components, 225
high-activity isotopes, 220
high-activity products, 218
high-activity waste, 225
high-activity waste stream, 225
high-level tank wastes, 231
high-level waste forms, 226
high-level waste tanks, 230
high-pressure vessels, 229
highways, 172
historical controls, 252
HLW, 231
Hobart cement mixer, 168
Hobart table-top mixer, 208
hollow microspheres of silica, 158
hopeite, 113, 114, 117, 121
hot and deep wells, 178
hot crude, 172, 191
hot pressing, 3
human body, 90, 153, 197
human culture, 157
Hume–Rothery rules, 88
hydrargillite, 61, 122, 124, 132
hydration, 184
hydraulic cements, 1–3, 8
hydrocarbon environment, 191
hydrocarbon gases, 192
hydrocarbons, 24
hydrochloric acid, 49
hydrogen bond, 1, 87, 90
hydrogen bonding, 87
hydrogen electrode, 79
hydrothermal treatment, 122
hydroxides, 201
hydroxy-, 92
hydroxyapatite, 30, 90–92, 143, 152, 190, 205, 230, 234, 246, 249
hydroxypyromorphite, 206

I

Idaho National Engineering and Environmental Laboratory, 209, 225
ignitability, 228, 230, 239
ignitability test, 239
ignitable waste stream, 206
IL, 173
imaginary galvanic cell, 78
immobilization of radioactive contaminants, 221
immobilization of radioactive elements, 221
impermeable barrier, 192
impermeable seals, 185
incinerated residues, 217
incineration, 198, 218
incinerator ash, 161
India, 5
Indonesia, 190
industrial activity, 158
industrial waste streams, 158, 159, 205
industrial wastewater, 205
infectious diseases, 245
inorganic contaminants, 199, 201
inorganic hazardous contaminants, 212
inorganic polymers, 190
inorganic waste, 197
inorganic waste streams, 241
Instron machine, 193
insulating cements, 160
insulation, 159
insulator, 171, 191
interatomic bonds, 85
internal energy, 64, 65
internal stresses, 122
International Standards Institute, 180
interparticle bonds, 2
interparticle diffusion, 1
inventories of radioactive waste, 217
investment materials, 19
ionic, 2, 86, 87
ionic bond, 2, 86
ionic conductivity, 86
ionic crystals, 87
ionic radii, 181
ionization constant, 45, 58–60
ions, 94
iron carbide, 166
iron debris, 241
iron industry, 166
iron mine tailings, 141, 159
iron tailings, 158
islands, 168

J

Jamaica, Guyana, 168
 Jamaican bauxite, 10
 Jamaican red mud, 10
 Japan, 190
 Japan Petroleum Exploration Company, 190
 joule heating, 183
 joules, 64

K

K-25, 240
 K-25 debris waste streams, 232
 K-25 plant at Oak Ridge, 230
 K-27 plants, 240
 Kanthal loop, 239
 Kanthal wire, 228
 kaolin, 3
 kinetics of hazardous waste stabilization, 212
 Kola, 30
 Kyushu, 190

L

lacunae, 247
 large-scale stabilization, 202
 laterite, 10, 11
 lateritic, 5
 lateritic soils, 5, 10, 11, 135, 141
 lattice dynamical model, 70
 lattice point, 64
 LAW, 226, 238
 leachability index, 231
 leachate, 209
 leachate water, 208
 leaching index, 228, 233, 238, 239
 leaching levels, 208–210
 leaching performance, 208
 LI, 231, 232, 234, 239, 241
 LI for contaminants, 238
 lightweight grout, 160
 limestone, 1, 157, 175, 185, 193
 limestone areas, 201
 linear, 43
 linear expansion coeff, 160
 linings in furnaces, 157
 liquid nitrogen, 174, 192
 liquid salt wastes, 217
 liquid waste streams, 210
 load-bearing strength, 198
 load factor, 158
 long chain, 48
 long-lived isotopes, 220
 loose and fixed contamination, 240

loss on ignition, 167
 lost circulation, 181, 183, 185
 low cost housing, 158
 low-activity streams, 218
 low-activity waste, 225
 low-activity waste stream, 225
 low-NO_x burners, 161
 low-pressure zones, 180
 lünebergite, 101, 102

M

machine oils, 166
 machine tool, 166
 machining swarfs, 141
 macro-defect-free, 2
 macroencapsulation, 219, 221, 237, 240, 241
 macroencapsulation technique, 237
 macroions, 3
 magnetic forces, 70
 magnetite, 23, 75, 84, 135–137, 166
 manufacturing cost, 154
 marine environment, 9
 marine resources development foundation, 8, 12
 mass balance, 76
 material radioactive, 93
 Mayak, P.R., 225
 MCC-1, 227, 228, 232, 233
 membranes, 1
 mercury column, 184
 metakaolin, 3
 metal abundance, 41
 metal swarfs, 166
 metallic bonds, 86
 microencapsulation, 206, 207, 221, 232, 233, 237
 mild steel, 185
 millidarcies, 184, 191
 mine tailings, 205
 mineral accretion process, 6, 8, 12
 mineral waste, 23, 29
 mining and civil engineering, 178
 mixed, 197
 mixed waste streams, 207
 moderators, 121
 moduli of rupture, 106
 molds, 51
 molecular radii, 181
 monazite, 93, 94
 monomers, 48
 monopatch, 173
 monozites, 218
 montmorillonite, 10

Morocco, 30
 mortar, 105, 106
 motors, 240
 MSW, 201, 205
 MSW ash, 206
 municipal sewage, 204
 municipal solid waste, 161, 201
 musculature, 252

N

National Academy of Sciences, 218
 natural fiber, 5, 169
 natural gas, 178
 natural resources, 158
 neutron absorption coefficient, 160
 neutron shield, 171
 newberyite, 20, 22, 102–104, 107, 109, 117, 122
 Nile river, 7, 12
 Nile silt, 5, 12
 nitrate waste, 239
 nitrate waste forms, 236, 239
 nitrate waste streams, 238
 nitrogen gas cylinder, 184
 nonflammable waste forms, 241
 nonignitable ceramic, 206
 nonleachable glass matrix, 218
 nonlinear viscosity, 183
 nonspontaneous dissolution, 69
 nonspontaneous dissolution reaction, 69
 nonspontaneous reaction, 67
 nonthermal methods, 198
 nonthermal stabilization, 199
 nonthermal stabilization technology, 218
 nonthermal treatment, 198, 199
 normalized leaching rate, 227, 231, 238
 Northern Canada, 172
 northslope, 178
 NRC land disposal requirement, 236
 nuclear age, 217
 nuclear energy, 217
 nuclear industries, 241
 nuclear materials, 160
 Nuclear Regulatory Commission, 226
 nuclear shield, 241
 nuclear waste encapsulation, 3
 nuclear weapons, 217
 nucleation sites, 194
 nylon, 169

O

Oak Brook, 173
 Oak Ridge, 240

Oak Ridge K-25 plant, 231
 ocean beds, 178
 off-gas treatment systems, 218
 offshore, 180, 194
 offshore well, 195
 oil, 178, 186
 oil and gas wells, 70, 177
 oil and natural gas industry, 177
 oil and natural gas wells, 177, 181
 oil drilling and completions, 4
 oil field cements, 23, 180
 oil field drilling cements, 157
 oil field service companies, 180
 oil fields, 24, 166, 172, 177
 oil well, 180, 187, 193
 oil well cements, 101, 180
 oil well platforms, 182
 onshore wells, 195
 opaque solid, 114
 organic chemicals, 199
 organisms, 5, 9
 orthophosphoric acid, 30, 43
 orthopedic substitutions, 247
 osteoblasts, 246–248
 osteocytes, 247
 osteoid, 246
 osteons, 247, 248
 oxidation, 75, 76
 oxidation reaction, 76–79
 oxychloride, 4
 oxychloride cements, 4
 oxysalt, 3
 oxysalt cements, 4
 oxysulfate cements, 4

P

paddle, 183
 paddle assembly, 183
 particles, 132
 passivation layer, 125
 PCT, 226, 227, 231–233, 237, 238
 Pennsylvania turnpike, 174
 peptide chains, 246
 periodic configurations, 86
 periodic table, 53, 89
 periodontal defect filling, 251
 permafrost, 160, 177, 178, 186, 187
 permafrost formation, 172, 191
 permafrost phosphate sealant, 191
 permafrost region, 172, 177, 181, 191
 permafrost-sealant, 186
 permafrost well, 186

permeability, 184, 191, 192
 permeable reactive barrier, 230
 petrochemical, 197
 pH stabilization, 205
 pharmaceutical, 197
 phosphate amendment, 205
 phosphate-based permafrost cement, 192
 phosphate bonded cements, 3
 phosphate ceramic waste forms, 208
 phosphate concrete, 29
 phosphate fertilizers, 30
 phosphate form, 211, 221
 phosphate gel, 117
 phosphate glues, 21, 75
 phosphate ores, 30, 31
 phosphate stabilization, 204, 212
 phosphate stabilizer, 204, 205
 phosphate tetrahedra, 94
 phosphate tetrahedrons, 93
 phosphate treatment, 206, 211, 212
 phosphate treatment of radioactive wastes, 212
 phosphate washing, 204, 206, 207, 212
 phosphatic clay, 206
 phospho-silicate ceramicrete, 149–151
 phosphogypsum, 175
 phosphoric acid, 29, 43
 physical encapsulation, 204, 219
 physical microencapsulation, 221
 physiological environment, 153
 pipe sections, 192
 pipeline supports, 172
 pipelines, 172
 piping sections, 240
 pitchblende, 223
 plaque, 114
 plaster of paris, 1, 245
 plutonium and uranium extraction process, 225
 plutonium separation process, 225
 PO₄ polyhedron, 88, 89
 PO₄ tetrahedron, 89
 polyalkenoate, 3
 polyalkaonate cements, 3, 4
 polycarboxylate cements, 3
 polyions, 3
 polymer cements, 249
 polymer fibers, 169
 polymeric coating, 101
 polymerization, 18
 polyphase ceramics, 218
 polyphosphonic cements, 3
 porcelain, 17
 porcelain dental cements, 121
 Portland, 191

Portland cement, 1, 2, 29, 107, 152, 154, 157, 168, 172, 175, 177, 190, 191, 240, 251
 Portland cement concrete, 139, 152
 Portland cement products, 168
 potential–pH relation, 136, 137
 potholes, 151, 172
 pottery, 1, 157
 Pourbaix diagrams, 223
 Pourbaix's treatment, 84
 power plants, steel slag, 159
 power production, 217
 pozzalanic, 162
 pre-calibrated potentiometer, 183
 precalcination, 101, 116
 precalcined, 116
 pressure, 71, 79, 80, 180, 181, 186
 pressure cell, 183
 pressure gauge, 229
 process liquids, 217
 product consistency test (PCT), 227
 prosthodontic crowning, 251
 protective shelters, 5
 protein, 246
 protons, 18
 Pu-containing combustion residue, 234
 pulp capping, 251
 pumping time, 177, 178, 181, 187, 194, 195
 PUREX, 225
 pyramids, 12
 pyrex beakers, 229
 pyromorphites, 206, 91
 pyrophoric, 135, 166, 229, 234
 pyrophoric components, 229
 pyrophoricity, 229, 230, 234
 pyrophosphoric acid, 43

Q

quaternary metal phosphate, 206

R

rabbit, 252
 radiation chemical yield, 235
 radioactive, 19, 23, 30, 107, 197, 206, 219, 225
 radioactive and hazardous contaminants, 94, 95, 218, 220, 226
 radioactive components, 24, 218, 219, 221, 225
 radioactive constituents, 218
 radioactive contaminant, 95, 197, 199, 206, 210, 217, 219, 220, 221, 227, 228
 radioactive elements, 206, 212
 radioactive isotope, 75, 202, 220, 224, 228

- radioactive materials, 160
 - radioactive minerals, 218
 - radioactive objects, structural ceramics, 160
 - radioactive supernatant, 210
 - radioactive waste, 197, 199, 208, 217, 221, 224, 226
 - radioactive waste encapsulation, 160
 - radioactive waste forms, 206, 227
 - radioactive waste immobilization, 221
 - radioactive waste management complex, 209
 - radioactive waste materials, 217
 - radioactive waste streams, 209, 217, 218, 220, 222, 229, 230
 - radioactive wastes stabilization, 217
 - radioactively contaminated cement debris, 151
 - radioactively contaminated debris, 240
 - radioactivity, 175
 - radiological risks, 217
 - radiolysis, 228–230, 235
 - radiolysis effects, 228
 - radiolysis tests, 241
 - radiolysis yield, 236
 - radiolytic decomposition, 235
 - radiolytically generated hydrogen, 226
 - rapid prototyping, 248, 252
 - RCRA limit, 200
 - RCRA metals, 199, 202
 - recycling, 23
 - recycling metal values, 159
 - recycling of the contaminants, 197
 - recycling of waste, 197
 - red mud, 10, 11, 135, 141, 159, 166–168
 - redox conditions, 81
 - redox potential, 77, 79, 83
 - redox reaction, 76–81
 - reducers of water demand, 2
 - reductant, 75, 78, 84
 - reduction (redox) reactions, 76
 - reduction mechanism, 75, 83, 84, 140
 - reduction reaction, 76–79
 - reduction–oxidation diagrams, 234
 - reference electrode, 79
 - refractory, 21, 101, 157
 - refractory applications, 107
 - refractory bricks, 121
 - refractory cement, 3
 - refractory components, 49
 - refractory materials, 105
 - refractory products, 1, 105
 - regulatory limit for Hg leaching, 204
 - regulatory limits, 208
 - regulatory requirements, 210
 - repository, 93, 220, 226
 - Resource Recovery and Conservation Act, 199
 - retardant, 101, 178
 - retardation, 101, 102
 - Reynolds chemical company, 128
 - rheology, 181, 183
 - ring, 43
 - ring polymers, 48
 - road repair, 158, 172
 - road repair materials, 106, 157
 - road-based and permafrost applications, 160
 - road-based applications, 160
 - roads, 172
 - rock core samples, 193
 - rocks, 24
 - Rocky Flats, 210, 223, 234, 235
 - Rocky Flats ash waste, 230
 - root canal, 249
 - root canal obturation, 251
 - rotational viscometer, 183
 - rotor speed, 183
 - rudimentary tools, 157
 - Russia, 30, 151
 - Russian Federal Nuclear Center at Sarov, 241
 - Russian Federation, 225
- S**
- saline, 201
 - saline water, 195
 - salt supernatant, 230, 232
 - salt sludge, 232
 - salt waste components, 220
 - salt waste forms, 236, 239
 - salt waste stabilization, 236
 - salt waste streams, 225, 237, 239
 - salt waste tanks, 231
 - salts, 202
 - sand, gravel, ash, soil, 29
 - sandstone, 193
 - saturated gel, 12
 - saturation, 12
 - Savannah River, 225, 231
 - Savannah River site, 230, 234
 - saw dust, 158, 166, 239
 - scaled loss, 173
 - scaling, 173
 - scanning electron micrograph, 10, 99, 109, 150, 169, 250
 - scanning electron photomicrograph, 108, 140, 141, 249
 - schertelite, 20, 104–106
 - sea organisms, 5, 9
 - sea shells, 5, 9
 - sea water, 5, 10, 177

- seal, 185
- sealant, 185, 191, 192
- second law of thermodynamics, 64
- secondary waste, 198, 208
- secondary waste streams, 198, 199, 218
- secondary wastes from the separation, 218
- sedimentary rocks, 5
- self-radiation, 223, 228
- SEM, 130, 131
- SEM micrograph, 161, 165, 172
- separation processes, 218
- separation technologies, 218
- serpentine, 10
- serpentinite, 19
- set sealant, 185
- shale, 185
- shallow well, 186, 187, 193
- shear bond strength, 160, 173
- shell, 5, 178
- shield, 52
- short-lived isotopes, 220
- shredded styrofoam, 159
- silica, 5, 29
- silicotitanate waste forms, 233
- silicotitanates, 233
- simulated downhole environment, 181
- simulated Pu-contaminated ash, 210
- simulated salt waste, 230
- simulated salt waste streams, 230
- simulated seawater, 195
- simulated sludge, 211
- simulated solid waste, 211
- simulated supernatant, 237
- simulated supernate waste, 211
- simulated tank waste streams, 236
- sintered ceramics, 23
- skeletal system, 245, 246
- slags, 161, 166
- sludge, 198, 211, 236–238
- sludge streams, 237
- sludge waste form, 237, 238
- sludge waste streams, 238
- slurry cup, 183
- slurry density, 191
- smelter slags, 205
- soft tissues, 153
- sol–gel process, 53, 57
- sol–gel science, 122
- solar energy, 7
- solid solution, 88, 116
- solidification, 5, 19, 23, 198, 199, 205, 209
- solidification of low-level radioactive waste, 97
- solidified waste forms, 218
- sols, 137, 58
- solubility, 63
- solubility product, 59, 126
- solubility product constant, 58, 59, 63, 66, 69, 70, 72, 73, 124, 152, 207, 222
- solvent, 51
- South Asia, 5
- South-West United States, 5
- sparsely soluble, 10, 11, 23, 75, 98, 153, 201, 202, 204, 211, 212
- sparsely soluble bases, 12
- sparsely soluble components, 201
- sparsely soluble compounds, 10, 201
- sparsely soluble form, 221
- sparsely soluble oxide, 53, 55, 58, 201, 210
- sparsely soluble solids, 53
- specific activity (Ci/g), 220, 235
- specific gravity, 247
- specific heat, 65, 70–72, 126, 185
- spektr conversion at Snezhinsk, 241
- spent nuclear fuel rods, 217
- spontaneous dissolution, 67
- spontaneous reaction, 67, 69
- sprayable coatings, 160
- stability of water, 81–83
- stability regions of water, 81, 83
- stabilization, 19, 23, 97, 198–202, 204–208, 210, 211, 218, 221–224, 226, 231, 232, 234, 241
- stabilization and solidification, 198
- stabilization approach, 202
- stabilization factor, 201
- stabilization kinetics, 202
- stabilization matrix, 224
- stabilization mechanisms, 24, 238
- stabilization method, 200
- stabilization of chromium, 210
- stabilization of hazardous contaminants, 212
- stabilization of hazardous metal oxides, 75
- stabilization of hazardous metals, 202, 224
- stabilization of Hg, 208, 209
- stabilization of Ra, 235
- stabilization of radioactive and hazardous waste streams, 157
- stabilization of radioactive and hazardous wastes, 5
- stabilization of technetium, 230
- stabilization procedure, 198
- stabilization process, 198, 210, 218
- stabilization treatment, 203

stabilized matrix, 234
stabilized product, 204
stabilized waste, 207, 210
stabilizers, 212
stabilizing chemicals, 199
standard chemical potential, 79
standard enthalpy, 71
standard Gibbs free energies, 81
standard potentials, 81
standard redox potential, 79
standard temperature, 71, 79, 80
standard temperature and pressure, 79
standard thermodynamic state, 79
standardized tests, 226
static downhole temperature, 178
static temperature, 179, 180, 186, 187
statistical–mechanical approach, 63
steam, 121
steel, 247
steel industry slag, 161
stercorite, 105
stirrer, 184
stoichiometric coefficients, 77
stoichiometric formula, 154
stoichiometry, 107
strength, 23, 192
strength (compressive), 18
striations, 100
structural and nuclear materials, 161
structural ceramic, waste management, 160
structural ceramics, oil well cements, waste encapsulation, 160
structural clay products, 16
structural material, 154, 157–160, 172
structural material in permafrost regions, 158
structural products, 41, 158, 159
struvite, 20, 104–108
styrofoam, 192
styrofoam sheets, 174
styrofoam, wood chips, cenospheres, 160
sulfidation, 211
sulfide forms, 207
sulfide immobilization, 208
sulfide stabilization, 204, 207
sulfide treatment, 207
Sumatra, 190
supernatant, 225, 230, 231, 236–238
supernatant waste form, 233, 238
surface area, 10, 185, 194, 198, 200, 227, 233, 237, 239
surface-to-volume ratio, 239

surrogate, 208, 229, 234
surrogate waste, 208, 239
surrogate waste form, 211
surrogate waste streams, 208, 234
swarf, 135, 141, 158, 159, 166–168

T

tank waste streams, 223
Tatra Mountains, 143
TCLP, 200, 201, 205, 209–211, 227, 232–235, 237, 238
TCLP leachate, 211, 234, 235, 237
TCLP result, 210, 211
TCLP test, 200, 208, 226
technetium-containing radioactive waste, 210
technological materials, 157
Temple, 6
Tennessee, 240
tensile strength, 17, 18, 117, 121, 147, 148, 153, 154, 246, 247
ternary diagram, 153
terra cotta, 168
tertiary metal phosphates, 206
tetrahedra, 91–93
tetrahedral crystal structure, 89
tetrahedron, 89, 92
TGA, 109
themocouple, 183
therapeutic effects, 17
thermal conductivity, 121, 158, 160, 191, 192
thermal cycling, 147
thermal cycling resistance, 148
thermal expansion coefficient, 65, 148
thermal expansion, 147
thermal stability, 157
thermal treatment, 198, 199
thermally insulating structural products, 159
ThermaLock, 178, 190, 196
thermodynamic model of dissolution, 63
thermodynamic parameter, 65–67, 71, 72
thermodynamic potentials, 63–65
thermodynamic properties, 52
thermogravimetric analysis, 108, 186
thermometer, 184
third law of thermodynamics, 65
third world countries, 168
tidal waves, 7
titanium, 247
titration test, 100

tooth enamel, 18, 114
torque, 183
toughness, 30
toxic chemicals, 197
Toxicity Characteristic Leaching Procedure (TCLP), 199, 227
toxicological studies, 199
translucency, 17, 18
translucent, 22
translucent product, 121, 143
transuranic, 228, 230, 235
transuranic ash, 236
transuranic elements, 23
trauma, 245
treated ash, 205
treated waste streams, 226
triple super phosphate, 32, 205
tritiated water, 236
tubing, 240
tumors, 245

U

U-contaminated groundwater and soil, 205
ultimate compressive, 118
ultimate tensile strength, 252
ultrasonic bath, 233
ultrasonic signals, 8
ultrasound signal, 123
underground, 178
underground repository temperature, 226
underwater construction, 178
uniaxial press, 185
United States, 30, 152, 158, 161, 173, 205, 217, 219, 225, 226
universal treatment standard, 200
University of Minnesota, 175
Unocal Corp., 178, 190
Unocal's geothermal well, 190
uranium tailings, 217
uranyl, 94
urea formaldehyde, 24
US Department of Energy, 208, 217, 230
US Environmental Protection Agency, 199, 226, 227
utility fly ash, 161, 209
utility industry, 161
utility plants, 161, 201
utility supply lines, 152
UTS, 210, 211, 237
UTS limit, 200, 209, 237

V

value-added products, 158, 168
valves, 240
van der Waals bonds, 2, 86, 87
van der Waals forces, 2, 89
vermiculite, 208
viscosity, 161, 186
vitrification, 202, 218
vitrification process, 218
volatile organic compounds, 24
volcanic ash, 161

W

wüstite, 75, 78, 135
WAC, 220, 226, 230, 238, 241
waring blender, 183
washed waste, 207
waste, 226, 232, 241
waste acceptance criteria, 219, 220, 226, 230
waste chemicals, 198
waste form, 29, 198, 206–209, 211, 212, 218–220, 226–229, 231, 233–239, 241
waste form matrix, 221
waste forms of silicotitanates, 233
waste loading, 210, 237
waste management, 4, 23, 41, 159
waste packages, 228
waste repositories, 217
waste stabilization, 200, 219
waste stream, 158, 166, 197–199, 201–210, 217–220, 222, 223, 226, 230–232, 236, 237
waste stream composition, 217
waste-to-energy facilities, 205
wastewater, 197, 201, 210, 232, 233
water absorption, 149
water of crystallization, 46
water shut off, 178, 185
weapons waste, 242
Western Carpathians, 143
wheelabrator technologies, 204
whisker reinforcement, 169
whisker-reinforced ceramic, 150
whiskers, 150
wollastonite, 19, 30, 108, 147, 149, 150, 154, 160, 174, 186, 249
wollastonite and class F fly ash, 187
wollastonite-based Ceramicrete, 150
wollastonite-containing Ceramicrete, 249, 251
wollastonite-filled Ceramicrete, 149

wood, cellulose, 169
wood chips, saw dust, 158, 159, 166
wood composites, 169
wood dust, 239
wrist fracture, 252

X

X-ray diffraction, 22, 101, 102, 104, 108, 122, 148,
150, 151, 164, 166, 167, 229
X-ray diffraction analyses, 223
X-ray diffraction output, 163
X-ray diffraction pattern, 101, 129, 130, 140, 148, 153,
166, 234, 237, 249, 250
X-ray *diffraction* studies, 237, 238
X-ray diffraction technique, 21

X-ray pattern, 129
X-ray photoelectron spectroscopy, 148
XPS, 148
XRD analysis, 129
XRD patterns, 129

Y

yield stress, 186
Young's modulus, 247
Yucca mountain, 238

Z

zinc phosphate gels, 114

This page is intentionally left blank